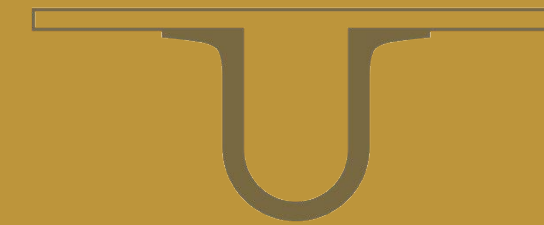UNIVERSIDADE Ð
COIMBRA

Tiago Daniel Almeida Rodrigues

AGEing fat – Exploring the mechanisms of glycation-induced microvascular dysfunction in adipose tissue

Tese no âmbito do Programa de Doutoramento em Ciências da Saúde – ramo de Ciências Biomédicas, orientada pela Professora Doutora Raquel Maria Fino Seiça e Professor Doutor Paulo Nuno Centeio Matafome e apresentada à Faculdade de Medicina da universidade de Coimbra.

Março de 2019

Faculdade de Medicina da Universidade de Coimbra

AGEING FAT – EXPLORING THE MECHANISMS OF GLYCATION-INDUCED MICROVASCULAR DYSFUNCTION IN ADIPOSE TISSUE

Tiago Daniel Almeida Rodrigues

Tese no âmbito do Programa de Doutoramento em Ciências da Saúde - ramo de Ciências Biomédicas, orientada pela Professora Doutora Raquel Seiça e pelo Professor Doutor Paulo Matafome, e apresentada à Faculdade de Medicina da Universidade de Coimbra.

Março de 2019

UNIVERSIDADE Ð
COIMBRA

Dedico este percurso aos que a vida levou demasiado cedo…

ACKNOWLEDGEMENTS

GLOBAL INDEX

RESUMO

Introdução e objectivos: O tecido adiposo tem um papel crucial no metabolismo, sendo actualmente reconhecido como um órgão endócrino, que produz e potencialmente liberta mais de 600 factores envolvidos em diversos processos fisiológicos. Quando disfuncional associa-se a insulinorresistência marcada e desregulação metabólica, contribuindo para o desenvolvimento de obesidade patogénica e diabetes tipo 2.

A glicação induzida pelo metilglioxal, sobretudo em condições de hiperglicemia crónica, é uma das vias de disfunção microvascular, podendo ocorrer no tecido adiposo e, consequentemente, prejudicar a sua função. As abordagens terapêuticas baseadas no "*glucagon-like peptide-1*" (GLP-1), cirurgia metabólica e tratamento com análogos do GLP-1, têm efeitos pleiotrópicos, nomeadamente na homeostasia do tecido adiposo e na sinalização da insulina e tolerância à glicose. Assim, a nossa hipótese é que a glicação induzida pelo metilglioxal afecta a vasculatura, a expansibilidade e a funcionalidade do tecido adiposo periepididimal, podendo ser um alvo de terapêuticas baseadas no GLP-1, através de mecanismos dependentes da enzima glioxalase-1. Neste sentido, o nosso principal objectivo foi avaliar a disfunção microvascular induzida pela glicação e o seu impacto na função do tecido adiposo, explorando os mecanismos envolvidos e o papel de terapias baseadas no GLP-1.

Métodos: Ratos Wistar mantidos com metilglioxal e/ou dieta rica em gordura, foram usados no estudo da rede vascular e função do tecido adiposo periepididimal, visando nomeadamente a hipóxia no tecido e a insulinorresistência local e sistémica. Pela primeira vez, a ressonância magnética com contraste, um método imagiológico dinâmico, e o ensaio de angiogénese de tecido adiposo de rato, foram desenvolvidos de forma a quantificar o fluxo sanguíneo no tecido adiposo periepididimal e a angiogénese,

respectivamente. Adicionalmente, foi avaliado o papel da actividade da glioxalase-1 na função do tecido adiposo visceral e no metabolismo sistémico, numa coorte de doentes obesos diabéticos e não diabéticos. O papel das terapias baseadas no GLP-1 na glicação do tecido adiposo, foi avaliado em ratos diabéticos tipo 2 (GK) tratados com liraglutido (modelo farmacológico) e ratos GK mantidos com dieta hipercalórica, e submetidos a gastrectomia vertical "*sleeve*" (modelo cirúrgico). Foram estudados os mecanismos dependentes da glioxalase-1 e o perfil metabólico do tecido adiposo e sistémico. O papel do liraglutido na prevenção da incapacidade angiogénica causada pelo metilglioxal e na modulação da angiogénese dependente da glioxalase-1 no tecido adiposo, foi avaliado através do *matrigel plug* e do ensaio de angiogénese de tecido adiposo, respectivamente. Foi aplicado o teste Kruskal-Wallis (com múltiplas comparações entre pares), sendo $p < 0,05$ considerado como critério de significância.

Resultados: Pela primeira vez, o nosso grupo demonstrou que a suplementação de metilglioxal a ratos com obesidade induzida por dieta gorda afecta o fluxo sanguíneo e a capilarização do tecido adiposo periepididimal, causando hipóxia e resistência local à insulina, bem como insulinorresistência muscular e sistémica e intolerância à glicose. Por sua vez, o ensaio de angiogénese do tecido adiposo mostrou diminuição da capilarização dependente da dose de metilglioxal e da inibição da glioxalase-1.

Os doentes resistentes à insulina mostraram um declínio progressivo das funções da célula β pancreática e do tecido adiposo, exacerbado nos doentes obesos diabéticos, nomeadamente diminuição sérica do colesterol HDL e da adiponectina e diminuição da actividade da glioxalase-1 no tecido adiposo. A actividade desta enzima no tecido adiposo visceral dos doentes obesos correlacionou-se negativamente com a HbA1c.

Nos modelos animais, a gastrectomia vertical "*sleeve*" e o tratamento com liraglutido, restauraram os níveis e a actividade da glioxalase-1 no tecido adiposo periepididimal.

Mais ainda, o tratamento com liraglutido aumentou os níveis de factores vasoactivos e angiogénicos, bem como a sensibilidade à insulina. No ensaio *matrigel plug*, o liraglutido preveniu a diminuição da angiogénese causada pelo metilglioxal e aumentou a angiogénese do tecido adiposo periepididimal, de forma dependente da glioxalase-1.

Conclusões: A glicação induzida pelo metilglioxal prejudica a expansibilidade e função do tecido adiposo periepididimal, contribuindo para o desenvolvimento de insulinorresistência e obesidade patogénica. A diminuição da actividade da enzima glioxalase-1 no tecido adiposo acompanha a sua progressiva deterioração funcional, e está correlacionada com a desregulação metabólica em doentes obesos. Além disso, a glioxalase-1 constitui um alvo das abordagens terapêuticas baseadas no GLP-1, ao melhorar a função do tecido adiposo e a sensibilidade à insulina, prevenindo a desregulação metabólica precoce, o desenvolvimento de obesidade não saudável e diabetes tipo 2.

Palavras-chave: Tecido adiposo, Glicação, Microvasculatura, Angiogénese, Metilglioxal, GLP-1, Liraglutido, Insulinorresistência, Obesidade; Diabetes tipo 2.

ABSTRACT

Background and aims: Adipose tissue has a crucial role in metabolism and is nowadays recognized as an endocrine organ that produces and potentially secrets more than 600 factors involved in several physiological processes. Adipose tissue dysfunction is associated with increased insulin resistance and systemic dysmetabolism, which contributes to the development of metabolically unhealthy obesity and type 2 diabetes. Methylglyoxal-induced glycation is commonly associated with microvascular dysfunction, namely during chronic hyperglycemia, being a hypothetic factor underlying the impairment of adipose tissue microvasculature and ultimately, tissue dysfunction. Glucagon-like peptide-1 (GLP-1) based therapeutic approaches, specifically metabolic surgery and GLP-1 analogue treatment, have pleiotropic effects, including improved adipose tissue homeostasis, insulin signalling and glucose tolerance. Thus, we hypothesised that methylglyoxal-induced glycation has adverse effects on periepididymal adipose tissue vasculature, expandability and function, which could be targeted by GLP-1-based strategies through glyoxalase-1-dependent mechanisms. Accordingly, our main goal was to evaluate the role of glycation-induced microvascular dysfunction in adipose tissue function, exploring the mechanisms involved and the role of GLP-1-based therapies.

Methods: Wistar rats supplemented with methylglyoxal and/or maintained with high-fat diet, were studied regarding periepididymal adipose tissue vasculature and function, namely addressing tissue hypoxia and local and systemic insulin resistance. For the first time, dynamic contrast-enhanced magnetic resonance imaging and adipose tissue angiogenesis assay have been used to quantify rat periepididymal adipose tissue blood flow and angiogenesis, respectively. Additionally, the role of glyoxalase-1 activity in

human visceral adipose tissue and systemic metabolism was assessed in a cohort of obese patients (diabetic and non-diabetic). The role of GLP-1-based therapies on adipose tissue glycation was studied in type 2 diabetic Goto-Kakizaki rats (GK) maintained with high-calorie diet and submitted to sleeve gastrectomy (surgical model) and liraglutide-treated GK rats (pharmacological model). The glyoxalase-1-dependent mechanisms in adipose tissue and systemic metabolic profile were studied, as well as the role of liraglutide in preventing methylglyoxal-induced impairment of angiogenesis and modulating glyoxalase-dependent angiogenesis in adipose tissue by matrigel plug and adipose tissue angiogenesis assays, respectively. Kruskal-Wallis test (all pairwise multiple comparisons) was applied, being $p<0.05$ considered as the criterion for significance.

Results: For the first time, our group demonstrated that methylglyoxal supplementation to high-fat diet-induced obese rats impairs periepididymal adipose tissue capillarization and blood flow, causing increased periepididymal adipose tissue hypoxia and insulin resistance as well as systemic and muscle insulin resistance and glucose intolerance. In turn, the adipose tissue angiogenic assay showed decreased capillarization after dose-dependent methylglyoxal exposure and glyoxalase-1 inhibition.

Insulin resistant patients have shown a progressive decline in pancreatic β-cell and adipose tissue function, which were exacerbated in diabetic obese patients, including decreased serum HDL cholesterol and adiponectin and visceral adipose tissue glyoxalase-1 activity. In visceral adipose tissue from obese patients the activity of this enzyme was negatively correlated with HbA1c.

Animal models of vertical sleeve gastrectomy and liraglutide treatment have shown restored periepididymal adipose tissue levels and activity of glyoxalase-1. Liraglutide-treated rats also showed increased levels of periepididymal adipose tissue angiogenic and vasoactive factors, and insulin signalling. Moreover, liraglutide prevented negative

methylglyoxal-induced effects on matrigel plug assay, being also effective in increasing periepididymal adipose tissue angiogenesis in a glyoxalase-1-dependent manner.

Conclusions: Methylglyoxal-induced glycation impairs periepididymal adipose tissue expandability and function, contributing to insulin resistance and to the onset of metabolically unhealthy obesity. Lower visceral adipose tissue glyoxalase-1 activity follows the progressive decline of adipose tissue function, and is negatively associated with metabolic dysregulation in obese patients. Furthermore, glyoxalase-1 is a target for GLP-1-based therapeutic approaches, improving periepididymal adipose tissue function and insulin sensitivity, preventing early metabolic dysregulation, metabolically unhealthy obesity and type 2 diabetes development.

Keywords: Adipose tissue, Glycation, Microvasculature, Angiogenesis, Methylglyoxal, GLP-1, Liraglutide, Insulin resistance, Obesity, Type 2 diabetes.

GRAPHICAL ABSTRACT
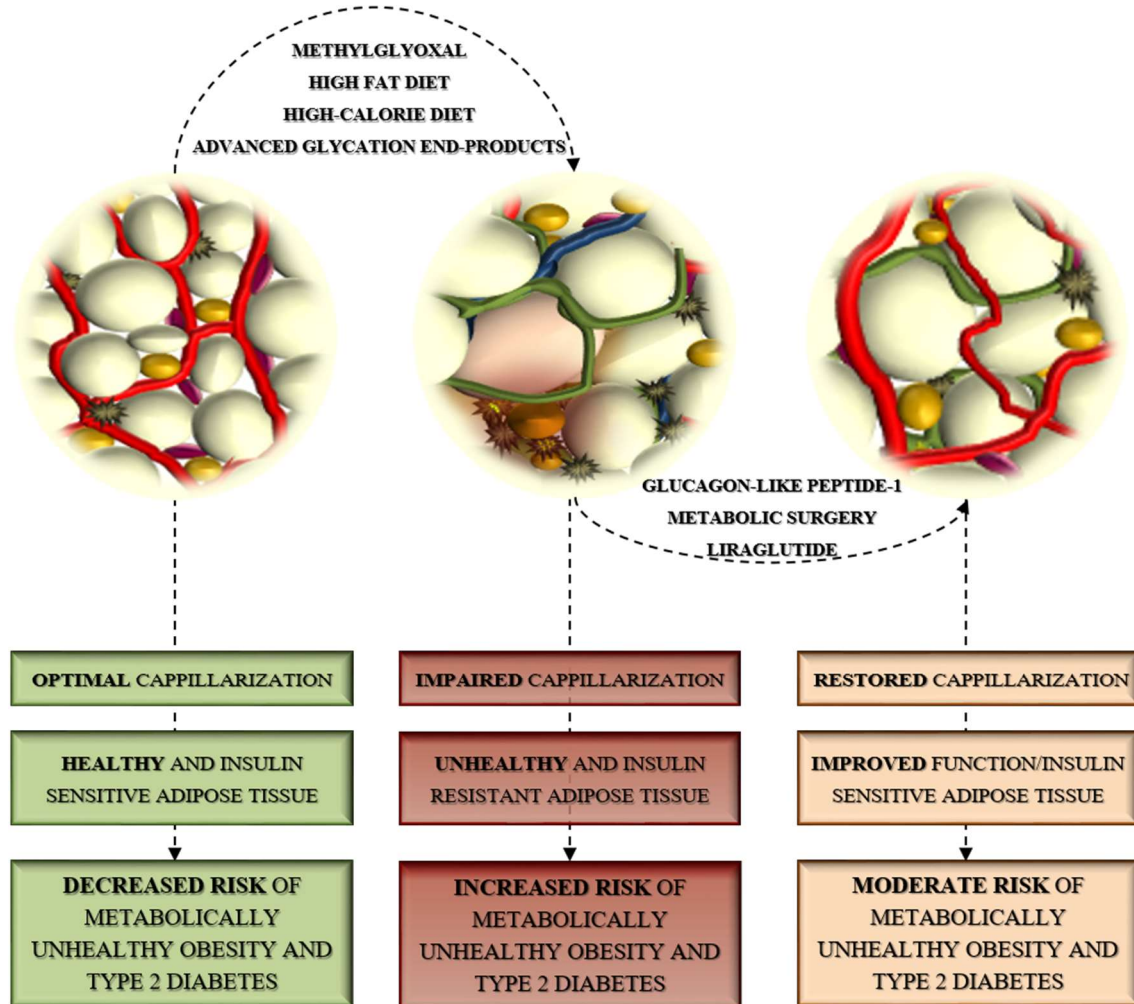
PhD - PUBLICATIONS, ORAL COMMUNICATIONS AND PRIZES

Publications

- Patrícia Santos-Oliveira, António Correia, **Tiago Rodrigues**, Teresa Ribeiro-Rodrigues, Paulo Matafome, Juan Rodríguez-Manzaneque, Raquel Seiça, Henrique Girão, Rui Travasso. **The Force at the Tip-Modelling Tension and Proliferation in Sprouting Angiogenesis**. PLoS Computational Biology 2015;11: e1004436.

- Paulo Matafome, **Tiago Rodrigues**, Raquel Seiça. **Glycation and hypoxia: two key factors for adipose tissue dysfunction**. Current Medicinal Chemistry 2015;22: 2417-37.

- Paulo Matafome, **Tiago Rodrigues**, Cristina Sena, Raquel Seiça. **Methylglyoxal in Metabolic Disorders: Facts, Myths, and Promises**. Medicinal Research Reviews 2017;37: 368–403.

- **Tiago Rodrigues**, Paulo Matafome, José Sereno, José Almeida, João Castelhano, Luís Gamas, Christian Neves, Sónia Gonçalves, Catarina Carvalho, Amina Arslanagic, Elinor Wilcken, Rita Fonseca, Ilda Simões, Silvia Vilares Conde, Miguel Castelo-Branco, Raquel Seiça. **Methylglyoxal-induced glycation changes adipose tissue vascular architecture, flow and expansion, leading to insulin resistance**. Scientific Reports 2017;7: 1698.

- Mário Ribeiro, José Castelhano J, Lorena I. Petrella, José Sereno, **Tiago Rodrigues**, Christian Neves, Liliana Letra, Filipa I. Baptista, Raquel Seiça, Paulo Matafome, Miguel Castelo-Branco. **High-fat diet induces a neurometabolic state characterized by changes in glutamate and N-acetylaspartate pools associated with early glucose intolerance: An in vivo multimodal MRI study**. Journal of Magnetic Resonance Imaging 2018;48: 757–766.

- Hans Eickhoff, **Tiago Rodrigues**, Inês Neves, Daniela Marques, Diana Ribeiro, Susana Costa, Raquel Seiça, Paulo Matafome. **Effect of sleeve gastrectomy on angiogenesis and adipose tissue health in an obese animal model of type 2 diabetes**. (under review - obesity surgery).

- **Tiago Rodrigues**, Patricia Borges, Laura Mar, Miguel Albano, Hans Eickhoff, Daniela Marques, Catarina Carrêlo, Bruno Almeida, Salomé Pires, Margarida Abrantes, Beatriz Martins, Cristina Uriarte, Filomena Botelho, Pedro Gomes, Sónia Silva, Raquel Seiça, Paulo Matafome. **Targeting adipose tissue glyoxalase system with GLP-1 to improve capillarization and insulin sensitivity** (in preparation).

Oral communications

- **Tiago Rodrigues**, Paulo Matafome, José Sereno, José Almeida, João Castelhano, Luís Gamas, Christian Neves, Sónia Gonçalves, Catarina Carvalho, Amina Arslanagic, Elinor Wilcken, Rita Fonseca, Ilda Simões, Silvia Vilares Conde, Miguel Castelo-Branco, Raquel Seica. **A modulação do sistema da glioxalase pelo liraglutido melhora a função vascular do tecido adiposo e contribui para um melhor controlo metabólico na diabetes tipo 2**. XLVII Reunião da Sociedade Portuguesa de Farmacologia (SPF). Coimbra, 2 a 4 de Fevereiro de 2017.

- **Tiago Rodrigues**, Paulo Matafome, José Sereno, José Almeida, João Castelhano, Luís Gamas, Christian Neves, Sónia Gonçalves, Catarina Carvalho, Amina Arslanagic, Elinor Wilcken, Rita Fonseca, Ilda Simões, Silvia Vilares Conde, Miguel Castelo-Branco, Raquel Seica. **A glicação prejudica a arquitectura vascular, a irrigação e expansão do tecido adiposo, causando insulino-resistência**. 13º Congresso Português de Diabetes (SPD). Vilamoura, 10 a 12 de Março de 2017.

- **Tiago Rodrigues**, Daniela Marques, Inês Neves, Hans Eickhoff, Catarina Carrêlo, Diana Ribeiro, Beatriz Martins, Carlos Fontes-Ribeiro, Sónia Santos, Raquel Seiça, Paulo Matafome. **Increasing GLP-1 levels is a route to improve adipose tissue angiogenesis, contributing to a better metabolic outcome**. 53st Annual Meeting of the European Association for the Study of Diabetes (EASD). Lisboa, Portugal, 11 a 15 de Setembro de 2017.

- **Tiago Rodrigues**, Patrícia Borges, Catarina Carrêlo, Laura Mar, Hans Eickhoff, Bruno Almeida, Daniela Marques, Salomé Pires, Margarida Abrantes, Beatriz Martins, Cristina Uriarte, Pedro Gomes, Sónia Silva, Raquel Seiça, Paulo Matafome. Modulação da glioxalase-1 pelo GLP-1: Impacto na capilarização e sensibilidade à insulina do tecido adiposo. 15º Congresso Português de Diabetes, Vilamoura, Portugal, 8 a 10 de março de 2019.

Prizes

- **Tiago Rodrigues**, José Almeida, José Sereno, João Castelhano, Christian Neves, Rita Fonseca, Sónia Gonçalves, Luís Gamas, Miguel Castelo-Branco, Paulo Matafome e Raquel Seiça. **AGEing fat: methylglyoxal-induced glycation impairs adipose tissue expansion causing systemic dysmetabolism in high-fat diet-fed rats**.

  Best scientific poster, 750 euros, presented at VII Annual Meeting of IBILI, 2015.

- Raquel Seiça, **Tiago Rodrigues**, Paulo Matafome, José Sereno, José Almeida, Luís Gamas, João Castelhano, Christian Neves, Sónia Gonçalves, Catarina Carvalho, Amina Arslanagic, Elinor Wilcken, Rita Fonseca, Ilda Simões, Silvia Vilares Conde, Miguel Castelo-Branco. **The echo of type 2 diabetes: magnetic resonance as a strategy to detect glycation-induced adipose tissue microvascular lesions and preventing unhealthy obesity and type 2 diabetes**.

  "Prémio Nacional de Diabetologia", 20000 euros, "Sociedade Portuguesa de Diabetologia", 2016.

- **Tiago Rodrigues**, Paulo Matafome, José Sereno, José Almeida, João Castelhano, Luís Gamas, Christian Neves, Sónia Gonçalves, Catarina Carvalho, Amina Arslanagic, Elinor Wilcken, Rita Fonseca, Ilda Simões, Silvia V. Conde, Miguel Castelo-Branco, Raquel Seiça. **Methylglyoxal-induced glycation changes adipose tissue vascular architecture, flow and expansion, leading to insulin resistance.**

  "Menção honrosa da bolsa Pedro Eurico Lisboa Lilly/SPD", 1000 euros, "Sociedade Portuguesa de Diabetologia", 2018.

- **Tiago Rodrigues**, Patrícia Borges, Catarina Carrêlo, Laura Mar, Hans Eickhoff, Bruno Almeida, Daniela Marques, Salomé Pires, Margarida Abrantes, Beatriz Martins, Cristina Uriarte, Pedro Gomes, Sónia Silva, Raquel Seiça, Paulo Matafome. Modulação da glioxalase-1 pelo GLP-1: Impacto na capilarização e sensibilidade à insulina do tecido adiposo. 15º Congresso Português de Diabetes, Vilamoura, Portugal, 8 a 10 de março de 2019.

  "Prémio SPD/MEDINFAR Diabetes/2019", 1500 euros, "Sociedade Portuguesa de Diabetologia", 2019.

- **Tiago Rodrigues**, Patrícia Borges, Catarina Carrêlo, Laura Mar, Hans Eickhoff, Bruno Almeida, Daniela Marques, Salomé Pires, Margarida Abrantes, Beatriz Martins, Cristina Uriarte, Pedro Gomes, Sónia Silva, Raquel Seiça, Paulo Matafome. Modulação da glioxalase-1 pelo GLP-1: Impacto na capilarização e sensibilidade à insulina do tecido adiposo. 15º Congresso Português de Diabetes, Vilamoura, Portugal, 8 a 10 de março de 2019.

  "Prémio de Melhor Comunicação Oral de Investigação Fundamental", 400 euros, "Sociedade Portuguesa de Diabetologia", 2019.

LIST OF ABBREVIATIONS

ACE	Angiotensin converting enzyme
AGE	Advanced glycation end-products
AKT/PKB	Protein kinase b
AMPK	AMP-activated protein kinase
ANG-1	Angiopoietin-1
ANG-2	Angiopoietin-2
AngI	Angiotensin I
AngII	Angiotensin II
ANGPTL4	Angiopoietin-like 4
AT	Adipose tissue
AT1	Angiotensin type 1 receptor
AT2	Angiotensin type 2 receptor
AUC	Area under the curve
BAT	Brown adipose tissue
BMI	Body mass index
cAMP	Cyclic adenosine monophosphate
CD31	Cluster of differentiation 31
CD36	Cluster of differentiation 36
CEL	N-epsilon (carboxyethyl)lysine
CML	N-carboxymethyl-lysine
DPP-4	Dipeptidyl peptidase-4
EC	Endothelial cell
ELISA	Enzyme-linked immunosorbent assay
eNOS	Endothelial nitric oxide synthase
ERK1/2	Extracellular signal-regulated kinase 1/2
FATP	Fatty acid transport protein
FFA	Free fatty acids
GK	Goto-Kakizaki
GLO-1	Glyoxalase-1
GLO-2	Glyoxalase-2
GLP-1	Glucagon-like peptide-1

GLP-1R	Glucagon-like peptide-1 receptor
GLUT-1	Glucose transporter-1
GLUT-4	Glucose transporter-4
GSH	Reduced glutathione
HbA1c	Glycated hemoglobin
HIF-1alpha	Hypoxia inducible factor-1 alpha
HIF-2alpha	Hypoxia inducible factor-2 alpha
HOMA	Homeostatic model assessment for insulin resistance
HOMA2IR	Homeostasis model assessment 2 insulin resistance index
HSL	Hormone-sensitive lipase
HUVEC	Human umbilical vein endothelial cell
ICAM-1	Intercellular adhesion molecule-1
IHC	Immunohistochemistry
IKK	Kinase of the inhibitor of NF-κB
IL	Interleukine
iNOS	Inducible nitric oxide synthase
IPGTT	Intraperitoneal glucose tolerance test
IPITT	Intraperitoneal insulin tolerance test
IQR	Interquartile range
IR	Insulin resistance
IRS-1	Insulin receptor substrate-1
ITT	Insulin tolerance test
IκBα	NF-κB inhibitor alpha
JNK/SAPK	C-jun n-terminal kinase/Stress-activated protein kinase
LPL	Lipoprotein lipase
MCP-1	Monocyte chemoattractant protein-1
MG	Methylglyoxal
MHO	Metabolically healthy obesity
MHO	Metabolically healthy obesity
MIF	Migration inhibitory factor
MMP	Matrix metalloproteinases
MRI	Magnetic resonance imaging
MUO	Metabolically unhealthy obesity

NF-κB	Nuclear factor-kappa B
NO	Nitric oxide
PAS	Periodic acid-schiff
pEAT	Periepididymal adipose tissue
PEPCK	Phosphoenolpyruvate carboxykinase
PI3K	Phosphatidylinositol-4,5-bisphosphate 3-kinase
PKC	Protein kinase C
PPAR-gamma/γ	Peroxisome proliferating-activated receptor-gamma/γ
RAGE	Advanced glycation end-product receptor
RAS	Renin-angiotensin system
SCD-1	Stearoyl-CoA desaturase-1
SEM	Standard error of the mean
SOCS	suppressor of cytokine signalling
SOD1	Superoxide dismutase 1
TG	Triglycerides
TGF-β	Transforming growth factor-β
Tie-2	Angiopoietins receptor-2
TLR	Toll-like receptors
TNF-α	Tumor necrosis factor-alpha
TZD	Tiazolidinediones
UCP-1	Uncoupling Protein-1
VAT	Visceral adipose tissue
VEGF	Vascular endothelial growth factor
VEGFR2	VEGF receptor 2
W	Wistar Han
WAT	White adipose tissue
WB	Western blotting

FIGURES INDEX

TABLE INDEX

THESIS OUTLINE

This thesis is divided in five chapters, which content is summarized below:

The first chapter includes a comprehensive introduction to the thesis, about previous findings and concepts.

Chapter two is composed by a scientific framework to explain the rationale of our research, scientific hypothesis and objectives.

Material and methods are detailed in chapter three, being rat adipose tissue angiogenesis assay development and use totally described.

Chapter four, which consists of results and highlights and detailed discussions, are divided in two sections: the first includes the effects of methylglyoxal-induced glycation during adipose tissue expandability and the second, the GLP-1-based therapies against adipose tissue glycation, exploring the role of glyoxalase-1.

Chapter five provides global considerations and conclusions.

Chapter 1 - INTRODUCTION

1. Adipose tissue in health and disease

1.1 Adipose tissue as a cryptic organ

Obesity is a multifactorial, complex and potentially preventable disease. However, has reached epidemic proportions worldwide. Nowadays obesity affects, along with overweight, over a third of world's population. In Europe, overweight and obesity affect 30-70% and 10-20% of adult individuals, respectively (Guilherme et al., 2008; Ng et al., 2014; Stevens et al., 2012; World Health Organization, 2000). In Portugal, data from 2015 demonstrated that 67.6% of adult population is overweighted and 28.7% are obese. Women are more obese, but diabetes prevalence is higher in man. Diabetes prevalence confirmed by HbA1c levels, diabetes medication or diabetes diagnosis was 13.3% of Portuguese population (Barreto et al., 2016; Observatório Nacional da Diabetes, 2016).

In addition, several authors claimed the existence of metabolically healthy obesity (MHO) and metabolically unhealthy obesity (MUO), based on the fact that different metabolic profiles and outcomes, as well as comorbidities that are seen in obese population (Gonçalves et al., 2016; Hinnouho et al., 2014; Naukkarinen et al., 2014). In fact, recent studies suggested that impaired metabolic outcomes and MUO were highly associated with early development and progression of type 2 diabetes (Boonchaya-anant and Apovian, 2014; Hinnouho et al., 2014; Kusminski et al., 2016; Uribarri et al., 2015a).

During the last three decades, the number of people with diabetes mellitus increased four times, meaning that worldwide 1 in 11 adults have diabetes. There are individuals with higher genetic predisposition to type 2 diabetes. However, unhealthy diets and lifestyle deficits largely contribute to increase all body adiposity, commonly described by body mass index (BMI), and abdominal fat accumulation, which is highly associated with detrimental metabolic effects. These lifestyle behaviours and adiposity alterations are recognized as

common triggers to this global burden, increasing the risk of type 2 diabetes development (Figure 1.1) (Kusminski et al., 2016; Smith, 2015; Wild et al., 2004; Zheng et al., 2017).
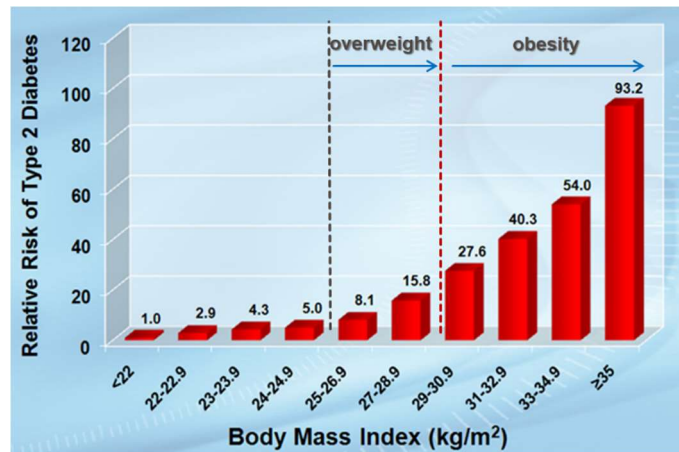
Figure 1.1 - Increased adiposity and type 2 diabetes risk
The figure shows the relative risk of type 2 diabetes development associated with body mass index increase. Overweight and obesity patients have a higher relative risk. Adapted from Colditz GA et al., 1995.

In the last two decades of intense research, the perspective of adipose tissue (AT) as a merely fat storing organ has changed considerably. AT physiology knowledge has deeply changed from the classical view, known by adipocyte's capacity to store triglycerides during postprandial and release fatty acids during interdigestive and fasting states. Despite the fact that the capacity to store and release fatty acids, responding to systemic energetic clues, involves AT in the regulation of whole body metabolism, AT is currently recognized as a highly complex and multifactorial endocrine organ able to influence all systems, including glucose and lipid homeostasis, energy expenditure, food consumption, immune system, vasculogenesis, coagulation, matrix remodelling and so forth. Consequently, the influence

of AT secretome goes far beyond the metabolism regulation (Guilherme et al., 2008; Rutkowski et al., 2015; Scherer, 2006, 2018; Trujillo and Scherer, 2006).

Impaired AT function is commonly associated with hypoxia, fibrosis and inflammation. In turn, these impaired function leads to dyslipidemia, hyperinsulinemia and hyperglycemia, contributing to progressive insulin resistance, metabolically unhealthy obesity and type 2 diabetes (Galic et al., 2010; Guilherme et al., 2008; Maury and Brichard, 2010; Olefsky and Glass, 2010; Scherer, 2018).

Adipose tissue distribution and adipocyte phenotypes

White adipose tissue distribution occurs in two anatomical compartments, commonly defined as visceral and subcutaneous fat depots, which are significantly different in their cellular/molecular mechanisms. Despite the fact that both may be expanded during overnutrition, enlarged visceral depots are highly associated with metabolic disorders, while subcutaneous depots are considered healthier. Epidemiological studies revealed that visceral AT accumulation, commonly seen in males (apple shape), contributes to metabolically unhealthy phenotype, when compared to subcutaneous accumulation, which is frequently observed in women, namely in lower extremities (pear shape) (Giordano et al., 2016; Pellegrinelli et al., 2016; Scherer, 2018).

In human infants, under physiological conditions, brown adipose tissue (BAT) is mainly located in supraclavicular region, contributing to heat production through energy expenditure. However, during adulthood brown adipose depot almost disappears, although adult humans may develop thermogenic AT in the paraspinal and supraclavicular depot and around large blood vessels following several signalling clues. In line with this, several authors are developing white AT browning-based strategies in order to increase energy

expenditure by uncoupling protein-1 (UCP-1)-dependent mechanisms and through increased fatty acid consumption (Ghaben and Scherer, 2019; Iacobini et al., 2018; Peschechera and Eckel, 2013; Shimizu and Walsh, 2015; Sidossis and Kajimura, 2015; Sun et al., 2014).

Adipocyte subtypes, from white to brown, are identified by their colour, regarding triglyceride (TG) and mitochondrial content (Figure 1.2). White adipocytes are well known by high-triglyceride content in one lipid droplet (approximately 90% of cell volume) and peripheral nuclei and decreased presence of mitochondria, while brown adipocytes have several but smaller lipid droplets (approximately 50% of cell volume) and increased mitochondria-derived metabolic rate (Giordano et al., 2016).

More recently, brite/beige adipocytes have been identified as an intermediate phenotype, which may be raised from white/brown adipocytes following signalling clues. In fact, browning and whitening processes occur in AT, converting adipocytes in accordance to nutritional/environmental changes (Giordano et al., 2016; Lee et al., 2013). These adipocyte subtypes with increased mitochondrial content are associated with non-shivering thermogenesis primarily regulated by nervous system, controlling energy and glucose/lipid homeostasis (Lee et al., 2013; Sidossis and Kajimura, 2015).
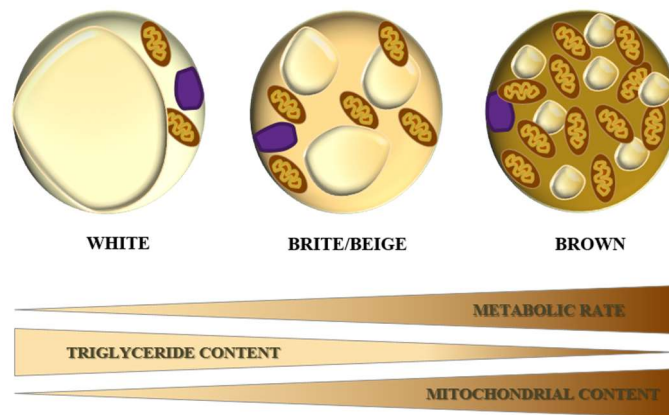
Figure 1.2 – Adipocyte phenotypes and associated metabolic rate
The schematic figure shows the spectrum of adipocyte phenotypes, namely concerning triglyceride and mitochondrial content. Metabolic rate capacity is increased in brite/beige and brown adipocytes, given the fact that mitochondrial content is significantly superior.

Adipose tissue composition and vasculature

Adipose tissue formation during the embryonic development is primarily shaped by vascular network and perivascular extracellular matrix formation. Subsequently, adipocytes are developed from progenitor cells, being each adipocyte surrounded by at least one blood vessel (Mannerås-Holm and Krook, 2012; Rutkowski et al., 2009; Tran et al., 2012).

Adipose tissue has a dense network of blood vessels responsible for factors, nutrients and oxygen transport. AT microvasculature is highly dynamic in accordance to nutritional fluxes, being significantly different between fat depots of different locations (Corvera and Gealekman, 2014a; Gealekman et al., 2011; Rodrigues et al., 2013a).

In addition to adipocytes, AT is composed by several cell types, being a highly heterogeneous and dynamic tissue severely expanded by increased adipocyte volume (hypertrophy) and number (hyperplasia). The stromovascular fraction is shaped by preadipocytes, endothelial and mesenchymal progenitor/stem cells, as well as fibroblasts and

several leucocytes, namely increased presence of M2 macrophages. The dynamic adaptation of these cells during tissue expansion or regression determine AT plasticity and maintain tissue function (Ghaben and Scherer, 2019; Guilherme et al., 2008; Kusminski et al., 2016). Despite the fact that mature adipocyte turnover is quite low (approximately 10 years in human), the formation of new adipocytes from preadipocytes and other stromovascular-derived cells (adipogenesis) may become an important strategy to improve adipocyte hyperplasia. This is particularly important, because adipose tissue vascularization and expansion is facilitated by adipocyte hyperplasia instead of hypertrophy, contributing to improved AT function (Arner et al., 2010; Rutkowski et al., 2009; Spalding et al., 2008; Tran et al., 2012). During embryonic development, the vascular network and extracellular matrix of AT are developed even before adipocytes differentiation as already mentioned. Recent data show that the expansion of AT vascular network potentiated by angiogenic factors is associated with increased proliferation of human brite/beige adipocyte progenitors, which may be fully differentiated in triglyceride-filled mature adipocytes (Christiaens and Lijnen, 2010; Ghaben and Scherer, 2019; Min et al., 2016; Neels et al., 2004; Tran et al., 2012).

Adipogenesis is a highly regulated process whereby progenitor cells known as preadipocytes originate fully differentiated mature adipocytes. This process is divided in two main steps: firstly, preadipocytes are developed and then, following signalling clues, begin a differentiation program. This dynamic process occurs during adulthood and is associated with hyperplasia-derived healthy AT expandability. It was described that healthy vasculature may be an important source of preadipocytes, meaning that angiogenesis and adipogenesis are mutually regulated and may be targeted to improve lipid handling and AT plasticity (Cao, 2007; Ghaben and Scherer, 2019; Min et al., 2016; Tran et al., 2012).

During adulthood, the vascular network of AT is crucial for nutrient and factors fluxes, being easily observable even in highly expanded AT depots. In physiological conditions, adipocytes are surrounded by fenestrated capillaries, which are rich in trans-endothelial channels allowing a better communication between adipocytes and endothelial cells (EC) (Christiaens and Lijnen, 2010; Min et al., 2016; Neels et al., 2004; Rutkowski et al., 2009). Furthermore, the expansion and regression of AT as well as the vascular network remodelling might be highly dynamic, even in adulthood, being both mutually regulated and changed during prolonged alterations of nutritional fluxes, affecting tissue function and secreted factors (Rutkowski et al., 2009; Tilg and Moschen, 2006).

In line with recent findings, the crosstalk between adipocytes and vasculature is crucial for AT adaptation during exacerbated expansion and hypoxic conditions, challenging tissue plasticity and lipid storage capacity. Despite the fact that those mechanisms involved in this adipovascular coupling are partly unknown, recent data reinforce the role of adipocytes- and endothelial cells-derived extracellular vesicles/exosomes, containing factors involved in inter-cell/organs communication during fasting/postprandial states, but also far beyond metabolic signals (Figure 1.3) (Rodrigues et al., 2013a; Scherer, 2018).
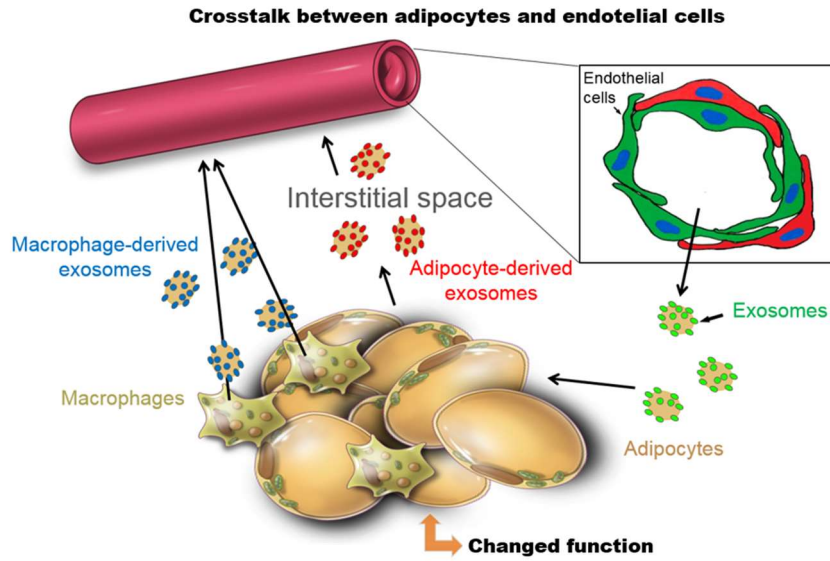
Figure 1.3 – Changed function after exosomes communication between adipocytes and endothelial cells
The schematic figure shows exosome-mediated communication between adipocytes and endothelial cells. In fact, this signalling molecules may affect AT and vascular function, namely during adaptations to stress signals. Adapted from Scherer et al. 2008.

Lipid handling and storage by adipocyte

Mature white adipocytes are well known by their expandability and lipid storage capacity, being a critical place to safely store fatty acids within lipid droplet, preventing lipotoxicity in other cell types as well as ectopic fat deposition and lipid-derived insulin resistance (Guilherme et al., 2008; Konige et al., 2013; Scherer, 2006).

TG storage is highly regulated by a number of interconnected and coordinated mechanisms. Firstly, TG synthesis, a process called esterification, occurs from one molecule of glycerol and three fatty acyl chains, which are included in lipid droplet. Given the fact that adipocytes have a limited ability to store glycogen, all the glucose that is not consumed in cell metabolism is transformed into glycerol and incorporated as well in triglycerides pool (Guilherme et al., 2008; Reshef et al., 2003; Scherer, 2006). On the other hand, fatty acids

are either directly synthesized within the adipocyte via de novo lipogenesis or indirectly from TG-enriched particles hydrolysis, such as chylomicrons or liver-derived lipoproteins. TGs derived from food or liver production, bind to cluster of differentiation 36 (CD36) in adipocyte membrane and are subsequently hydrolysed by lipoprotein lipase (LPL). Then, free fatty acids (FFA) are transported by several family members of fatty acid transport protein (FATP) to adipocyte cytoplasm and captured by the fatty acid binding protein, which prevent their free circulation in the cell and the consecutive activation of inflammatory and stress pathways. Together with glucose-derived glycerol, fatty acids are finally esterified into TGs and stored in lipid droplets (Dragos et al., 2017; Guilherme et al., 2008; Rutkowski et al., 2015; Scherer, 2006).

The lipid droplets are coated by a family of proteins called perilipins. Despite the fact that lipid droplets formation and regulation are under investigation, perilipin proteins are known by their regulatory role in lipid storage and metabolism and may be targeted to improve lipid handling and adipocyte function (Giordano et al., 2016; Rutkowski et al., 2015).

During fasting, interdigestive period, physical exercise, or stress/cold exposure, FFA are released from lipid droplets within adipocytes, a process known as lipolysis, in order to be involved as a key metabolic fuel (β-oxidation) of catalytic tissues. Lipolysis is a highly complex process mostly regulated by neuroendocrine signalling. Contra-regulatory hormones, like glucagon, cortisol, growth and thyroid hormones and adrenaline, and sympathetic stimulation increase adipocyte's cAMP levels, leading to PKA activation. In turn, activated protein kinase A (PKA) phosphorylates and activates AGTL/HSL following perilipin phosphorylation/degradation, which originates FFA release into circulation, being used in energy demanding tissues (Arner, 2005; Benito, 2011; Guilherme et al., 2008; Nielsen et al., 2014; Reilly and Saltiel, 2017).

In contrast, insulin has a crucial regulatory role in adipocyte metabolism, specially stimulating nutrient storage (lipogenesis) and inhibiting catabolic events (lipolysis). Thus, insulin is responsible for lipolysis inhibition during digestive state, through the inhibition of adenylate cyclase, the main enzyme involved in cAMP synthesis and ATGL/HSL. Conversely, is the main stimulus to triglyceride esterification and nutrient uptake by adipocytes (Czech et al., 2013; Reilly and Saltiel, 2017; Rutkowski et al., 2015).

Insulin receptor phosphorylation and activation of the insulin receptor substrate-1 (IRS-1) initiates a signalling pathway, which involves phosphatidylinositol-4,5-bisphosphate 3-kinase (PI3K) and protein kinase b (AKT/PKB) activation. Among other actions, the activation of this signalling cascade leads to the translocation to the membrane of glucose transporter-4 (GLUT-4)-containing vesicles, allowing enhanced GLUT-4-mediated glucose uptake. Insulin promotes glucose uptake and LPL activity on received TGs, which are converted in glycerol and FFA, respectively, and further incorporated in triglyceride pool (Czech, 2017; Kusminski et al., 2016; Virtanen et al., 2002).

The activity of the peroxisome proliferation-activated receptor-ϒ (PPAR-ϒ) controls the events involved in lipid handling/esterification, being also activated by the pharmacological class of tiazolidinediones (TZD) (Kusminski et al., 2016). The genes controlled by the activation of PPAR-γ include proteins involved in fatty acid uptake (FATP, CD36 and LPL), metabolism (phosphoenolpyruvate carboxykinase and stearoyl-CoA desaturase-1), storage (perilipin-A) and oxidation (adiponectin and uncoupling protein-1) (Guilherme et al., 2008; Pino et al., 2012).

PPAR-γ activation also inhibits cellular inflammatory pathways due to the reduction of cytoplasmatic FFA, specifically nuclear factor-kappa B (NF-κB) pathway, and therefore, promotes improved lipid handling and insulin sensitivity. In addition, peroxisome proliferation-activated receptor-α (PPARα) also controls the expression of genes involved

in lipid oxidation, which are more expressed in tissues with higher catabolic activity, namely liver, skeletal muscle and brown AT. PPARα may be regulated by adiponectin and by drugs, including TZDs, fibrates and metformin, increasing β-oxidation of fatty acids in mitochondria (Guilherme et al., 2008; Kersten and Stienstra, 2017; Odegaard et al., 2007).

White adipose tissue secretome

White adipose tissue produces and potentially releases a broad range of factors (more than 600), commonly known as adipokines, that may be changed in several diseases, namely obesity and type 2 diabetes. The adipokines are involved, among others, in glucose and lipid metabolism, food intake and energy expenditure, angiogenesis and vascular homeostasis, reproduction and immunity (Blüher and Mantzoros, 2015; Kusminski et al., 2016; Rutkowski et al., 2009, 2015; Scherer, 2018; Vázquez-Vela et al., 2008).

Leptin was the first factor originally identified as a product of AT, and its discovery markedly changed the view about this tissue. It is almost exclusively produced by the adipocyte (95% particularly in subcutaneous adipocyte) and its circulating levels are proportional to the fat mass. Among other actions, leptin induces food intake reduction and energy expenditure, acting directly on hypothalamic and extra hypothalamic sites. Leptin is also effective in vasorelaxation (eNOS-dependent nitric oxide production), but chronic hyperleptinemia may lead to increased inflammatory pathways and hypertension, as well as endothelial dysfunction through nitric oxide (NO) depletion, endothelin signalling and ROS production (Blüher and Mantzoros, 2015; Boydens et al., 2012; Golay and Ybarra, 2005; Houben et al., 2012; Lorincz and Sukumar, 2006; Matafome et al., 2017a; Meier and Gressner, 2004; Nielsen et al., 2009; Rajala and Scherer, 2003).

Adiponectin is mainly produced in AT and a progressive decrease in its circulating levels is observed in AT dysfunction. It is an important insulin sensitizer and highly responsible for lipid metabolism and energy expenditure. Besides being recognized by antidiabetic actions, adiponectin has anti-inflammatory and anti-apoptotic effects on several cell types, as well as important vascular effects, such as vasodilation (increased eNOS-dependent NO production), and prevention of endothelial dysfunction (decreases ROS and endothelial cell/macrophage activation) and proliferation/migration of vascular smooth muscle cells. Adiponectin circulates in several molecular forms: globular, trimer (low-molecular weight), hexameric (middle-molecular weight) and multimer (high-molecular weight - HMW) isoform. HMW isoform is composed by several hexamers and has the most important long-term activity in comparison to the other isoforms, having pleiotropic effects and highly complex regulatory functions, which are not fully understood (Blüher and Mantzoros, 2015; Boydens et al., 2012; Houben et al., 2012).

Pharmacological activators of PPAR-γ, glitazones and insulin, are known to increase adiponectinemia. In turn, adiponectin secretion is inhibited by inflammatory pathways activation and cAMP, which are involved in metabolic decline and insulin resistance. Circulating adiponectin levels are inversely correlated with several metabolic disorders, including metabolically unhealthy obesity, type 2 diabetes and related comorbidities (Kusminski et al., 2016; Rajala and Scherer, 2003; Riera-Guardia and Rothenbacher, 2008; Scherer, 2018; Tilg and Moschen, 2006; Wang and Scherer, 2016). Interestingly, increased adiponectinemia is associated with potential beneficial role in healthy aging and extended life span, which have been demonstrated in centenarian women (Gondo et al., 2006) and transgenic mice expressing high levels of human adiponectin (Kadowaki et al., 2014; Otabe et al., 2007).

In human, resistin is mainly produced by AT macrophages and is a pro-inflammatory adipokine associated with local and systemic insulin resistance as well as exacerbated lipolysis and ectopic fat deposition. Higher levels of resistin are commonly seen in models of obesity and type 2 diabetes. In mice slightly overexpressing resistin in AT, it was observed resistin-mediated increase in central leptin resistance and pronounced insulin resistance. Resistin is also a vasoactive factor involved in endothelial dysfunction and coronary heart disease (Asterholm et al., 2014; Blüher and Mantzoros, 2015; Kusminski et al., 2016).

The renin-angiotensin system (RAS) is important in blood pressure regulation and AT blood flow and function. Although angiotensinogen is mainly produced in the liver, AT may become the second higher source of angiotensinogen in obese individuals due to fat mass expansion (Kalupahana and Moustaid-Moussa, 2012). Angiotensinogen is cleaved by renin enzyme into AngI, which in turn is subsequently converted in AngII by angiotensin converting enzyme (ACE) (60% of AngII production), chymase and cathepsin G (Negro, 2008; Weir, 2007a). AngII receptors type 1 (AT1) are the most expressed and responsible for AngII actions, such as vasoconstriction, aldosterone production in the adrenal glands as well as salt and water tubular retention (Steckelings et al., 2009; Weir, 2007a, 2007b).

There are others AT-derived factors associated with vasoactive actions, omentin-1 (vasorelaxation), visfatin (inflammation and vascular smooth muscle and endothelial cells growth stimulation), TNF-α (ROS production, inflammation and endothelial dysfunction), IL-6 (endothelial dysfunction after long-term exposure) and apelin (NO-dependent vasorelaxation) (Figure 1.4) (Agabiti-Rosei et al., 2018; Boydens et al., 2012; Houben et al., 2012).

In obese patients, inflammation-dependent perivascular fat dysfunction changes secretome (decreased adiponectinemia and increased leptinemia, TNF-α and IL-6 levels), contributing to vasoconstriction, smooth muscle cell proliferation and endothelial dysfunction (Giordano

et al., 2016; Houben et al., 2012; Iantorno et al., 2014). Although perivascular AT may have an important role in local vessel regulation (physical support, vasodilator and anti-inflammatory effects), all AT depots may contribute to global vascular alterations through endocrine actions (Boydens et al., 2012; Farb et al., 2012a; Iantorno et al., 2014).

Adipokines are also associated with several physiological and pathophysiological processes, such as immunity (tumor necrosis factor-alpha – TNF-α, interleukin-1β, interleukin-6 – IL-6, interleukin-8, interleukin-10, C reactive protein, osteopontin, macrophage chemoattractant protein-1 – MCP-1, progranulin, adipsin, acylation-stimulating protein, serum amyloid A3), adipogenesis (chemerin), thermogenesis (fibroblast growth factor 21, bone morphogenetic protein 7), glucose homeostasis (visfatin, vaspin, dipeptidyl peptidase-4 - DPP-4, retinol binding protein 4), hypertension (angiotensinogen), cell adhesion (plasminogen activator inhibitor-1), angiogenesis/vascular function (vascular endothelial growth factor - VEGF, apelin, cathepsins) and growth (fibronectin, transforming growth factor-β – TGF-β, insulin growth factor-1) (Blüher and Mantzoros, 2015; Kusminski et al., 2016; Scherer, 2016; Trujillo and Scherer, 2006).

Newly discovered adipokines and their mechanisms in health and disease further increase the complexity of processes, which are under intense research in order to find physiologic regulation/function as well as potential biomarkers, adipokine analogues and therapeutic targets. Furthermore, AT secretome in obesity, evaluated by gene expression may be changed in 60% as well as adipokine receptor distribution in target tissues (Blüher and Mantzoros, 2015; Kusminski et al., 2016; Scherer, 2016).
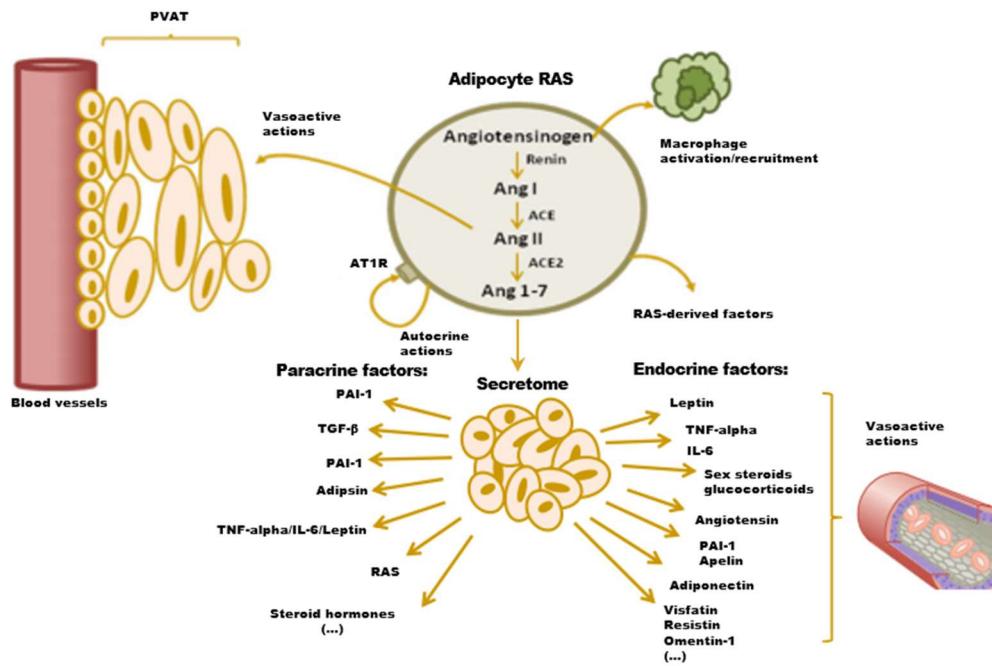
Figure 1.4 – Adipose tissue-derived vasoactive factors

Adipokines and other factors with vasoactive actions, which are secreted by adipose tissue. IL-6 - interleukin-6; PAI-1 - plasminogen activator inhibitor type 1; TGF-β - transforming growth factor-β; TNF-α - tumor necrosis factor-α; Ang I/II - angiotensin I/II; Ang1-7 - angiotensin 1-7; ACE - angiotensin converting enzyme; ACE2 - angiotensin converting enzyme 2; AT1R - AngI/II angiotensin type 1 receptor; RAS - renin-angiotensin system; PVAT - perivascular AT. Adapted from Agabiti-Rosei et al., 2018.

1.2 Impaired adipose tissue expandability

Adipocyte hypertrophy and inflammation

During AT expansion, adipocyte differentiation favours tissue hyperplasia and angiogenesis, allowing a regular oxygenation. However, if adipocytes become more hypertrophic, existent capillaries suffer remodelling and dilation to increase blood supply. Thus, expansion or retraction of the AT microvasculature is permanently required following adipocyte alterations. Indeed, this plasticity is particularly important after adiposity changes, in order to prevent the development of hypoxic regions (Christiaens and Lijnen, 2010; Mannerås-Holm and Krook, 2012; Pellegrinelli et al., 2016; Rodrigues et al., 2013a; Rutkowski et al., 2009).

Excessive nutritional fluxes in adipose tissue may lead to adipocyte hyperplasia and/or hypertrophy. Hyperplasia is typically associated with decreased metabolic dysregulation as it allows a better vascularization and oxygenation. Hypertrophy, in turn, may result from impaired adipogenesis. The adipocytes continually accumulate TGs in lipid droplets, that may lead to exacerbated cell hypertrophy and accumulation of secondary products of lipid metabolism, such as diacylglycerols and ceramides, leading to local inflammation (Figure 1.5), and therefore insulin resistance and lipolysis, which are mutually potentiated (Ghaben and Scherer, 2019; Guilherme et al., 2008; Gustafson et al., 2009; Qatanani and Lazar, 2007; Reilly and Saltiel, 2017; Tilg and Moschen, 2006).

a) Normal adipocyte from a lean subject

b) Hipertrofic adipocyte from an obese subject
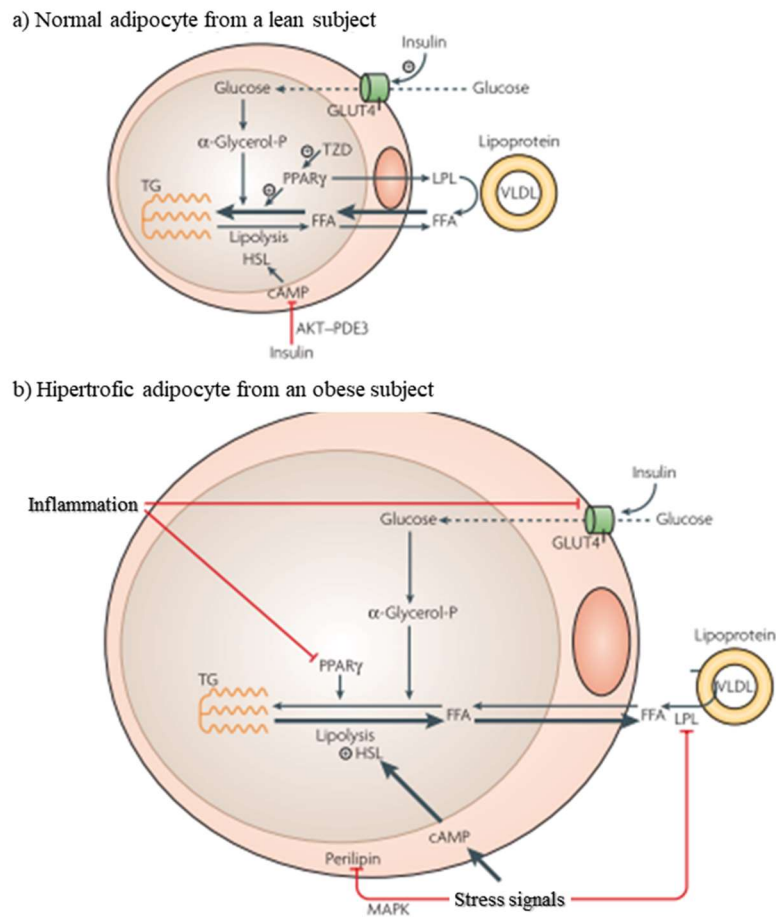
Figure 1.5 – Insulin signalling and inflammation effects in normal and hypertrophic adipocytes.

The schematic figure shows adipocyte insulin signalling: glucose and FFA uptake used in triglycerides esterification and inhibition of lipolysis. On the other hand, AT inflammation leads to insulin resistance and decreased esterification through PPAR-γ actions and ultimately, increased lipolysis and FFA release. TZD - tiazolidinediones; HSL - hormone-sensitive lipase; cAMP - cyclic adenosine monophosphate; FFA - free fatty acids; TG - triglyceride; LPL - lipoprotein lipase; VLDL - very low density lipoprotein; AKT - protein kinase b; GLUT4 - glucose transporter 4; MAPK - mitogen activated protein kinase; PPAR-γ - peroxisome proliferating-activated receptor- γ. Adapted from Guilherme et al. 2008.

The exacerbated accumulation of FFA in adipocyte cytoplasm (via diacylglycerol and ceramides formation) and in circulation (via toll-like receptor 4) directly inhibit insulin signalling through NF-κB-dependent mechanisms. Despite the fact that inhibition of substrate uptake by inflammatory mechanisms represent a physiological response aiming to decrease adipocyte hypertrophy, long-term signalling leads to increased glucose and lipid dysmetabolism and chronic insulin resistance (Guilherme et al., 2008; Qatanani and Lazar, 2007; Reilly and Saltiel, 2017; Tilg and Moschen, 2006).

The activation of inflammatory mechanisms completely changes AT secretome, impairing adipokines expression and favouring the secretion of pro-inflammatory factors, including TNF-α, IL-6, MCP-1, VEGF, leptin and resistin, while decreasing adiponectin secretion. Besides, changing adipocyte metabolism and secretome, these products also influence tissue vascularization, and angiogenesis and leukocyte recruitment (increasing pro-inflammatory M1 macrophages), causing a positive inflammatory feedback in the tissue (Blüher and Mantzoros, 2015; Corvera and Gealekman, 2014b; Ghaben and Scherer, 2019; Guilherme et al., 2008; Reilly and Saltiel, 2017; Rutkowski et al., 2015; Tilg and Moschen, 2006; Vázquez-Vela et al., 2008; Wellen and Hotamisligil, 2005). In fact, these inflammatory mechanisms worsened in obesity and prolonged in time are responsible for increased circulating FFA, which may accumulate ectopically, causing lipotoxicity in muscle and liver. Chronically, this may cause functional and structural lesions in such tissues and may conduct to systemic insulin resistance and ultimately to type 2 diabetes development (Boden et al., 2005; Czech et al., 2013; Guilherme et al., 2008; Kaneto et al., 2010; Scherer, 2018).

Activation of inflammatory pathways originates increased AT fibrosis (Buechler et al., 2015; Pellegrinelli et al., 2016). Decreased M2 and increased M1 macrophage levels in AT, leads to a pro-inflammatory environment associated with extra cellular matrix (ECM) alterations, causing excessive deposition of fibrotic material. Chronically, M1 macrophages, in addition

to hypoxia-inducible transcription factor-1alpha (HIF-1alpha) and TGF-β pathways activation, initiates profibrotic mechanisms, inhibits PPAR-γ–mediated adipogenesis and increases vessel rigidity, being associated with decreased vascular and tissue plasticity contributing to impaired AT expandability and functionality (Ghaben and Scherer, 2019; Halberg et al., 2009; Rutkowski et al., 2009; Tran et al., 2012).

Impaired adipose tissue angiogenesis

As noted above, healthy AT expansion critically depends of angiogenesis and a highly dynamic vasculature. There are AT anatomical locations as well as depot-specific angiogenic mechanisms. Angiogenesis is a highly dynamic and complex process involved in AT adaptation to hypoxia, namely during AT expansion (AT may reach 40% of body composition in obese patients) (Cao, 2013; Gealekman et al., 2011; Mannerås-Holm and Krook, 2012; Reilly and Saltiel, 2017; Rutkowski et al., 2009).

In adulthood, new capillary growth from pre-existing vasculature involves vascular EC proliferation and migration, matrix remodelling, intercellular junctions/communication, formation of lumen, anastomosis with other blood vessels, organization of perivascular supporting cells and blood circulation. This complex process of fully functional blood vessel is highly regulated by several factors, including VEGF, angiopoietins-1/-2 (ANG-1 and ANG-2), matrix metalloproteinases (MMP), adipokines and other growth factors. ECs are highly plastic cells, that may be in a long-term quiescent state or underwent rapid proliferation by hypoxia/growth factors stimulation (De Bock et al., 2013; Corvera and Gealekman, 2014a; Lijnen, 2008; Rodrigues et al., 2013a).

In response to angiogenic stimulus, endothelial tip cells (characterized by filopodia and VEGF sensing capacity) have higher levels of vascular endothelial growth factor receptor 2

(VEGFR2) and delta-like 4 (ligand for Notch), allowing navigation towards VEGF gradient, induction of stalk phenotype in adjacent ECs and sprout formation. Endothelial stalk cells elongate the branch by proliferating after tip cells, being highly regulated by Notch, VEGF/VEGFR2 and other signalling clues. VEGF is the only angiogenic factor specific for ECs, stimulating its proliferation (increased CD31, EC marker) and migration, and the expression of proteolytic enzymes and blood vessels formation, being considered one of the most potent drivers for AT angiogenesis (De Bock et al., 2013; Cao, 2013; Corvera and Gealekman, 2014a; Vona-Davis and Rose, 2009).

Although several VEGF isoforms are involved in AT angiogenic process, most of VEGF actions in AT are dose-dependent and mediated by VEGF-A (Christiaens and Lijnen, 2010; Neels et al., 2004). VEGF-A introduced in BAT restores capillary rarefaction, tissue dysfunction and lipid and glucose homeostasis in mice challenged by a high-fat diet, suggesting a beneficial role of VEGF-A in healthy BAT (Sun et al., 2014). More recently, Robciuc and collaborators, demonstrated that increased VEGF-B overexpression in adipose tissue leads to enhanced activation of VEGFR2 by VEGF-A (increased bioavailability), which leads to improved AT angiogenesis, metabolic health and insulin sensitivity (Rafii and Carmeliet, 2016; Robciuc et al., 2016). VEGF, in AT, is mainly produced and released by stromal cells and mature adipocytes since the first embryonic stage, being the paracrine action crucial in the adjacent cells/capillaries (Christiaens and Lijnen, 2010; Neels et al., 2004). During tissue expansion, VEGF is also produced by recruited inflammatory cells, namely monocyte-derived macrophage. In fact, VEGFR2 blockage inhibits angiogenesis and preadipocyte proliferation, suggesting VEGF-mediated preadipocyte differentiation (Cao, 2007, 2013; Hausman and Richardson, 2004; Tam et al., 2009). In accordance, transgenic mice with VEGF overexpression in (brown/white) AT have shown increased protection against high-fat diet-induced hypoxia and inflammation (Elias et al., 2012).

However, animal models of obesity and obese patients have higher circulating VEGF levels, which have been decreased following weight loss (Gómez-Ambrosi et al., 2010). Indeed, contradictory reports may also be influenced by the different characteristics of the genetic models when compared to diet-induced obese models, as well as the stage of AT dysfunction and related mechanisms (Rodrigues et al., 2013a).

According to recent data, VEGF overexpression may be useful during AT expansion, allowing sustained angiogenesis and preventing local hypoxia and chronic activation of inflammatory pathways and ultimately, insulin resistance establishment (Elias et al., 2012; Rutkowski et al., 2015; Scherer, 2018). In contrast, VEGF inhibition may be useful in the context of pre-existing AT dysfunction, reducing exacerbated inflammation induced by the most pro-inflammatory and hypertrophic adipocytes (Sun et al., 2012). Nevertheless, VEGF-dependent mechanisms in AT dysfunction are still controversial and partly unknown.

Inflammation drives angiogenesis as well, being macrophage particularly active in VEGF and ANG-2 (Tie-2–dependent blood vessel remodelling) secretion and in the remodelling of the extracellular matrix (Carmeliet and Jain, 2011; Rodrigues et al., 2013a). AT resident leukocytes have shown highly pro-angiogenic actions through cytokines and growth factors release. Even in lean models, vascularization of AT was reduced after macrophage removal (Ye, 2008).

Although insulin and AMP-activated protein kinase (AMPK) may induce VEGF expression and angiogenesis, its main regulators are the HIFs (Treins et al., 2002; Vona-Davis and Rose, 2009; Ye, 2008). Indeed, data from our colleagues have shown that HIF-1α stabilization under hypoxic conditions may get compromised by hyperglycemia, contributing to different observations regarding VEGF expression in experimental models of obesity and type 2 diabetes (Bento et al., 2010b, 2010c).

Angiopoietin-1 (ANG-1) and angiopoietin-2 (ANG-2) have opposite effects on blood vessel stabilization. ANG-1 increases vessel stability and interaction of endothelial cells with supporting cells (pericytes and smooth muscle cells) and extracellular matrix. ANG-1 also triggers TGF-β expression and structural proteins, such as integrins, fibrin and vitronectin (Hausman and Richardson, 2004; Hemmeryckx et al., 2010; Lijnen, 2008). Conversely, ANG-2 expression is mainly stimulated during vascular remodelling, namely under hypoxic conditions, being its receptors commonly co-localized with VEGF receptors (Bento et al., 2010b; Hausman and Richardson, 2004). ANG-2 is essential for vessel remodelling and growth, given the fact that it turns cell interactions weaker, allowing VEGF-induced EC proliferation, migration and reorganization. Nevertheless, VEGF signalling blockage following ANG-2-induced cell destabilization may originate vessel dysfunction (Bento et al., 2010b; Hausman and Richardson, 2004).

Regarding TGF-β, it is further produced by adipocytes and stromal cells under hypoxic conditions, regulating the deposition of extracellular matrix and leading to vessel stabilization (Halberg et al., 2009). Chronically, hypoxia and inflammation lead to TGF-β-mediated fibrosis, which is a feature commonly observed in dysfunctional AT from obese individuals. Consequently, increased fibrosis originates a progressive decline in tissue and blood vessels plasticity, being a known characteristic related to impaired AT expandability and function (Christiaens and Lijnen, 2010; Hausman and Richardson, 2004; Ye, 2008).

Considering adipokine-mediated AT angiogenesis, most of the known pro and anti-angiogenic factors are produced by many of the cells present in AT, being particularly active through endocrine and paracrine actions and may become dysregulated by adipose tissue dysfunction during obesity. Firstly, *in vitro* studies demonstrated a strong angiogenic role of leptin by acting in endothelial cell receptors, promoting proliferation/migration and ECs survival through the inhibition of apoptosis (Cao, 2007; Christiaens and Lijnen, 2010;

Hausman and Richardson, 2004; Lijnen, 2008). In fact, leptin increases VEGF and MMP production, what may explain ECs effects and blood vessel growth/remodelling as well as the formation of fenestrated capillaries (Cao, 2013; Lijnen, 2008). In turn, adiponectin has been primarily suggested as an anti-angiogenic adipokine involved in pro-apoptotic mechanisms in ECs and ultimately, balancing the angiogenic effects of leptin. (Cao, 2013; Vona-Davis and Rose, 2009). In contrast, several authors have shown adiponectin-mediated increase of AT angiogenesis and endothelial progenitor cells (Adya et al., 2012; Shibata et al., 2008). Future studies are required, to clarify the effects of these adipokines and the involvement of other adipose tissue factors.

Adipose tissue hypoxia and microvascular dysfunction

As discussed earlier, AT dysfunction is related to decrease adipogenesis and to impaired angiogenesis. In the past, it was hypothesized that the hypertrophic adipocytes volume may become higher than the oxygen diffusion distance, leading to local hypoxia (Hosogai et al., 2007; Trayhurn, 2013; Trayhurn et al., 2008a). However, Goossens and collaborators showed a reduced number of adipocytes bigger than the oxygen diffusion distance in human obese AT (Goossens, 2008; Goossens and Blaak, 2015; Goossens et al., 2011). Consequently, future studies are required to fully describe the mechanisms regarding adipocyte oxygen consumption and AT hypoxia in obesity.

In line with previous findings, hypoxic regions observed in AT from obese patients might be caused by impaired tissue blood flow, capillarization or oxygenation (Figure 1.6) (Corvera and Gealekman, 2014a; Gealekman et al., 2004, 2011; Matafome et al., 2015; Rodrigues et al., 2013c; Scherer, 2018).
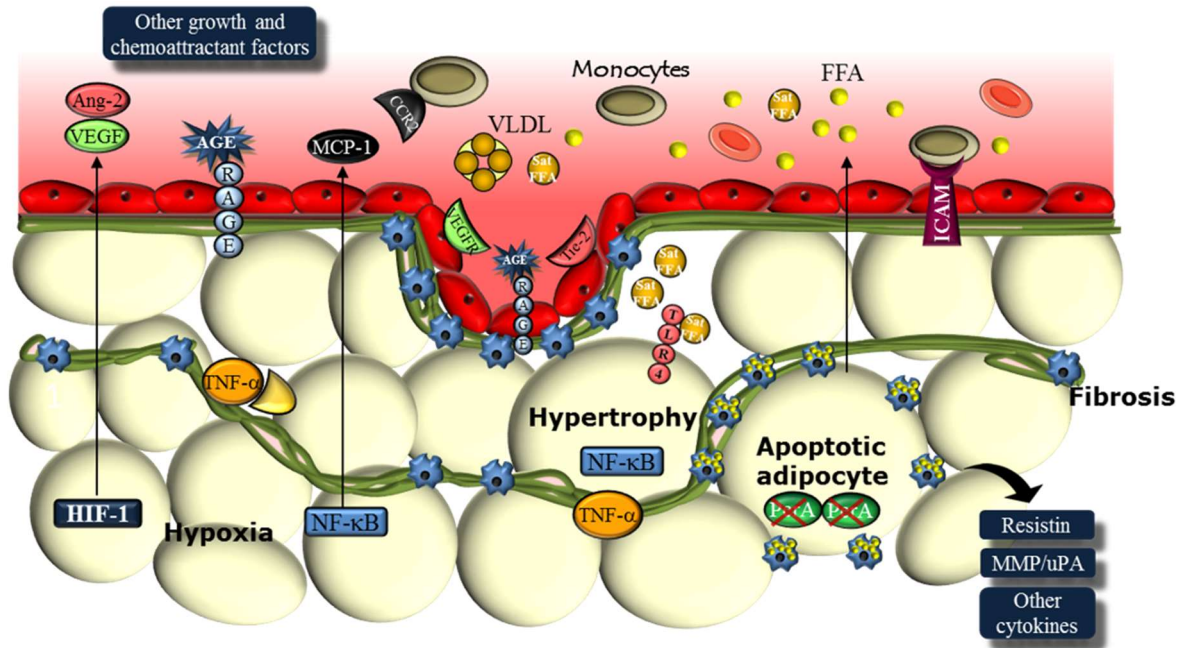
Figure 1.6 – Events occuring in adipose tissue under sustained hypoxia

Adipose tissue undergoing an inappropriate growth of the vascular network during tissue expansion leads to increased hypoxia. Besides, adipocyte hypertrophy and decreased plasticity (increased fibrosis) leads to impaired adaptation to hypoxia, and consequently, activation of inflammatory pathways, adipocyte death and macrophage recruitment. Overall, adipose tissue function and metabolic homeostasis are disturbed, contributing to exacerbated insulin resistance and ectopic fat deposition as well as to higher risk of type 2 diabetes development. Ang-2 - angiopoietin-2; CCR2 - cytokines receptor; FFA - free fatty acids; FFA-Sat - saturated free fatty acids; HIF-1 - hypoxia inducible factor-1; ICAM - intercellular adhesion molecule; NF-κB - nuclear factor kappa b; MCP-1 - monocyte chemo-attractant protein-1; MMPs - matrix metalloproteinases; PerA - perilipin-A; Tie-2 - angiopoietins receptor; TLR4 - toll-like receptor 4; TNF-α – tumour necrosis factor alpha; uPA - plasminogen activator urokinase-type; VEGF - vascular endothelial growth factor; VEGFR - VEGF receptor; VLDL - very-low density lipoprotein.

In the last years, several studies have shown increased hypoxia in the AT of genetic and diet-induced obese animal models. Several experimental approaches showed higher accumulation of a hypoxia probe (pimonidazole) and lactate production (endogenous marker of hypoxia) as well as decreased endothelial cell markers and blood supply (Frayn and Karpe, 2013; Hosogai et al., 2007; Matafome et al., 2015; Rodrigues et al., 2013a; Trayhurn, 2013; Ye et al., 2007).

Under physiologic conditions, HIFs (constituted by oxygen-sensitive - α and oxygen-insensitive - β subunits) are hydroxylated in proline residues using oxygen as substrate by prolyl hydroxylases, which leads to constant ubiquitination and degradation by proteasome. Thus, HIFs half-life is really short, being constantly produced and rapidly degraded under normoxic conditions (Bento and Pereira, 2011; García-Martín et al., 2016; Semenza, 2004). However, during hypoxia the lack of oxygen inhibits proline-hydroxilases, leading to HIFs stabilization/activation and HIF-dependent upregulation of several genes involved in cell survival and adaptation to hypoxic conditions (García-Martín et al., 2016; Semenza, 2004; Wood et al., 2009). These genes are involved in angiogenesis and vasoactive function, including VEGF, angiopoietins (ANG-1 and ANG-2), angiopoietin-like 4 (ANGPTL-4), MMPs, leptin and plasminogen activators. Moreover, anaerobic conditions are favoured by genes responsible for the metabolic shift, increasing glycolysis pathway (Yamakawa et al., 2003; Cao, 2007; Hosogai et al., 2007; Ye, 2009; Christiaens and Lijnen., 2010; Goossens et al., 2011). Hypoxia response is mainly done by HIF-1 and HIF-2 transcription factors, being HIF-1alpha considered pro-inflammatory through macrophage M1-dependent mechanisms, while HIF-2alpha is associated with decreased inflammation (macrophage M2) as well as healthy AT and increased insulin sensitivity (Aouadi, 2014; Choe et al., 2014; García-Martín et al., 2016).

In line with these findings, chronic hypoxia activation leads to sustained activation of AT stress/inflammatory pathways (protein kinase C - PKC, NF-κB, C-jun n-terminal kinase/Stress-activated protein kinase - JNK) and secretome alterations (increased circulating levels of TNF-α, MCP-1, IL-6, MMPs), which are commonly associated with diminished AT nutrient uptake and insulin sensitivity, contributing to exacerbated lipolysis and ectopic fat deposition (Glassford et al., 2007; Guilherme et al., 2008; Halberg et al., 2009; He et al., 2011; Trayhurn et al., 2008b; Ye, 2008). Inflammatory pathways impair insulin signalling, given the fact that serine kinases negatively phosphorylate the insulin receptor and its substrate, which are normally activated by phosphorylation in tyrosine residues (Czech, 2017; Guilherme et al., 2008; Wellen and Hotamisligil, 2005). Besides metabolic alterations, hypoxia-induced inflammation also has a major impact on the secretory profile of AT from obese mice and culture human adipocytes, including decreased PPAR-γ-mediated downregulation of adiponectin production, which leads to diminished anti-inflammatory and insulin sensitizer effects (Hosogai et al., 2007; Wang and Scherer, 2016; Wang et al., 2007). In contrast, other adipokines and factors like leptin, resistin, visfatin, MCP-1, migration inhibitory factor, TNF-α and VEGF are highly increased by prolonged hypoxia, contributing to exacerbated inflammation, angiogenesis and insulin resistance (Juge-Aubry et al., 2005; Maury and Brichard, 2010; Scherer, 2006, 2018; Tilg and Moschen, 2006).

Regarding increased AT hypoxic regions during tissue expansion, it has been demonstrated the consequent activation of inflammatory and other response pathways (HIF-1alpha/HIF-2alpha-dependent regulation of macrophage M1/M2 phenotype), causing significant secretome changes, progressive metabolic decline, insulin resistance and impaired lipid handling/storage, which represent known triggers to AT dysfunction, unhealthy metabolically obesity and type 2 diabetes development (Figure 1.7) (Aouadi, 2014;

Guilherme et al., 2008; Iacobini et al., 2018; Matafome et al., 2015; Rodrigues et al., 2013a; Rutkowski et al., 2015; Scherer, 2016; Tilg and Moschen, 2006; Ye et al., 2007). Future studies are required to describe the mechanisms involved as well as possible therapeutic approaches aiming to protect AT from prolonged hypoxia.
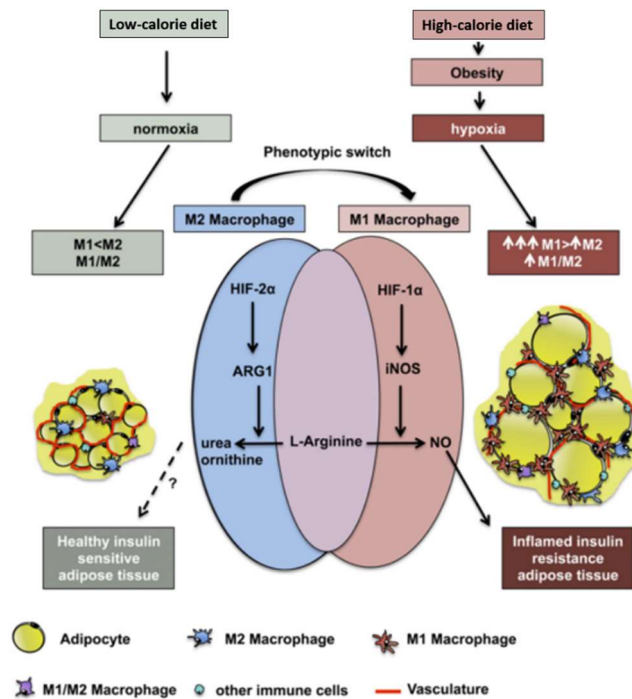
Figure 1.7 - Hypoxia-derived mechanisms in macrophage phenotype during diet-induced AT expansion
The representative figure shows an hypothetical model for HIF-1alpha/HIF-2alpha effects on macrophage inflammatory phenotype during increased AT expansion and insulin resistance. High-calorie diets are commonly associated with impaired AT expandability and increased hypoxia, being hypoxia-inducible factors responsible for AT adaptation to hypoxia and macrophage M1/M2 phenotype. Consequently, HIF-2alpha may promote healthy AT by preventing inflammation and insulin resistance. HIF-1α – hypoxia-inducible factor 1 alpha; HIF-2 α - hypoxia-inducible factor 2 alpha; ARG1 - arginase 1; iNOS - inducible nitric oxide synthase; NO – nitric oxide. Adapted from Aouadi, 2014.

Adipose tissue microvascular dysfunction may precede many of the alterations observed in unhealthy AT during obesity, and thus it is not a secondary event in AT dysfunction. In this regard, limited capillarization was recently shown in AT explants from obese donors, potentially causing hypoxia. However, reduced AT blood flow was observed to be independent of obesity per se, and shown to be more associated with insulin resistance (Cao, 2013; Gealekman et al., 2012; Mannerås-Holm and Krook, 2012; Rodrigues et al., 2013a; Rutkowski et al., 2009). In obese patients and animal models, it was demonstrated a 30-40% reduction of AT blood flow, in part due to regression or dysfunction of the vascular network (Goossens, 2008; Ye, 2008). We have shown that even in normal rats, a partial reduction of blood supply in one single fat depot (left periepididymal adipose tissue) causes hyperinsulinemia forty eight hours after the surgery (Rodrigues et al., 2013b), suggesting that decreased AT blood flow may trigger important local and systemic metabolic alterations, contributing to insulin resistance and glucose dysmetabolism (Rodrigues et al., 2013a; Rutkowski et al., 2009).

Data from our and other laboratories propose that vasoactive and angiogenic factors may in fact, be negatively regulated by glycation, a process caused by reducing sugars. Even if not all the studies have been performed in AT, existing data supporting the idea that glycation potentiate the effects of vasoconstriction factors, while impairing AT angiogenesis. Consequently, these mechanisms may decrease AT blood flow and thus induce tissue hypoxia (Matafome et al., 2015; Rodrigues et al., 2013a).

In AT arterioles, decreased perfusion may be impaired by endothelium-dependent relaxation disability (Farb et al., 2012b; Georgescu et al., 2011). Indeed, blood pressure and regional blood flow may change in accordance to neural, endocrine and paracrine regulation of vascular tonus (Figure 1.8). Postprandial or physical exercise-derived stimulus may change microvascular perfusion through capillary recruitment in peripheral tissues such as skeletal

muscle and AT (Boydens et al., 2012; Dimitriadis et al., 2007; Karpe et al., 2002). In agreement, in lean insulin-sensitive subjects, postprandial visceral AT blood flow may increase by 2-4 times. However, in insulin resistant obese and type 2 diabetic patients, postprandial insulin-mediated vasodilatation and delivery of substrates to peripheral tissues may become impaired, decreasing lipid handling and AT oxygenation (Frayn and Karpe, 2013; Karpe et al., 2002; Lambadiari et al., 2015).

Besides, sympathetic nervous system affects blood pressure and AT vasculature, being tightly associated with AT metabolic processes. Thus, α2-adrenergic stimulus is associated with vasoconstriction during fasting states. In contrast, vasodilatation is promoted by β2-adrenergic stimulation. Sympathetic coordination of AT blood flow may be associated with other vasoactive factors, namely in fasting and physical exercise states (Figure 1.8) (Galitzky et al., 1993; Sotornik et al., 2012; Villela et al., 2009).
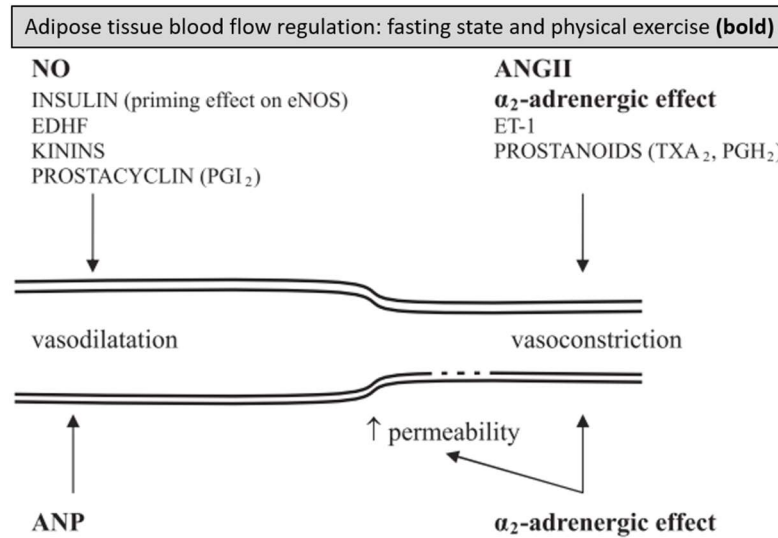
Figure 1.8 – Adipose tissue blood flow regulation during fasting and physical exercise

The representative figure shows vasoactive factors involved in AT blood flow regulation, being fasting and physical exercise-derived hypothetic mechanisms shown. ANGII - angiotensin II; ANP - atrial natriuretic peptide; EDHF - endothelium-derived hyperpolarizing factor; eNOS - endothelial nitric oxide synthase; ET-1 - endothelin-1; PGH2 - prostaglandin H2; PGI2 - prostaglandin I2/prostacyclin; TXA2 - thromboxan A2. Adapted from Sotornik et all., 2012.

Adipose tissue dysfunction and clinical outcome

The chronic activation of inflammatory pathways and impaired AT expandability may lead to adipose tissue dysfunction, metabolic dysregulation and insulin resistance in obesity and type 2 diabetes (Figure 1.9). Adipose tissue seems to be pivotal in the clinical outcome, given its contribution to insulin resistance and glucose and lipid dysmetabolism as well as the autocrine, paracrine and endocrine impact of adipokines. Indeed, AT dysregulation may be highly associated with the development and progression of several disorders among others type 2 diabetes, hepatic and cardiovascular diseases, and even some types of cancer, due to the impairment of local and systemic dysmetabolism (Figure 1.10) (Galic et al., 2010; Guilherme et al., 2008; Hocking et al., 2010; Maury and Brichard, 2010; Rutkowski et al., 2015; Scherer, 2016, 2018; Tilg and Moschen, 2006). Although several underlying

mechanisms remain to be addressed, such evidences suggest the modulation of AT angiogenesis and blood flow as potential targets in improving insulin sensitivity (Kusminski et al., 2016; Mannerås-Holm and Krook, 2012; Reilly and Saltiel, 2017; Scherer, 2018).
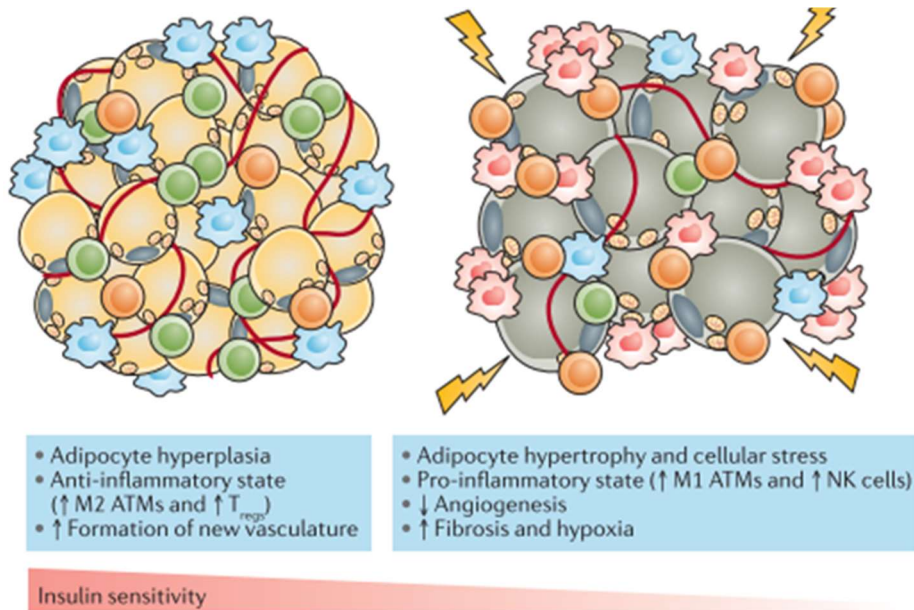
Figure 1.9 - Healthy and unhealthy adipose tissue expandability

The schematic figure represents AT features during healthy and unhealthy conditions. Adipocyte hiperplasia is associated with better AT function, angiogenesis, oxigenation, controlled inflammation and ultimatly, higher insulin sensitivity. On the oher hand, hypertrofic adipocytes are associated with higher insulin resistance caused by stress and inflammatory pathways activation, decreased angiogenesis and increased hypoxia and fibrosis. M1/M2 ATMs, light blue cells - M1/M2 AT macrophage; T_{regs}, green cells - regulatory T cells; NK, orange cells - natural killer cells. Adapted from Kusminski *et al*. 2016.
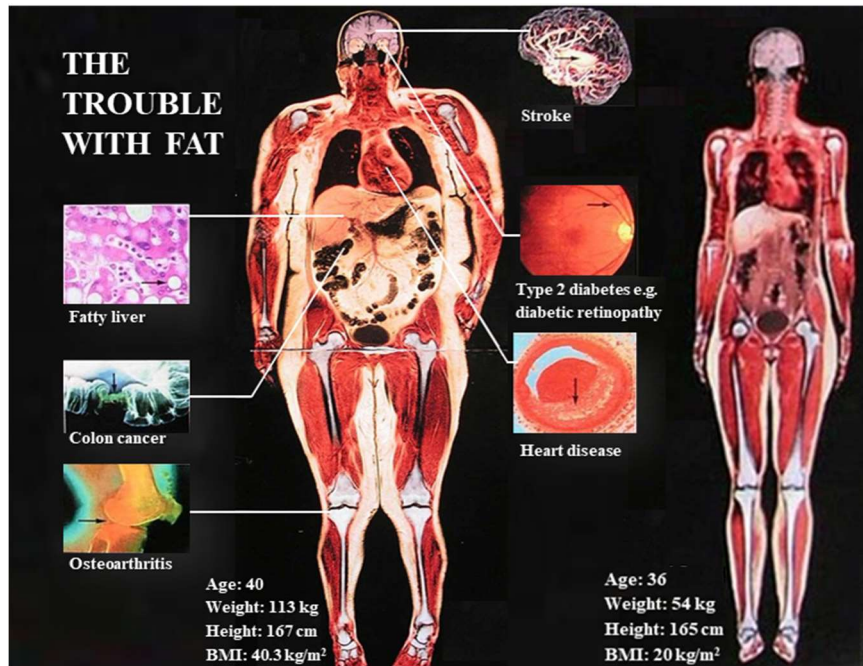
Figure 1.10 - The trouble with fat and obesity-related diseases

The magnetic resonance imaging image shows fat amount and distribution in two female patients with body mass index (BMI) of 40.3 kg/m^2 and 20 kg/m^2. Addictionally, common obesity-related diseases are described Adapted from dietdatabase.com/obesity-facts, 2016.

2. Glycation in biological systems

2.1 MG-induced glycation

Glycation and vascular effects

Non-enzymatic glycosylation (terminology frequently applied to food alterations), also named glycation (endogenous effects), was firstly described by Louis-Camille Maillard, in the XX century (Maillard, 1912). Briefly, this reaction occurs spontaneously between reducing sugars (glucose, fructose and others) and amino residues in proteins, lipids and nucleic acids (Brownlee, 2005; Goldin et al., 2006; Negre-Salvayre et al., 2009; Rabbani and Thornalley, 2011).

During evolution, organisms have developed endogenous protective mechanisms against reductive sugar-derived damage. Firstly, the predominant use of glucose in biological systems, which is the least reactive sugar when compared to other sugars with more reducing activity. Secondly, cells store most of sugars in non-reactive forms, such as glycogen, profoundly reducing metabolic intermediates such as fructose and methylglyoxal (MG) as well as advanced glycation end products (AGE) formation and derived effects (Rabbani and Thornalley, 2015; Wang and Chang, 2010).

Endogenous glycation changes physical and chemical properties of biomolecules, leading to impaired biological function, in a sequential process through reactions and molecular rearrangements, which originate schiff bases, amadori products and ultimately AGE (Goldin et al., 2006; Negre-Salvayre et al., 2009). Additionally, AGE may be also formed from glucose metabolism-derived intermediary products such as gliceraldehyde-3-phosphate, dihydroxyacetone-phosphate and MG. In fact, MG is a well-known and strong precursor of AGE, and its levels are elevated in prediabetes and type 2 diabetic patients as well as in

sugar-rich foods prepared at high-temperatures (Desai et al., 2010; Matafome et al., 2013, 2015, 2017b; Negre-Salvayre et al., 2009).

MG is one of the key drivers of glycation and was firstly identified as a key intermediate of glucose metabolism in animals, plants and microorganisms (Dakin and Dudley, 1913; Neuberg, 1913). MG is a highly reactive dicarbonyl aldehyde produced directly from fructose (through aldolase B catalyzation) and aminoacetone (through semicarbazide-sensitive amine oxidase catalyzation) as well as from glyceraldeyde-3-P (G3P), during glycolysis and glycerogenesis (glycerol production during triglyceride synthesis), which are exacerbated in obesity and type 2 diabetes (Brownlee, 2001, 2005; Chan et al., 2007; Liu et al., 2011a; Masania et al., 2016a). Moreover, fructose administration in experimental models demonstrated increased MG formation while aldolase B knockout prevents MG formation from fructose (Liu et al., 2011a).

Regarding MG reactivity in biological systems, it is able to react with DNA, lipids and proteins (mainly through arginine, lysine and cysteine residues) producing a broad range of AGE. MG interaction with lysine residues leads to the formation of 6-{1-[(5S)-5-ammonio-6-oxido-6-oxohexyl]- 4-methyl- imidazolium-3-yl}-L-norleucine) (MOLD) and N-epsilon (carboxyethyl)lysine (CEL), whereas through argine modifications originate N_δ-(5-hydro-5-methyl-4-imidazolon-2-yl)- L-ornithine (MG-H1) and argpyrimidine, from the imidazolones family (Figure 1.11) (Ahmed et al., 1997; Falone et al., 2012; Goldin et al., 2006; Kim et al., 2012b; Maessen et al., 2015; Nagaraj et al., 2012; Rabbani and Thornalley, 2008; Xue et al., 2011b).
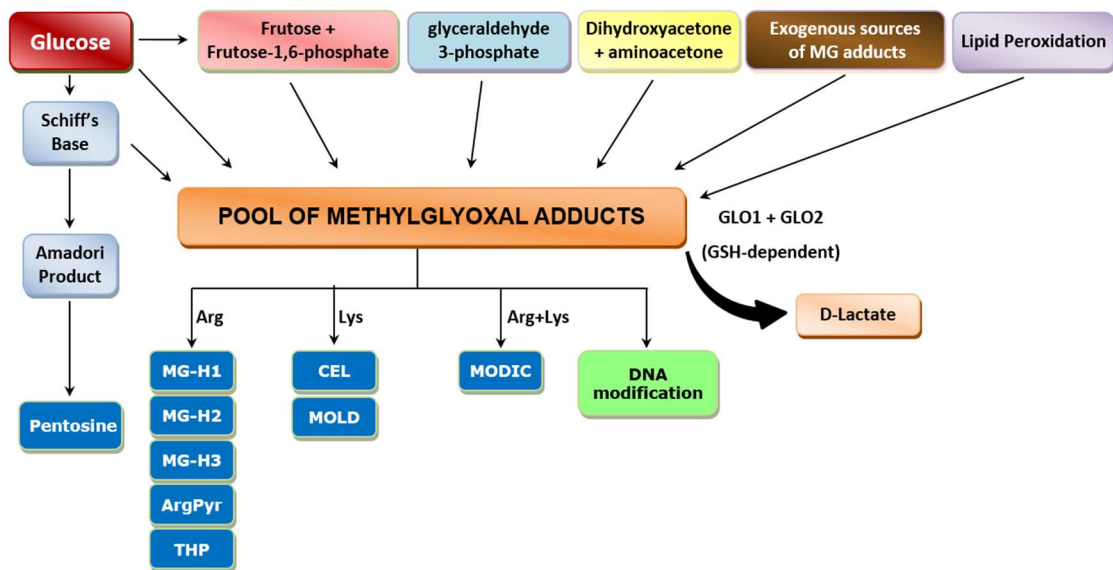
Figure 1.11 – Sources of MG and AGE formation

Glycolysis is the most important source of MG. MG is formed from several intermediary products and from auto-oxidation of glucose. Other sources of MG are fructose, lipid peroxidation and dietary glycotoxins. MG accumulation through impaired glyoxalase system, leads to MG-induced adducts, such as: arginine residues to form the AGE, MG-H1, MG-H2, MGH3, argpyrimidine, and THP; lysine to form CEL and the lysine dimer MOLD. MG crosslink with arginine and lysine produces MODIC. AGE - advanced glycation end products; Arg - arginine; ArgPyr - argpyrimidine; CEL - N-epsilon (carboxyethyl)lysine; Lys - lysine; MG - methylglyoxal; MG-H1 - N δ -(5-methyl- 4-imidazolon-2-yl)-L-ornithine; MG-H2 - 2-amino-5-(2-amino-5-hydro-5-methyl-4-imidazolon-1-yl)pentanoic acid; MG-H3 - 2-amino-5-(2-amino-4-hydro-4-methyl-5-imidazolon-1 -yl)pentanoic acid; MODIC - 2-ammonio-6-({2 – [4- ammonio-5-oxido-5-oxopently)amino]-4-methyl-4,5-dihydro-1H-imidazol-5-ylidene}amino)hexanoate); MOLD - 6-{1-[(5S)-5-ammonio-6-oxido-6-oxohexyl]- 4-methyl- imidazolium-3-yl}-L-norleucine); THP - Nδ-(4-carboxy-4,6- dimethyl-5,6-dihydroxy-1,4,5,6-tetrahydropyrimidine-2-yl)-L-ornithine); GLO-1 - glyoxalase-1; GLO-2 - glyoxalase-2; GSH - reduced glutathione.

Important biological effects of MG, namely in what concerns to diabetic microvascular complications, are likely to derive from its increased endogenous production, caused by exacerbated intracellular glucose levels. In type 2 diabetes, chronic hyperglycemia selectively damage cells, such as endothelial cells and mesangial cells, because glucose transport rate does not decline rapidly, leading to sustained intracellular high glucose levels and ultimately, microvascular complications (Brownlee, 2001, 2005; Goldin et al., 2006; Negre-Salvayre et al., 2009). In addition, although dietary MG and AGE-modified peptides, commonly known as glycotoxins, are partially absorbed from the diet and are mostly excreted in urine, it is thought that they may interfere with biological systems through a progressive accumulation, causing cell and tissue dysfunction and early aging-dependent mechanisms (Goldin et al., 2006; Leung et al., 2014; Matafome et al., 2015; Negre-Salvayre et al., 2009; Poulsen et al., 2014; Vlassara and Striker, 2013). This may be particularly important in patients who have impaired kidney function and therefore, a limited ability to excrete these harmful products in urine, contributing to increased damage and ultimately nephropathy development and progression (Adolphe et al., 2012; Negre-Salvayre et al., 2009; Rabbani and Thornalley, 2014a, 2015; Schalkwijk, 2015).

MG is found in several natural products, including honey, which has also high levels of antioxidants, but mostly in processed alimentary products such as commercial beverages (Kalapos, 2013; Nemet et al., 2006; Tan et al., 2008; Wang and Chang, 2010). Furthermore, different MG concentrations were found in high-fructose corn syrup, milk, coffee and cheese from different producers (Ahmed et al., 2005; Gensberger et al., 2013; Spanneberg et al., 2012; Tan et al., 2008). Altogether, there is growing evidence that many alimentary products are very rich in highly reactive dicarbonyls, such as MG, which leads to increased AGE. However, the effects of a prolonged exposure to dietary MG and AGE are still partially unknown. In addition, previous studies implicated the cooking method, time of storage and

foods having high glycemic index, in the amount of dietary MG generated and possibly absorbed (Maessen et al., 2015; Nemet et al., 2006; Vlassara and Striker, 2013).

Despite the fact that exogenous AGE have long been described as insignificant contributors to diseases, recent studies have shown that they may potentiate the negative effects from endogenous AGE (Maessen et al., 2015; Uribarri and He, 2015; Uribarri et al., 2015a; Vlassara and Striker, 2013). In accordance, chronic MG infusion (60 mg/kg/day subcutaneous minipump during 28 days) to healthy Sprague-Dawley rats resulted in impaired AT insulin signalling and glucose tolerance (Dhar et al., 2011). MG administration in a stepwise manner (i.p. 5 days/week, 50-75 mg/kg during 7 consecutive weeks) to normal Wistar rats, induced diabetes-like microvascular changes such as, loss of ECs, ECM thickening, increased AGE receptor (RAGE) mediated inflammation and TGF-β production, namely in glomerular tufts and tubular epithelial cells (Berlanga et al., 2005).

Our group developed a rat model with prolonged oral MG administration (diluted in the daily water, 50-75 mg/kg/day during 14 weeks) to Wistar rats, that resulted in tissue and plasma MG concentrations similar to non-obese type 2 diabetic Goto-Kakizaki (GK) rats. This MG-induced model of AT glycation did not present insulin resistance but showed several AT structural and functional alterations. In fact, we observed increased markers of AT dysfunction (inflammation, fibrosis and VEGF/ANG-2 ratio), suggesting MG-induced effects on AT microvasculature (angiogenesis/blood flow regulation) and impaired adaptation to local hypoxia (Matafome et al., 2012).

Fructose, a known reducing sugar, when supplemented (fructose-enriched diet during 9 weeks) to Sprague-Dawley rats, leads to decreased activation of insulin pathway in AT, suggesting that exogenous ingestion of reducing sugars may, in fact, impairs AT metabolism (Jia and Wu, 2007). Besides, in a study of Hofmann et al., the consumption of AGE- (N-carboxymethyl- lysine - CML) and MG-enriched diets (supraphysiological MG doses)

caused insulin resistance and glucose intolerance, nonetheless only in diabetic *db/db* mice, showing slightly effects on normal mice (Hofmann et al., 2002).

Indeed, the major concern of the existing studies is the use of MG/AGE exacerbated doses in normal rats, for instance using intraperitoneal injections, and to the best of our knowledge, few studies compare the effects on biological systems with similar endogenous levels observed in a phenotypic diabetic model (Berner et al., 2012; Brownlee, 2001; Cantero et al., 2007; Gaens et al., 2014; Hofmann et al., 2002; Kim et al., 2012b; Maessen et al., 2015; Masterjohn et al., 2013a; Matafome et al., 2015; Schalkwijk, 2015; Sena et al., 2012; da Silva et al., 2017; Tikellis et al., 2014; Wang et al., 2015a).

Until the last years, AT microvascular dysfunction was thought to be a consequence of sustained hyperglycemia, as shown for common diabetic microvascular complications, including retinopathy or nephropathy. Nevertheless, AT dysfunction occurs since early stage of type 2 diabetes development, even before chronic hyperglycemia, being glycation a possible link (Guilherme et al., 2008; Rodrigues et al., 2013a; Rutkowski et al., 2015; Scherer, 2018). In agreement, our group showed that MG-induced AT microvascular lesions were time-dependent and partially restored by the dicarbonyl scavenger drug pyridoxamine. Altogether, these results suggest that progressive AGE accumulation in AT leads to early microvascular dysfunction (Rodrigues et al., 2013; Rutkowski et al., 2009).

In vitro, MG exposure leads to impaired insulin signalling (decreased p-AKT and p-extracellular signal–regulated kinase 1/2 - ERK1/2) in L6 muscle cells (Riboulet-Chavey et al., 2006), and insulin-stimulated insulin receptor activation (p-IR) and downstream effectors (p-PI3K and p-AKT) in the pancreatic β-cell line (INS-1E) (Fiory et al., 2011). Besides, MG-treated 3T3-L1 adipocytes have shown impaired insulin signalling, including diminished activated forms of IRS-1 and PI3K (Jia and Wu, 2007).

Several studies have also shown that MG-induced DNA-AGE interactions may contribute to the age-related decrease of genomic function. Furthermore, glycated lipid, including low-density lipoproteins (LDL) and very low-density lipoproteins (VLDL) represent a major concern, since their function may be changed. In fact, increased glycation during type 2 diabetes impairs LPL and VLDL degradation, contributing to hypertriglyceridemia, increased inflammation and oxidative stress (Baynes, 2002; Goldin et al., 2006; Matafome et al., 2012; Negre-Salvayre et al., 2009; Rabbani et al., 2014; Roberts et al., 2003; Tames et al., 1992).

Regarding AGE-induced effects on biological systems, they are mainly caused by MG crosslinks with biomolecules, including the change of protein structure/function and turnover, affecting circulating, intracellular and extracellular matrix proteins. Therefore, the most abundant plasmatic proteins, hemoglobin and albumin, are highly glycated. Despite the fact that glycated hemoglobin (HbA1c) is not directly formed from MG, represents a reliable marker for monitoring glycemic control in diabetic patients (Goldin et al., 2006; Negre-Salvayre et al., 2009; Rabbani and Thornalley, 2012; World Health Organization, 2011).

In ECM matrix, proteins such as collagen, vitronectin, laminin or elastin usually have a low turnover rate, being preferential targets for glycation. Consequently, glycated proteins have impaired cell attachment and function, causing dysfunction (Goldin et al., 2006; Negre-Salvayre et al., 2009; Rabbani and Thornalley, 2008). Thus, MG-induced glycation on intracellular proteins leads to changes in critical pathways, for instance those involved in cell response to hypoxia, contributing to HIF-1α stabilization even under regular oxygenation (Bento and Pereira, 2011). Besides, MG induces several alterations in cellular systems responsible for modified proteins degradation, namely via proteasome and lysosome-mediated degradation (Bento et al., 2010a; Padival et al., 2003).

As discussed above, AT expansion is associated with hypoxia, which represents a powerful trigger to induce angiogenesis. However, even using a relatively short period of MG administration in order to avoid its long-term effects, it was demonstrated that MG decreases angiogenesis and the ability of AT to adapt to a surgery-induced reduction of blood supply (Rodrigues et al., 2013b). More, in this animal model with MG-induced glycation, a partial decrease of blood supply caused a higher activation of inflammatory pathways and perilipin-A degradation, as well as decreased PPAR-γ tissue levels and adiponectinemia, suggesting adipocyte dysfunction (Rodrigues et al., 2013b).

A number of studies showed that diabetic patients and animal models commonly have impaired vascularization ability. This was described to be caused by hyperglycemia and specifically by AGE accumulation, given the fact that glyoxalase-1 (GLO-1) overexpression, the key limiting enzyme involved in MG degradation, restored hypoxia-induced VEGF expression (Bento and Pereira, 2011; Bento et al., 2010b; Brownlee, 2001, 2005).

On the other hand, AGE act in RAGE to trigger intracellular signals, for instance sustained activation of inflammatory pathways and TGF-β signalling, leading to fibrosis and higher deposition of glycated ECM. RAGE receptor recognizes two major types of ligands, CML adducts and imidazolones (MG-induced), causing NF-κB activation, which in turn, leads to increased RAGE levels, that may constitute a positive feedback loop (Brownlee, 2005; Goldin et al., 2006; Matafome et al., 2012, 2013; Negre-Salvayre et al., 2009; Xue et al., 2011a; Yan et al., 2003; Yao and Brownlee, 2010).

Additionally, exacerbated RAGE expression was seen in aorta, retina and kidney of diabetic patients, while in streptozotocin-induced diabetic rats, RAGE blocking diminished albuminuria and glomerular mesangial growth (Negre-Salvayre et al., 2009). RAGE silencing in apoE-/- mice results in decreased atheromas and adipocyte size as well as increased adiponectinemia (Ueno et al., 2010).

In line with previous findings, excessive RAGE activation induces GLO-1 downregulation, while RAGE knockdown is associated with decreased MG formation (Ramasamy et al., 2012; Yao and Brownlee, 2010). Furthermore, RAGE-mediated NF-κB activation is thought to be redox-dependent, as well as increasing protein kinase C, p21, ERK1/2, p38 and JNK activation. Consequently, NF-κB activates the expression of adhesion molecules, VEGF, cytokines, TNF-α and RAGE itself (Goldin et al., 2006; Hattori et al., 2001; Negre-Salvayre et al., 2009; Yao and Brownlee, 2010).

Regarding AGE sensing and clearance, there are specific receptors such as, R1, R2, R3 and circulating soluble RAGE form that may be involved. However, to the best of our knowledge, intracellular signalling was not described and they are likely to act mainly in AGE scavenging and detoxification, opposing or balancing RAGE effects (Cai et al., 2008, 2010; Goldin et al., 2006; Lu et al., 2004; Negre-Salvayre et al., 2009).

MG was shown to activate several stress pathways such as the mitogen-activated protein kinases JNK and p38 in osteoblasts, Jurkat leukemia cells and ECs in a redox-dependent manner (Chan et al., 2007; Yamawaki et al., 2008). Moreover, MG was also able to activate ERK1/2 by a mechanism independent of redox signalling in endothelial cells and fibroblasts (Akhand et al., 2001; Du et al., 2003). Although these findings suggest different mechanisms involved in MG-dependent actions, including extracellular and intracellular alterations, chronic alterations, dose-dependent changes and tissue specific alterations are in part unknown (Figure 1.12).
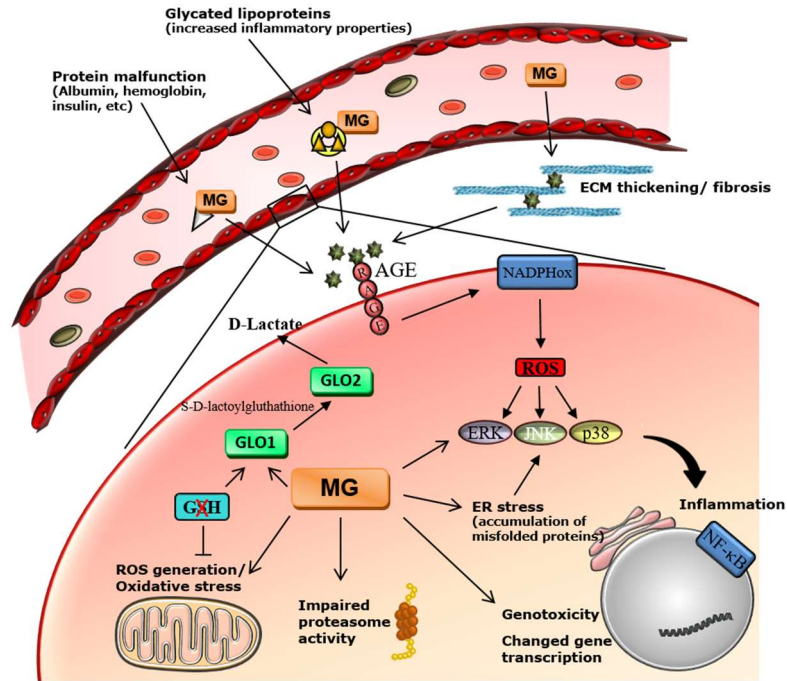
Figure 1.12 – MG-induced glycation: extracellular and intracellular mechanisms

Circulating MG reacts with several biomolecules (proteins and lipoproteins), leading to its impaired function. Glycated ECM changes collagen and other stuctural proteins, contributing to ECM thickening and exacerbated fibrosis. AGE-mediated RAGE activation triggers several intracellular stress and inflammatory pathways, causing exacerbated production of reactive oxygen species and misfolded proteins, which are associated with genotoxicity (chemical modification of DNA), ER stress, impaired proteasome activity and ultimately, cell dysfunction and death. Glyoxalase system is critical in MG control, but GSH depletion inhibiths GLO-1 activity, which is the key limiting enzyme in MG degradation. AGE – advanced glycation end products; MG - methylglyoxal; GLO-1 - glyoxalase-1; GLO-2 - glyoxalase-2; GSH - reduced glutathione; ECM - extracellular matrix; ERK - extracellular signal-regulated kinase; JNK - c-jun N-terminal kinase; NADPHox - nicotinamide adenine dinucleotide phosphate oxidase; NF-kB - nuclear factor kappa B; ROS - reactive oxygen species.

2.2 Mechanisms of MG detoxification and scavenging factors

Although cells produce relatively low amounts of MG in normal conditions, its formation is a natural consequence of glucose and lipid metabolism. Thus, cells developed specialized mechanisms and systems to detoxify harmful substances into innocuous products. In fact, the impact of MG in biological systems is mostly avoided (more than 99% under physiological conditions) by a specific enzymatic system known as the GLO system, which is present in several species and well conserved during evolution (Rabbani and Thornalley, 2011, 2012, 2014b).

Regarding enzyme activity, GLO-1 is the key limiting enzyme in glyoxalase system, which converts MG into an intermediary product known as S-D-lactoylglutathione. Subsequently, GLO-2 is responsible for S-D-lactoylglutathione conversion into D-Lactate (Figure 1.12 and 1.13). Furthermore, GLO-1 is glutathione (GSH)-dependent, being the activity of the enzyme affected by GSH levels and therefore, enzyme activity critically depends of the antioxidant/oxidative status of the cell (Figure 1.12 and 1.13) (Falone et al., 2012; Masania et al., 2016a; Rabbani et al., 2014). Other enzymes such as aldo-keto reductases, alpha-dicarbonyl/L-xylulose reductase and aldehyde dehydrogenase are also involved in MG degradation, but with much smaller activity when compared to glyoxalase system (>99%) (Goldin et al., 2006; Maessen et al., 2015; Negre-Salvayre et al., 2009; Rabbani and Thornalley, 2014b; Rabbani et al., 2014).

Nevertheless, even if MG reacts and modify proteins, cells also have the ability to degrade a small percentage of these adducts through amadoriases as well as proteasome and lysosome degradation (Bento et al., 2010a; Grimm et al., 2012; Negre-Salvayre et al., 2009). Furthermore, an important part of circulating AGE and dicarbonyl adducts are eliminated in the kidney. AGE and dicarbonyl adducts with peptides are filtered in the glomerulum,

degraded in the lysosomes of tubular and mesangial cells and eliminated as AGE-amino acids (Nakajou et al., 2005; Negre-Salvayre et al., 2009; Rabbani and Thornalley, 2014a).

Regarding experimental models of obesity and type 2 diabetes, several have demonstrated diminished GLO-1 activity in visceral AT, which may be related to HIF-1α, as well as increased hyperglycaemia-derived formation of MG, depletion of antioxidant defences and other unknown mechanisms (Lee et al., 2014; Masania et al., 2016a; Rabbani and Thornalley, 2011).

In addition, human GLO-1 expression and activity is highly regulated by several unknown mechanisms and, as recently found, responsive elements that may change the cellular levels of the enzyme in response to insulin (IRE-insulin-response element), antioxidant/oxidative factors (ARE-antioxidant response-element), metal regulation (MRE-metal-response element), mitogenic stimulus (E2F4-early gene 2 factor isoform 4), cellular homeostasis (AP-2α-activating enhancer- binding protein 2α) and is in fact, a hotspot for copy number variation (Masania et al., 2016a; Rabbani and Thornalley, 2011; Rabbani et al., 2014).

MG is also a potent inducer of oxidative stress (Brownlee, 2001; Desai et al., 2010; Negre-Salvayre et al., 2009). MG inhibits mitochondrial permeability transition, while increases the activity of several prooxidant enzymes, namely NADPH oxidase, leading to the production of ROS, hydrogen peroxide and peroxynitrite in isolated mitochondria and in several tissues (Chang et al., 2005; Dhar et al., 2008; Kalapos et al., 1993; Remor et al., 2011). Furthermore, it reduces antioxidants such as GSH (Amicarelli et al., 2003), glutathione peroxidase and reductase (Paget et al., 1998) in different cell types (Desai et al., 2010). Okuno and colleagues, recently demonstrated healthy adipose tissue expansion in diet-induced obese mice having overexpression of catalase and SOD1 in adipocytes, while glutathione depletion, specifically in these cells, resulted in impaired adipose tissue expandability (Okuno et al., 2018). Consequently, depletion of cell GSH levels decreases

GLO-1 activity, while increases cellular MG levels, which contributes to a self-perpetuating cycle of ROS/AGE formation. Indeed, GSH depletion is commonly observed during chronic hyperglycemia, contributing to early aging-dependent mechanisms and progressive increase in type 2 diabetes microvascular complications (Brownlee, 2001, 2005; Goldin et al., 2006; Maessen et al., 2015; Negre-Salvayre et al., 2009; Rabbani and Thornalley, 2011).
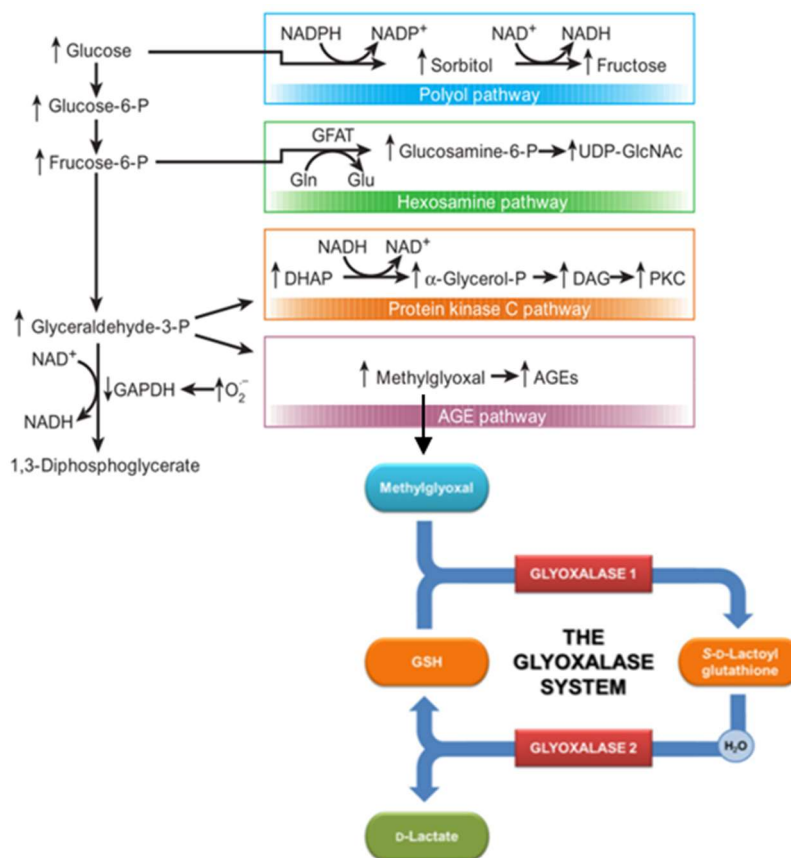
Figure 1.13 – Chronic hyperglycemia increases glycolysis-derived methylglyoxal, contributing to glyoxalase system overflow and microvascular complications
The schematic figure shows endothelial cells upregulated pathways, during chronic hyperglicemia (type 2 diabetes). Thus, more glucose originates higher glycolisys-derived secondary products, namely methylglyoxal. Methylglyoxal may react with biomolecules (AGE formation) or may be degradade by glyoxalase system (GLO-1 and GLO-2). GAPDH - glyceraldehyde 3-phosphate dehydrogenase; AGE - advanced glycation end-products; NAD$^+$/NADH - nicotinamide adenine dinucleotide; DAG - diacylglycerol; UDP - uridine diphosphate; GlcNAc - N-acetyl glucosamine; GSH - reduced glutathione; GFAT - glutamine fructose-6-phosphate amidotransferase; DHAP - dihydroxyacetone phosphate; Gln - glutamine; Glu – glutamate. Adapted from Brownlee et al., 2001 and Maessen et al., 2015.

In accordance, diabetic or hyperglycemic-induced microvascular complications are developed (Figure 1.13), as well as dysfunction of endothelial/progenitor cells, renal tubular epithelial and mesangial cells, retinal pericytes and bone marrow cells, which are improved by GLO-1 overexpression (Kim et al., 2012a; Shinohara et al., 1998; Vulesevic et al., 2014). Furthermore, GLO-1 overexpression was shown to protect from glucose-induced MG, ROS and AGE formation, being a promising strategy to develop therapeutic approaches against microvascular lesions (Masania et al., 2016a; Rabbani et al., 2014, 2016; Xue et al., 2016). Interestingly, elevated AGE levels are not prevented by intensive glycemic control in diabetic patients, leading to increased cardiovascular events (Group, 1998; Koska et al., 2018; Patel et al., 2008). Thus, several authors raised the hypothesis of "metabolic memory", based on the fact that increased MG formation may be acquired from endogenous metabolism, causing progressive AGE accumulation and ROS production even following tight blood glucose control (Ceriello et al., 2009).

In the past, several studies have explored the role of scavenger drugs (aminoguanidine, pyridoxamine and N-Acetyl-Cysteine) in preventing AGE formation and the associated pathophysiological burden (Almeida et al., 2013; Gaens et al., 2012; Rodrigues et al., 2013c; Thieme et al., 2016). In fact, all have shown decreased *in vivo* AGE accumulation, ROS formation, and ECM deposition, as well as improved vessel thickening of diabetic animal models (Chetyrkin et al., 2008; Fan et al., 2011; Goldin et al., 2006; Kim et al., 2012b). Furthermore, several natural and exogenous compounds were studied, including soy isoflavones, several flavonoids, phlorotannins from algae, sulforaphane from broccoli, fruit triterpenes, red wine resveratrol or polyunsaturated FFA, which showed decrease of *in vivo* and *in vitro* MG formation and effects through MG scavenging or increased GLO-1 levels/activity-dependent mechanisms (Jia et al., 2006; Liu and Gu, 2012; Liu et al., 2011b;

Lu et al., 2008; Maher et al., 2011; Muthenna et al., 2012; Schalkwijk, 2015; Taneda et al., 2010; Wang et al., 2010).

In 1999, Beisswenger and collaborators showed that increased MG levels in diabetic patients, were decreased by metformin in a dose-dependent fashion (Beisswenger et al., 1999). More recently, Kinsky and collaborathors identified imidazolinone formation from metformin interaction with MG (Kinsky et al., 2016). Thus, metformin, the most used oral anti-diabetic, contributes to prevent microvascular diabetic complications, independently of antihyperglycemic actions (Beisswenger et al., 1999; Kinsky et al., 2016; Madiraju et al., 2018).

Given the fact that glycation lowering strategies may prevent or at least delay the development of diabetic microvascular complications, several approaches have been employed in the last years. Indeed, our group demonstrated the efficacy of the vitamin B6 derivative, pyridoxamine, even a late intervention, in restoring MG-induced effects on AT microvascular lesions and in heart survival pathways under ischemia conditions (Almeida et al., 2013; Rodrigues et al., 2013c). In the last years, Schalkwijk and collaborators have been highly dynamic in pyridoxamine study and use against MG-induced glycation in biological systems, specifically targeting vascular dysfunction. In fact, they are running a clinical trial addressing the beneficial effects of pyridoxamine in type 2 diabetic patients, focusing on vascular effects (Engelen et al., 2013; Maessen et al., 2016b; Schalkwijk, 2015).

More recently, Thornalley and collaborators have developed a new formulation (trans-resveratrol-hesperetin) to induce higher GLO-1 activity. Interestingly, this clinical intervention resulted in diminished insulin resistance and vascular inflammation/dysfunction, contributing to improved glucose tolerance in overweight and obese patients (Masania et al., 2016a; Xue et al., 2016).

New GLO-1 inducers and new formulations/associations or natural compounds are required and the mechanisms involved should be fully described in the near future. Targeting GLO-1 activity may potentially prevent metabolically unhealthy obesity and type 2 diabetes development and progression, as well as vascular complications (Maessen et al., 2016b; Masania et al., 2016b; Rabbani and Thornalley, 2011; Rodrigues et al., 2013a; Schalkwijk, 2015; Watson et al., 2011; Xue et al., 2016).

3. Targeting "adiposopathy" to prevent metabolically unhealthy obesity and type 2 diabetes - exploring incretin-based therapeutic approaches

Abdominal obesity is characterized by exacerbated visceral adipose tissue (VAT) expansion, which occurs after prolonged excessive caloric intake and reduced physical exercise, usually present in overweighed and obese subjects, a well-known risk-factor for type 2 diabetes, cardiovascular and liver diseases and cancer (Galic et al., 2010; Goossens, 2008; Hinnouho et al., 2014; Kiess et al., 2008; Kusminski et al., 2016; Liu et al., 2010; Pais et al., 2009; World Health Organization, 2000; Ye, 2008). Thus, AT has become a crucial target in order to prevent/delay such diseases. In fact, several therapeutic strategies are under development, including adipokine-based and other pharmacological approaches, as well as bariatric/metabolic surgical procedures. These strategies seek improved adipose tissue functionality, such as through energy expenditure (browning), vasculature, inflammation/fibrosis as well as insulin resistance and glucose homeostasis (Kusminski et al., 2016; Rutkowski et al., 2015; Scherer, 2018). Overall, preserved AT plasticity and increased lipid handling, may contribute to improve tissue homeostasis, preventing metabolically unhealthy obesity and type 2 diabetes development.

Pleiotropic actions of Glucagon-like peptide-1 and DPP-4-mediated degradation

GLP-1 is a gut-derived incretin hormone, produced from proglucagon and mainly released by L-cell in distal small intestine. GLP-1 is cleaved from GLP-1(1-37), which originates two bioactive circulating forms, GLP-1(7-37) and GLP-1(7-36)amide. It is mainly regulated by nutritional signals, namely sugars and lipids, as well as neural and hormonal signals. In fact,

plasma GLP-1 levels rise really fast, even before direct nutrient stimulation of gut L-cells (Drucker, 2006, 2018; Ladenheim, 2015).

The incretin concept is characterized by significantly higher insulin secretion from pancreatic β-cells after oral glucose stimulation, in comparison to intravenous glucose load in normal subjects. Thus, enteroendocrine cells release incretin hormones, namely glucose-dependent insulinotropic polypeptide (GIP) and GLP-1 proportionally to oral glucose load delivered (Cho et al., 2014; Drucker, 2006, 2018).

Interestingly, unlike GIP, the pleiotropic effects of GLP-1, including potentiating glucose-dependent insulin secretion and glucose homeostasis, are preserved in diabetic animal models and humans. Although controversial, it is thought that GLP-1 actions are mostly G-protein coupled GLP-1 receptor-dependent, being its receptors present in multiple tissues and organs (central and peripheral nervous system, gastrointestinal system, liver, kidney, heart, pancreas, muscle and adipose tissue), where it exerts beneficial effects (Figure 1.14) (Cho et al., 2014; Drucker, 2018; Drucker and Nauck, 2006).
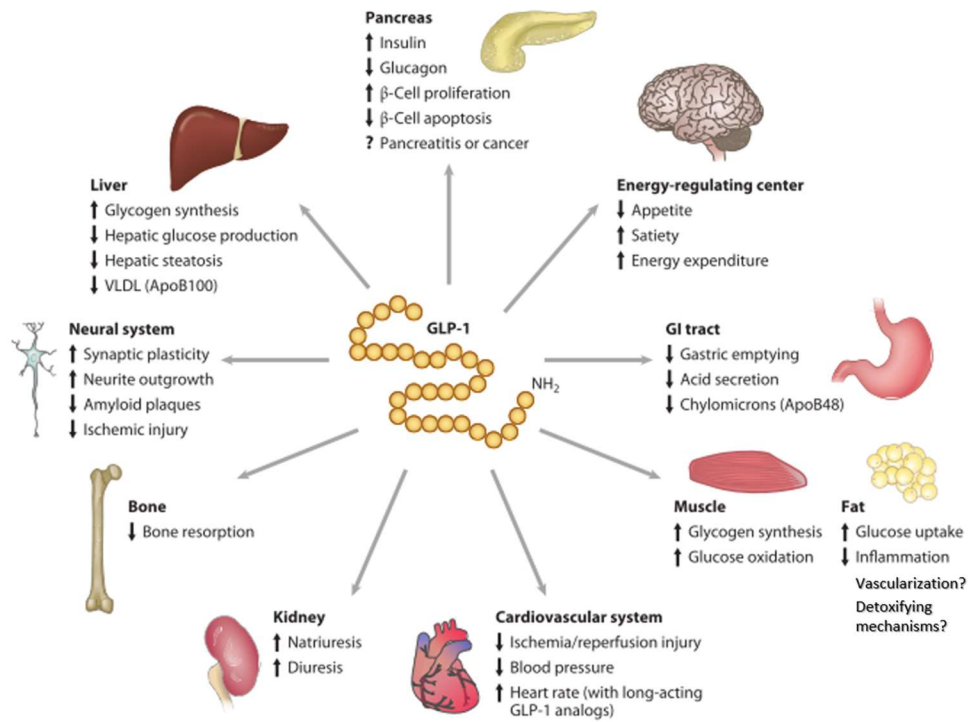
Figure 1.14 – GLP-1-mediated pleiotropic effects

GLP-1 receptor is present in several tissues and organs, although the most known physiological mechanism occurs in endocrine pancreas. GLP-1 exerts several effects, namely regulating energy metabolism, such as, improved nutrient handling (decreased food intake and gastric emptying) and anabolic/catabolic processes (nutrient storage in adipose tissue and use in skeletal muscle and liver). In addition, it may also be benefical on cardiovascular and neuronal health, kidney and bone function as well as on hepatic steatosis and adipose tissue dysfunction, specifically preventing ectopic fat. GLP-1 - glucagon-like peptide-1 ; VLDL – very low density lipoprotein; NH$_2$ - amide. Adapted from Cho et al,. 2014.

Circulating GLP-1 has a really short half-life (approximately 2 minutes), due to rapidly DPP-4-induced degradation and renal clearance. In fact, a substantial degradation of GLP-1 by DPP-4, occurs even before it reaches portal and systemic circulation. Thus, DPP-4 inhibitors increase GLP-1 half-life and circulating levels, allowing sustained postprandial GLP-1 actions. Interestingly, DPP-4 was previously described as an adipokine, which is highly released from visceral adipose tissue of obese and insulin-resistant patients. Furthermore, DPP-4 may act in skeletal muscle cells and adipocytes, inducing insulin resistance and decreased nutrient uptake, which may represent a counterbalancing mechanism with GLP-1 (Blüher and Mantzoros, 2015; Drucker, 2006; Lamers et al., 2011).

GLP-1 receptor (GLP-1R) mediated effects (through adenylyl cyclase-dependent cAMP production) lead to improved β-cell health and survival (via PI3K) even following increased insulin biosynthesis/secretion. Besides, α-cells are inhibited (paracrine signals from β-cells), decreasing glucagon secretion, which contributes to improved glucose homeostasis (Cho et al., 2014; Drucker, 2018).

In adipose tissue, to the best of our knowledge, GLP-1-mediated effects are different among fat depots, specifically between visceral and subcutaneous. GLP-1 promotes preadipocyte differentiation, being also effective in reducing lipogenic genes, while increases lipolytic markers in human-derived adipose tissue explants (Challa et al., 2012; Consoli et al., 2017). GLP-1 acts on angiogenesis, promoting increased proliferation/differentiation of endothelial progenitor cells, through increased VEGF signalling (Xiao-Yun et al., 2011). GLP-1 also induced angiogenesis in a dose-dependent manner using pharmacological doses (200nM to 1000nM) in human umbilical vein endothelial cell (HUVEC). Moreover, signalling studies demonstrated increased GLP-1-induced angiogenesis through PI3K/Akt, PKC as well as nitric oxide pathways (Aronis et al., 2012, 2013). Considering adipose tissue angiogenesis, GLP-1R presence and GLP-1-mediated effects on adipocytes are still controversial. GLP-1

actions in adipose tissue may also derive from GLP-1R-independent mechanisms. Although GLP-1 actions in AT and specifically in AT angiogenesis are still controversial, it has been demonstrated increased AT glucose uptake, lipolytic and anti-inflammatory actions after liraglutide (GLP-1R agonist) treatment, contributing to improved metabolic outcome (Cho et al., 2014; Drucker, 2018). Nevertheless, future studies are required to describe GLP-1R-dependent/independent mechanisms in adipose tissue, given the fact that may reveal therapeutic opportunities.

Bariatric/metabolic surgery: beyond body weight loss effects

In the mid-1950s, the concept of bariatric surgery as a strategy to control body weight was created from patients with stomach or intestine diseases like cancer or ulcer, which were treated by surgical procedures and experienced significant postoperative weight loss. Thus, artificial malabsorbtion syndromes were created, known as two variants of the jejuno-ileal bypass, which have been used to reduce nutrient uptake (Buchwald, 2002; Jenkins et al., 2005; Payne and DeWind, 1969).

In 1960s, Edward Mason was pioneer using a restrictive/malabsorptive gastrointestinal procedure, known as gastric bypass (Mason and Ito, 1969). In a well-known publication from 1992 "Is Type II Diabetes Mellitus a surgical disease?", Pories and collaborators reported type 2 diabetes remission in 78% of patients submitted to gastric bypass (Pories, 1992; Pories et al., 2006a). Furthermore, in 1995 same authors were incredulous and the publication "Who Would Have Thought It? An Operation Proves To Be the Most Effective Therapy for Adult-Onset Diabetes Mellitus" was a crucial driven to scientific community find bariatric/metabolic surgery-derived mechanisms in improved glucose tolerance and type 2 diabetes remission (Pories et al., 2006b).

At the beginning, the alterations of gastrointestinal tract were thought to cause weight loss by gastric restriction- and/or malabsortive-derived effects. Thus, bariatric surgery procedures have been developed in order to maximize long-term body weight effects as well as preventing side effects. Besides, surgical procedures have been integrated in three generic lines regarding alterations in stomach volume and intestinal nutrient uptake: malabsorptive, malabsorptive/restrictive, and purely restrictive (Buchwald, 2002). Each approach has advantages and disadvantages and therefore, the procedures used are in accordance with clinical data and individually adjusted to clinical aims. Despite the fact that several anatomical procedures have been developed (Figure 1.15), improved glucose tolerance and type 2 diabetes remission have been observed in most cases, being the gastric bypass the most effective (Batterham and Cummings, 2016; Cefalu et al., 2016).
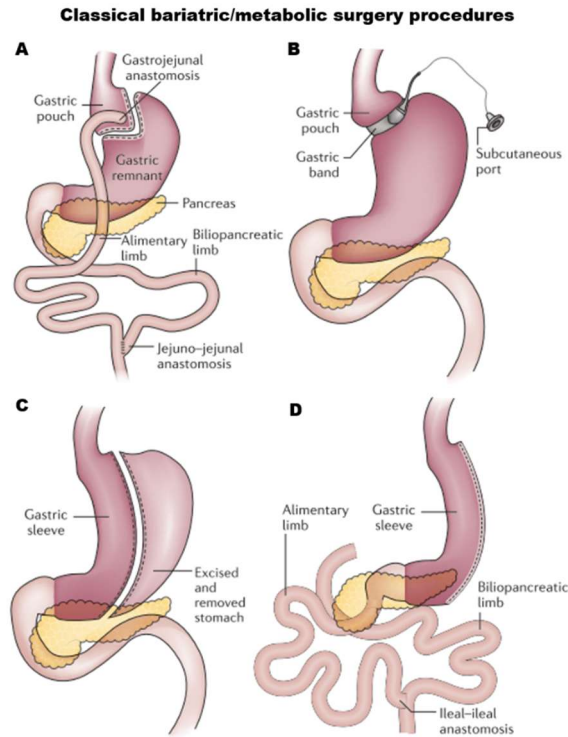
Figure 1.15 –Established bariatric/metabolic surgery procedures

The figure shows four types of bariatic/metabolic surgery procedures used in obese patients. A) The stomach volume is divided into two, being digestive continuity a small chamber and food directly reachs proximal jejunum; B) An inflatable silicon ring decreases stomach entrance, slowing food flow; C) 80% of stomach volume is excised, leading to increased gastric empting; D) Reduction of stomach volume and malabsorption of nutrients regarding biliopancreatic diversion with duodenal switch. Adapted from Nguyen *et al*., 2016.

In line with these findings, terminology has changed, being bariatric surgery applied to obese patients aiming weight loss, while metabolic surgery terminology is mostly used, focusing clinical and metabolic benefits introduced, to obese pre-diabetic and type 2 diabetic patients (Rubino, 2013). Although the underlying mechanisms are partially unknown, most of the metabolic surgery-derived beneficial effects on glucose and insulin resistance begins within days after surgical procedures, even before significant reduction of body weight (Batterham and Cummings, 2016).

Body weight loss is thought to play an important role in long-term alterations. However, early mechanisms are mostly explained by gut anatomical and functional changes, being highly dependent of the surgical procedure. Thus, gastric bypass and sleeve gastrectomy, which are frequently used, have been associated with enhanced caloric restriction, nutrient/bile emptying and delivery to distal intestine. Conversely, both surgical procedures differ in stomach fundus excision performed in sleeve gastrectomy, while duodenum and partial jejunum exclusion is applied in gastric bypass. Recently, Batterham and Cummings described the potential mechanisms/mediators of metabolic surgery in glucose homeostasis and insulin resistance (Figure 1.16) (Cefalu et al., 2016; Rubino, 2013; Rubino et al., 2016).
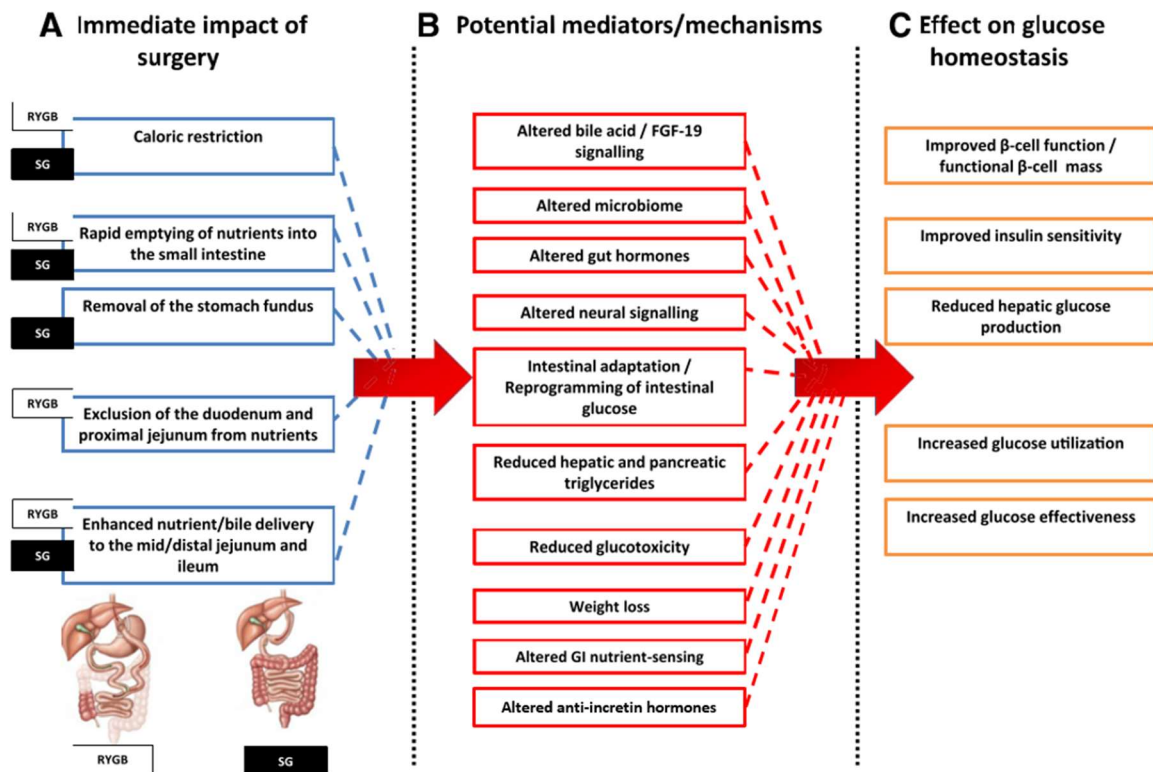
Figure 1.16 – Time-dependent effects of the most used metabolic surgery procedures in glucose homeostasis and insulin resistance

The schematic figure shows the hipothetical bariatic/metabolic surgery-dependent pleiotropic mechanisms and mediators involved in improved glucose tolerance and insulin resistance in obese and type 2 diabetic patients. RYGB – Roux-en-Y gastric bypass; GI – gastrointestinal; FGF-19 – fibroblast growth factor-19; SG – sleeve gastretomy. Adapted from Batterham *et al*., 2016.

In line with this, several mechanisms responsible for multifactorial postoperative effects on metabolic control than weight loss-dependent mechanisms have been identified using clinical and animal studies, namely incretin hormones, microbiome, and gut-derived peripheral/central pathways (Figure 1.17) (Batterham and Cummings, 2016; Nguyen and Varela, 2017).
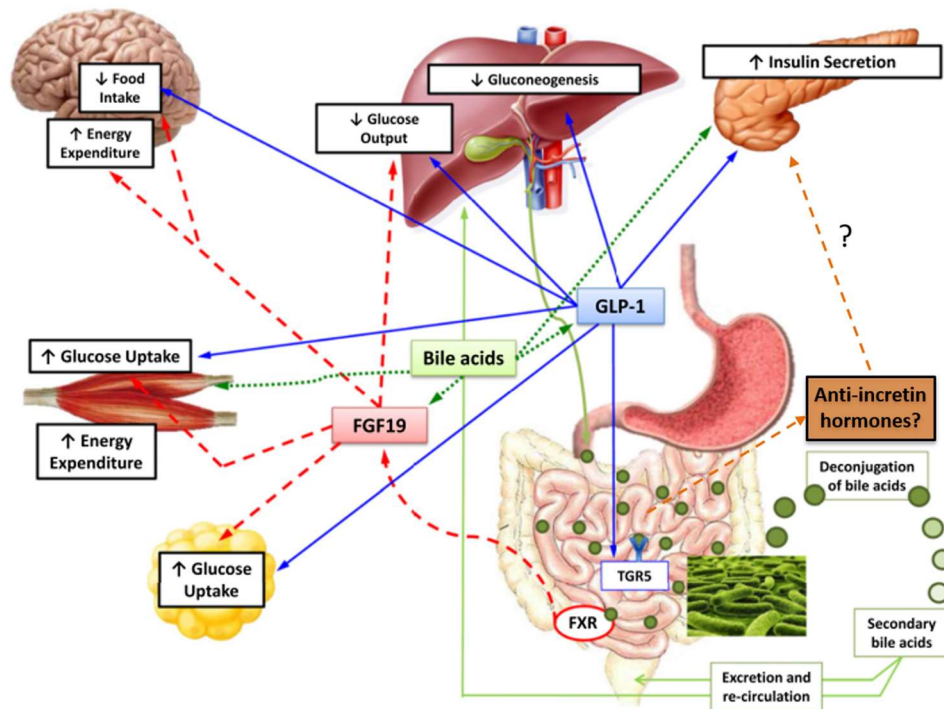
Figure 1.17 – Bariatric/metabolic surgery-derived multifactorial mechanisms
The figure shows bariatric/metabolic surgery-dependent pleiotropic mechanisms improving glucose intolerance and insulin resistance in obese and type 2 diabetic patients. GLP-1 – glucagon-like peptide-1; FGF - 19 – fibroblast growth factor-19; TGR5 – membrane-type receptor for bile acids; FXR – farnesoid X receptor. Adapted from Batterham *et al.*, 2016.

Based on animal studies, several authors postulated the existence of anti-incretin hormones, and nutrient-stimulated gut-derived neuroendocrine signals mainly located at proximal intestine and responsible for counterbalance incretins and other beneficial factors involved in insulin signalling and glucose homeostasis (Figure 1.17). Despite the fact that in humans anti-incretin factors are unknown, a factor named decretin was identified in drosophila (Alfa et al., 2015; Kamvissi et al., 2015). In line with this, gastric bypass surgeries have been associated with long-term occurrence of severe hypoglycemias in some patients. Given the fact that proximal intestine exclusion leads food directly to proximal jejunum, these counterbalance mechanisms are excluded, while beneficial factors, namely GLP-1-delivery,

is increased (Batterham and Cummings, 2016; Drucker, 2018; Kamvissi et al., 2015; Ladenheim, 2015).

Regarding GLP-1 signalling, is nowadays widely accepted that metabolic surgery leads to improved postprandial incretin levels and consequently, increased β-cell function/protection and insulin secretion. It is thought that alterations to gastrointestinal tract originated by metabolic surgery, cause faster and higher stimulation of L-cells, contributing to increased postprandial GLP-1 levels. However, it is believed that there are GLP-1R-independent effects on peripheral tissues, including increased insulin sensitivity, weight loss and bile acids signalling that remain partially unknown (Figure 1.17) (Cho et al., 2014; Drucker, 2018).

On the other hand, based on animal models and clinical observations, metabolic surgery improves bile acids actions. Postprandially, bile acids are thought to be involved in metabolism and energy homeostasis, namely acting through farnesoid X and G-coupled TGR5 receptors to increase ileal-derived enterokine fibroblast growth factor-19 and GLP-1 and peptide YY (PYY) levels, which are associated with increased insulin signalling and glucose dysmetabolism improvement (Batterham and Cummings, 2016; Cho et al., 2014).

In line with these findings, the effects of metabolic surgery should be fully addressed in near future, including related mechanisms of other gut-derived hormones and co-activators as well as gut microbiome and vagal activity.

Long-acting actions of liraglutide, a known GLP-1 receptor agonist

Liraglutide developed by Novo Nordisk under the brand name Victoza, is a long-acting GLP-1 analogue, which was firstly approved to type 2 diabetes and more recently to obesity. Given the fact that GLP-1 protein is changed in one amino acid highly targeted by DPP-4 and bound to a palmitic acid that allows additional interactions with plasma proteins, circulating time is significantly increased (10-14 hours). Thus, prevention of DDP-4-induced degradation and reduced absorption in tissues contribute to the longer half-life and sustained biological effects, namely glucose-lowering and body weight loss actions (Ladenheim, 2015; Marso et al., 2016).

Liraglutide has pleiotropic effects, as well as GLP-1 itself, being involved in reduced food intake, body weight loss and improved metabolic outcome in both animal and human studies. Human studies also revealed increased efficacy of liraglutide in reducing visceral instead subcutaneous AT, when compared to lifestyle interventions (Santilli et al., 2015). Animal models demonstrated liraglutide action in preadipocyte proliferation and inhibition of cell apoptosis. The reduction of lipogenic signals in VAT of db/db obese mice, driven by activation of AMPK and inhibition of AKT, cause decreased body weight gain and VAT depots, as well as diminished expression of the lipogenic transcription factors PPARγ and C/EBPα (Shao et al., 2015).

Liraglutide beneficial actions have been demonstrated in several clinical trials. It was shown to improve glucose and HbA1c levels (Liraglutide Effect and Action in type 2 diabetes – LEAD 1-5) (Blonde and Russell-Jones, 2009), reduce body weight in obese individuals (Effect of Liraglutide on Body Weight in Non-diabetic Obese Subjects or Overweight Subjects With Co-morbidities - SCALE) (Pi-Sunyer et al., 2015), and decrease cardiovascular complications among patients with type 2 diabetes (Liraglutide Effect and

Action in Diabetes: Evaluation of Cardiovascular Outcome Results - LEADER) (Jones, 2016).

Despite the fact that few studies have addressed liraglutide actions in angiogenesis, several beneficial effects were demonstrated, including restored angiogenesis in palmitate-induced endothelial dysfunction using HUVECs (Ke et al., 2016), VEGF-dependent angiogenesis and long-term recovery in a mice model of focal cerebral ischemia (Ke et al., 2016), improvement of transplanted islet through angiogenic mechanisms (Langlois et al., 2016), cardiac microvascular endothelial cells after hypoxia/reoxygenation damage (Zhang et al., 2016) and cardiac regeneration in a rat model of myocardial infarction (Qi et al., 2017). Altogether, these observations may provide a rationale for using liraglutide to improve angiogenesis in other tissues and models, namely adipose tissue.

Chapter 2 - SCIENTIFIC FRAMEWORK AND HYPOTHESIS AND AIMS

1. Scientific framework and hypothesis

Several years ago, AT was mostly described as a specialized tissue in triglyceride storage and particularly involved in lipid homeostasis. However, in the last years, remarkable insights have been gained about some processes and nowadays AT is known as a multifactorial organ involved in multi-organ physiology, including the regulation of food intake and energy expenditure and insulin sensitivity. Interestingly, so far the endocrine actions of AT are known to involve more than 600 factors produced and potentially released, changing other tissues and organs physiology. The implications of secretome changes to other tissues are still far from being completely understood, namely during adipose tissue dysfunction and metabolically unhealthy obesity,

Ten years ago, our laboratory was involved in a project to study the effects of methylglyoxal/glycation in type 2 diabetes. We were able to show that methylglyoxal supplementation unbalances the ratio between VEGF and Angiopoietin-2 (ANG-2), with negative consequences on retina vessels, which are commonly affected in diabetes (Bento et al., 2010b). Moreover, we have shown that methylglyoxal induces endothelial dysfunction in rat's aorta and impaired activation of stress pathways in the heart during ischemia (Crisóstomo et al., 2013; Sena et al., 2012). At the time, little was known about the mechanisms of adipose tissue dysfunction in obesity and the involvement of glycation in such process was completely unknown. Thus, one of the first objectives was to understand the impact of methylglyoxal-induced glycation in adipose tissue function. In May of 2010, I started an internship dedicated to this project; we have demonstrated that MG supplementation causes functional and structural changes in adipose tissue, even when studying a lean animal model (Matafome et al., 2012). Then, we hypothesized that MG effects on AT could be restored or at least reduced by pyridoxamine, a methylglyoxal

scavenger drug. Even using a delayed intervention, a condition highly common in type 2 diabetes therapeutic approaches, we demonstrated a microvascular AT improvement after pyridoxamine administration (Rodrigues et al., 2013c).

Subsequently, we formulated the hypothesis that methylglyoxal could impair AT adaptation to reduced blood flow. Thus, during my master thesis project we developed a surgical animal model in order to reduce left periepididymal adipose tissue (pEAT) blood flow. Methylglyoxal-supplemented animals challenged with left pEAT blood flow reduction demonstrated impaired adaptation, which contributed to increased AT and systemic dysmetabolism (Rodrigues et al., 2013b). Altogether, these previous results were crucial to formulate several questions and hypothesis that were included in the PhD project.

Regarding the PhD project, we hypothesized that methylglyoxal-supplemented animals challenged with a high-fat diet would have reduced AT capillarization and blood flow, leading to pEAT dysfunction and insulin resistance. Briefly, this hypothesis was corroborated and, in fact, methylglyoxal-induced glycation during tissue expansion originated all features associated with AT dysfunction, metabolically unhealthy obesity and ultimately, type 2 diabetes development.

Secondly, we considered that similar negative effects of glycation could occur in obese human VAT, governing the development of metabolically unhealthy obesity as well as progressive type 2 diabetes development and progression. This hypothesis was corroborated using VAT, blood samples and clinical data from obese subjects undergoing bariatric/metabolic surgeries at *Centro Hospitalar e Universitário de Coimbra – Hospital Geral - Covões* (CHUC - CHC).

Thirdly, previous data from our group demonstrated that metabolic surgery is able to increase AT angiogenesis (Eickhoff et al., 2015) and postprandial GLP-1 levels in type 2 diabetic GK rats (Eickhoff, in revision). Based on this, we hypothesized that GLP-1 or

liraglutide, a human GLP-1 analogue, could increase pEAT angiogenesis and improve tissue and systemic metabolism. Moreover, knowing that GLP-1 has antioxidant actions, we also hypothesized that GLP-1-mediated effects could be GLO-1-dependent or at least involved in enzyme modulation, for instance changing enzyme levels or activity in pEAT. Thus, using normal and diabetic rats we applied two strategies based on GLP-1 signalling, vertical sleeve gastrectomy and liraglutide administration. AT angiogenesis assay was used to explore the direct involvement of GLO-1 in liraglutide-induced improvement of pEAT angiogenesis. Overall, knowing the negative effects of methylglyoxal-induced glycation in pEAT, namely on angiogenesis and metabolic function, GLO-1 become a promising therapeutic target to prevent AT vascular and metabolic dysfunction. In fact, healthy AT may avoid or delay the transition from metabolically healthy to unhealthy obesity and ultimately, to prevent chronic insulin resistance and type 2 diabetes development and progression.

2. Graphical framework

2012 — Methylglyoxal causes structural and functional alterations in adipose tissue in Wistar rats

2013 — Methylglyoxal further impairs adipose tissue metabolism after partial decrease of blood supply

2013 — Pyridoxamine improves adipose tissue microvascular lesions caused by methylglyoxal

2014 — A vascular piece in the puzzle of adipose tissue dysfunction

2015 — Start of the PhD project start - glycation-derived microvascular dysfunction in adipose tissue expandability and functionality, exploring the mechanisms involved and GLP-1-based therapeutic approaches

2015 — Glycation and hypoxia: two key factors for adipose tissue dysfunction

2015 — "Melhor poster científico", VII Annual Meeting of IBILI

2016 — "Prémio Nacional de Diabetologia - SPD"

2016 — Methylglyoxal in Metabolic Disorders

2017 — Methylglyoxal-induced glycation changes adipose tissue vascular architecture, flow and expandability, leading to insulin resistance

2018 — "Menção Honrosa da Bolsa Pedro Eurico Lisboa Lilly/SPD"

2018 — High-fat diet induces a neurometabolic state with early glucose intolerance

2019 — Effect of sleeve gastrectomy on angiogenesis and adipose tissue health in an obese animal model of type 2 diabetes (in revision)

2019 — "Prémio SPD/MEDINFAR Diabetes/2019"

2019 — Targeting adipose tissue glyoxalase system with GLP-1 to improve capillarization and insulin sensitivity (in preparation)

2019 — "Prémio de Melhor Comunicação Oral de Investigação Fundamental"

3. Objectives

Main objective

- To study the effects of glycation on adipose tissue microvasculature and the impact on tissue expandability and function, exploring the mechanisms involved and GLP-1-based therapeutic approaches.

Specific objectives

- To evaluate the consequences of methylglyoxal-induced AGE accumulation in adipose tissue, namely vascular dysfunction during diet-induced tissue expansion and local and systemic metabolic alterations;

- To develop a rat adipose tissue angiogenesis assay in order to study adipose tissue capillarization as well as a sophisticated imaging technique based on magnetic resonance to study adipose tissue blood flow;

- To determine glyoxalase-1-dependent mechanisms, specifically its levels and activity, in animal models and humans adipose tissue;

- To explore the role of increased GLP-1 signalling, using metabolic surgery (vertical sleeve gastrectomy) and liraglutide (human GLP-1 analogue), including the effects on adipose tissue angiogenesis, detoxifying mechanisms and metabolic outcome;

- To identify if GLP-1-derived effects on adipose tissue angiogenesis are glyoxalase-1-dependent.

Chapter 3 - MATERIAL AND METHODS

1. Reagents/equipment

Unless stated, all common reagents and products were acquired from Sigma - Merck (USA) and Fisher Scientific - Thermo Fisher Scientific (USA). All the standard equipment used is from our laboratory. When there is some specificity or characteristic required from the equipment it is stated.

Antibodies used

Calnexin, VEGFA, CD31, HIF-1 alpha, (AB0037, AB0063, AB0092, AB0112, Sicgen, Portugal), β-actin, (A5316, Sigma - Merck, USA), PPAR-γ, AKT, p-AKT(Ser473), VEGFR2, PI3K, p-eNOS(Ser1177), eNOS (#2443, #9272, #4058, #2479, #4249, #9571, #32027 Cell Signalling, USA), ANG-2, F4/80, perilipin-A, GLUT-4, p-IR(Y1361), GLO-1, C/EBPalpha, PGC1alpha, ANGPTL4, AT1, HIF-2 alpha, GLP-1R (Ab8452, Ab74383, Ab3526, Ab65267, Ab60946, Ab96032, Ab40764, Ab191838, Ab2920, Ab9391, Ab8365, Ab186051 Abcam, UK), CD11c, CD206 (bs-2058R, bs-2664R Bioss, USA) TIE-2, IRβ, Catalase, SOD1 (sc-324, sc-57342, sc-271803, sc-101523 SantaCruz Biotechnology, USA), CEL (KH025, TransGenic Inc, Japan).

2. Animal model studies

2.1 Animal maintenance and experimental groups

Wistar Han (W) and Goto-Kakizaki rats from our breeding colonies at Faculty of Medicine, University of Coimbra were kept under standard conditions of ventilation, temperature (22-25ºC), humidity (50-60%) and light (12h light/dark). The experimental protocols have been approved by the local Institutional Animal Care and Use Committee (ORBEA IBILI-FMUC 03-2015). All the procedures were performed in accordance with the European Union Directive for Protection of Vertebrates Used for Experimental and Other Scientific Ends (2010/63/EU) and by users licensed by the Federation of Laboratory Animal Science Associations (FELASA).

Experimental groups for MG-induced glycation during adipose tissue expansion in diet-induced obese rats

In order to study glycation effects in diet-induced obese rats, forty-eight male Wistar rats with 8 months old were randomly divided in four groups (n=12/group): 1) Control group (Ct) maintained with standard diet (SD) (5% triglycerides, 21% proteins, 45% carbohydrates, AO3, SAFE, France); 2) Methylglyoxal group (MG) supplemented with standard diet and MG administration; 3) High-fat (HF) diet-fed group (HFD); 4) High-fat diet-fed group and MG administration (HFDMG). Twelve age-matched non-obese type 2 diabetic GK rats feeding a standard diet (GK group) were used as a model of endogenous glycation due to the presence of chronic hyperglycemia (Figure 3.1).

High-fat diet and MG administration: the HFD and HFDMG groups were maintained with a balanced high-fat diet created from AO3 standard diet (40% triglycerides, 10% carbohydrates and 26% proteins, 231 HF, SAFE, France), during 18 weeks (8 to 12 months old). MG was administered diluted in daily water (100 mg/Kg/day), during the same time and as described before (Matafome et al., 2012; Rodrigues, 2013).

Figure 3.1 – Schematic representation of experimental groups: methylglyoxal-induced glycation effects during adipose tissue expansion

The figure shows experimental design followed to evaluate the effects of glycation suplementation during 8 to 12 months old. MG (100 mg/Kg/day) was diluted in daily water and SD and HF were monitored. Ct, MG and GK groups were always mantained with SD. Ct – Wistar rats twelve months old; MG – Wistar rats twelve months old with MG supplementation from eight to twelve months old; HFD - HF diet-fed Wistar rats from eight to twelve months old; HFDMG - HF diet-fed and MG-supplemented Wistar rats from eight to twelve months old; GK - Goto-Kakizaki; SD – standard diet; HF – high fat.

Experimental groups for sleeve gastrectomy experiments in obese type 2 diabetic GK rats

Evaluation of vertical sleeve gastrectomy effects on adipose tissue from obese type 2 diabetic GK rats was done using eight male Wistar Han with one month old and thirty-two age-matched non-obese diabetic GK rats (n=8/group), which were randomly assigned to the following groups: standard diet-fed Wistar (W) and GK rats (GKSD); GK rats maintained with high-calorie diet (20% high-fat/20% high-sucrose – HF/HS) (GKHFD group) and submitted to sham surgery (GKHFDSh) or sleeve gastrectomy (GKHFDSl) at four months old.

High-calorie diet and vertical sleeve gastrectomy and sham surgeries: W and GKSD groups were always fed with a standard diet (AO3, above mentioned). In turn, GK rats (GKHFD, GKHFDSh and GKHFDSl) were also fed with a balanced high-calorie diet between 1 and 6 months old (Figure 3.2). The randomized animals at 4 months old assigned to surgery (GKHFDSl and GKHFDSh) were starved overnight and surgical interventions occurred under intraperitoneal anaesthesia using chlorpromazine (3 mg/kg body weight, Laboratórios Vitória, Portugal) and ketamine (75 mg/kg body weight, Pfizer Inc, USA). After shaving the abdomen area, the skin was disinfected with a 4% polividone-iodine solution (MEDA Pharma, Portugal). A midline incision was performed using a scalpel blade and the abdominal cavity opened. The stomach volume was reduced around 80% using a bulldog clamp curved to dissect the greater curvature including the lower part of the stomach and the aglandular forestomach with ligation of the short gastric vessels in accordance to a technique previously described (de Bona Castelan et al., 2007; Eickhoff et al., 2015). After dissection and disinfection with a 4% polividone-iodine solution (MEDA Pharma, Portugal) it was performed a continuous double-armed suture with 4/0 midterm absorbable synthetic

glyconate monofilament (Monosyn® - B. Braun, Germany). After completing surgery and rinsing the abdomen with sterile saline, meloxicam (1 mg/kg body weight, Boehringer Ingelheim GmbH, Germany) diluted in sterile saline was deposited inside peritoneal cavity for postoperative analgesia. The abdominal wall was closed in all animals by continuous mass closure with a 3/0 short-term absorbable suture (Safil Quick® - B. Braun, Germany). In addition, the postoperative care (5 days) included supplementation with liquid diet (Forticare from Nutricia - Danone Group, France), subcutaneous analgesia with meloxicam (1 mg/Kg of body weight) and antibiotics (doxycycline, 5 mg/Kg of body weight, Pfizer Inc, USA) mixed to drinking water during 5 days.

In animals assigned to sham surgery, the surgical procedure was similar, but without alteration of the stomach volume. Thus, the stomach was mobilized and exposed during an interval of 30 minutes, which was similar to the time used to perform the vertical sleeve gastrectomy. Accordingly, analgesia was administered inside intraperitoneal cavity and the abdominal wall was also closed by continuous mass closure with a 3/0 short-term absorbable suture (Safil Quick® - B. Braun, Germany). The postoperative care was the same used for sleeve gastrectomy animals.
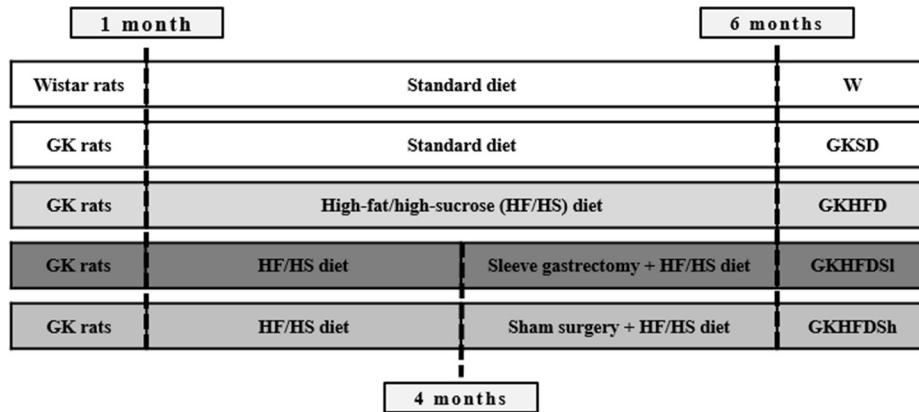
Figure 3.2 – Schematic representation of experimental groups: metabolic surgery effects on adipose tissue function of diet-induced obese and diabetic GK rats

The figure shows the experimental design followed to study metabolic surgery (vertical sleeve gastrectomy) effects on high-calorie-induced obese GK animals. Age-matched GK rats mantained with high-calorie diet were randomly assigned to GKHFD, sham surgery and vertical sleeve gastrectomy groups. Surgical procedures were performed at 4 months old and animals were sacriced at 6 months old. W and GKSD control groups were always maintained with SD until sacrifice. W – Wistar rats 6 months old fed a standard diet; GKSD – Goto-Kakizaki rats 6 months old fed a standard diet; GKHFD - Goto-Kakizaki rats 6 months old fed a high-fat and high-sucrose diet for 5 months; GKHFDSl – GKHFD submitted to sleeve gastrectomy at 4 months old; GKHFDSh – GKHFD submitted to sham surgery at 4 months old. GK - Goto-Kakizaki; HF - high-fat; HS - high-sucrose.

Experimental groups for liraglutide treatment in control Wistar and diabetic GK rats

In order to explore liraglutide effects on adipose tissue, twenty-four age-matched male Wistar Han and Goto-Kakizaki rats fourteen weeks old were always maintained with SD (AO3) and randomly divided in 4 groups (n=6/group): Wistar (W) and non-obese type 2 diabetic GK rats (GK), which were injected subcutaneously with an isotonic solution (1 μL/g of body weight using sterile NaCl 0,9%) in order to mimic injection effects on control groups; Wistar (WLira) and GK (GKLira) groups, which were submitted to subcutaneous injection of liraglutide (200 μg/Kg), twice a day (at 9am and 7pm), during 14 days (Victoza - novo nordisk, Denmark). Body weight was daily registered in order to adjust liraglutide dose (Figure 3.3).

	14weeks		16 weeks	
Wistar rats		Standard diet + saline twice/day		W
GK rats		Standard diet + saline twice/day		GK
Wistar rats		Liraglutide 200 μg/Kg s.c. twice/day		WLira
GK rats		Liraglutide 200 μg/Kg s.c. twice/day		GKLira
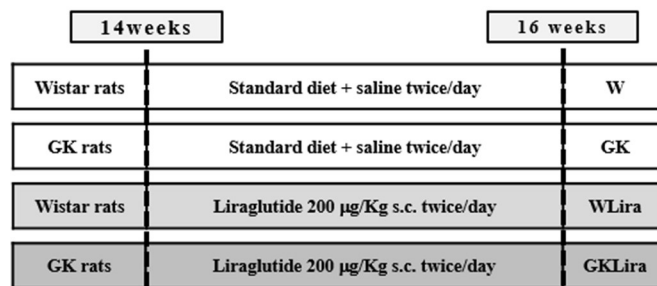
Figure 3.3 – Schematic representation of experimental groups: liraglutide effects on adipose tissue angiogenesis and function

The figure shows the experimental design regarding vehicle (NaCl 0.9%) or liraglutide (200 μg/Kg) (Victoza - Novo Nordisk, Denmark) treatment to Wistar and GK animals during two weeks (14-16 weeks old). All animals were maintained with standard diet until sacrifice. W – Wistar rats 16 weeks old; GK – Goto-Kakizaki rats 16 weeks old; WLira – Wistar rats 16 weeks old with liraglutide treatment during 14 days; GKLira – Goto-Kakizaki rats 16 weeks old with liraglutide treatment during 14 days. S.C. - subcutaneous injection.

Experimental groups for matrigel plug angiogenesis assay using Wistar rats

Matrigel plug angiogenesis assay is a well-known approach to study pro/anti-angiogenic factors, which was used to explore the actions of MG, liraglutide or both in combination. After overnight defrost at 4ºC, matrigel phenol red free (BD, UK) was supplemented with 50 U/mL of heparin (Merck, USA) and 100 nM of liraglutide (Lira group), 250 µM of MG (MG group) and both (100 nM + 250 µM, Lira + MG group) (mixed 2 hours at 4ºC). Using Wistar rats sixteen weeks old, 0.6 mL of supplemented matrigel phenol red free were injected subcutaneously in dorsal area (Figure 3.4).

16 weeks		17 weeks
Wistar rats	Matrigel + heparin 50 U/mL	Ct
Wistar rats	Matrigel + heparin 50 U/mL + MG 250 µM	MG
Wistar rats	Matrigel + heparin 50 U/mL + Lira 100 nM	Lira
Wistar rats	Matrigel + heparin 50 U/mL + Lira 100 nM + MG 250 µM	Lira + MG

Figure 3.4 - Schematic representation of experimental groups: liraglutide and methyglyoxal effects on matrigel plug angiogenesis

The figure shows the experimental design regarding methylglyoxal (250 µM) and liraglutide (100 nM) effects in matrigel plug angiogenesis assay using Wistar rats (16-17 weeks old). All animals were maintained with standard diet until sacrifice. Ct – Wistar rats 17 weeks old injected with matrigel suplemented with heparin 50 U/mL; MG – Wistar rats 17 weeks old injected with matrigel suplemented with heparin 50 U/mL and methylglyoxal 250 µM; Lira – Wistar rats 17 weeks old injected with matrigel suplemented with heparin 50 U/mL and liraglutide 100 nM; Lira + MG – Wistar rats 17 weeks old injected with matrigel suplemented with heparin 50 U/mL and methylglyoxal 250 µM and liraglutide 100 nM. MG – methylglyoxal; U – units; Lira – liraglutide.

2.2 *In vivo* procedures, sample collection and blood and tissue analysis

Magnetic resonance imaging

In order to evaluate *in vivo* adipose tissue blood flow in rat models, a highly sophisticated contrast-enhanced (DCE) magnetic resonance imaging (MRI) study was performed using a BioSpec 9.4 T MRI scanner (Bruke, Biospin, Ettlingen, Germany). Animals (n=6/group) were kept anesthetized by isoflurane (2-3%) with 100% O_2 with body temperature and respiration monitoring (Instruments SA - Stony Brook, USA). A body quadrature transmit/receive volume coil with 71/112 mm of inner/outer diameter was used. Images were acquired with a fat-saturated T1-weighted gradient-echo sequence with parameters: TR/TE=301.5/2.5ms, FA=50°, FOV=65×65mm^2, matrix size=169×169, 40 slices (axial orientation), slice thickness=1.0mm, 40 dynamics, scan time per dynamic=51s, total scan time=34mins. The contrast agent (Gadovist® - LUSAL, Portugal) was administered intraperitoneally, after the acquisition of 3 baseline dynamics. Tissue enhancement curves were obtained offline using homemade software implemented in Matlab (v2013a, Mathworks, Natick, Mass) and intensity variation was quantified in regions of interest (ROIs) as a function of time. The area under the curve (AUC) was calculated to indirectly quantify visceral AT blood flow, which was normalized to skeletal muscle intensity in studied animal groups (Ct, MG, HFD, HFDMG and GK).

Adipose tissue hypoxia

In order to study AT hypoxic regions, pimonidazole was intraperitoneally injected (60 mg/Kg, 40', n=3/group) in a specific set of twelve months old animals (Ct, MG, HFD, HFDMG and GK). Pimonidazole is a specific probe to study hypoxia, which under hypoxic conditions in tissues leads to adducts formation with proteins, being further detected using specific antibodies (Millipore, USA). Thus, the Hypoxia Probe Kit (Millipore, USA) was used to assess pEAT hypoxia by Western blotting (WB) and hypoxic regions using immunohistochemistry (IHC) as described before (Matafome et al., 2012).

The matrigel plug angiogenesis assay

After one week, animals (n = 3/condition) previously injected with supplemented matrigel were anesthetized by intraperitoneal anaesthesia using chlorpromazine (3 mg/kg body weight, Laboratórios Vitória, Portugal) and ketamine (75 mg/kg body weight, Pfizer Inc., USA). Under anaesthesia, animals were shaved in neck area and the skin was disinfected with a 4% polividone-iodine solution (MEDA Pharma, Portugal). Using surgical forceps and scissors, the jugular vein was exposed and animals were catheterized (BD, USA) in order to administer (100 mg/Kg of body weight) Evans blue dye (NaCl 0.9% plus 100 mg/mL of Evans Blue, Sigma - Merck, USA). The Evans blue dye has high affinity to serum albumin in circulating blood, therefore, all animal tissues and specifically the matrigel plug are perfused with time. Higher accumulation of Evans blue dye in matrigel plug is associated with higher density of functional blood vessels.

After forty minutes of Evans blue perfusion, animals were sacrificed by cervical displacement and the matrigel plugs excised using forceps and scissors. Matrigel plugs were

washed in PBS, embedded in cryomatrix (Thermo Fisher Scientific, USA) and immediately stored at -20ºC.

Crimomatrix embedded samples were sectioned (9 μm/slice) using a cryostat (LEICA CM3050S, Germany). Slices were placed in previously Poly-L-Lysine-coated microscope slides (Thermo Fisher Scientific, USA) and stored at -20ºC.

Slides were warm up to room temperature and washed 3x5' in Milli-Q water at RT. Using ice-cold methanol, slices were simultaneously fixated and permeabilized during 15'. After, slices were washed again 3x5' with PBS and incubated with PBS supplemented with (0.1 μg/ml) DAPI dye (Thermo Fisher Scientific, USA) during 15'. Once again, slices were washed 3x5' in PBS, dried at RT and coverslips were mounted using one drop of mounting medium (DAKO, USA).

Images were acquired (50X) in a Zeiss Axio Observer Z1 with an incorporated camera and using Zeiss software (Zeiss, Germany). Cells nuclei were stained with DAPI (blue colour) and blood vessels observed due to Evans Blue dye (red colour).

Body weight and blood glucose and triglycerides levels

In overnight fasted rats, body weight was recorded and glycemia [fasting and at 1 and 2 hours during intraperitoneal glucose tolerance test (IPGTT) using 1.8 g of glucose/Kg (Braun Medical, Portugal)] was measured using blood from the tail vein (Glucometer Elite from Bayer, Germany). The results were used to perform the area under the curve of IPGTT.

In six hours fasted animals, insulin (0.25 UI/Kg) (100 UI/mL, Humulin – Lilly, USA) was intraperitoneally injected to study insulin sensitivity, being glycemia measured before and 15', 30', 60' and 120' after injection (Glucometer Elite from Bayer, Germany). The results were used to calculate the area under the curve of intraperitoneal insulin tolerance test (IPITT).

After overnight fasting, tail vein-derived blood was used to determine serum triglyceride content using specific reactive test stripes (Accutrend Plus - Roche, Germany).

Serum and plasma samples collection

Immediately before sacrifice, animals were submitted to intraperitoneal anaesthesia using chlorpromazine (3 mg/Kg body weight, Laboratórios Vitória, Portugal) and ketamine (75 mg/Kg body weight, Pfizer Inc., USA) and blood samples were collected through cardiac puncture. The blood collected was divided to BD Vacutainer and BD Vacutainer K3E (BD, UK), then centrifuged (15' at 3500 rpm and 4ºC) in order to isolate serum and plasma samples, respectively, which were aliquoted and stored (ultra-low freezer -80ºC) for further analysis.

Tissue collection

Under anaesthesia effect, the sacrifice was done by cervical displacement and the abdominal cavity was open using forceps and a surgical scalpel. The internal organs were exposed and pEAT was collected. In turn, skeletal muscle was excised using scissors and forceps from inner thigh. Both tissues were immediately stored in ultra-low freezer (-80ºC) or in 10% formalin (overnight at room temperature) and subsequently in 70% ethanol until paraffin inclusion.

Adipose tissue GSH levels

GSH levels were determined using the Glutathione assay kit (Merck, USA). Firstly, 150 mg of pEAT were rapidly frozen in liquid nitrogen to obtain a fine powder. Then, 100 mg of pEAT powder were vortexed with 300 μL of 5% 5-sulfosalicylic Acid (SSA) solution. Solution was completed with 700 μl and samples were homogenized with a potter and piston, kept on ice during 10' and centrifuged (10' 10000 rpm at 4ºC). The supernatant volume was collected and recorded to be used as the original sample volume in glutathione determination. Then, plate layout was created by pipetting blank reagent (10 μL of SSA), standard curve (10 μL of several sample dilutions) and diluted samples (10 μL) [95 mM potassium phosphate buffer, pH=7.0, 0.95 mM EDTA, 0.038 mg/mL (48 μM) NADPH, 0.031 mg/mL DTNB, 0.115 U/mL glutathione reductase, and 0.24% 5-sulfosalicylic acid]. Using a multichannel pipette, 150 μL of working solution was added to each well and the plate kept undisturbed at RT during 5'. Subsequently, 50 μL of NADPH (0,16 mg/mL) were added to each well using a multichannel pipette and the absorbance was measured using a

microplate reader (Synergy HT - Biotek, USA) set to 412 nm with 1 minute of interval until 5 minutes. Consequently, the assay quantifies the nmoles of GSH per mL of sample, being presented as pmoles of GSH per gram of pEAT.

Serum and adipose tissue glyoxalase-1 activity

GLO-1 activity was measured through the GLO-1 activity assay kit (Sigma - Merck, USA), in native conditions, using serum samples diluted (1:2) and 50 mg of pEAT homogenized in 1 mL of ice-cold buffer (Tris 50 mM and NaCl 150 mM pH=8). Tissue homogenates were centrifuged (15' 14000 rpm 4ºC) and protein-rich supernatants were collected and kept on ice. The collected supernatants and diluted serum samples were divided (40 µL/each) into two independent centrifuge tubes, being one the sample reaction tube and the other the sample blank tube. Master mix (assay buffer plus MG plus GSH) was prepared as described and 160 µL were added to sample tubes and kept 20' at RT. The reaction was stopped and protein was precipitated by adding 70 µL of 4 M perchloric acid and tubes were kept on ice during 15'. Following this incubation, samples were centrifuged (5' 14000 rpm at 4ºC) and 200 µL of collected supernatant were placed on a 96-well UV microplate. In sample blank tubes the protein was initially precipitated by adding 70 µL of 4 M perchloric acid on ice during 15'. After that, 160 µL of master mix was added and tubes were undisturbed for 20' at RT. As before, sample blank tubes were centrifuged (5' 14000 rpm at 4ºC) and supernatants collected to 96 well UV multiwell plate. Using a microplate reader (Synergy HT - Biotek, USA) the absorbance was recorded at 240 nm, and the results were calculated and expressed as units per gram of pEAT (one unit of GLO-1 is the amount of enzyme that

convert one μmole of S-lactoylglutathione from MG and GSH per minute at pH=6.6 and 25ºC).

Western Blotting

Sample preparation: as before, pEAT (300 mg) and skeletal muscle (100 mg) collected and stored as previously desbribed, were homogenized in 1 mL of ice-cold lysis buffer [0.25 M Tris-HCl; 150 mM NaCl; 1% Triton X-100; 0.5% SDS; 1 mM EDTA; 1 mM EGTA; 20 mM NaF; 2 mM Na3VO4; 10 mM β-glycerophosphate; 2.5 mM sodium pyrophosphate; 10 mM PMSF and 40 μL of proteases inhibitor cocktail/g of tissue (Merck, EUA), pH=7.7] as described (Matafome et al., 2012; Rodrigues, 2013). The whole cell lysates were collected to centrifuge tubes and were always kept on ice. This was followed by centrifugation (14000 rpm 20' 4ºC), which allowed the separation of lipids (top layer), membranes and nucleic acids (bottom pellet), and supernatant (protein-rich fraction), being the last collected into a new centrifuge tube. Then, supernatants were aliquoted and stored (-80ºC) and protein quantification was performed following manufacturer instructions (Thermo Fisher Scientific, USA). Additionally, samples were diluted 1:2 with 2 times concentrated laemmli buffer [62.5 mM Tris, 1% SDS, 1.25 mL glycerol, 0.01% (w/v) bromophenol blue, pH=6.8] and calculations were made in order to load 40 μg of protein in each well. Finally, samples were sonicated (5'' and 50% amplitude), boiled (3' at 95-100ºC) and vortexed immediately before the loading into the polyacrylamide gel.

Vertical electrophoresis (SDS-PAGE): using specific equipment (BIO-RAD, USA), the polyacrylamide gels (4-15%, 0.75-1.5 mm 10 wells) were done using the solutions of resolving (0.75 M Tris-HCl, 0.2% SDS, pH=8.8) and stacking (0.25 M Tris-HCl, 0.2% SDS, pH=6.8) plus acrylamide, Milli-Q water, ammonium persulfate and TEMED. Resolving

solution (6-15% of acrylamide) was polymerized in the bottom and few drops of propanol solution were used to avoid air bubbles. After polymerization and propanol removal, stacking solution (4% of acrylamide) was added and wells formed. After stacking polymerization, the electrophoresis system was filled with running buffer (125 mM Tris-base, 480 mM glycine, 1% SDS, pH=8.8), the precision plus protein standard (BIO-RAD, EUA) and samples loaded into the wells, being the voltage always constant during protein migration. Thus, the protein separation in denaturing conditions allowed its separation accordingly to the molecular weight, which was followed by using a precision plus protein standard and bromophenol-blue indication.

Protein transference from acrylamide gel to PVDF membrane: PVDF membranes (GRiSP Research Solutions, Portugal) were activated in methanol (30''), hydrated in Milli-Q water (1') and maintained (30') in CAPS solution (50 mM CAPS, 2% NaOH, 10% methanol, pH=11) until transfer sandwich assembly. Using a transfer system (BIO-RAD, USA), the proteins were moved from polyacrylamide gel to the PVDF membrane with constant amperage (750 milliamperes 1-3 hours). After protein transference, the membrane was quickly washed with TBST solution (250 mM Tris, 1.5 mM NaCl pH=7.6 plus 0.5% Tween20), blocked (1-2h) with albumin solution (5% albumin in TBS solution) and washed again (30'-1h) with TBST solution.

Incubation with antibodies: primary antibodies against our target proteins were diluted (TBST solution 0.01% Tween20 plus 0.05% BSA) to working concentration, being the membranes incubated overnight at 4ºC. After this, membranes were washed (1h) in TBST solution at room temperature. Secondary antibodies were diluted to working concentration (TBST solution 0.01% Tween20 plus 0.05% BSA), and used (2h at RT) in accordance to the required target, including anti-mouse (GE Healthcare, UK), anti-rabbit and anti-goat (Bio-

Rad, USA). Finally, membranes were washed (2h at RT) using TBST solution which was completely replaced tree times.

Bands acquisition and quantification: membranes were revealed using ECL substrate (GRiSP Research Solutions, Portugal) in a Versadoc system (BioRad, USA) and analyzed with Image Quant® (Molecular Dynamics, USA). Results were calculated and presented as %Ct/loading control.

Plasma free fatty acids levels

Using plasma samples, FFA were assessed using the FFA assay kit (ZenBio, USA). Briefly, non-esterified fatty acids were converted into fatty acyl-CoA thiol esters by Acyl-CoA synthetase plus ATP, Mg, and CoA. Then, acyl-CoA derivatives plus oxygen and AcylCoA oxidase produced hydrogen peroxide. Subsequently, peroxidase induced the oxidative condensation of 3-methyl-N-ethyl-N-(β-hydroxyethyl)-aniline with 4-aminoantipyrine, which formed a purple product that absorbed light, which was further calculated from the optical density measured at 540-550 nm (Synergy HT - Biotek, USA and ZenBio, NC, USA).

Plasma insulin levels

Briefly, insulin levels (pg/mL) of plasma samples were assessed through a solid phase two-site enzyme immunoassay rat insulin ELISA kit (Mercodia, Sweden). Basically, two different monoclonal antibodies against different insulin epitopes were used to target insulin. Then, peroxidase-conjugated anti-insulin antibodies converted 3,3',5,5'-tetramethylbenzidine (TMB) to a colorimetric product, measured spectrophotometrically at 450 nm (Synergy HT - Biotek, USA).

Serum adiponectin and leptin levels

Serum adiponectin (µg/mL) and leptin (ng/mL) were determined using, respectively, the Rat Adiponectin immunoassay kit and Rat Leptin immunoassay kit (Thermo Fisher Scientific, USA). Briefly, these solid-phase ELISA sandwiches use immobilized antibodies against adiponectin and leptin in pre-coated wells of the supplied microplates. The solid-phase ELISA sandwiches were further completed by adding an enzyme-linked secondary antibody and TMB as enzyme substrate, which produced a measurable signal at 450 nm (Synergy HT - Biotek, USA) proportional to adiponectin or leptin levels.

Histological colorimetric assays and adipocyte area

Paraffin-embedded tissue sections (4µm) of pEAT (n=3/group), were submitted to paraffin removal processes, using xylol (3x3' at RT) and subsequently, progressive hydration (EtOH 100%/70%/30% 1x3'/each and Milli-Q water 1x3' at RT). Tissue sections were blocked (10% goat serum in PBS, 30'-1h at RT) and stained with Periodic Acid-Schiff (PAS) or Masson Trichrome staining in order to identify glycated material and fibrosis, respectively. After this, tissue sections were washed again and coverslips were mounted using mounting medium (DAKO, Japan). Finally, images (100X) were captured in a Zeiss microscope with incorporated camera (Germany). These images were also used to determine mean adipocyte area (the number of adipocytes was determined in at least 10 fields/slice).

Immunohistochemistry

Briefly, after sequential paraffin removal as described before, tissue sections were washed (3x5' with PBS 0.05% Tween20 at RT), blocked (10% goat serum in PBS, 30'-1h at RT) and incubated overnight (at 4ºC) with primary antibodies against specific epitopes of pimonidazole adducts, CEL and F4/80, which were diluted in PBS (supplemented with 0.01% BSA). Always at RT, sections were washed (3x5' with PBS 0.05% Tween20) and incubated with secondary antibodies peroxidase-linked during two hours (IHC peroxidase Kit, Chemicon, USA). After washing (3x5' with PBS 0.05% Tween20), DAB (diaminobenzidine) was used as substrate, being the excess removed (3x5' with PBS 0.05% Tween20). Finally, sections were stained with hematoxylin, washed (3x5' with PBS 0.05% Tween20) and coverslips were mounted using mounting medium (DAKO, USA). The images were acquired using a morphometric microscope with an incorporated camera and Zeiss software (Zeiss, Germany).

3. Human study

3.1 Study design and groups

After approval from the Ethical Comittee of CHUC and FMUC, patients have been consecutively informed and recruited to a prospective and longitudinal study entitled "*Estudo Anátomo-Morfológico do Tecido Adiposo na Obesidade*". This cohort of patients (diabetic and non-diabetic) attending general or obesity surgery consultation was developed at Serviço de Cirurgia - *Centro Hospitalar e Universitário de Coimbra – Hospital Geral - Covões"* (CHUC - CHC). The inclusion criteria were adjusted to metabolic/bariatric surgical criteria, but only patients aged between 25 and 65 years old were included. The exclusion criteria were active inflammatory and chronic diseases, including neurodegenerative diseases and active tumours. Patients submitted to previous restrictive (sleeve gastrectomy) or mal-absorptive (gastric bypass or duodenal switch) surgical procedures were excluded, as well as patients under type 2 diabetes medication other than metformin, including GLP-1 analogues, DPPIV inhibitors or insulin.

A total of 140 obese patients (113 women and 27 men) were divided into four groups according to fasting glucose, HbA1c and the homeostasis model assessment 2 insulin resistance index Ox-HOMA2IR (Oxford, UK). Thus, insulin sensitive and normoglycemic patients (Ox-HOMA2IR<1) were allocated to insulin sensitive group (insulin sensitive – IS group, n=20). Insulin resistant patients (Ox-HOMA2IR>1), but normoglycemic (fasting glycemia<100mg/dL and HbA1c<5.7%) were included in the insulin resistant and normoglycemic group (IR normoglycemic group, n=66). Additionally, all insulin resistant patients (Ox-HOMA2IR>1) with fasting blood glucose between 100 and 125 mg/dL or HbA1c between 5.7% and 6.4% were further allocated to prediabetes group (IR pre-diabetic group, n=34). Type 2 diabetic patients, diagnosed or with clinical presentation (fasting blood

glucose superior to 125 mg/dL or HbA1c superior to 6.4%) were included in type 2 diabetes

group (IR Diabetic group, n=20).

3.2 Clinical data and sample collection

Firstly, in the day before surgery, patients were submitted to a comprehensive clinical evaluation and data collection. Fasting peripheral blood was collected, and serum and plasma isolated and stored (at -80 ºC) for further analysis. Blood analysis included a broad range of general clinical parameters, including fasting glucose, insulin, HbA1c, HDL cholesterol and triglycerides, by automatic analyser as well as adiponectin and leptin by DuoSet ELISA kits. Additionally, using software developed by Oxford University, Ox-HOMA2IR index as well as the percentage of insulin sensitivity (%S) and β-cell function (%β) were calculated from fasting glucose and insulin levels (Oxford, UK). During surgery intervention, visceral white AT samples were collected from obese patients undergoing elective abdominal surgery (cholecystectomy for uncomplicated biliary calculi) and/or bariatric/metabolic surgery. Clinical data was inserted into a dedicated data base using SPSS Statistics software, version 24.0 (IBM, USA).

3.3 Blood and adipose tissue analysis

Serum adiponectin and leptin levels

Using DuoSet ELISA kits (R&D Systems, USA), we developed sandwich immunoassays in human serum samples. Firstly, high binding plates (Corning, USA) were incubated overnight at RT with adiponectin and leptin capture antibodies. Unlinked antibodies were washed out with 400 μL 3*5' PBS, being the blockage (300 μL/well of PBS 1% BSA 1h at RT) performed and washing step repeated again to remove unlinked BSA. Subsequently, immobilized antibodies targeted standards with known concentrations as well as diluted (1:5000 for adiponectin and 1:200 for leptin) serum samples, loading 100 μL/well 2 hours at RT. After PBS wash (400 μL 3*5'), ELISA sandwich was completed by detection antibody incubation during 2 hours at RT, being the plate washed again (400 μL 3*5' PBS), to remove unlinked detection antibodies. Streptavidin-HRP (100 μL) was incubated 20' at RT and protected from direct light. The plate was washed again with 400 μL 3*5' PBS, being 100 μL of substrate solution added 20' at RT and protected from light. Stop solution (50 μL) was added to each well and plate was read using a plate reader (Synergy HT - Biotek, USA) set to 450 nm, corrected to 540 nm. The results were plotted using a computer software able to generate a four parameter logistic curve-fit.

Adipose tissue glioxalase-1 activity assay

GLO-1 activity in human visceral AT was determined using an enzymatic assay (Sigma - Merck, USA) and the method was described in chapter 3 and section 2.2.

4. *Ex vivo* angiogenic assays

4.1 Aortic ring angiogenis assay

The formation of new blood vessels from existing ones is a complex process known as angiogenesis. Aortic ring assay was a valuable tool to understand angiogenic processes and involved mechanisms. It was developed by Nicosia and collaborators and recently updated in order to become more versatile (Aplin and Nicosia, 2015; Aplin et al., 2008; Nicosia et al., 1982). This assay was implemented in our laboratory and further adapted to our experimental conditions and models. Briefly, aortic rings from rat aorta are subsequently embedded in specific matrices, that allow the formation of new sprouting vessels. In fact, the aortic rings allow time-dependent and factor-dependent growth or regression of new sprouting microvessels, which may be observed by light microscopy during the assay and further quantified. Thus, the presence of the same cell types that are responsible for *in vivo* angiogenic process was very valuable to understand the elementary mechanisms of angiogenesis and yet, is nowadays recognized as a crucial tool to study angiogenesis and angiogenic factors (Aplin and Nicosia, 2015; Aplin et al., 2008; Baker et al., 2012).

In this assay, Wistar rats (4-8 weeks old) were submitted to anaesthesia and sacrificed by cervical displacement. After this, thoracic area was shaved and disinfected with EtOH 70%. Using disinfected forceps and a surgical scissor, internal organs were removed allowing aorta collection to a falcon tube containing ice-cold Opti-MEM supplemented with 1X Penicillin/Streptomycin (Pen/Strep) and 50 µM Gentamycin (Gent) (Thermo Scientific, USA).

Under supplementary sterile conditions working in a vertical laminar flow hood, aorta was dissected and washed several times using ice-cold Opti-MEM supplemented with 1X Pen/Strep and 50 µM Gent. Disinfected forceps and a surgical scissor were used to clean and

cut aortic rings, which were placed in a petri dish containing ice-cold Opti-MEM supplemented with 1X Pen/Strep and 50 µM Gent, until matrix inclusion.

Type 1 collagen from rat tail (Millipore - Merck, USA) was used as matrix, which was prepared on ice and always using ice-cold reagents. Concentrated type 1 collagen was diluted in high-glucose DMEM growth medium, containing phenol red indicator, to a final concentration of 1.5 mg/mL (Figure 3.8A-B). This solution presented a yellow colour (Figure 3.8B) and based on phenol red indicator this colour indicated a pH slightly acid. Thus, NaOH 0,1 M was used to change pH to marginally basic, which was identified by the pink colour solution (Figure 3.8C). Mixture was kept on ice to avoid premature type 1 collagen assembly. As quickly as possible, each aortic ring was embedded in 60 µL of collagen type 1 mixture in a 96 well plate (Corning, USA) using clean forceps. Experimental conditions were created in the centre of the plate, being the remaining wells filled with PBS solution to prevent plate dehydration. Plate was undisturbed 15' in the laminar flow hood. However, to complete collagen assembly, plate was kept 30' inside a cell incubator at 37ºC and 5% CO_2.After collagen assembly, 150 µL of warm (37ºC) Opti-MEM supplemented with 2,5% FBS (Gibco - Thermo Fisher Scientific - USA) and antibiotics (1X Pen/Strep and 50 µM Gent) were added to each well. Half of the culture medium volume was replaced every second day until the end of the experiment. Images were captured in a Zeiss Axio Observer Z1 with an incorporated camera and using Zeiss software (Zeiss, Germany). However, image processing and quantifications were done in ImageJ software (USA) using Wacom Intuos Pro (software version 6.3.21-7, Japan).

In order to study MG effects on aortic ring angiogenesis assay, experimental conditions were created through the incubation of aortic rings with supplemented culture medium plus MG (50 µM, 100 µM, 250 µM, 500 µM and 1000 µM from Sigma - Merck, USA), (n=6 explants/condition and n=3 independent experiments).

4.2 Adipose tissue angiogenesis assay

Adipose tissue angiogenesis assay

In the past, the study of angiogenic process was based on *in vitro* models in order to study new mechanisms, or more recently, allowing faster drug screenings regarding angiogenic effects. Nonetheless, several significant achievements have been derived from the aortic ring angiogenesis assay, which is much more complex, reproduce important mechanisms and processes, namely those involving the interplay between several cell types.

On the other hand, the AT angiogenesis assay has been developed as an adaptation of the aortic ring angiogenesis assay, in order to explore AT-specific mechanisms and processes. This assay was firstly developed using human and mice AT samples, and showed the relationship between AT angiogenic capacity and metabolic and physiological conditions from the donor. Interestingly, the assay also demonstrated that angiogenic capacity is fat depot-dependent and may be changed by several factors, namely insulin resistance. Consequently, this assay became a crucial tool to identify and characterize endogenous and exogenous factors with pro/anti-angiogenic actions in AT vasculature. However, Corvera's group was not able to develop this assay using AT explants from rat (Gealekman et al., 2008, 2011; Rojas-Rodriguez et al., 2014).

Most of our research models of obesity and type 2 diabetes are developed using rat strains, including experimental models submitted to specific diets, pharmacological factors or surgical approaches. Based on in vivo experiments using rat models, we also formulated several hypothesizes regarding impaired AT angiogenesis and blood flow. Altogether, these reasons were our driven to develop a new optimized protocol to study rat pEAT angiogenesis.

Development of rat adipose tissue angiogenesis assay using matrigel matrix

First of all, we followed the initial protocol developed by Corvera's group, using pEAT explants (~1 mm^3) from rats aged between 9-23 weeks (Gealekman et al., 2008; Rojas-Rodriguez et al., 2014). Although we have been able to see several sprouts from AT explants in matrigel matrix, after several weeks of protocol optimizations the results were not satisfactory and the increase in sprouting formation was not consistent (Figure 3.5A). To improve sprouting formation, we decreased rat's age (4-5 weeks old) in order to increase cell proliferation potential; in fact, it was observed a slightly rise of angiogenic capacity, but still insufficient. We also confirmed that supplemented endothelial growth medium (EGM-2MV, from LONZA - USA) was better than dulbecco's modified eagle's medium (DMEM, from Gibco - Thermo Fisher Scientific - USA) supplemented with 10% fetal bovine serum (FBS, from Gibco - Thermo Fisher Scientific - USA) (Figure 3.5B). Additionally, knowing that hypoxia is a crucial stimulus to angiogenesis, we developed the assay under hypoxic conditions (1% and 11%), but once again the results were not satisfactory (Figure 3.5C-D) and in several explants sprouting formation was not observed. Altogether, these experiments revealed that this assay is highly sensitive to rat age, technical procedures and temperature. However, even after several experimental improvements, sprouting formation was not consistently preserved between the explants/experiments. Consequently, we were forced to rethink the protocol and all the reagents used, as well as to search for detailed information about this type of assay in literature.
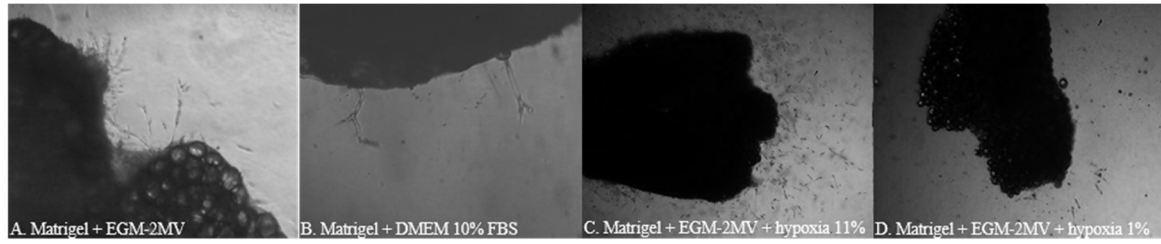
Figure 3.5 - Rat adipose tissue angiogenesis assay development using matrigel matrix

The figure shows representative image of pEAT explants capillarization, which were collected from Wistar rats (4-5 weeks old) embedded in matrigel matrix. Then, explants were submitted to several experimental conditions, including EGM-2MV (A), DMEM plus 10% FBS (B) and EGM-2MV plus hypoxia 11% (C) and 1% (D). EGM-2MV - supplemented endothelial growth medium; DMEM - dulbecco's modified eagle's medium; FBS - fetal bovine serum.

Rat adipose tissue angiogenesis assay using collagen type 1 matrix

Subsequently, we designed a new protocol based on the aortic ring assay and AT angiogenesis assay, originally developed by Nicosia and Gealekman and respective collaborators (Aplin and Nicosia, 2015; Aplin et al., 2008; Baker et al., 2012; Gealekman et al., 2008; Rojas-Rodriguez et al., 2014). Thus, based on our protocol and previous experiments, we introduced some alterations in order to achieve reproducible and consistent results. Primarily, the replacement of matrigel matrix for type 1 collagen from rat tail (Millipore -Merck, USA), which is not supplemented with growth factors, the manipulation is easier, the visibility using light microscopy is better and concentration may be changed in order to adjust physical properties (Figure 3.6).
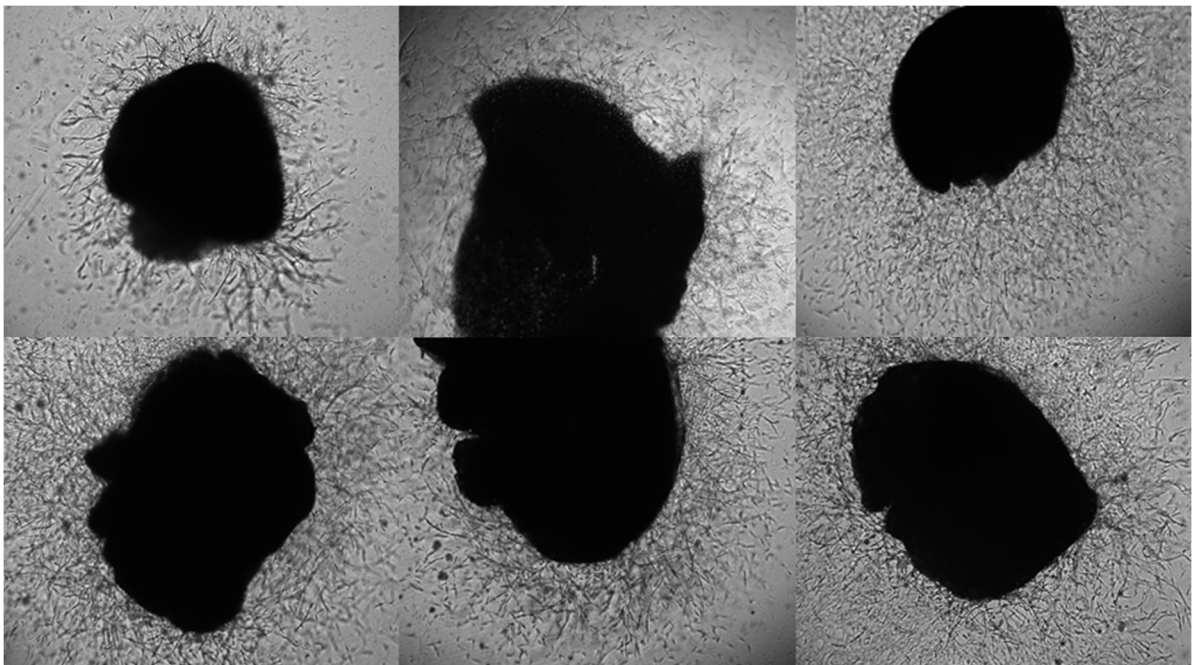
Figure 3.6 – Improved rat adipose tissue angiogenesis assay using collagen matrix
The figure shows representative image of optimized rat pEAT angiogenesis assay. Explants from Wistar rats (4-5 weeks old) were embedded in collagen type 1 matrix (1-2 mg/mL), fed with EGM-2MV and image were taken 4-6 days later. EGM-2MV - supplemented endothelial growth medium.

Optimized protocol for rat adipose tissue angiogenesis assay

After optimization, the rat AT angiogenesis assay used pEAT from Wistar rats 4-5 weeks old. The animals were sacrificed by cervical displacement, the abdominal area was partially disinfected by EtOH 70% and then, the cavity was opened using disinfected forceps and a surgical scalpel. The internal organs were exposed and pEAT was collected using disinfected forceps and a scissor. The collected AT was immediately introduced in a 50 mL falcon with 30 mL of sterile ice-cold basal EGM (Lonza – USA) supplemented with 1X Pen/Strep (Gibco - Thermo Fisher Scientific - USA) and 50 µg/mL of Gent (Gibco - Thermo Fisher Scientific - USA).

Using a vertical laminar flow hood, the tissue was washed tree times in petri dishes with sterile ice-cold basal EGM supplemented with Pen/Strep and Gent (Figure 3.7A). Using sterilized forceps and a surgical scalpel, the pEAT was cut in small pieces (~1mm^3), commonly referred as explants, which were placed in a petri dish containing ice-cold basal EGM supplemented with Pen/Strep and Gent (Figure 3.7B-H). Immediately before embedding in collagen matrix, pEAT explants were placed in the centre of the well of a 96 well plate (Corning, USA) (Figure 3.7I).
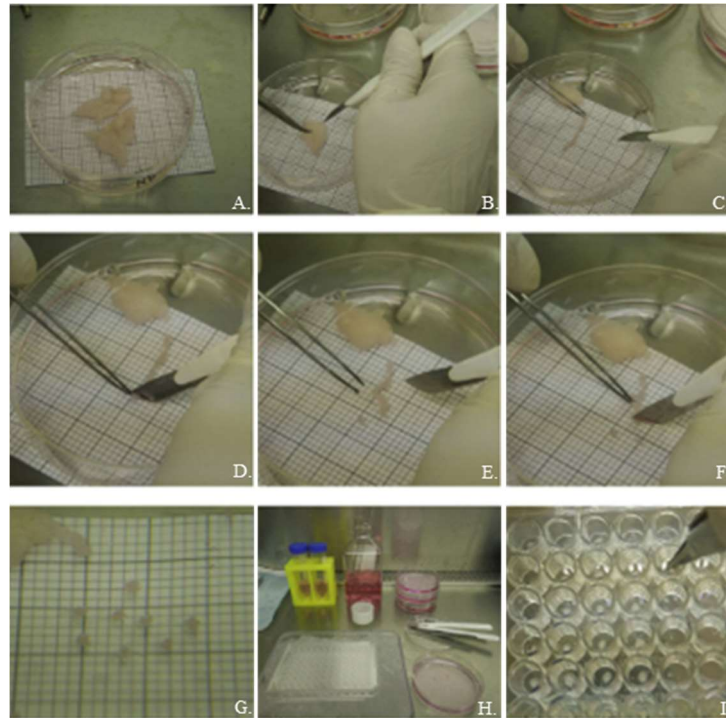
Figure 3.7 – Preparation of rat-derived periepididymal adipose tissue explants

The figure shows representative image of pEAT explants preparation and plate distribution. AT was washed 3 times with ice-cold EGM suplemented with antibiotics (A), explants were prepared using scalpel blade and forceps (B-F), sellected by volume (G) collected to a petri dish with fresh EGM (H) and subsequently distributed in 96-well microplate (I). EGM – basal endothelial growth medium. Adapted from Rojas-Rodriguez et al. 2014.

In turn, the matrix solution was prepared with ice-cold reagents and was always kept on ice in order to delay collagen assembly. Firstly, type 1 collagen was diluted in high-glucose DMEM growth medium to a final concentration of 1.5 mg/mL (Figure 3.8A). This mixture resulted in a yellow solution (Figure 3.8B). Based on phenol red indicator, this colour indicated a pH slightly acid that was adjusted using NaOH 0.1 M to achieve a physiological pH identified by the pink colour ((Figure 3.8C).

The embedding process was done by adding one AT explant to a flat-bottom 96-well plate (Corning, USA) and 60 µL of recently prepared collagen solution. Although ice-cold solution delayed temporarily the collagen assembly, small pEAT explants were embedded as fast as possible in order to avoid early assembly and matrix damage. After embedding all explants, the plate was left undisturbed in the laminar flow hood 15' in order to allow partial collagen assembly. The explants were mostly distributed in the centre of the plate and the remaining wells were filled with DMEM supplemented with Pen/Strep and Gent in order to prevent dehydration and temperature changes (Figure 3.8D). The assembly process was only completed after 30' in a cell incubator (37ºC and 5% CO_2).
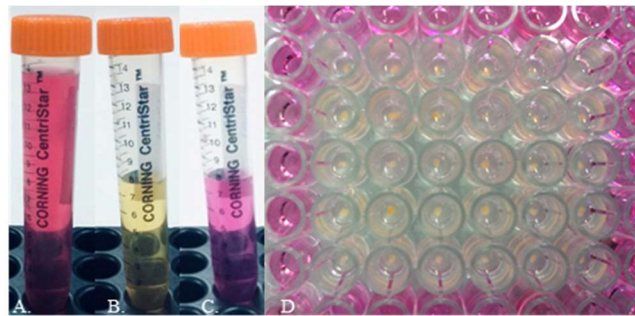
Figure 3.8 - Collagen type 1 matrix preparation and embedding process

The figure shows representative image of collagen dilution and plate preparation. Collagen type 1 from rat tail was diluted in DMEM with phenol red indicator (A), leading to a yellow solution (B). This solution was kept on ice and pH was slightly adjusted with NaOH to a pink colour solution (C), and explants were embedded using 60 µL of recently prepared collagen solution. - EGM - basal endothelial growth medium; DMEM - dulbecco's modified eagle's medium; NaOH – sodium hydroxide.

Supplemented growth medium (EGM-2MV - fetal bovine serum, Gent, human epithelial growth factor, hydrocortisone, human fibroblast growth factor, VEGF, R3-insulin growth factor, ascorbic acid) was added (150 µL/each well) at 37ºC. The different conditions studied

in this assay were done through the dilution of several factors in EGM-2MV growth medium, which were compared to EGM-2MV and EGM-2MV plus the vehicle (PBS/DMSO). During the time of the assay, the growth medium was changed every second day (half of the total volume).

Images were captured in a Zeiss Axio Observer Z1 with an incorporated camera and using Zeiss software (Zeiss, Germany). Image processing and quantifications were done in ImageJ software (USA) and using Wacom Intuos Pro (software version 6.3.21-7, Japan). Representative image are shown (Figure 3.9A-C). The area of capillarization was calculated and normalized for explant area (Figure 3.9A). Tubular (sprout) length was also determined as a measure of cell organization and capillary integrity as described before (Santos-Oliveira et al., 2015)(Figure 3.9B). Regarding vessel density, images were transformed in black/white images by applying a standard threshold, which allowed the quantification of signal intensity in the area of capillarization (Figure 3.9C).
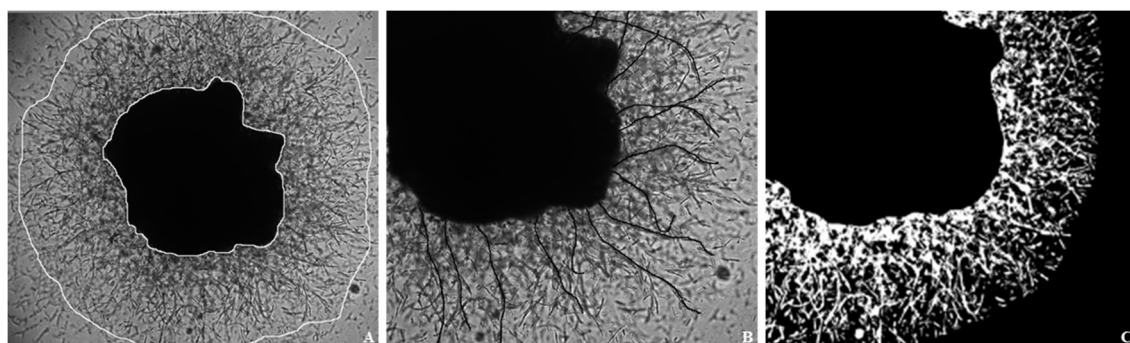
Figure 3.9 – Quantification of rat adipose tissue angiogenesis assay
The figure shows representative image of rat AT angiogenesis quantifications, using ImageJ software (USA) and three different approaches: area of capillarization normalized to explant area (A); Sprout length (B); vessel density (C). Explant was embedded in collagen type 1 matrix (1.5 mg/mL), fed with EGM-2MV and image were taken 6 days later. EGM-2MV - supplemented endothelial growth medium.

In order to study glycation-derived effects on AT angiogenesis, the AT explants were incubated with control medium/DMSO vehicle or MG (50 µM, 100 µM, 250 µM, 500 µM and 1 mM from Sigma - Merck, USA), GLO-1 inhibitor s-p-bromobenzylglutathione cyclopentyl diester (BBGC 20 µM from Sigma - Merck, USA) and with BBGC 20 µM in combination with MG 250 µM (n=6 explants/condition and n=3 independent experiments). Regarding pEAT angiogenesis, liraglutide-mediated effects were explored in preventing MG-induced impairment. Thus, AT explants were exposed to liraglutide (Lira - 50 nM), GLO-1 inhibitor (BBGC - 10 µM) and MG (MG - 250 µM) as well as respective combinations (Lira 50 nM + BBGC 10 µM and Lira 10 nM + MG 250 µM).

Human adipose tissue angiogenesis assay

Human visceral adipose tissue angiogenesis assay was firstly developed by Corvera's group (Gealekman et al., 2011; Rojas-Rodriguez et al., 2014). We were able to develop human AT angiogenesis assay, using the same conditions for rat adipose tissue angiogenesis assay and achieving sustained sprout formation (Figure 3.10). Such protocols may allow future studies of the angiogenic process and factors in human samples.
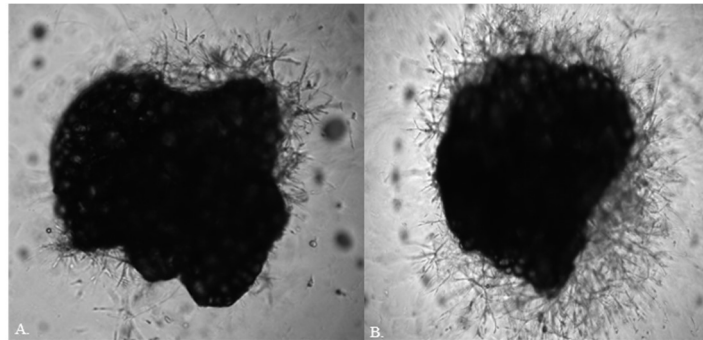
Figure 3.10 - Human adipose tissue angiogenesis assay
Visceral AT excised from a human obese donor during a bariatric/metabolic surgery procedure. The ex vivo assay was developed during eight days in matrigel matrix (A) and type 1 collagen matrix (1.5 mg/mL) (B) and both were maintained with supplemented endothelial growth medium and representative images (50X) are shown.

5. Statistical analysis

5.1 Animal model studies

All data are presented as mean ± SEM per group. Given the relatively small sample size (n=6-12), the non-parametric Kruskal-Wallis test (all pairwise multiple comparisons) was applied to determine all statistical differences between the groups, using the SPSS Statistics software, version 24.0 (IBM, USA). The alpha level of significance for all experiments was 0.05 and $p < 0.05$ was considered as the criterion for significance.

5.2 Human study

Patients data was collected to SPSS statistics software, version 24.0 (IBM, USA). All the data are shown as median and interquartile range (IQR) per group, being descriptive statistics and sample size the factors followed to apply non-parametric statistical tests. Additionally, non-parametric hypothesis tests and Spearman's correlations were applied, alpha level of significance for all experiments was 0.05 and $p < 0.05$ was considered as the criterion for significance.

Chapter 4 - RESULTS AND DISCUSSION

1. Glycation-induced impaired adipose tissue expandability and function

1.1 Results

Based on previous data regarding MG effects on adipose tissue, we formulated a scientific question: is MG-induced glycation able to impair adipose tissue microvasculature and expandability, leading to metabolic dysregulation?

Consequently, we hypothesized reduced periepididymal adipose tissue capillarization, blood flow and expandability, that may increase tissue hypoxia and dysfunction, contributing to metabolic dysregulation and insulin resistance in MG-treated animals challenged with a high-fat diet.

In order to evaluate MG-induced AGE accumulation during periepididymal adipose tissue expansion, we developed an animal model maintained with a high-fat and supplemented with MG, which was compared to a model of endogenous glycation (type 2 diabetic GK rats). Adipose tissue vasculature and function were studied as well as systemic metabolic alterations. A specific protocol of magnetic resonance imaging and adipose tissue angiogenesis assay have been developed to study adipose tissue blood flow and explore the role of MG-induced glycation in adipose tissue angiogenesis, respectively.

MG and HFD increases pEAT glycation, similarly to diabetic GK rats

GLO-1 is the key limiting enzyme in glyoxalase system. However, enzyme levels and activity may be changed, namely by oxidative status and insulin resistance. Serum-derived GLO-1 activity was significantly decreased in GK animals, when compared to Ct, MG and HFD groups ($p<0.05$ vs Ct and HFD; $p<0.01$ vs MG). Although GLO-1 activity in HFDMG group was significantly decreased when compared to MG group ($p<0.05$ vs MG), no alterations were observed in relation to Ct group (Figure 4.1A). Regarding GLO-1 activity and levels in pEAT, no alterations were seen between experimental groups (Figure 4.1A). Ne(carboxyethyl)lysine (CEL) is an AGE specifically derived from the MG reaction with lysine residues, which may accumulate in AT following local formation or intestinal absorption of MG-lysine adducts. Thus, CEL levels were significantly higher in HFDMG ($p<0.05$ vs Ct; $p<0.01$ vs HFD) and GK groups ($p<0.05$ vs HFD) (Figure 4.1B).
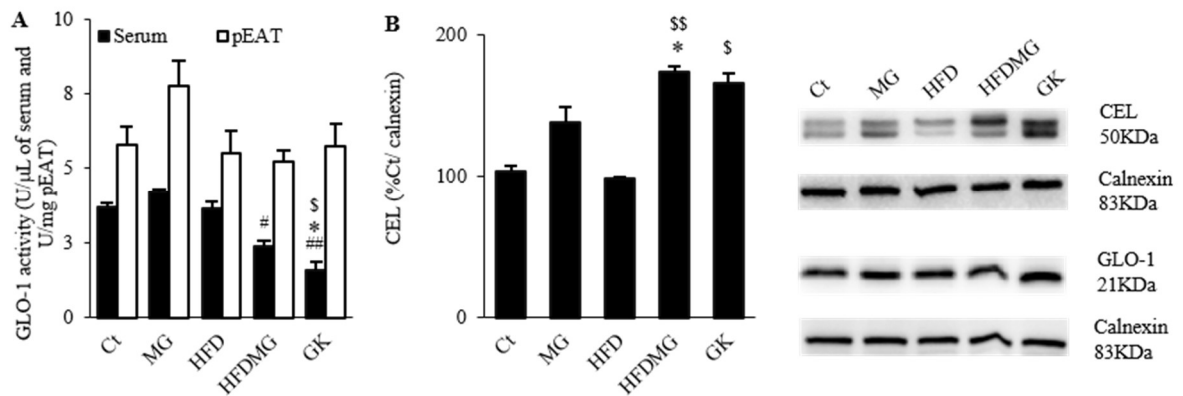
Figure 4.1 – Methylglyoxal-induced glycation and high-fat diet combination decreases serum glyoxalase-1 activity while increase CEL levels in pEAT, similarly to diabetic GK rats

Serum-derived (U/µL) and pEAT (U/g of pEAT) GLO-1 activity were evaluated using GLO-1 activity assay kit (A). CEL and GLO-1 levels in pEAT were calculated by WB (B) and representative WB images are shown (WB panel). Ct – Wistar rats twelve months old; MG – Wistar rats twelve months old with MG supplementation from eight to twelve months old; HFD – HF diet-fed Wistar rats from eight to twelve months old; HFDMG – HF diet-fed and MG-supplemented Wistar rats from eight to twelve months old; GK – Goto-Kakizaki rats twelve monts old. GLO-1 – glyoxalase-1; WB – western blotting; pEAT – periepididymal adipose tissue; CEL – Ne(carboxyethyl)lysine. Bars represent means ± standard error of the mean (SEM), n = 6-8/group. * vs Ct; # vs MG; $ vs HFD. 1 symbol $p<0.05$; 2 symbols $p<0.01$.

Glycation increases glycoconjugates and fibrosis in periepididymal adipose tissue

Increased PAS (glycoconjugates), Masson Trichrome (fibrosis) and CEL staining were observed in pEAT from MG-treated groups (MG and HFDMG) and non-obese type 2 diabetic GK rats, which are associated with AT dysfunction and decreased plasticity (Figure 4.2A-C). In accordance, macrophage marker F4/80 was also increased in MG-treated groups (MG and HFDMG) and in GK rats, suggesting increased inflammation in pEAT (Figure 4.2D).

A. Periodic Acid-Schiff (PAS) in pEAT (100X)
B. Masson Trichrome in pEAT (100X)
C. CEL in pEAT (100X)
D. Macrophage marker F4/80 in pEAT (100X)
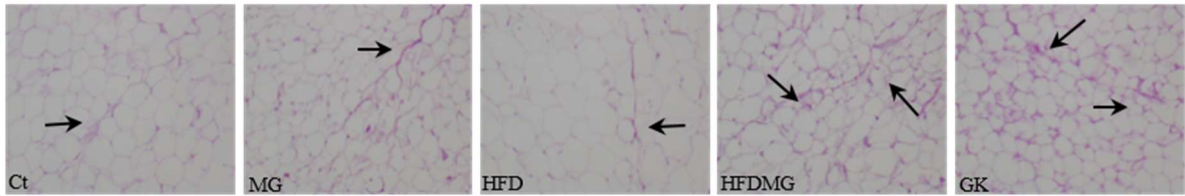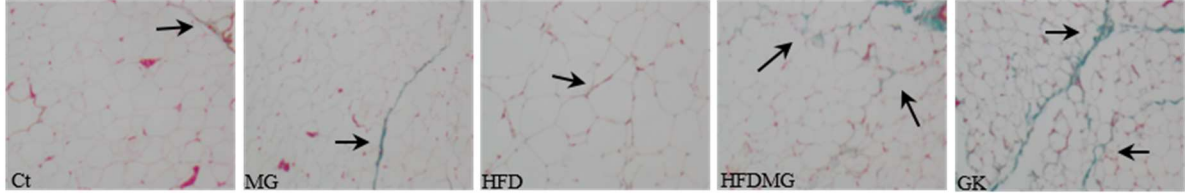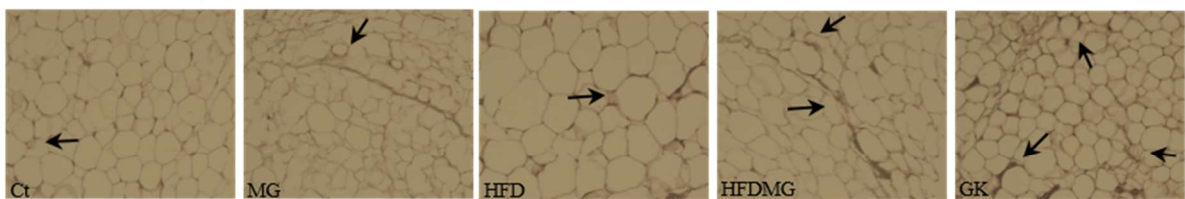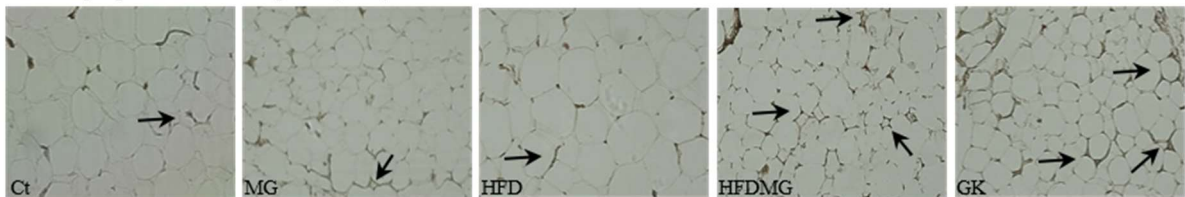
Figure 4.2 - Methylglyoxal-supplemented groups show increased glycation and fibrotic material as well as macrophage infiltration in periepididymal adipose tissue, similarly to GK rats

Histological analysis shows PAS (100X) (A) and Masson Trichrome (100X) (B). CEL (C) and F4/80 (D) IHC were performed in pEAT. Representative image are shown (A-D). Ct – Wistar rats twelve months old; MG – Wistar rats twelve months old with MG supplementation from eight to twelve months old; HFD - HF diet-fed Wistar rats from eight to twelve months old; HFDMG – HF diet-fed and MG-supplemented Wistar rats from eight to twelve months old; GK – Goto-Kakizaki rats twelve monts old. n = 6-8/group. IHC – immunohistochemistry; pEAT – periepididymal adipose tissue; PAS – periodic acid-schiff.

Glycation reduces periepididymal adipose tissue blood flow

For the first time, we were able to develop a procedure to evaluate AT blood flow *in vivo* using dynamic contrast-enhanced magnetic resonance imaging (DCE-MRI) (Figure 4.3A-C). The accumulation curve of the contrast product was evaluated during 34 minutes. The fold increase in relation to the basal signal was calculated at each dynamic scan and the AUC was determined. Enhancement curves of representative animals of each group (Figure 4.3A) have shown rapid contrast product accumulation in pEAT, which is higher in control rats and reduced in groups submitted to MG supplementation (MG, HFDMG). Accordingly, the AUC was significantly reduced in these groups and in GK rats, showing decreased pEAT blood flow (Figure 4.3B). Representative DCE-MRI image at baseline and dynamic 15 are shown (Figure 4.3C).
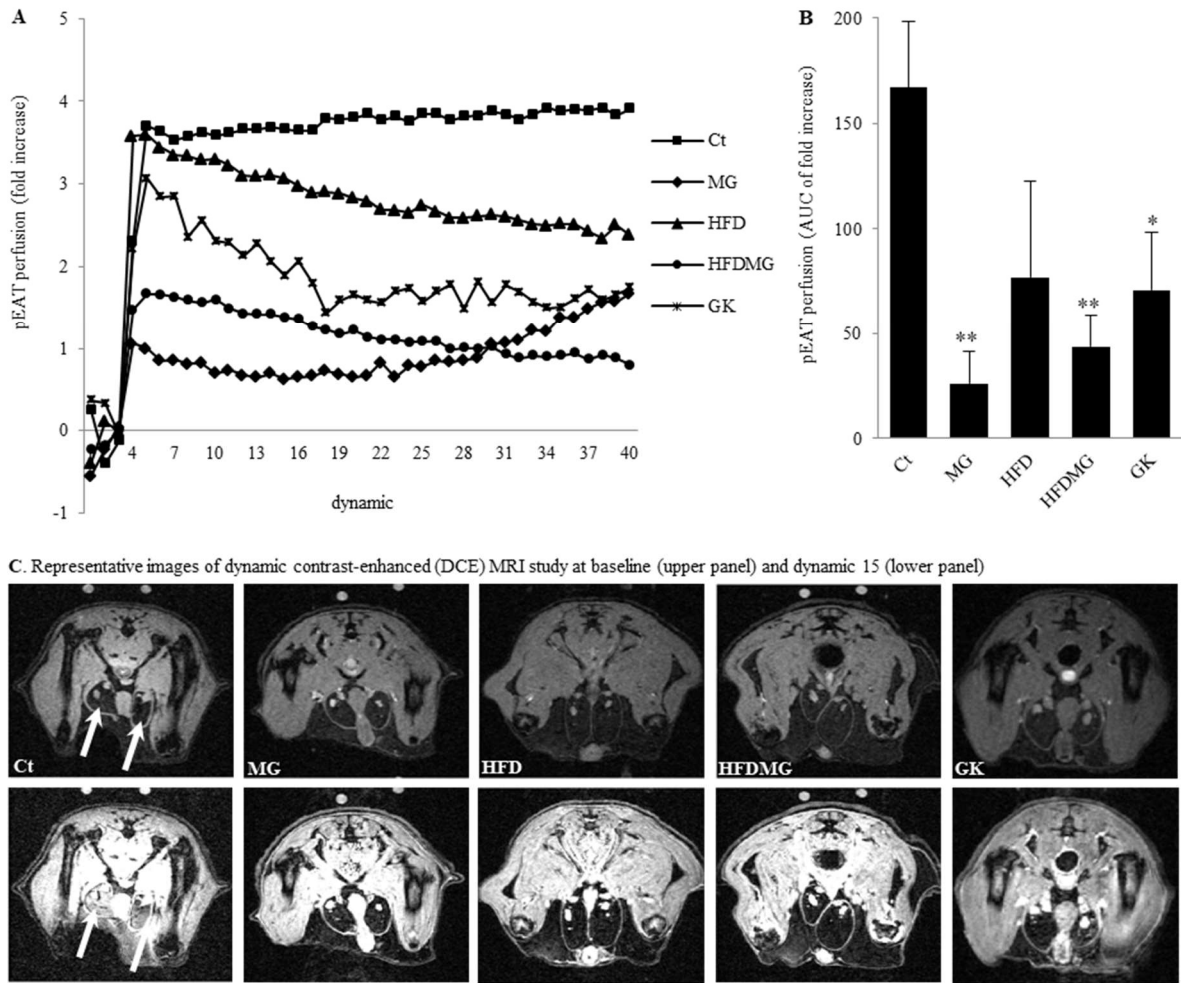
Figure 4.3 - Glycation decreases periepididymal adipose tissue blood flow

Blood flow was evaluated through the AUC of a DCE-MRI study (A-B). Representative image at baseline and dynamic 15 are shown (C). Ct – Wistar rats twelve months old; MG – Wistar rats twelve months old with MG supplementation from eight to twelve months old; HFD – HF diet-fed Wistar rats from eight to twelve months old; HFDMG – HF diet-fed and MG-supplemented Wistar rats from eight to twelve months old; GK – Goto-Kakizaki rats twelve monts old. AUC – area under the curve; pEAT – periepididymal adipose tissue; MRI – magnetic resonance imaging. Bars represent means ± SEM, n = 6-8/group. * vs Ct. 1 symbol $p<0.05$; 2 symbols $p<0.01$.

Glycation in diet-induced obese rats originates periepididymal adipose tissue hypoxia

Hypoxia was quantified through the accumulation of pimonidazole adducts, by WB and histological analysis. No significant differences were observed in HFD and MG groups (Figure 4.4A). However, the HFDMG ($p < 0.001$ vs Ct) and GK ($p < 0.05$ vs Ct) groups showed increased pimonidazole accumulation in pEAT (Figure 4.4A-B). Interestingly, pEAT hypoxia is present in a lean model of type 2 diabetes and increased in HFDMG group, suggesting impaired AT blood flow and hypoxia adaptation mechanisms.
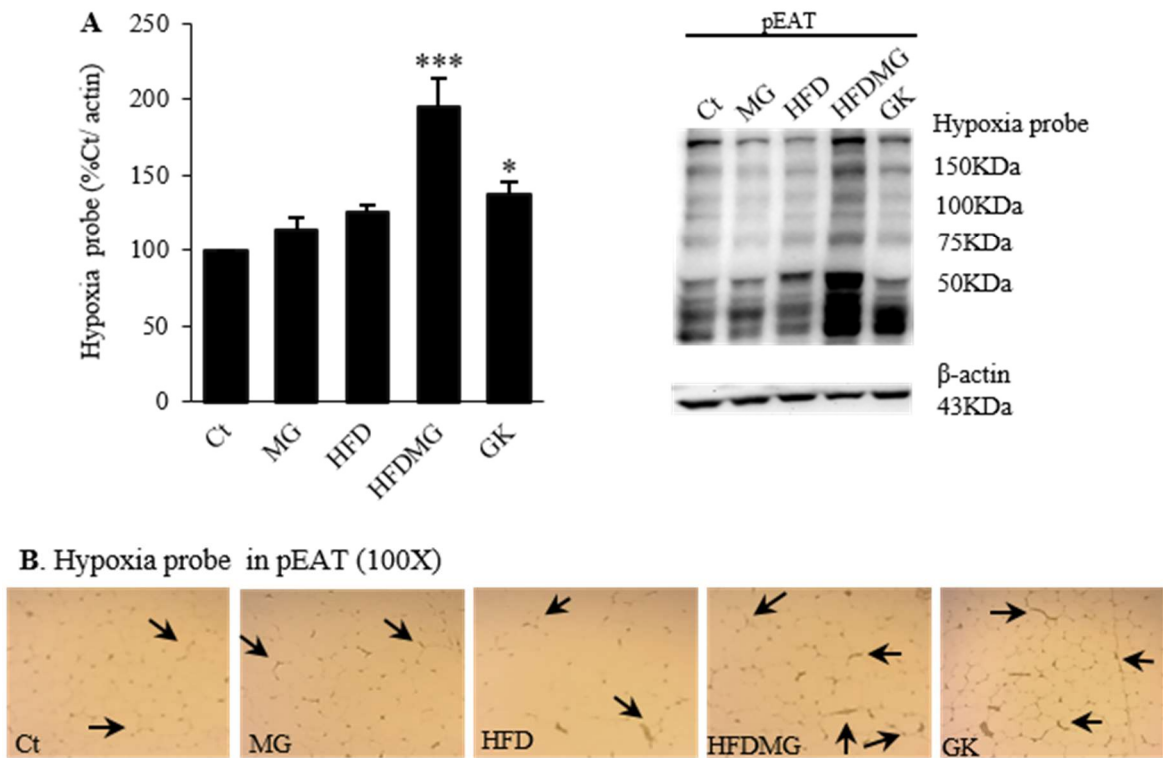
Figure 4.4 – Methylglyoxal-induced glycation combined with high-fat diet leads to periepididymal adipose tissue hypoxia

Hypoxia was assessed using an antibody against pimonidazole adducts by WB quantification (A) and IHC (100X) (B). Ct – Wistar rats twelve months old; MG – Wistar rats twelve months old with MG supplementation from eight to twelve months old; HFD – HF diet-fed Wistar rats from eight to twelve months old; HFDMG – HF diet-fed and MG-supplemented Wistar rats from eight to twelve months old; GK – Goto-Kakizaki rats twelve monts old. IHC – immunohistochemistry; WB – western blotting; pEAT – periepididymal adipose tissue. Bars represent means ± SEM, n = 6-8/group for WB and n = 3 for IHC. * vs Ct. 1 symbol p<0.05; 3 symbols p<0.001.

Combination of glycation and high-fat diet impairs pEAT expandability

AT expansion was assessed through the fat pad weight (pEAT), adipocyte area and indirectly by circulating leptin. HF diet-fed groups (HFD and HFDMG) have eaten less food when compared to standard diet-fed groups (Ct, MG and GK) (Table 4.1). However, HFD group had increased body and pEAT weight (Table 4.1). HFDMG group showed a smaller increase of pEAT weight and no differences in body weight, although they have eaten similar amounts of food as compared to the HFD group (Table 4.1). Age-matched GK rats had lower body weight than Wistar rats, without major differences in pEAT weight (Table 4.1). HF diet-induced AT expansion (HFD group) caused increased circulating leptin levels ($p<0.001$ vs Ct; $p<0.01$ vs MG) and adipocyte area ($p<0.05$ vs Ct; $p<0.01$ vs MG), which were not fully observed in the HFDMG group (leptin: $p<0.05$ vs Ct) (Figure 4.5A-B).

Table 4.1 - Food intake and body and periepididymal adipose tissue weight.

Group	Ct	MG	HFD	HFDMG	GK
Food (g/rat/day)	22.9 ± 0.7	24.3 ± 1.6	15.1 ± 1.1**##	14.4 ± 0.7**##	$25.7 \pm 0.6$$$$ &&&
Body weight (g)	508.8 ± 11.4	508.9 ± 18.4	652.7 ± 35.8**##	571.6 ± 27.3	398.7 ± 7.7*#$$$ &&&
pEAT weight (g)	5.5 ± 0.4	5.9 ± 1.1	16.8 ± 2.5**#	14.2 ± 1.4*	2.8 ± 0.3###&&&

Ct – Wistar rats twelve months old; MG – Wistar rats twelve months old with MG supplementation from eight to twelve months old; HFD – HF diet-fed Wistar rats from eight to twelve months old; HFDMG – HF diet-fed and MG-supplemented Wistar rats from eight to twelve months old; GK – Goto-Kakizaki rats twelve months old. pEAT – periepididymal adipose tissue. Data represent mean ± SEM, n = 12/group. * vs Ct; # vs MG; $ vs HFD; & vs HFDMG. 1 symbol $p<0.05$; 2 symbols $p<0.01$; 3 symbols $p<0.001$.
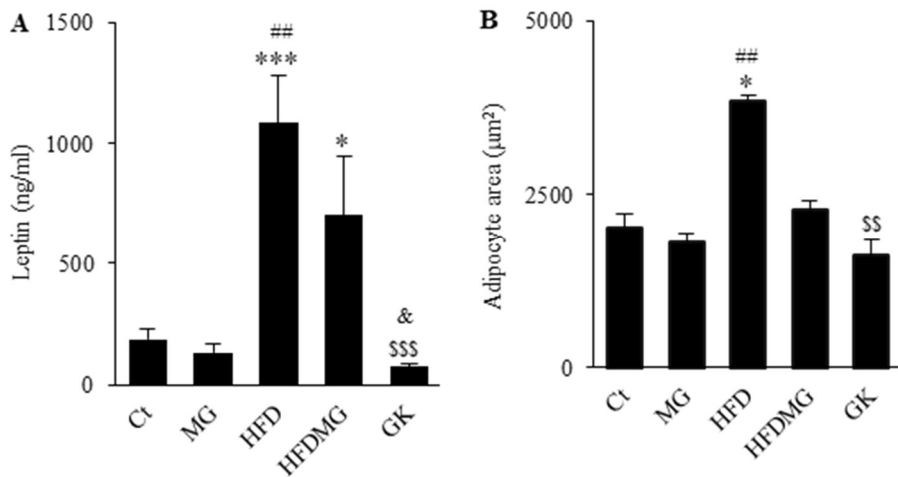
Figure 4.5 – High-fat diet increases serum leptin levels and adipocyte area, which was not observed in HFDMG group

Serum leptin levels were assessed by ELISA kit (A). Adipocyte area was evaluated through the number of adipocytes counted in each field of histological images (10 fields/rat, 100X) (B). Ct – Wistar rats twelve months old; MG – Wistar rats twelve months old with MG supplementation from eight to twelve months old; HFD – HF diet-fed Wistar rats from eight to twelve months old; HFDMG – HF diet-fed and MG-supplemented Wistar rats from eight to twelve months old; GK – Goto-Kakizaki rats twelve monts old. Bars represent means $\pm$ SEM, n = 6-8/group. * vs Ct; # vs MG; $ vs HFD; & vs HFDMG. 1 symbol p<0.05; 2 symbols p<0.01; 3 symbols p<0.001.

Combination of methylglyoxal-induced glycation and high-fat diet decreases periepididymal adipose tissue angiogenesis

Adequate angiogenesis is determinant for AT expandability and when hypoxia regions are generated during physiological tissue expansion, the hypoxia-inducible factors are activated as a mechanism to increase angiogenesis. Despite the fact that no changes were observed in HIF-1alpha, decreased HIF-2alpha expression in HFDMG ($p<0.01$) and GK ($p<0.05$) groups was observed when comparing with MG and HFD groups (Figure 4.6A). Decreased HIF-2alpha expression in AT has been associated with increased macrophage M1 phenotype, pro-inflammatory status and impaired adipose tissue functionality. Accordingly, MG and HFDMG rats had increased M1 levels ($p<0.05$ vs Ct and HFD groups), but no differences were observed for the M2 phenotype (Figure 4.6B). Besides increased number of M1 macrophage, dysregulation of HIFs expression may hamper angiogenesis as well. Our group showed aberrant capillary formation in retinal pigment epithelium cells and pEAT after MG-induced HIF-1alpha degradation and imbalance of VEGF/ANG-2 ratio (Bento et al., 2010b; Matafome et al., 2012). In fact, a similar imbalance of VEGF/ANG-2 ratio was observed in our results, including in the MG-supplemented groups (MG $p<0.05$ vs Ct and HFDMG $p<0.01$ vs Ct) and GK rats ($p<0.05$ vs Ct) (Figure 4.6C). This was coincident with increased levels of the endothelial cell marker CD31 in MG ($p<0.05$ vs Ct) and HFDMG ($p<0.05$ vs Ct) groups, what may denote a compensatory endothelial cell proliferation and formation of aberrant capillaries (Figure 4.6A). Angiotensin II receptor type 1 (AT1) was decreased in HFD ($p<0.01$ vs MG) and GK ($p<0.01$ vs MG) groups. No alterations were observed for ANGPTL4 levels in pEAT, which is an important factor involved in AT hypoxia response (Figure 4.6D).
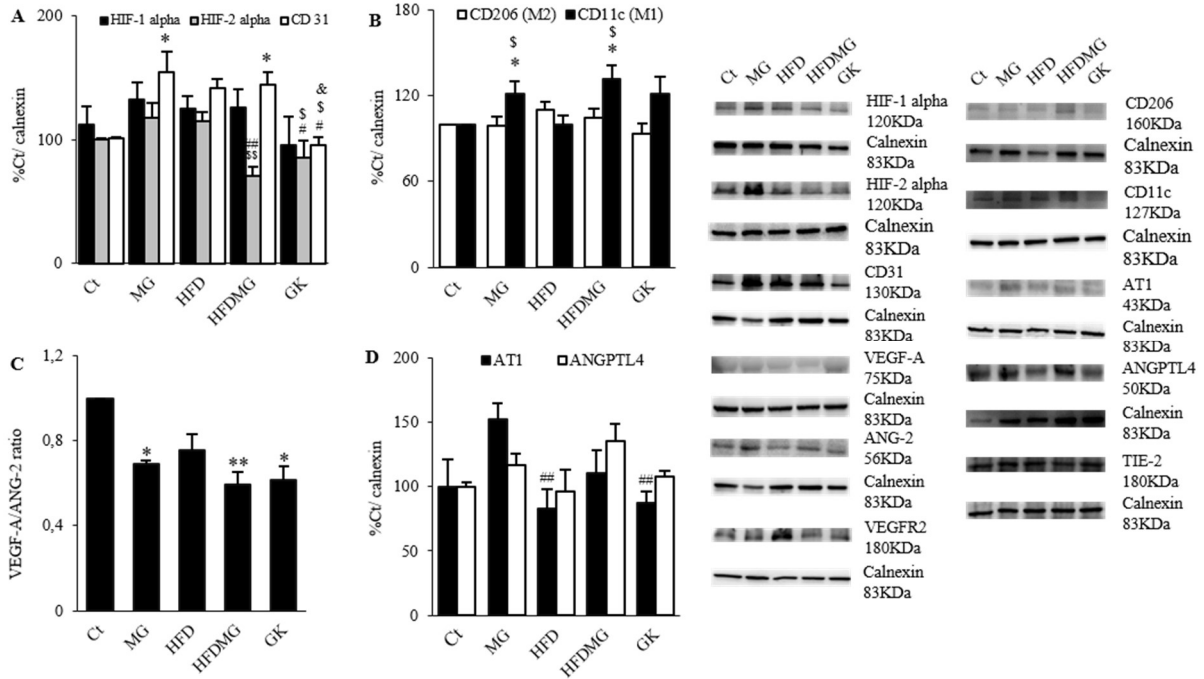
Figure 4.6 – Methylglyoxal-induced glycation during adipose tissue expansion hampers angiogenesis pathways and vascular function and remodelling

The levels of HIF-1alpha, HIF-2alpha, CD31 (A), CD11c, CD206 (B) VEGF/ANG-2 ratio (C), ANGPTL4 and AT1 (D) were determined by WB and representative images are shown. Ct – Wistar rats twelve months old; MG – Wistar rats twelve months old with MG supplementation from eight to twelve months old; HFD – HF diet-fed Wistar rats from eight to twelve months old; HFDMG – HF diet-fed and MG-supplemented Wistar rats from eight to twelve months old; GK – Goto-Kakizaki rats twelve monts old. HIF-1alpha/HIF-2alpha – hypoxia inducible factor alpha-1 and 2; WB – western blotting; CD31 – endothelial cell marker; CD11c/CD206 – macrophage M1/M2 phenotype; VEGF – vascular endothelial growth factor; ANG-2 – angiopoitin-2; AT1 – angiotenesin 2 receptor-1; ANGPTL-4 – angiopoietin-like-4; VEGFR2 – vascular endothelial growth factor receptor-2; TIE-2 – angiopoitin receptor-2. Bars represent means ± SEM, n = 6-8/group. * vs Ct; # vs MG; $ vs HFD; & vs HFDMG; 1 symbol p<0.05; 2 symbols p<0.01.

Dose-dependent methylglyoxal effects on *ex vivo* angiogenesis assays

MG-induced negative effects on pEAT angiogenesis were corroborated by the AT and aortic ring angiogenesis assays, as shown in representative figures (Figure 4.7C-D). Incubation of AT explants with growing concentrations of MG demonstrated a progressive decline of endothelial cell capillarization area in the collagen matrix, but only using concentrations higher than 100μM (250 μM $p<0.05$ vs Ct; 500 μM $p<0.01$ vs Ct; 1000 μM $p<0.001$ vs Ct) (Figure 4.7A). However, MG concentrations between 50 μM and 100 μM caused a significant decrease of sprout length (100 μM $p<0.05$ vs Ct; 250 μM $p<0.05$ vs Ct; 500 μM $p<0.01$ vs Ct; 1000 μM $p<0.001$ vs Ct), showing that glycation-induced vessel destabilization precedes inhibition of cell proliferation and migration in the AT (Figure 4.7B). Additionally, dose-dependent MG-induced effects on angiogenesis were also confirmed using aortic ring assay (Figure 4.7D).
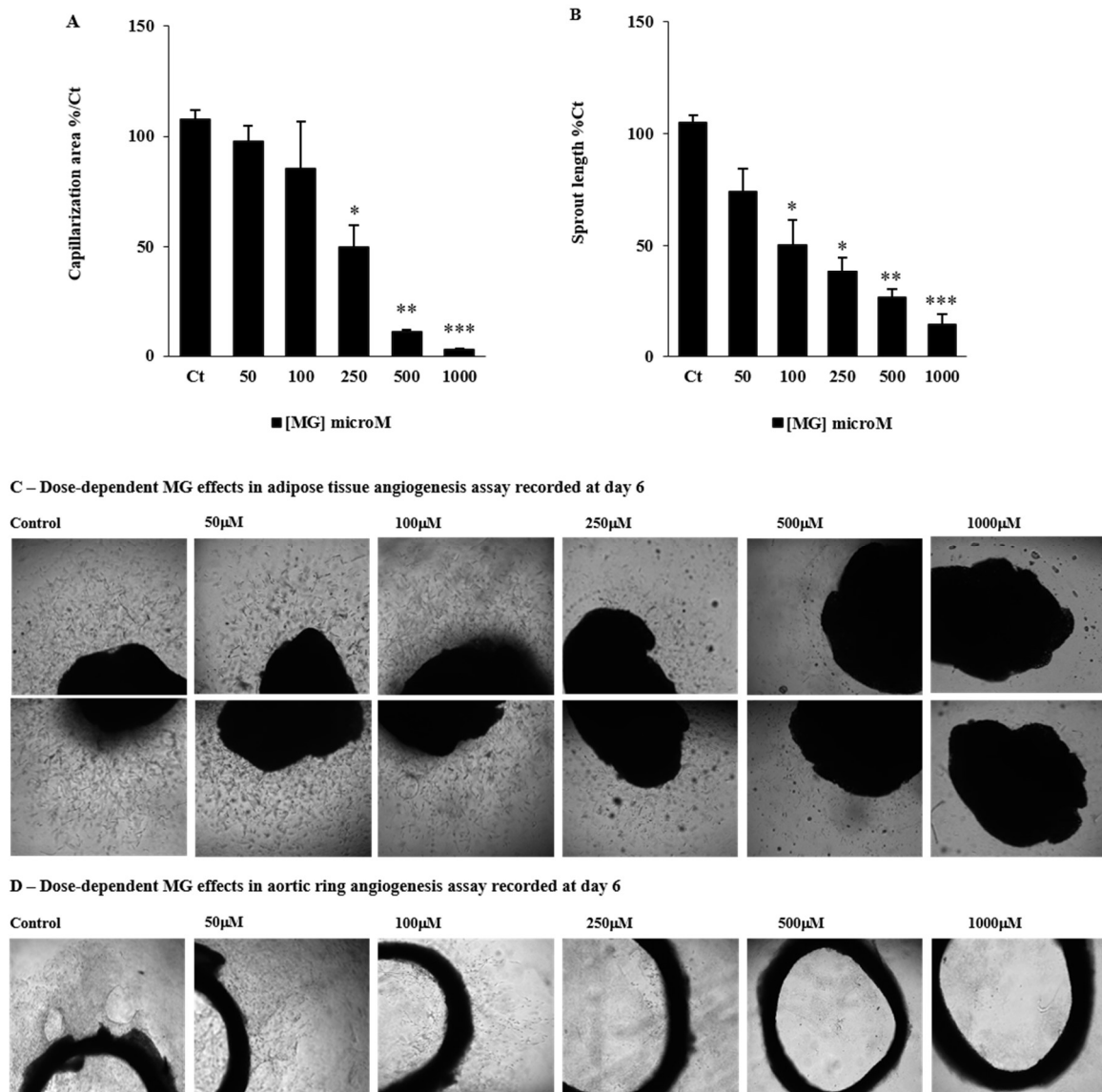
Figure 4.7 - Methylglyoxal decreases adipose tissue and aortic ring angiogenesis

The AT and aortic ring angiogenesis assays were developed (6 days) and used to evaluate the MG-induced effects of glycation in angiogenesis. Capillarization area (A) and sprout length (B) were calculated using ImageJ and Wacom Intuos Pro. Representative image of all conditions are shown in (C-D). AT angiogenesis assay: Ct – EGM-2MV plus vehicle (PBS) or MG (50-1000 μM); aortic ring angiogenesis assay: Ct – Opti-MEM suplemented with 2,5% FBS plus vehicle (PBS) or MG (50-1000 μM). EGM-2MV – supplemented endothelial growth medium; MG – methylglyoxal; PBS – phosphate-buffered saline. Bars represent means ± SEM, n = 6x3/condition. * vs Ct; 1 symbol $p < 0.05$; 2 symbols $p < 0.01$; 3 symbols $p < 0.001$.

Glyoxalase-1 inhibition and methylglyoxal further impair adipose tissue angiogenesis

GLO-1 inhibition leads to increased intracellular MG levels and ultimately, exacerbated AGE production. Using rat AT angiogenesis assay supplemented with MG (250 µM) or a selective inhibition of GLO-1 through BBGC (20 µM), we observed a significant reduction of capillarization area (MG $p<0.05$ vs Ct and BBGC $p<0.01$ vs Ct) (Figure 4.8A) and sprout length (MG $p<0.05$ vs Ct and BBGC $p<0.05$ vs Ct) (Figure 4.8B). Interestingly, this negative effect in pEAT angiogenesis (capillarization area and sprout length) was further enhanced when BBGC (20 µM) was combined with MG (250 µM) (MG + BBGC $p<0.001$ vs Ct) (Figure 4.8A-B), as shown in representative figures (Figure 4.8C).
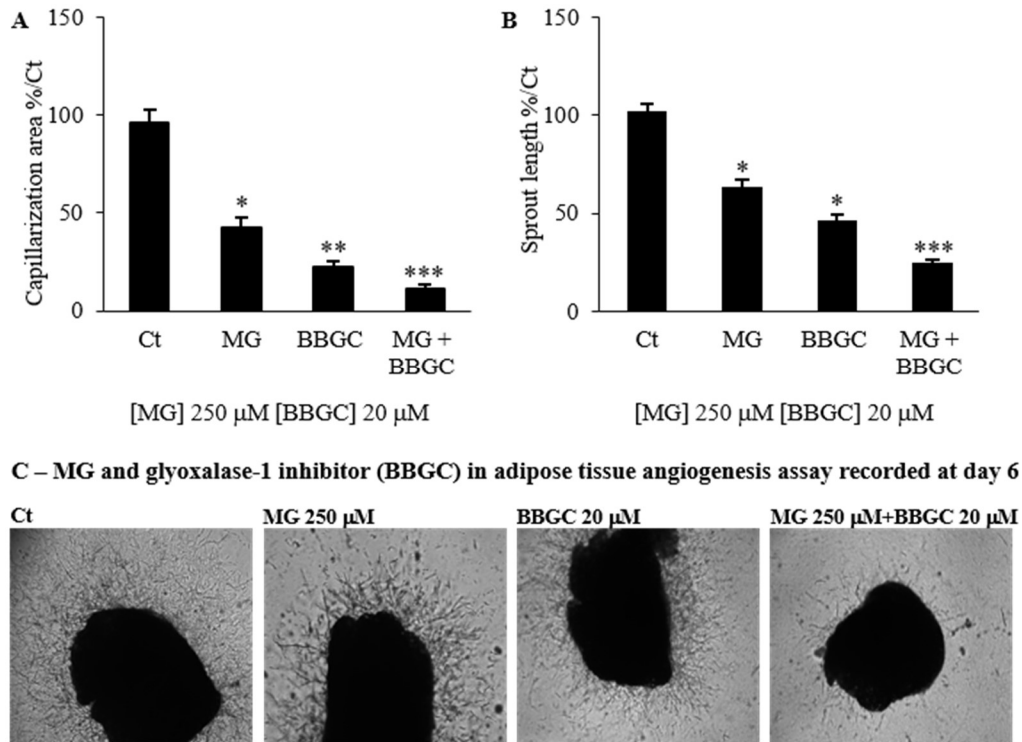
Figure 4.8 – Potentiated effect of GLO-1 inhibition plus MG on adipose tissue capillarization and sprout length

The AT angiogenesis assay was used to evaluate the MG and GLO-1 inhibitor BBGC-induced effects on AT angiogenesis. Capillarization area (A) and sprout length (B) were calculated using ImageJ and Wacom Intuos Pro, being representative image of all conditions shown (C). Ct – EGM-2MV plus vehicle (PBS); MG – EGM-2MV plus MG (250 µM); BBGC – EGM-2MV plus BBGC (20 µM); MG+BBGC – EGM-2MV plus MG (250 µM) and BBGC (20 µM). EGM-2MV – supplemented endothelial growth medium; MG – methylglyoxal; BBGC – s-p-bromobenzylglutathione cyclopentyl diester; PBS – phosphate-buffered saline. Bars represent means ± SEM, n = 6x3/condition. * vs Ct; 1 symbol p<0.05; 2 symbols p<0.01; 3 symbols p<0.001.

Glycation decreases adipose tissue insulin signalling in high-fat diet-fed rats

Methylglyoxal supplementation and HF diet separately had no major effects on the insulin receptor, PPARgamma (major regulator of lipid storage) and perilipin-A (regulator of lipolysis) levels. However, HF diet combined with MG supplementation induced a significant decrease of activated insulin receptor form ($p<0.05$ vs Ct and $p<0.01$ vs MG), similarly to non-obese type 2 diabetic rats ($p<0.05$ vs Ct and $p<0.01$ vs MG) (Figure 4.9A). No major differences were observed in phosphorylated AKT, PPAR-γ and the differentiation factors PGC1alpha and C/EBPalpha (Figure 4.9B-C and WB panel). Perilipin-A degradation is strongly inhibited by insulin and, accordingly, its levels were significantly reduced in the HFDMG group ($p<0.05$ vs Ct and $p<0.01$ vs MG) suggesting insulin resistance and higher susceptibility to lipolysis (Figure 4.9C). Thus, impairment of pEAT expandability induced by glycation results in impaired insulin signalling and lipid storage.
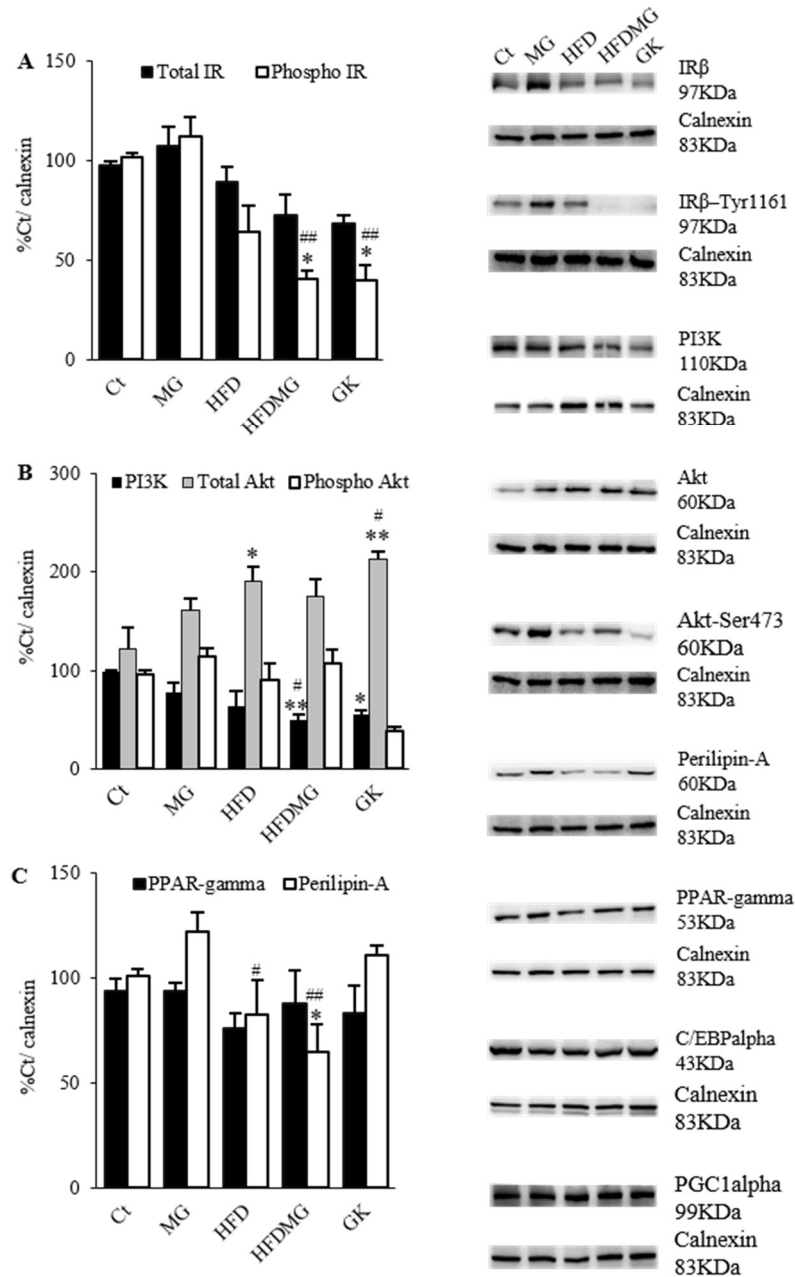
Figure 4.9 - Glycation impairs pEAT insulin signalling and lipid storage in high-fat diet-fed rats

Insulin signalling in pEAT was evaluated through WB quantification of activated and total forms of insulin receptor (A) and AKT (B). PPAR-gamma and perilipin-A levels in pEAT were also assessed by WB quantification to study lipid metabolism (C). Representative WB images are shown. Ct – Wistar rats twelve months old; MG – Wistar rats twelve months old with MG supplementation from eight to twelve months old; HFD – HF diet-fed Wistar rats from eight to twelve months old; HFDMG – HF diet-fed and MG-supplemented Wistar rats from eight to twelve months old; GK – Goto-Kakizaki rats twelve monts old. WB – western blotting; IRβ – insulin receptor beta; AKT – protein kinase b; PI3K – phosphatidylinositol-4,5-bisphosphate 3-kinase; PPAR-gamma – peroxisome proliferator-activated receptor gamma; C/EBPalpha – CCAAT-enhancer-binding protein alpha; PGC-1alpha – peroxisome proliferator-activated receptor gamma coactivator 1-alpha. Bars represent means ± SEM, n = 6-8/group.* vs Ct; # vs MG; 1 symbol $p<0.05$; 2 symbols $p<0.01$.

Glycation impairs skeletal muscle insulin signalling in high-fat diet-fed rats

Beyond AT insulin resistance, insulin signalling was also evaluated in skeletal muscle, which is a known target of insulin. MG supplementation or the HF diet separately had no effects on insulin signalling of skeletal muscle (Figure 4.10A-C). However, HF diet fed-rats submitted to MG-supplementation demonstrated a significant decrease in the levels of the insulin receptor ($p < 0.05$ vs MG; $p < 0.01$ vs Ct), AKT active form ($p < 0.01$ vs MG and HFD; $p < 0.001$ vs Ct) and GLUT-4 ($p < 0.05$ vs Ct and HFD; $p < 0.01$ vs MG) (Figure 4.10A-C). Such effects were very similar to GK rats, which also showed decreased phospho-insulin receptor ($p < 0.05$ vs Ct), total-IR ($p < 0.05$ vs MG and HFD; $p < 0.01$ vs Ct), phospho-AKT ($p < 0.01$ vs MG and HFD; $p < 0.001$ vs Ct) and GLUT-4 ($p < 0.05$ vs HFD; $p < 0.01$ vs Ct and MG) (Figure 4.10A-C). Such results show that glycation also impairs skeletal muscle insulin signalling, contributing to systemic insulin resistance and glucose intolerance.
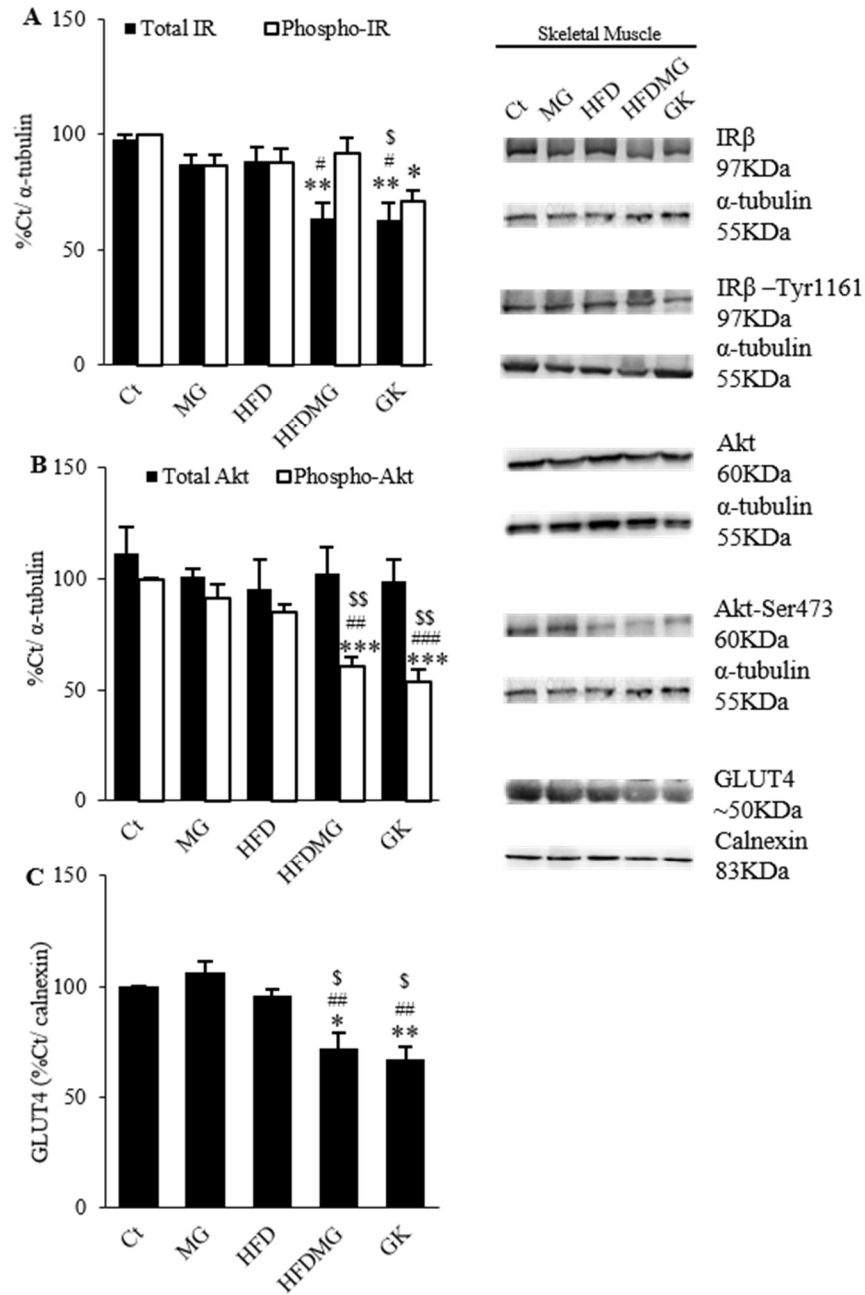
Figure 4.10 - Glycation decreased skeletal muscle insulin signalling in high-fat diet-fed rats

Skeletal muscle insulin signalling was evaluated through WB quantification of activated and total forms of insulin receptor (A) and AKT (B) as well as GLUT-4 transporter (C). Representative WB images are shown. Ct – Wistar rats twelve months old; MG – Wistar rats twelve months old with MG supplementation from eight to twelve months old; HFD – HF diet-fed Wistar rats from eight to twelve months old; HFDMG – HF diet-fed and MG-supplemented Wistar rats from eight to twelve months old; GK – Goto-Kakizaki rats twelve monts old. WB – western blotting; IRβ – Insulin receptor beta; AKT – protein kinase b; GLUT-4 – glucose transporter 4. Bars represent means ± SEM, n = 6-8/group. * vs Ct; # vs MG; $ vs HFD; 1 symbol p<0.05; 2 symbols p<0.01; 3 symbols p<0.001.

Glycation causes systemic dysmetabolism in high-fat diet-fed rats

MG and HF diet effects on systemic metabolism were assessed through the evaluation of glycemia (fasting and IPGTT), HbA1c, FFA, triglycerides, insulin and adiponectin levels. MG supplementation alone had no effect on such systemic parameters (Figure 4.11A-D; Table 4.2). Despite increased adiponectinemia, HFD rats developed glucose intolerance, with higher AUC during the IPGTT ($p < 0.001$ vs Ct and $p < 0.01$ vs MG), but no significant differences were observed for HbA1c, fasting glycemia, insulinemia and FFA and TG levels (Figure 4.11A-D; Table 4.2). In turn, HFDMG rats developed higher fasting FFA levels ($p < 0.05$ vs Ct), insulinemia ($p < 0.05$ vs Ct) and glucose intolerance (AUC) ($p < 0.05$ vs HFD; $p < 0.001$ vs Ct and MG) (Figure 4.11B-D). Moreover, MG-induced glycation in HF diet supplemented rats inhibited the compensatory increase of serum adiponectin levels ($p < 0.05$ vs HFD) observed in the HFD group ($p < 0.05$ vs CT and MG; $p < 0.001$ vs GK) (Figure 4.11A). Such features were similar to type 2 diabetic rats, which developed glucose intolerance ($p < 0.001$ vs Ct, MG, HFD and HFDMG), hypoadiponectinemia ($p < 0.001$ vs HFD) and increased FFA levels ($p < 0.01$ vs Ct), as well as hypoinsulinemia ($p < 0.05$ vs MG; $p < 0.01$ vs Ct; $p < 0.001$ vs HFD and HFDMG), due to age-dependent impaired β-cell function (Figure 4.11A-D). Altogether, such results show that glycation in HF diet fed-rats results in systemic insulin resistance and impaired glucose tolerance.

Table 4.2 - Fasting glycemia, HbA1c and serum triglyceride levels were performed after overnight fasting.

Group	Ct	MG	HFD	HFDMG	GK
Fasting glycemia (mg/dl)	68.5 ± 2.0	70.6 ± 1.4	70.9 ± 2.0	71.1 ± 1.6	91.7 ± 3.0***#$&
HbA1c (%)	3.2 ± 0.1	3.3 ± 0.1	3.3 ± 0.1	3.5 ± 0.1	5.6 ± 0.4
(mmol/mol)	(11.8 ± 1.5)	(13 ± 2.1)	(12.8 ± 0.9)	(15.4 ± 1.9)	(36 ± 6.8)***### \$\$\$ &&&
Triglycerides (mg/dl)	77.2 ± 6.4	69.3 ± 10.7	77.8 ± 5.4	62.3 ± 3.2	160.1 ± 23.1***### \$\$\$ &&&

Ct – Wistar rats twelve months old; MG – Wistar rats twelve months old with MG supplementation from eight to twelve months old; HFD – HF diet-fed Wistar rats from eight to twelve months old; HFDMG – HF diet-fed and MG-supplemented Wistar rats from eight to twelve months old; GK – Goto-Kakizaki rats twelve months old. HbA1c – glycated hemoglobin A1c. Data represent mean ± SEM, n = 12/group. * vs Ct; # vs MG; $ vs HFD; & vs HFDMG. 1 symbol p<0.05; 3 symbols p<0.001.
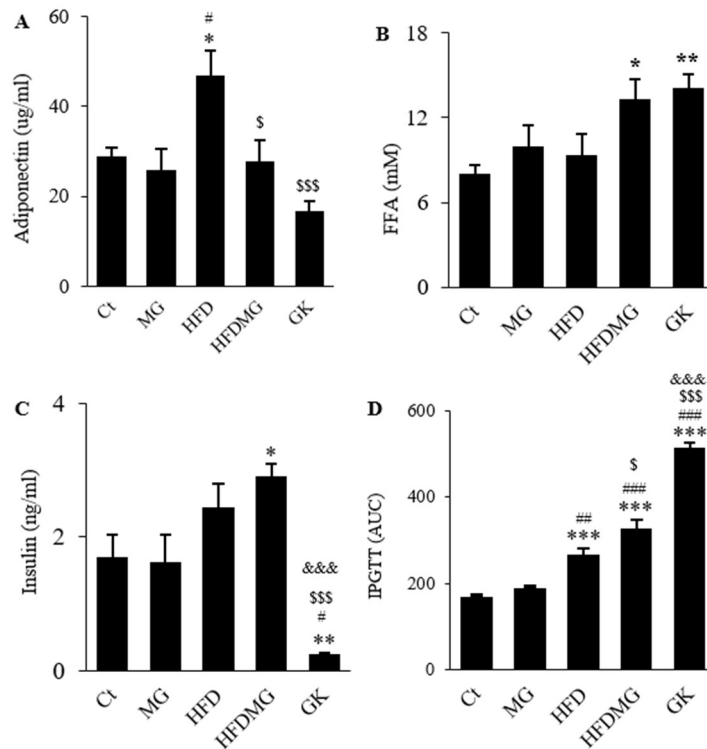
Figure 4.11 - Glycation increases systemic dysmetabolism in high-fat diet-fed rats

Circulating levels of adiponectin (A), FFA (B) and insulin (C) were quantified by ELISA (adiponectin and insulin) and by FFA assay kit (plasma FFA). Glucose intolerance was evaluated through the area under the curve of an IPGTT (D). Ct – Wistar rats twelve months old; MG – Wistar rats twelve months old with MG supplementation from eight to twelve months old; HFD – HF diet-fed Wistar rats from eight to twelve months old; HFDMG – HF diet-fed and MG-supplemented Wistar rats from eight to twelve months old; GK – Goto-Kakizaki rats twelve monts old. FFA – free fatty acids; IPGTT – intraperitoneal glucose tolerance test; AUC – area under the curve. Bars represent means ± SEM, n = 6-8/group. * vs Ct; # vs MG; $ vs HFD; & vs HFDMG; 1 symbol p<0.05; 2 symbols p<0.01; 3 symbols p<0.001.

1.2 Highlights

✓ Dynamic contrast-enhanced magnetic resonance imaging and rat adipose tissue angiogenesis assay are effective in evaluating adipose tissue blood flow and angiogenesis, respectively;

✓ Methylglyoxal-induced glycation impairs adipose tissue vascular architecture, flow and expandability;

✓ Compromised adipose tissue expandability and function lead to local and systemic insulin resistance and metabolic dysregulation;

✓ Methylglyoxal causes dose-dependent decrease of adipose tissue and aortic ring angiogenesis;

✓ Glyoxalase-1 inhibition results in decreased adipose tissue angiogenesis, being such effects enhanced under methylglyoxal exposure;

1.3 Discussion

In this study we investigated a new mechanism for AT dysfunction in obesity and type 2 diabetes. We demonstrate that glycation in pEAT has adverse vascular effects, impairing blood flow, hypoxia-response mechanisms and expandability, which are tightly associated with local and systemic insulin resistance and glucose dysmetabolism. AT dysfunction has been suggested to be caused by limited AT capillarization and expansion potential (Moreno-Indias and Tinahones, 2015; Rutkowski et al., 2009). This may be of particular relevance due to different metabolic outcomes of metabolically healthy (MHO) and unhealthy obesity (MUO), being the latter characterized by the earlier progression to insulin resistance and glucose dysmetabolism (Boonchaya-anant and Apovian, 2014; Hinnouho et al., 2014; Uribarri et al., 2015a).

Previously, we have shown that MG supplementation to Wistar rats impairs angiogenic markers and blood flow in AT, causing hypoxia, macrophage recruitment, hypoadiponectinemia and increased plasma FFA, but neither insulin resistance nor glucose dysmetabolism (Matafome et al., 2012). Such effects were partially reverted by a delayed treatment with pyridoxamine, a dicarbonyl scavenger drug (Rodrigue et al., 2013). We have also demonstrated that glycation impairs AT ability to adapt to hypoxia in a model of surgery-induced reduction of blood supply to the left pEAT, causing insulin resistance and adipocyte death (Rodrigues et al., 2013b). Based on such observations, we hypothesized that AT glycation may induce microvascular lesions that hamper blood flow and expandability during a diet-induced expansion and lead to AT dysfunction and insulin resistance in obesity. This would therefore provide a strong mechanistic framework to the MUO phenotype. To test this conceptual model, we developed an animal model with HF diet-induced AT expansion and MG supplementation. We used a diet specifically enriched in triglycerides in

order to induce physiological AT expansion and better isolate the variables of interest, while controlling for potential confounds. The effects of MG were compared with the endogenous glycation observed in non-obese type 2 diabetic GK rats.

MG supplementation in the diet increases the formation of stable MG adducts that are partially absorbed to the bloodstream, accumulate in different tissues and cause diabetes-like microvascular lesions (Berlanga et al., 2005; Golej et al., 1998). Our group demonstrated that our protocol results in plasma and AT MG levels (after derivatization) similar to those of diabetic rats and here we demonstrate that MG supplementation results in CEL levels in AT similar to diabetic GK rats (Matafome et al., 2012).

In order to evaluate AT blood flow, we have developed, validated and applied a new in vivo quantitative DCE-MRI technique to assess pEAT blood flow. In the past, we evaluated pEAT blood flow through the accumulation of the fluorescent dye Evans Blue. However, this histological technique is strongly influenced by adipocyte area, becoming inappropriate after HF diet-induced adipocyte hypertrophy (Matafome et al., 2012; Rodrigues et al., 2013b). Using DCE-MRI, we demonstrate a reduction of pEAT blood flow in MG-supplemented groups and diabetic rats.

Several authors suggested that hypoxia could be caused by limited oxygen diffusion due to adipocyte hypertrophy, being a trigger to AT metabolic and endocrine dysfunction (Guilherme et al., 2008; Halberg et al., 2009; Hosogai et al., 2007; Trayhurn et al., 2008a; Ye et al., 2007). Nonetheless, the AT from obese patients was shown to be hyperoxic and to have only a very small proportion of adipocytes with a diameter superior to 100µm (oxygen diffusion distance), increasing the controversy about the previous hypothesis (Goossens and Blaak, 2015; Goossens et al., 2011). Our results demonstrate that HF diet-induced AT expansion does not cause significant alterations in AT blood flow and formation of hypoxic regions. Remarkably, hypoxia was found when the HF diet was combined with MG, showing

that glycation-induced decreased blood flow leads to hypoxia when the AT is critically forced to expand.

Regarding the mechanisms involved in glycation-induced vascular lesions, some groups have introduced the concept of targeting AT angiogenesis to improve insulin sensitivity, based on decreased angiogenic ability of explants from obese donors (Cao, 2013; Corvera and Gealekman, 2014b; Gealekman et al., 2012; Mannerås-Holm and Krook, 2012; Rutkowski et al., 2009). This is in line with observations showing that AT blood flow was decreased in obese patients due to impaired arteriolar function (Farb et al., 2012a; Karpe et al., 2002). Given that hypoxia is the main trigger for angiogenesis, we evaluated the role of glycation on adaptation mechanisms to hypoxia and angiogenesis, as well as vascular tone. MG was shown to hamper acute HIF-1alpha stabilization in hypoxia, impairing cell response to hypoxia (Bento et al., 2010c). In fact, we show no long-term differences in HIF-1alpha levels. Nevertheless, recent studies demonstrated the involvement of HIF-2alpha in chronic cell adaptation to hypoxia and in preventing hypoxia-induced insulin resistance (Aouadi, 2014; García-Martín et al., 2016). Choe et al., demonstrated that HIF-2alpha expression in macrophage prevents M1 phenotype and their pro-inflammatory activity in AT (Aouadi, 2014; Choe et al., 2014). In addition, mice lacking HIF-2alpha had insulin resistance and glucose intolerance (Aouadi, 2014; Choe et al., 2014; García-Martín et al., 2016). Thus, while HIF-1alpha is important for the pro-inflammatory activation of M1 macrophage through iNOS induction, HIF-2alpha contributes to metabolic homeostasis by inhibiting such mechanisms (Aouadi, 2014; García-Martín et al., 2016). In our study, we show decreased HIF-2alpha expression in high-fat diet-fed rats with MG supplementation and in type 2 diabetic GK rats as well. Moreover, we observed an increased number of M1 macrophage in pEAT, which is in accordance with decreased HIF-2alpha levels. Such events may be responsible for a pro-inflammatory environment in the AT.

Our group demonstrated that MG-induced imbalance of VEGF/ANG-2 ratio inhibits tube-like formation, conducting to dysregulated endothelial cell proliferation and formation of aberrant capillaries (Bento et al., 2010b). In the present study, we show similar VEGF/ANG-2 ratio in HF diet-fed and control rats, but a decreased VEGF/ANG-2 ratio in HF diet-fed rats submitted to MG supplementation. Moreover, increased levels of the endothelial cell marker CD31 were observed, suggesting a higher number of endothelial cells and vessel disarrangement. Our data are also consistent with the findings of Jörgens et al., and Wang, et al., which observed VEGF downregulation and formation of aberrant vessels in methylglyoxal-treated zebrafish and inhibition of angiogenesis in MG-treated HUVECs (Jörgens et al., 2015; Wang et al., 2015b). The AT angiogenesis assay, an adaptation of the aortic ring assay, was developed by Corvera's laboratory, but only for human subcutaneous and mice pEATs (Gealekman et al., 2008; Rojas-Rodriguez et al., 2014). Based on the original one, we developed an assay for rat pEAT. Our results show that, higher MG concentrations or selective inhibition of its detoxification by GLO-1 impair the angiogenic process. However, before inhibiting cell proliferation and migration, MG destabilizes sprouts structure and affects their growth. This is in accordance with the findings of Liu et al., showing excessive endothelial cell proliferation in HUVECs (Liu et al., 2012), but the mechanisms involved are still controversial. While the authors of the first study have shown increased autophagy-dependent VEGFR2 degradation, the others have shown increased VEGFR2 autophosphorylation, which would lead to excessive endothelial cell proliferation (Jörgens et al., 2015; Liu et al., 2012). Thus, MG has been shown to decrease capillary structure and growth and here we extend these observations to AT vessels. Such events are likely to decrease AT blood flow and contribute to insulin resistance, but the mechanisms should be further elucidated in the future.

Karpe et al., observed impaired postprandial blood flow in AT and demonstrated that such events were associated with lower insulin sensitivity (Karpe et al., 2002). As well, Farb et al., described impaired arteriolar function in the AT of obese patients, which mechanisms remain to be uncovered (Farb et al., 2012a). Vascular tone is strongly influenced by the RAS and by factors influencing vascular integrity and permeability. The RAS is upregulated by AGE, increasing vascular damage in different tissues (Matafome et al., 2015). As well, AGE were recently shown to increase vascular permeability by upregulating ANGPTL4 expression. Our results are in accordance with such body of evidence, showing that AT glycation leads to a tendency of increase of AT1 and ANGPTL4 levels, which may impair vascular function.

Insulin resistance in fat depots contributes to increased spill-over of FFA to the circulation, ectopic deposition and the development of systemic insulin resistance (Goossens, 2008; Guilherme et al., 2008; Smith, 2015). Our present study demonstrates for the first time that accumulation of glycated products during pEAT expansion is associated with impaired insulin signalling in AT, perilipin-A loss and decreased adiponectin secretion. Moreover, such pEAT alterations were associated with systemic dysmetabolism, including decreased glucose tolerance, hyperinsulinemia, and increased plasma FFA and skeletal muscle insulin resistance. Our observations are in accordance with previous data from our laboratory and the studies of Gaens et al., and Uribarri et al., which showed that RAGE-mediated CML accumulation in AT is involved in adipokines dysregulation, suggesting the involvement of glycation in the progression from metabolically healthy to unhealthy obesity (Gaens et al., 2013, 2014; Uribarri et al., 2015b).

In sum, our results demonstrate that glycation impairs pEAT microcirculation and expandability, in particular when associated with high-fat diets and ensuing obesity. Thus, we propose the existence of adipovascular coupling mechanisms, based on the fact that blood

flow is critical for adipocyte function and, when decreased, it causes insulin resistance. This coupling is disrupted by glycation, impairing blood flow, adaptation to hypoxia and expansion potential, thus causing hypoxia and local and systemic insulin resistance and metabolic dysregulation (Figure 4.12). Although the mechanisms should be further addressed in the future, our results identify promising therapeutic targets in preventing metabolically unhealthy obesity and metabolic disorders.
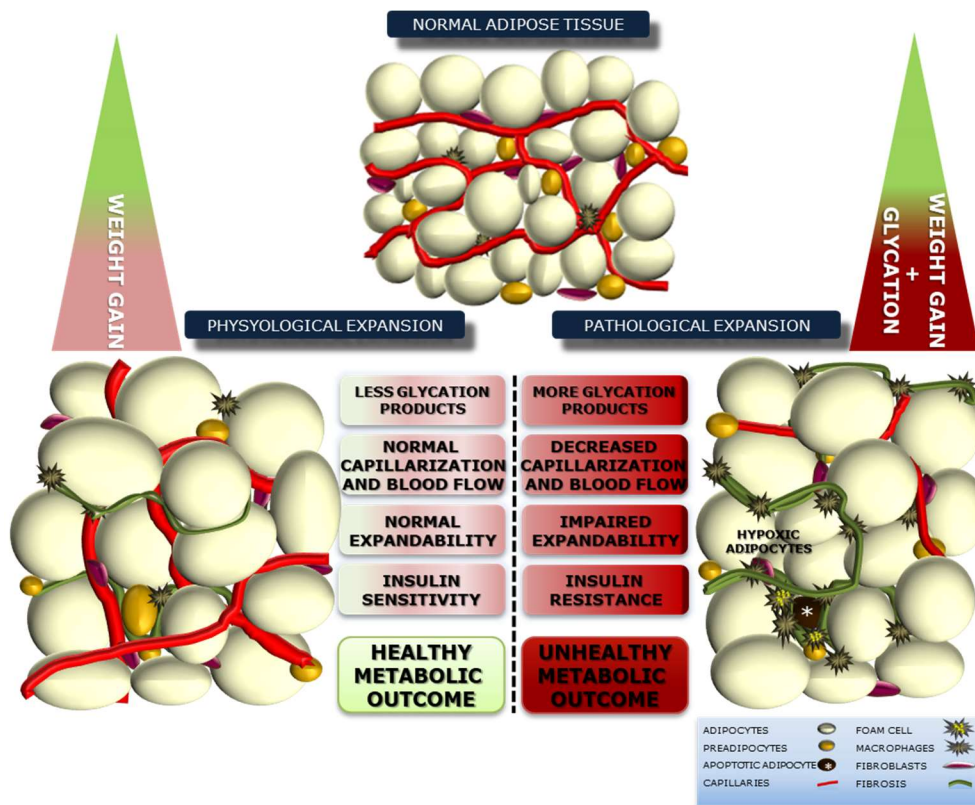
Figure 4.12 - Impact of glycation in adipose tissue expandability, causing pathological expansion with impaired capillarization and blood flow, as well as insulin resistance. Such mechanisms may contribute to secretome changes and glucose dysmetabolism and ultimately, metabolically unhealthy obesity and type 2 diabetes

2. Targeting adipose tissue glyoxalase system with GLP-1-based therapies

2.1 Results

Knowing the negative effects of MG-induced glycation in pEAT, including angiogenesis and metabolic function, GLO-1 was studied and become a promising therapeutic target to prevent AT dysfunction and vascular complications. Based on this, we formulated a scientific question: are GLP-1-based therapies able to target GLO-1-dependent mechanisms in order to improve adipose tissue vascularization and function?

In line with previous findings from animal models, we hypothesized similar negative effects of glycation in human visceral adipose tissue in obesity, governing tissue dysfunction and the development of metabolically unhealthy obesity as well as progressive type 2 diabetes development and progression. Recently, metabolic surgery was shown to increase adipose tissue angiogenesis and postprandial GLP-1 levels. Thus, we also hypothesized that GLP-1 or liraglutide, could be responsible for improved pEAT angiogenesis and tissue and systemic metabolism, involving GLO-1-dependent mechanisms.

In order to study the involvement of GLO-1-dependent mechanisms, enzyme levels and activity were studied in human and animal models samples, exploring the role of vertical sleeve gastrectomy and liraglutide in adipose tissue angiogenesis, detoxifying mechanisms and metabolic outcome. Furthermore, adipose tissue angiogenesis assay was used to specifically unravel the role of GLO-1-depentent actions of liraglutide (GLP-1 analogue) on adipose tissue angiogenesis.

2.1.1 Metabolic healthy and unhealthy obese patients regarding insulin resistance and visceral adipose tissue dysfunction

Obese patients were included in different groups according to their insulin resistance, fasting glucose and HbA1c levels. The metabolically healthy group (IS - insulin sensitive) was composed by subjects with normal fasting glycemia (81 mg/dL and IQR = 12 mg/dL) and HbA1c (5.45% and IQR = 0.45%) and normal Ox-HOMA2IR index (0.55 and IQR = 0.35). Higher Ox-HOMA2IR (>1) index was the determinant to include insulin resistant (IR) patients in IR normoglycemic group (2.22 and IQR = 1.6), IR pre-diabetic (1.98 and IQR = 1.1) or IR diabetic (2.2 and IQR = 3). IR normoglycemic group was comprised by insulin resistant patients, but with normal fasting glycemia (87 mg/dL and IQR = 15 mg/dL) and HbA1c (5.4% and IQR = 0.2%). IR pre-diabetic group included insulin resistant patients with prediabetes i.e. 100 mg/dL<fasting glycemia<126 mg/dL (96 mg/dL and IQR = 18 mg/dL) or 5.6%<HbA1c<6,5% (5.85% and IQR = 0.4%). Insulin resistant patients with type 2 diabetes i.e. fasting glycemia higher than 125 mg/dL (114,5 mg/dL and IQR = 40 mg/dL) or HbA1c higher than 6.4% (6,95% and IQR = 0.9%) were incorporated in IR diabetic group (Table 4.3). Interestingly, despite the fact that the metabolic outcome is different among groups, BMI was similar between them, which reinforces the importance of AT function instead of fat amount regarding metabolic consequences. In accordance with disease progression, pre-diabetic (IR pre-diabetic) (p<0.01 vs IR normoglycemic) and diabetic (IR diabetic) (p<0.01 vs IR normoglycemic) patients were older than insulin resistant but normoglycemic patients (IR normoglycemic) (Table 4.3).

Table 4.3 - Age, body mass index and metabolic parameters used to include patients into specific groups

Group Statistics				
Parameter	Group	Median	IQR	p value
Age (y)	IS	43	16	
	IR normoglycemic	41	14.3	
	IR pre-diabetic	49.5	15	p<0.01 vs IR normoglycemic
	IR diabetic	50.5	12.5	p<0.01 vs IR normoglycemic
BMI (Kg/m^2)	IS	41.8	8.23	
	IR normoglycemic	43.3	9.1	
	IR pre-diabetic	44.8	6.1	n.s.
	IR diabetic	44.6	9.5	
HOMA2IR	IS	0.55	0.35	
	IR normoglycemic	2.22	1.6	p<0.01 vs IS
	IR pre-diabetic	1.98	1.1	p<0.01 vs IS
	IR diabetic	2,2	3	p<0.01 vs IS
HbA1c (%)	IS	5.45	0.45	
	IR normoglycemic	5.4	0.2	
	IR pre-diabetic	5.85	0.4	p<0.001 vs IS and IR normoglycemic
	IR diabetic	6.95	0.9	p<0.001 vs IS and IR normoglycemic; p<0.01 vs IR pre-diabetic
Fasting glycemia (mg/dL)	IS	81	12	
	IR normoglycemic	87	15	
	IR pre-diabetic	96	18	p<0.001 vs IS and IR normoglycemic;
	IR diabetic	114,5	40	p<0.001 vs IS and IR normoglycemic; p<0.01 vs IR pre-diabetic

IS – patients with HOMA2IR<1; IR normoglycemic – patients with HOMA2IR>1 but normoglycemic; IR pre-diabetic – patients with HOMA2IR>1 and 99 mg/dL<fasting glycemia<126 mg/dL and/or 5.6%<HbA1c<6.5%; IR diabetic – patients with HOMA2IR>1, fasting glycemia and HbA1c higher than 125 mg/dL and/or 6.4%, respectively. BMI – body mass index; HbA1c – glycated hemogloblin; IQR – interquartil range; IR – insulin resistant/insulin resistance; HOMA2IR – homeostasis model assessment 2 insulin resistance index. Data are shown as median and IQR.

Increased leptin levels and triglyceridemia in obese subjects

Leptin is a known adipokine which is produced and secreted from AT, being leptin levels associated with fat amount instead of AT functionality. Although serum leptin levels were higher in all groups, no differences were observed between them, following the results observed for BMI, suggesting that metabolic alterations are primarily caused by AT function instead of fat amount (Figure 4.13A and Table 4.3). Fasting serum triglycerides levels, that may be associated with lipid dysmetabolism and insulin resistance, were increased in IR normoglycemic ($p<0.05$ vs IS) and IR diabetic ($p<0.01$ vs IS) groups, when compared to IS group (Figure 4.13B).
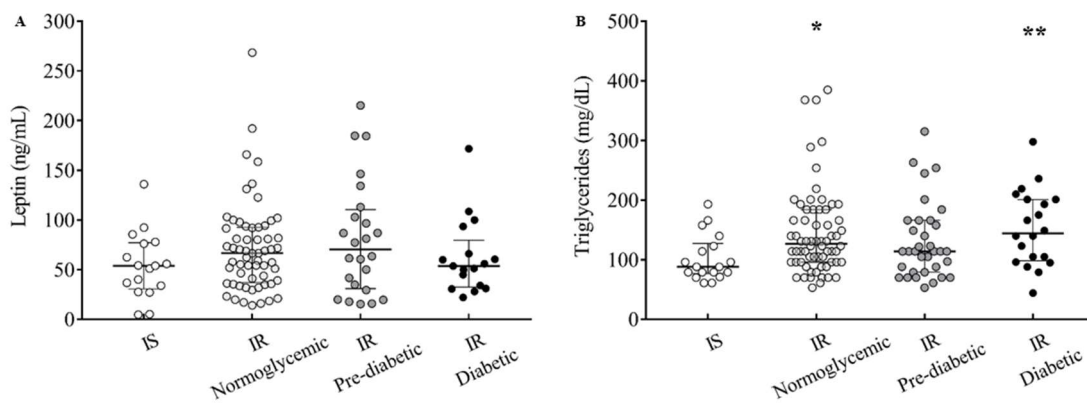
Figure 4.13 - Serum leptin and triglyceride levels in obese subjects
Fasting serum leptin levels were quantified using the Human Leptin DuoSet ELISA kit (A), while triglycerides were calculaded by automatic analyser (B). IS – patients with HOMA2IR<1; IR normoglycemic – patients with HOMA2IR>1 but normoglycemic; IR pre-diabetic – patients with HOMA2IR>1 and 99 mg/dL<fasting glycemia<126 mg/dL and/or 5.6%<HbA1c<6.5%; IR diabetic – patients with HOMA2IR>1, fasting glycemia and HbA1c higher than 125 mg/dL and/or 6.4%, respectively. IS – insulin sensitive; IR – insulin resistant; HbA1c – glycated hemogloblin; HOMA2IR – homeostasis model assessment 2 insulin resistance index. Data are shown in dots accordingly to each patient result/group plus median and interquartil range lines. * vs IS. 1 symbol $p<0.05$; 2 symbols $p<0.01$.

Decreased HDL cholesterol and adiponectinemia in type 2 diabetic obese subjects

AT dysfunction is associated with unbalanced cholesterol fluxes, including HDL cholesterol decrease as well as decreased adiponectin circulating levels. Obese pre-diabetic and type 2 diabetic patients have shown decreased circulating HDL cholesterol levels (IR pre-diabetic $p<0.05$ vs IS) (IR diabetic $p<0.01$ vs IS and $p<0.05$ vs IR normoglycemic) (Figure 4.14A). Accordingly, adiponectinemia was lower in diabetic patients (IR diabetic) when comparing to IS group ($p<0.01$), IR normoglycemic and IR pre-diabetic ($p<0.05$) groups, which suggests the decline of AT function in insulin resistant type 2 diabetic patients (Figure 4.14B).
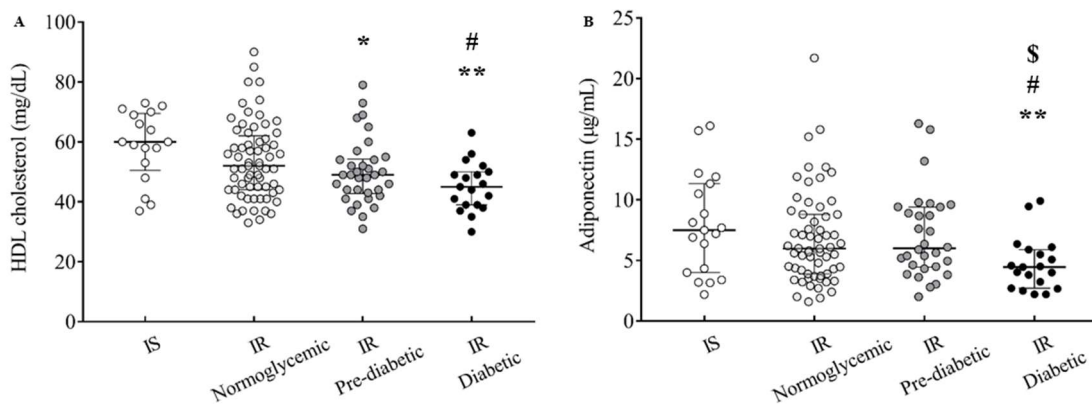
Figure 4.14 - Decreased HDL cholesterol and adiponectin levels in obese type 2 diabetic patients
Fasting HDL cholesterol levels were quantified by automatic analyser (A). Serum adiponectin levels were quantified using the Human Adiponectin DuoSet ELISA kit (B). IS – patients with HOMA2IR<1; IR normoglycemic – patients with HOMA2IR>1 but normoglycemic; IR pre-diabetic – patients with HOMA2IR>1 and 99 mg/dL<fasting glycemia<126 mg/dL and/or 5.6%<HbA1c<6.5%; IR diabetic – patients with HOMA2IR>1, fasting glycemia and HbA1c higher than 125 mg/dL and/or 6.4%, respectively. IS – insulin sensitive; IR – insulin resistant; HbA1c – glycated hemogloblin; HOMA2IR – homeostasis model assessment 2 insulin resistance index; HDL – high-density lipoprotein . Data are shown in dots accordingly to each patient result/group plus median and interquartil range lines. * vs IS; # vs IR normoglycemic; $ vs IR pre-diabetic. 1 symbol $p<0.05$; 2 symbols $p<0.01$.

Beta cell progressive decline and decreased visceral adipose tissue glyoxalase-1 activity in pre-diabetic and type 2 diabetic obese patients

Beta cell function index was higher in IR normoglycemic group than in the other groups ($p < 0.001$ vs IS and IR diabetic; $p < 0.01$ vs IR pre-diabetic) (Figure 4.15A). Moreover, IR pre-diabetic group also maintained increased index when comparing with IS and IR diabetic groups ($p < 0.001$ vs IS; $p < 0.05$ vs IR diabetic) (Figure 4.15A). As expected, IR diabetic group showed the lower beta cell function index of insulin resistant groups, resulting from the progressive deterioration of beta cell, which leads to compensatory insulin secretion failure. The quantification of GLO-1 activity in VAT has shown lower activity of this MG-detoxifying enzyme in IR pre-diabetic ($p < 0.05$ vs IS and $p < 0.01$ vs IR normoglycemic) and IR diabetic ($p < 0.05$ vs IS and $p < 0.01$ vs IR normoglycemic) groups (Figure 4.15B). The decrease of GLO-1 activity may be associated with higher accumulation of MG-adducts and glycation in adipose tissue, contributing to tissue dysfunction and insulin resistance.
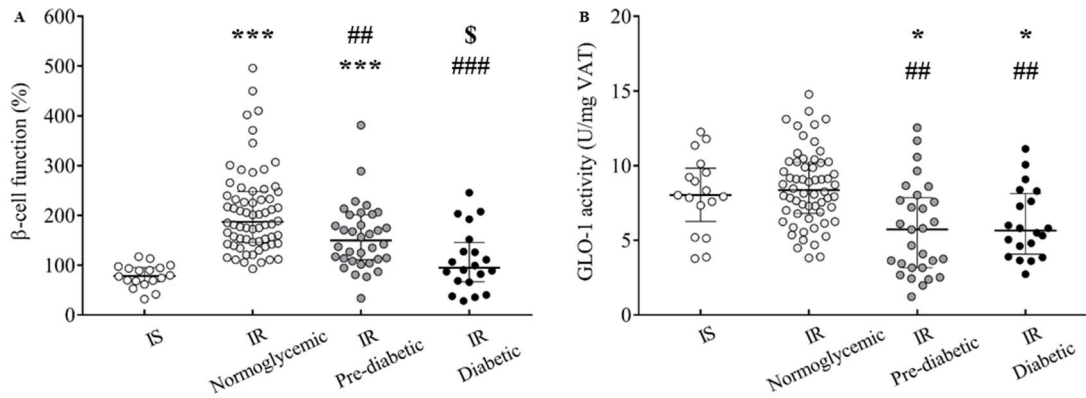
Figure 4.15 –Progressive β-cell decline and decreased visceral adipose tissue glyoxalase-1 activity in pre-diabetic and diabetic obese patients

The percentage of β-cell function was calculated using fasting blood insulin and glucose levels (A). The GLO-1 activity in human VAT samples was quantified using GLO-1 activity assay (B). IS – patients with HOMA2IR<1; IR normoglycemic – patients with HOMA2IR>1 but normoglycemic; IR pre-diabetic – patients with HOMA2IR>1 and 99 mg/dL<fasting glycemia<126 mg/dL and/or 5.6%<HbA1c<6.5%; IR diabetic – patients with HOMA2IR>1, fasting glycemia and HbA1c higher than 125 mg/dL and/or 6.4%, respectively. IS – insulin sensitive; IR – insulin resistant; HbA1c – glycated hemgloblin; HOMA2IR – homeostasis model assessment 2 insulin resistance index; GLO-1 – glyoxalase-1; VAT – visceral adipose tissue. Data are shown in dots accordingly to each patient result/group plus median and interquartil range lines. * vs IS; # vs IR normoglycemic; $ vs IR pre-diabetic. 1 symbol p<0.05; 2 symbols p<0.01; 3 symbols p<0.001.

Visceral adipose tissue glyoxalase-1 activity is negatively correlated with HbA1c in obese patients

Given the fact that GLO-1 gene has an insulin responsive element, this may be a mechanism involved in the regulation of GLO-1 activity (Rabbani et al., 2014). Insulin resistance may compromise VAT-derived GLO-1 activity. In fact, data from all patients originated a negative Spearman correlation (r'=-0.346; p<0.003) between HbA1c levels and VAT GLO-1 activity, meaning that poorer glycemic control in obese patients is associated with decreased AT GLO-1 activity (Figure 4.16A). No correlations were observed in any of the studied groups (Figure 4.16B-E).
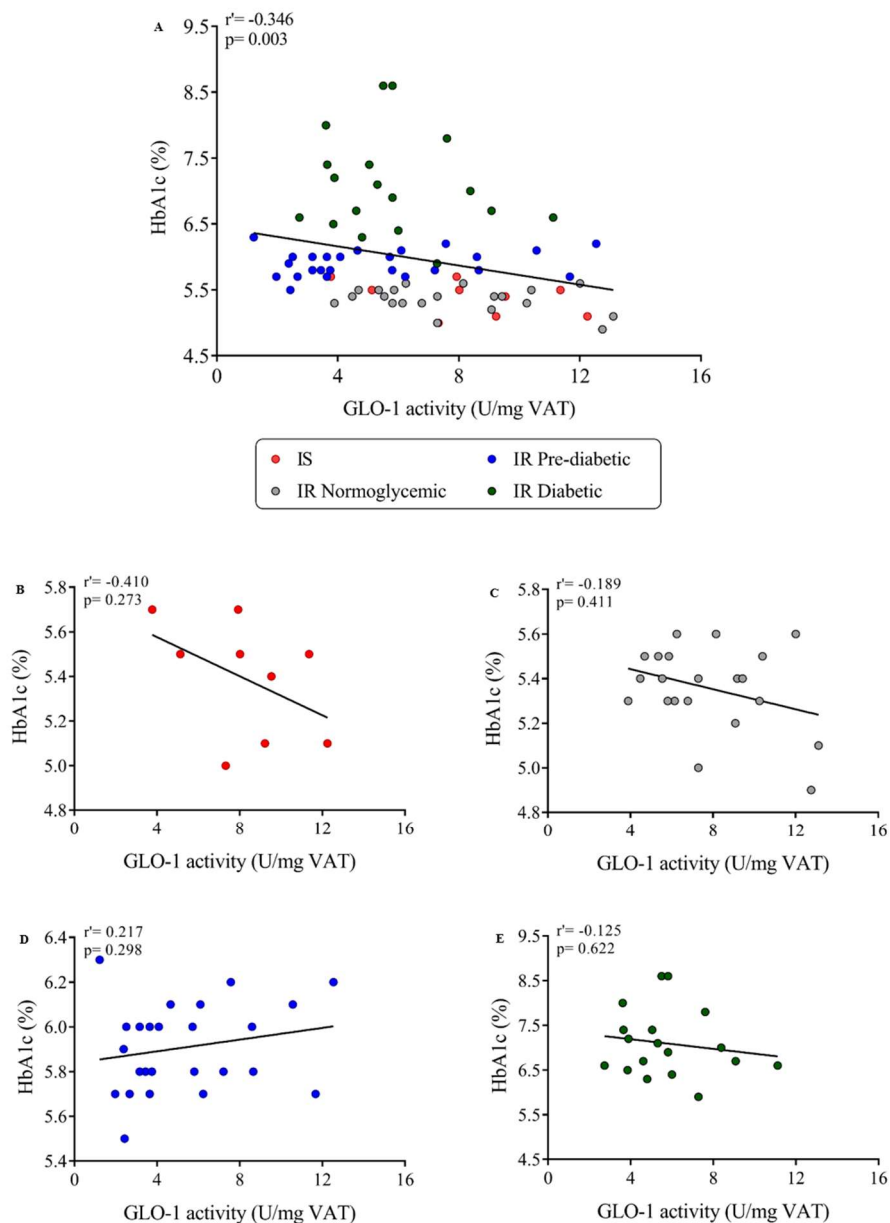
Figure 4.16 – Impaired glycemic control in obese patients is associated with decreased visceral adipose tissue glyoxalase-1 activity

Non-parametric Sprearman correlations were calculated from all data (A) or to each group (B-E), using HbA1c levels vs VAT-derived GLO-1 activity (kit from Sigma – Merck, USA). IS – patients with HOMA2IR<1 (B); IR normoglycemic - patients with HOMA2IR>1 but normoglycemic (C); IR pre-diabetic - patients with HOMA2IR>1 and 99 mg/dL<fasting glycemia<126 mg/dL and/or 5.6%<HbA1c<6.5% (D); IR diabetic – patients with HOMA2IR>1, fasting glycemia and HbA1c higher than 125 mg/dL and/or 6.4% (E), respectively. HbA1c – glycated hemoglobin; r' – Rho value; p – p value; U – units; VAT – visceral adipose tissue; IR – insulin resistant IS – insulin sensitive; HbA1c – glycated hemogloblin; HOMA2IR – homeostasis model assessment 2 insulin resistance index; GLO-1 – glyoxalase-1. Data are shown in dots accordingly to each patient result/group plus tendency lines.

Hyperinsulinemia is positively correlated with visceral adipose tissue glyoxalase-1 activity in pre-diabetic obese patients

Although insulin could change GLO-1 activity, no correlations were found between insulinemia and human VAT GLO-1 activity in all included patients (Figure 4.17A). However, pre-diabetic obese patients have shown a positive Spearman correlation between insulin levels and GLO-1 activity (r'=0.551; p=0.002). Accordingly, increased insulinemia in obese patients during prediabetes is associated with higher GLO-1 activity in VAT (Figure 4.17D). However, this association is lost in obese type 2 diabetic patients (Figure 4.17E).
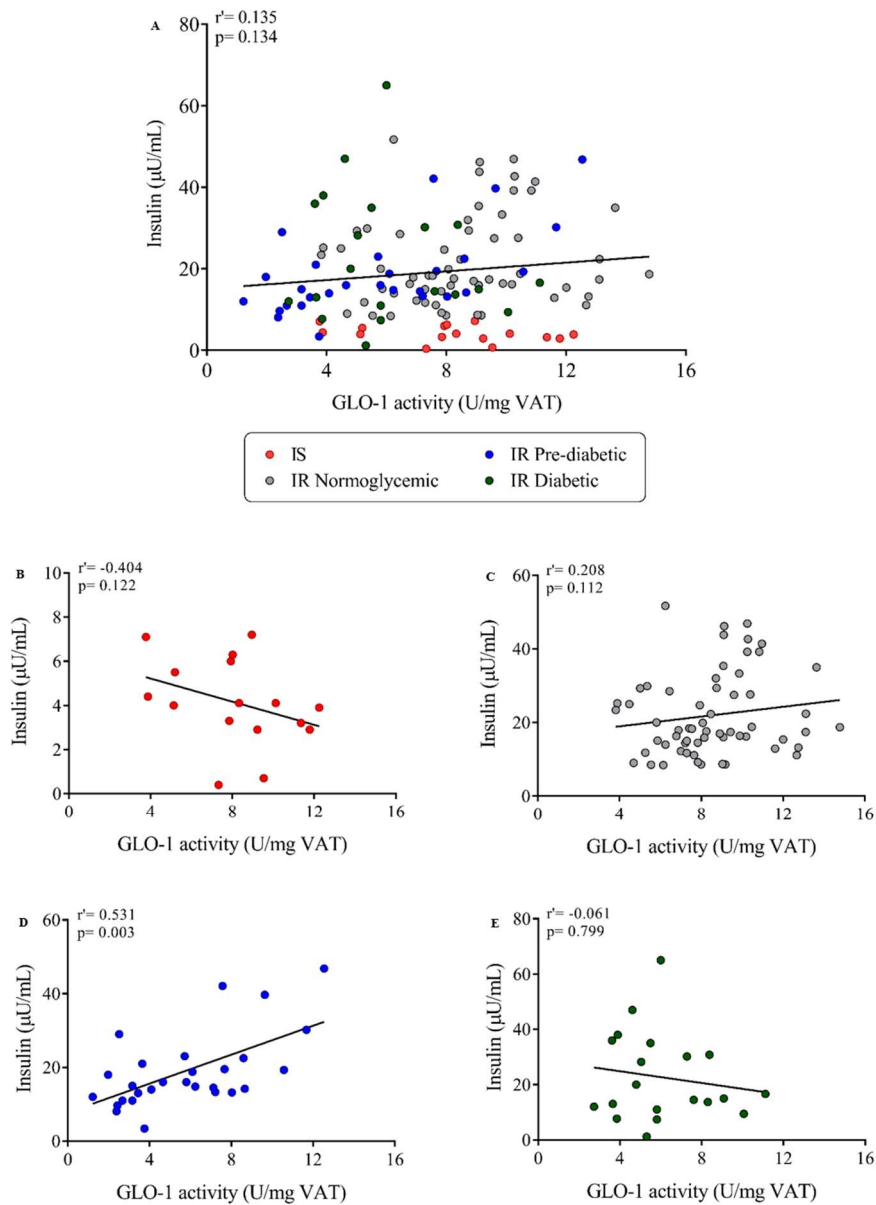
Figure 4.17 – Visceral adipose tissue glyoxalase-1 activity is increased following hyperinsulinemia in pre-diabetic obese patients

Non-parametric Sprearman correlations were calculated from all data (A) or to each group (B-E), using fasting insulin levels vs VAT-derived GLO-1 activity (kit from Sigma – Merck, USA). IS – patients with HOMA2IR<1 (B); IR normoglycemic - patients with HOMA2IR>1 but normoglycemic (C); IR pre-diabetic – patients with HOMA2IR>1 and 99 mg/dL<fasting glycemia<126 mg/dL and/or 5.6%<HbA1c<6.5% (D); IR diabetic – patients with HOMA2IR>1, fasting glycemia and HbA1c higher than 125 mg/dL and/or 6.4% (E), respectively. IS – insulin sensitive; IR – insulin resistant; HbA1c – glycated hemogloblin; HOMA2IR – homeostasis model assessment 2 insulin resistance index; r' – rho value; p – p value; U – units; VAT – visceral adipose tissue; GLO-1 – glyoxalase-1. Data are shown in dots accordingly to each patient result/group plus tendency lines.

Insulin resistance and visceral adipose tissue glyoxalase-1 activity in obese patients

In insulin sensitive patients, decreased insulin resistance (HOMA2) is associated with higher VAT GLO-1 activity (r' -0.547; p=0.037), reinforcing the relation between GLO-1 activity and metabolically healthy conditions (Figure 4.18B). This association is lost in insulin resistant but normoglycemic patients (Figure 4.18C). Interestingly, in pre-diabetic obese patients, insulin resistance is positively associated with higher VAT GLO-1 activity (r'=0.541; p=0.002), suggesting the existence of other compensatory mechanisms, that may be triggered by increased intracellular glucose levels and metabolic-derived signals (signalling through enhanced production of MG and other factors). However, this positive association is lost in obese type 2 diabetic patients (Figure 4.18E).
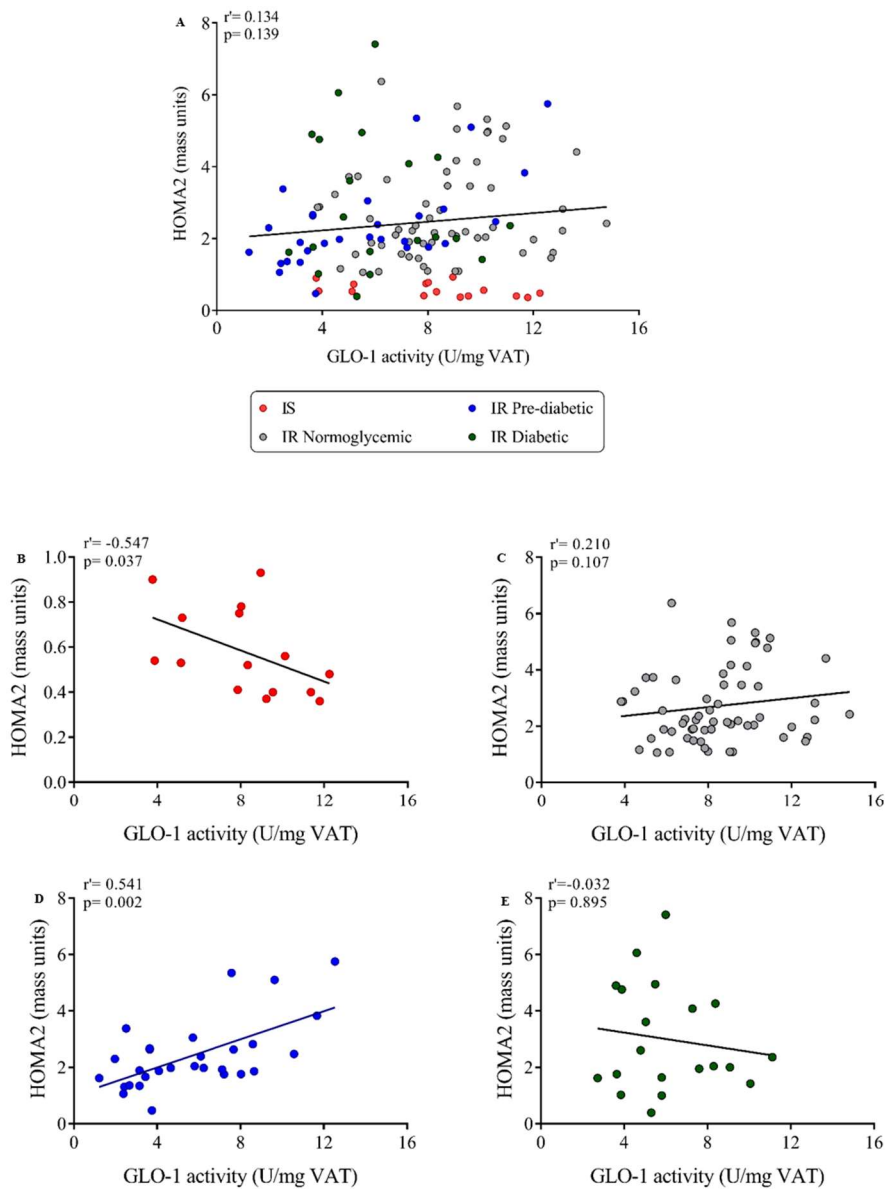
Figure 4.18 – Insulin resistance changes visceral adipose tissue glyoxalase-1 activity in obese patients
Non-parametric Sprearman correlations were calculated from all data (A) or to each group (B-E), using HOMA2 insulin resistance index vs VAT-derived GLO-1 activity (kit from Sigma – Merck, USA). IS – patients with HOMA2IR<1 (B); IR normoglycemic – patients with HOMA2IR>1 but normoglycemic (C); IR pre-diabetic – patients with HOMA2IR>1 and 99 mg/dL<fasting glycemia<126 mg/dL and/or 5.6%<HbA1c<6.5% (D); IR diabetic – patients with HOMA2IR>1, fasting glycemia and HbA1c higher than 125 mg/dL and/or 6.4% (E), respectively. IS – insulin sensitive; HbA1c – glycated hemogloblin; HOMA2IR – homeostasis model assessment 2 insulin resistance index; HOMA2 – homeostasis model assessment 2 index; IR – insulin resistant; r' – rho value;p – p value; U – units; VAT – visceral adipose tissue. Data are shown in dots accordingly to each patient result/group plus tendency lines.

2.1.2 Sleeve gastrectomy reduces glycated material accumulation in pEAT

Recently, data from our group demonstrated increased GLP-1 signalling after vertical sleeve gastrectomy as well as significantly improved adipose tissue angiogenesis and health. This model has shown reduced insulin resistance and improvement of PPAR-γ and several markers of sprouting regulation involved in angiogenesis and endothelial function (Eickhoff et al, 2015 and in revision). Using this model, vertical sleeve gastrectomy (GKHFDSl) in GK rats maintained with a high-calorie diet, resulted in diminished PAS positive material deposition and a slight reduction of CEL accumulation, which were increased in GK rats feeding standard diet (GKSD) and those feeding a high-calorie diet (GKHFD and GKHFDsh) (Figure 4.19A-B).
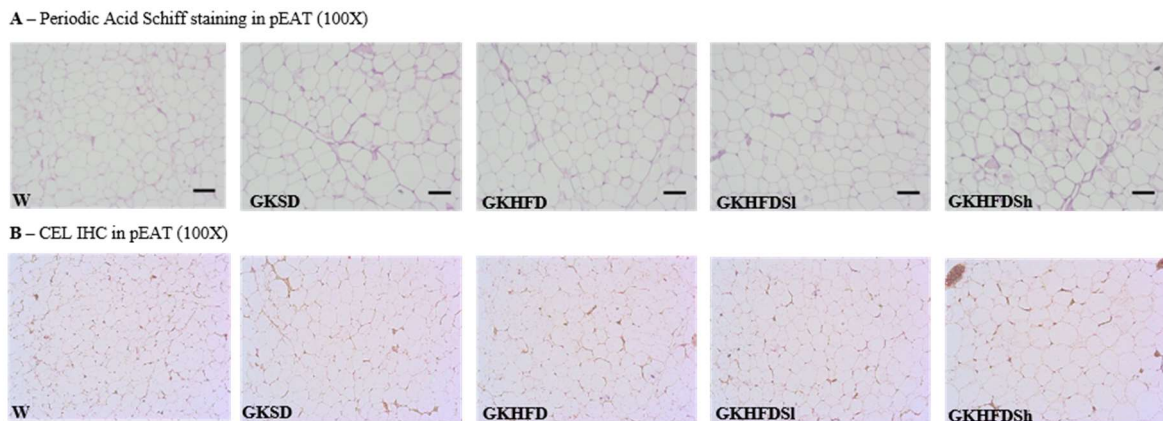
Figure 4.19 - Metabolic surgery decreases Periodic Acid-Schiff positive material and CEL in pEAT from GK rats fed a high-calorie diet

Histological analysis shows PAS (100X) staining (A) and CEL IHC (100X) (B). W – Wistar rats 6 months old fed a standard diet; GKSD – Goto-Kakizaki rats 6 months old fed a standard diet; GKHFD - Goto-Kakizaki rats 6 months old fed a high-calorie diet for 5 months; GKHFDSl – GKHFD submitted to sleeve gastrectomy at 4 months old; GKHFDSh – GKHFD submitted to sham surgery at 4 months old. CEL – Ne(carboxyethyl)lysine; pEAT – periepididymal adipose tissue; PAS – Periodic Acid-Schiff; IHC – immunohistochemistry. Representative image of PAS staining and CEL IHC are shown, n = 3/group.

Sleeve gastrectomy improves insulin sensitivity and systemic metabolism

GKHFD and GKHFDSh groups have eaten more calories per day than age-matched Wistar and GK animals maintained with standard diet (p<0.01 vs W and GKSD). Age-matched GK fed with SD are smaller than Wistar rats (p<0.001 vs W), while GK fed a high-calorie diet increased body weight, including GKHFD (p<0.05 vs GKSD) and GKHFDSh (p<0.01 vs GKSD) groups. However, GK animals submitted to high-calorie diet and vertical sleeve gastrectomy have shown decreased calorie ingestion (p<0.05 vs GKHFDSh), being body and pEAT weight similar to GKSD animals. Accordingly, weight gain between four and six months old was significantly lower in GKHFDSl group (p<0.05 vs GKSD; p<0.001 vs GKHFD and GKHFDSh) even maintaining the animals with high-calorie diet in this period. Accordingly, glucose homeostasis and insulin sensitivity were impaired by the high-calorie diet, but vertical sleeve gastrectomy (GKHFDSl) improved fasting glycemia (p<0.05 vs GKSD), IPITT-AUC (p<0.05 vs GKHFD) and glycemia at 2h during ITT (p<0.01 vs GKHFD) and HOMA (similar to GKSD). The impairment of lipid profile (serum triglycerides and cholesterol) induced by high-calorie diet was reverted by metabolic surgery (p<0.01 vs GKHFD and GKHFDSh). Despite the fact that pEAT GSH levels have a tendency to increase in GKHFDSl, there are no significant statistical differences between groups (Table 4.4).

Table 4.4 - Caloric intake and weight gain after sleeve gastrectomy. Body and pEAT weight, glycemic (6h fasting glycemia, HOMA, AUC during the IPITT and glycemia at the end of the IPITT) and lipid profile (6h fasting serum triglycerides and cholesterol levels) and pEAT GSH levels at the end of the experimental period.

Group	W	GKSD	GKHFD	GKHFDSl	GKHFDSh
Caloric ingestion (Kcal/rat/day)	63.7±1.5	64.4±1.3	81.4±4.4***##	69.9±4.7&	84.4±4.7***##
Body weight (g)	487±12	371.4±5.1***	405.9±47.2**#	389.7±8.4***	412±9.7*##
Weight gain 4-6 months (%)	10.8±1.5	11.6±2.3	17.2±1.7*#	3.3±2.1*#$$$&&&	16.7±1.4*#
Fasting glycemia (mg/dL)	81.1±1.8	207.6±15.8***	202.8±23.4***	142.5±9.9**#	166.4±19.5**
IPITT - AUC	135.6±3.1	242.1±20.8	365.6±36.2*****##	240.4±16.6**$	296±22.8*****##
IPITT – glycemia at 2h (mg/dL)	66.6±2.3	77.7±4.9**	141.8±18.8****#	89.6±4.3**$$	114.6±12.8***
HOMA	8.1±0.2	10.8±1.4	23.9±2.7**#	16.7±3.0	27.2±3.9**#
Triglycerides (mg/dL)	175.0±14.0	126.2±10.3	402.7±27.2******###	226±20.6#$$&&	381.1±28.7*****###
Cholesterol (mg/dL)	164.7±1.4	157.6±2.5	219.7±15.4*****###	167.4±5.3$$&&	209.8±16.6*****###
pEAT weight (g)	7.2±1.1	3.9±0.2	4.8±0.4	2.8±0.3***$$&&	5.2±0.5
pEAT GSH levels (nmol/mL)	15.7±4.2	13.7±7.5	14.2±5.6	21.1±3.0	18.4±7.1

W – Wistar rats 6 months old fed a standard diet; GKSD – Goto-Kakizaki rats 6 months old fed a standard diet; GKHFD – Goto-Kakizaki rats 6 months old fed a high-calorie diet for 5 months; GKHFDSl – GKHFD submitted to sleeve gastrectomy at 4 months old; GKHFDSh – GKHFD submitted to sham surgery at 4 months old. HOMA – homeostatic model assessment for insulin resistance; pEAT – periepididymal adipose tissue; GSH – reduced gluthathione; IPITT – intraperitoneal insulin tolerance test. Results are presented as mean ± SEM, n = 6-8/group. * vs W; # vs GKSD; $ vs GKHFD; & vs GKHFDSh. 1 symbol p<0.05; 2 symbols p<0.01; 3 symbols p<0.001.

Sleeve gastrectomy increases GLP-1 receptor and catalase levels in pEAT

In the pEAT, sleeve gastrectomy in rats fed a high-calorie diet resulted in a significant increase of GLP-1R levels ($p<0.01$ vs GKSD and GKHFD), which were decreased in GKHFD rats ($p<0.05$ vs W) (Figure 4.20A). Higher GLP-1R levels in pEAT may be associated with increased GLP-1 signaling, which is known to increase postprandially after vertical sleeve gastrectomy (Eickhoff et al., 2015). Furthermore, sleeve gastrectomy also resulted in a significant improvement of catalase levels ($p<0.05$ vs GKHFDSh; $p<0.01$ vs GKHFD), a known antioxidant enzyme, while no effects were observed in SOD1, which suggests the existence of mechanisms specifically involved in governing the expression and/or activity of several antioxidant and detoxification mechanisms (Figure 4.20B and WB panel).
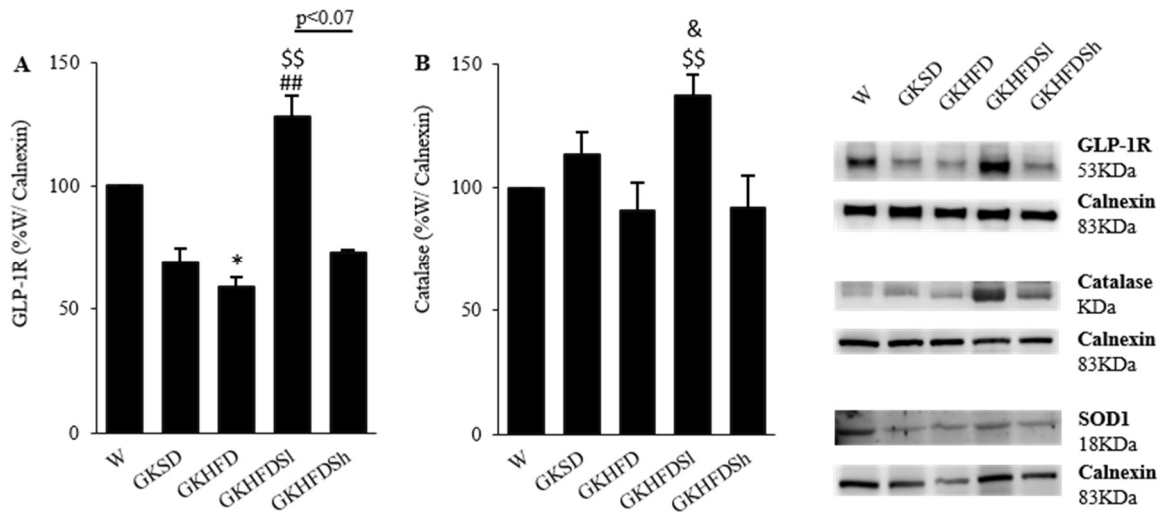
Figure 4.20 - Metabolic surgery increases GLP-1 receptor and catalase levels in pEAT

GLP-1R (A) and catalase (B) and SOD1 (WB right painel) levels were evaluated through WB quantification. Representative WB images are shown. W – Wistar rats 6 months old fed a standard diet; GKSD – Goto-Kakizaki rats 6 months old fed a standard diet; GKHFD – Goto-Kakizaki rats 6 months old fed a high-calorie diet for 5 months; GKHFDSl – GKHFD submitted to sleeve gastrectomy at 4 months old; GKHFDSh – GKHFD submitted to sham surgery at 4 months old. GLP-1R – glucagon-like peptide-1 receptor; SOD1 – superoxide dismutase 1; pEAT – periepididymal adipose tissue; WB – western blotting. Bars represent means ± SEM, n = 6-8/group. * vs W; $ vs GKHFD; & vs GKHFDSh; 1 symbol $p<0.05$; 2 symbols $p<0.01$.

Sleeve gastrectomy prevents lower glyoxalase-1 levels and activity in GK rats

GLO-1 is crucial in methylglyoxal degradation, preventing negative effects on AT angiogenesis and microvascular complications. GLO-1 levels were significantly decreased in GKSD ($p < 0.05$ vs W) as well as in GKHFD ($p < 0.01$ vs W) and GKHFDSh ($p < 0.01$ vs W) groups. However, GKHFDSl animals have shown increased GLO-1 levels in pEAT ($p < 0.07$ vs GKHFD; $p < 0.05$ vs GKHFDSh), being similar to W group (Figure 4.21A). Regarding GLO-1 activity in pEAT, there was a significant decrease in GKHFD ($p < 0.05$ vs W) and GKHFDSh ($p < 0.01$ vs W and $p < 0.05$ vs GKHFDSl), which was prevented in GKHFDSl group (Figure 4.21B).
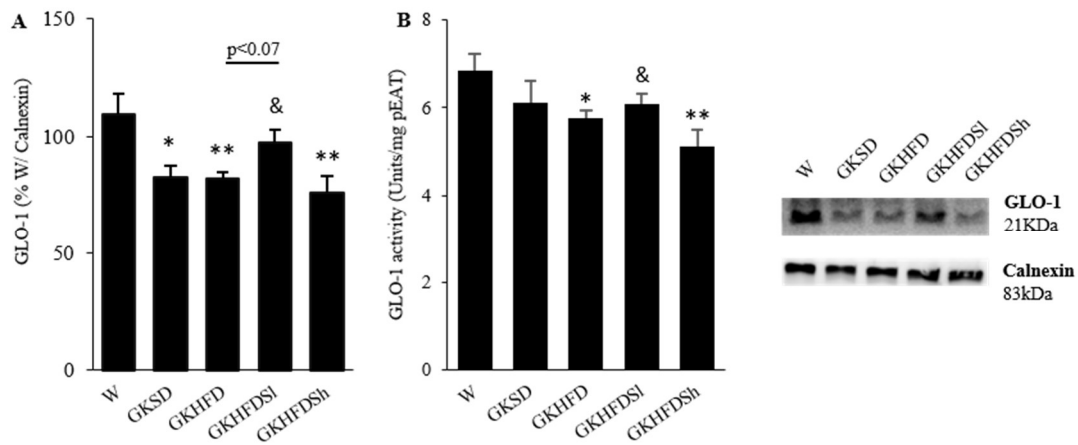
Figure 4.21- Metabolic surgery prevents glyoxalase-1 levels and activity decrease in pEAT
GLO-1 levels (A) and GLO-1 activity (B) were evaluated through WB quantification and GLO-1 activity assay, respectively. Representative WB images are shown in the right panel. W - Wistar rats 6 months old fed a standard diet; GKSD – Goto-Kakizaki rats 6 months old fed a standard diet; GKHFD – Goto-Kakizaki rats 6 months old fed a high-calorie diet for 5 months; GKHFDSl – GKHFD submitted to sleeve gastrectomy at 4 months old; GKHFDSh – GKHFD submitted to sham surgery at 4 months old. GLO-1 – glyoxalase-1; U – units; g – grams; pEAT – periepididymal adipose tissue; WB – Western Blotting. Bars represent means ± SEM, n = 6-8/group. * vs W; & vs GKHFDSh; 1 symbol $p < 0.05$; 2 symbols $p < 0.01$.

2.1.3 Liraglutide prevents methylglyoxal-induced decrease of angiogenesis in matrigel plug angiogenesis assay

Our group has recently shown that sleeve gastrectomy enhances the levels of angiogenic and vasoactive pathways in the pEAT from diet-induced obese GK rats, particularly VEGF and ANG-2 as well as the endothelial cell marker CD31 and the levels of endothelial nitric oxide synthase (Eickhoff, in revision). In the present work, we hypothesized that such effects may result from increased GLP-1 signaling on AT.

Firstly, we evaluated the angiogenic effects of liraglutide (GLP-1 analogue) and MG in matrigel plug angiogenesis assay. MG-supplemented matrigel decreased angiogenesis when compared to Ct (Figure 4.22A-B). Despite the fact that liraglutide-supplemented matrigel has not significantly increased angiogenesis (Figure 4.22C), MG-induced decrease of angiogenesis was fully prevented by liraglutide (Figure 4.22D).
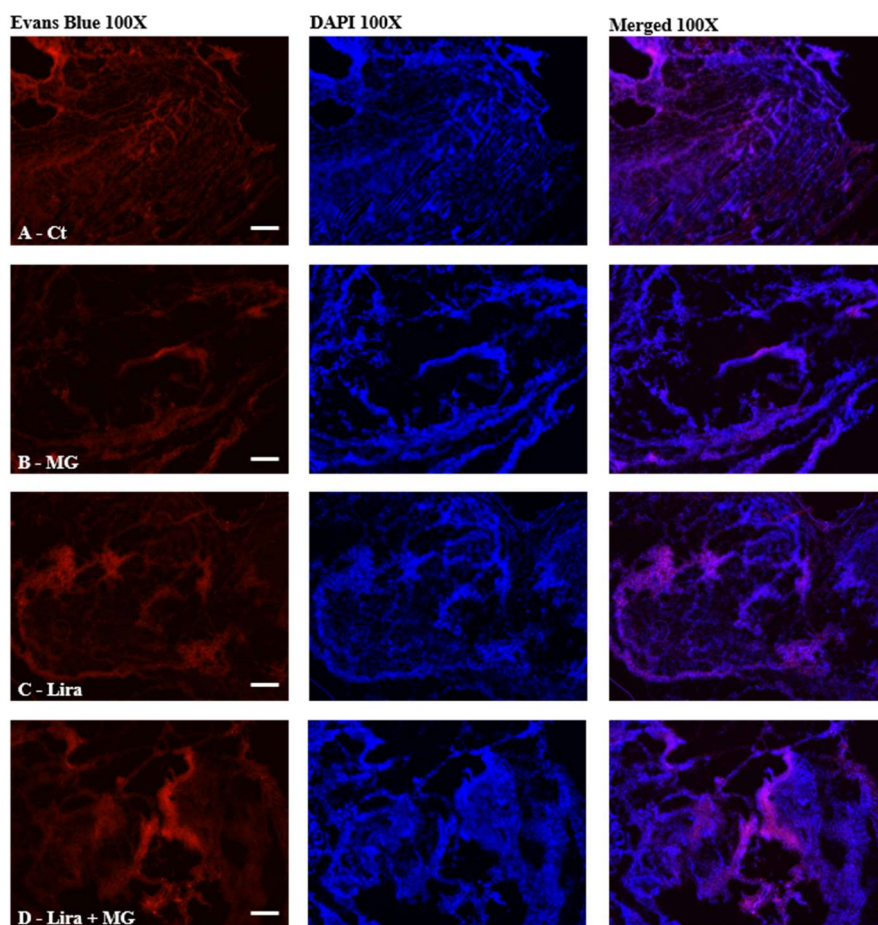
Figure 4.22 – Methylglyoxal decreases angiogenesis in matrigel, being this effect prevented by liraglutide
Matrigel plug assay was employed and matrigel-derived slices containing Evans blue were stained with DAPI. Representative image (Evans blue-red, DAPI-blue and merged staining, 50X) of all conditions are shown (A-D). Phenol red-free matrigel plus heparin (50 U/mL) was administered subcutaneously (A), supplemented with MG (B), liraglutide (C) or both (D). Ct – Wistar rats sixteen weeks old plus matrigel supplemented with heparin (50 U/mL); MG 250 μM – Wistar rats sixteen weeks old plus matrigel supplemented with heparin (50 U/mL) and MG (250 μM); Lira 100 nM – Wistar rats sixteen weeks old plus matrigel supplemented with heparin (50 U/mL) and liraglutide (100 nM); Lira 100 nM + MG 250 μM – Wistar rats sixteen weeks old plus matrigel supplemented with heparin (50 U/mL) and liraglutide (100 nM) and MG (250 μM). MG – methylglyoxal; Lira – liraglutide; DAPI – 4′,6-diamidino-2-phenylindole; n = 3/condition.

Liraglutide improves body weight, insulin signaling and lipid homeostasis in diabetic GK rats

Human GLP-1 analogue, liraglutide was used to explore GLP-1 specific effects on pEAT function, including angiogenesis and GLO-1-dependent mechanisms. As described before, non-obese type 2 diabetic rats have lower body weight, mild fasting hyperglycemia and marked glucose intolerance when compared with age-matched Wistar rats. Liraglutide treatment significantly reduced food consumption in normal ($p<0.05$ vs W) and type 2 diabetic rats ($p<0.05$ vs GK), leading to a significant reduction of body ($p<0.001$ vs W) and pEAT ($p<0.01$ vs W) weight in diabetic rats (Table 4.5 and Figure 4.23A). In addition, liraglutide-treated Wistar animals have shown decreased weight gain ($p<0.01$ vs W), when compared to W group (Table 4.5 and Figure 4.23A). As expected, type 2 diabetic GK animals (GK and GKLira) have shown increased fasting glycemia ($p<0.05$ vs W). However, the increased IPITT-AUC observed in GK rats ($p<0.01$ vs W) was not maintained after liraglutide treatment (GKLira) (Table 4.5 and Figure 4.23B), suggesting higher insulin sensitivity. No alterations were observed for cholesterol and pEAT GSH levels in experimental groups. Moreover, diabetic rats treated with liraglutide improved serum triglycerides and free fatty acids ($p<0.01$ vs GK) levels (Table 4.5 and Figure 4.23C). Altogether, these results reinforce the efficacy and pleiotropic actions of liraglutide, decreasing insulin resistance, body and pEAT weight and lipid levels in non-obese diabetic GK rats.

Table 4.5 - Food intake and weight gain during liraglutide treatment. Body and pEAT weight, glycemia and lipid profile (6h fasting) and pEAT GSH levels.

Group	W	GK	WLira	GKLira
Food consumption (g/rat/day)	16.9±0.6	18.3±1.6	11.2±0.8*	11.6±1.3*#
Body weight (g)	390.1±3.4	312.9±2.4**	361±8.8	302.5±7.3***
Weight gain (%)	0.2±0.5	1.2±0.6	-9.6±0.7**	-5.4±2.3*
Fasting glycemia (mg/dL)	84.1±2.4	140.5±25.3*	87.9±4.6	115.5±5.1*
Triglycerides (mg/dL)	106.1±9.0	207.5±52.3*	100.3±7.8	111.3±6.6
Cholesterol (mg/dL)	167.6±2.8	176.2±2.7	169.2±1.4	174±2.5
pEAT GSH levels (nmol/mL)	4.2±1.0	3.2±0.4	4.0±1.0	3.2±0.5
pEAT weight (g)	4.1±0.6	2.8±0.3	3.3±0.3	2.0±0.2**

W – Wistar rats 14 weeks old and saline administration during 2 weeks; GK – Goto-Kakizaki rats 14 weeks old and saline administration during 2 weeks; WLira – Wistar rats 14 weeks old with liraglutide administration during 2 weeks twice/day; GKLira – GK rats 14 weeks old with liraglutide administration during 2 weeks twice/day. GSH – reduced gluthathione; pEAT – periepididymal adipose tissue. Results are presented as mean ± SEM, n = 6/group. * vs Ct; # vs GK. 1 symbol $p<0.05$; 2 symbols $p<0.01$; 3 symbols $p<0.001$.
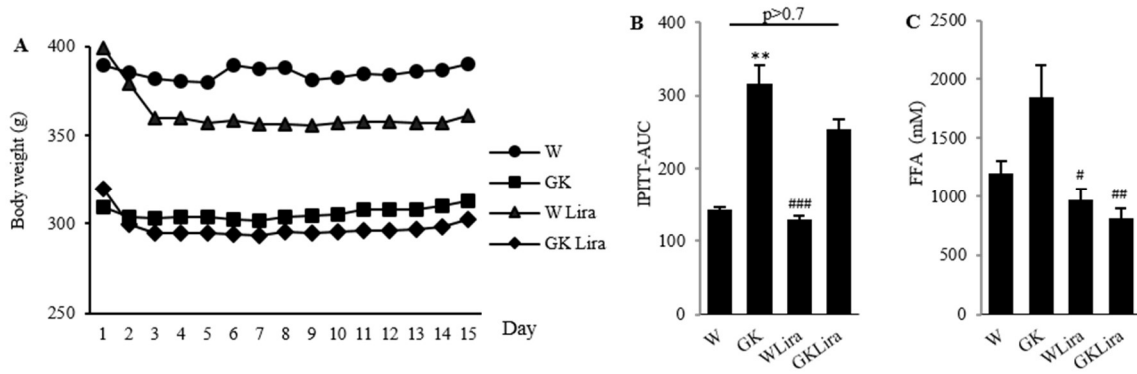
Figure 4.23 - Liraglutide decreases body weight and insulin resistance and circulating FFA in GK rats
Body weight was recorded daily during liraglutide treatment period (A). In order to evaluate insulin sensitivity, IPITT was performed and glucose levels assessed to calculate the AUC (B). Regarding serum FFA levels, samples were quantified using FFA assay kit (C). W – Wistar rats 14 weeks old and saline administration during 2 weeks; GK – Goto-Kakizaki rats 14 weeks old and saline administration during 2 weeks; WLira – Wistar rats 14 weeks old with liraglutide administration during 2 weeks twice/day; GKLira – GK rats 14 weeks old with liraglutide administration during 2 weeks twice/day. IPITT – intraperitoneal insulin tolerance test; AUC – area under the curve; FFA – free fatty acids. Bars represent means ± SEM, n = 6/group. * vs Ct; # vs GK. 1 symbol $p<0.05$; 2 symbols $p<0.01$; 3 symbols $p<0.001$.

Liraglutide increases insulin receptor activation in diabetic GK rats

Type 2 diabetic rats showed a tendency to lower activation of the insulin receptor (Tyrosine 1161) in pEAT, when compared to control rats. However, liraglutide administration resulted in increased IR-Tyr1161 levels in GK rats (p<0.01 vs GK) (Figure 4.24A). Liraglutide increased PPARgamma levels in pEAT in normal rats and not affects perilipin-A (Figure 4.24B), GLP-1R and GLUT-4 levels in normal and diabetic rats (WB panel).
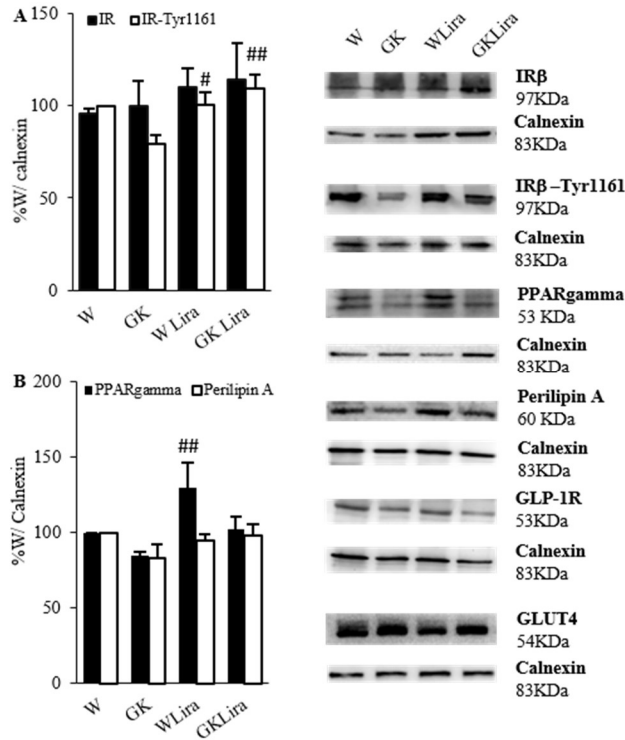
Figure 4.24 - Liraglutide increases insulin receptor activation in pEAT from diabetic GK rats
Insulin receptor (total and Tyr1161) (A) and PPAR-γ and perilipin-A levels (B) were evaluated through WB quantification. Representative WB image are shown in the right panel. W – Wistar rats 14 weeks old and saline administration during 2 weeks; GK – Goto-Kakizaki rats 14 weeks old and saline administration during 2 weeks; WLira – Wistar rats 14 weeks old with liraglutide administration during 2 weeks twice/day; GKLira – GK rats 14 weeks old with liraglutide administration during 2 weeks twice/day. WB – western blotting; IR – insulin receptor; pEAT – periepididymal adipose tissue; GLUT-4 – glucose transporter-4; GLP-1 – glucagon-like peptide-1; PPAR-gamma – peroxisome proliferator-activated receptor gamma. Bars represent means ± SEM, n = 6/group. # vs GK. 1 symbol p<0.05; 2 symbols p<0.01.

Liraglutide ameliorates pEAT response to hypoxia, vascular function and angiogenic pathways

HIF-2alpha is a known transcription factor involved in long-term adaptation to hypoxia as well as increased macrophage phenotype M2 and reduced inflammation status in pEAT. Type 2 diabetic rats have shown increased levels of HIF-2alpha after liraglutide treatment ($p < 0.05$ vs GK) (Figure 4.25A). The endothelial cell marker CD31, which was reduced in GK rats ($p < 0.01$ vs W) was slightly increased after liraglutide administration ($p < 0.05$ vs W) (Figure 4.25B). Regarding total and eNOS-Ser1177 levels in pEAT, although no significant alterations have occurred in GK groups, WLira group increased eNOS-Ser117 ($p < 0.01$ vs GK), meaning a tendency to increase when compared to control group (W) (Figure 4.25C). Type 2 diabetic rats showed decreased levels of the VEGF and angiopoietin receptors in pEAT, VEGFR2 ($p < 0.05$ vs W) and TIE-2 ($p < 0.05$ vs W), respectively, and liraglutide restored TIE-2 levels ($p < 0.05$ vs GK) (Figure 4.25D-E). Remarkably, an increase in pEAT VEGF levels (WLira $p < 0.01$ vs W; GKLira $p < 0.05$ vs GK) was observed in both liraglutide-treated groups (Figure 4.25D).
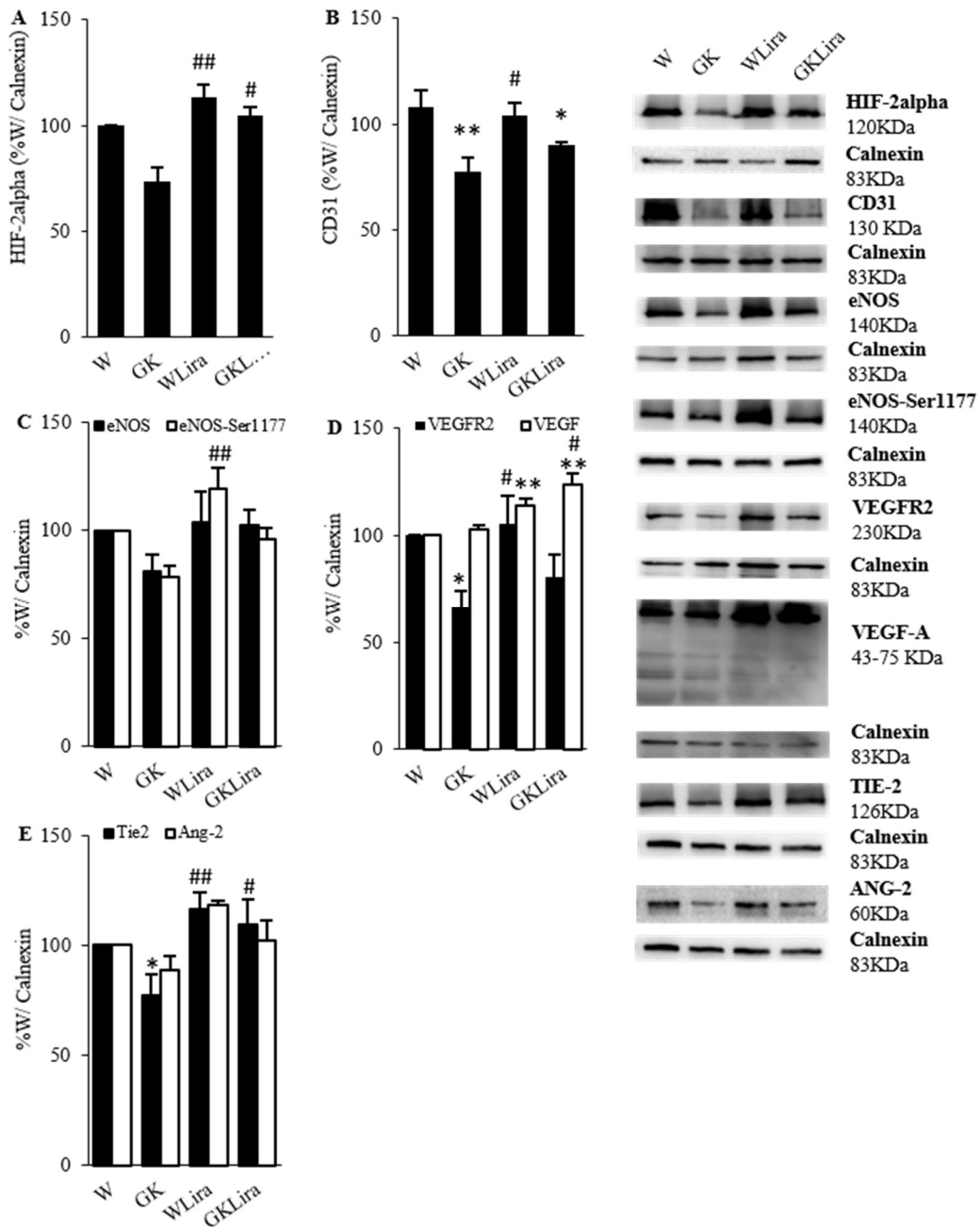
Figure 4.25 - Liraglutide ameliorates pEAT adaptation to hypoxia, vascular function and angiogenesis
HIF-2alpha (A), CD31 (B), eNOS (total and Ser1177) (C), VEGFR2/VEGF (D) and Tie-2/Ang-2 (E) levels
were evaluated through WB quantification. Representative WB images are shown in the right panel. W – Wistar
14 weeks old and saline administration during 2 weeks; GK – Goto-Kakizaki 14 weeks old and saline
administration during 2 weeks; WLira – Wistar 14 weeks old with liraglutide administration during 2 weeks
twice/day; GKLira – GK 14 weeks old with liraglutide administration during 2 weeks twice/day. WB – western
blotting; pEAT– periepididymal adipose tissue; HIF-2alpha – hypoxia inducible factor-2 alpha; CD31 – cluster
of differentiation 31/endothelial cell marker; eNOS – endothelial nitric oxide synthase VEGF – Vascular
endothelial growth factor; VEGFR2 – VEGF receptor 2; ANG-2 – Angiopoietin-2; TIE-2 – angiopietin
receptor-2. Bars represent means ± SEM, n = 6/group. * vs Ct; # vs GK. 1 symbol p<0.05; 2 symbols p<0.01.

Liraglutide restores glyoxalase-1 levels and activity in pEAT from diabetic GK rats

Type 2 diabetic GK rats had decreased GLO-1 levels ($p<0.05$ vs W) and activity ($p<0.05$ vs W) in pEAT, that were restored by liraglutide treatment (Figure 4.26A-B). No significant differences were observed for GSH levels between groups (Figure 4.26C).
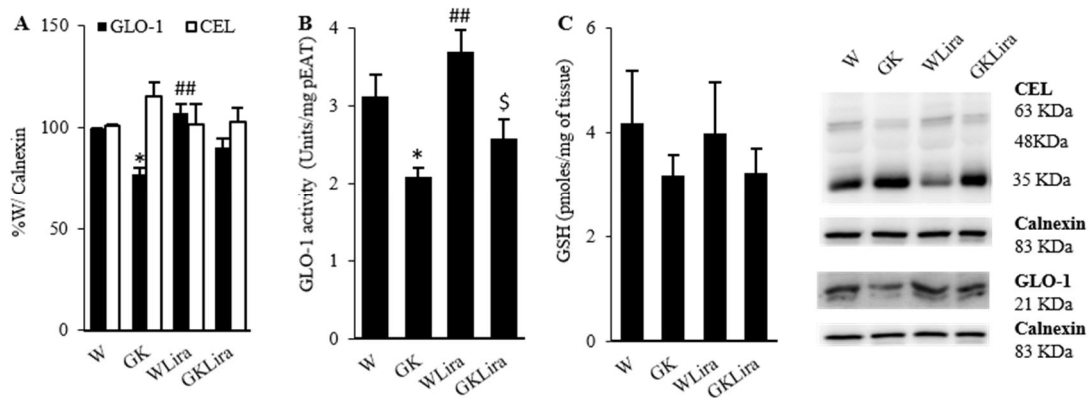
Figure 4.26 - Liraglutide restores glyoxalase-1 levels in pEAT from diabetic GK animals
GLO-1 and CEL levels were evaluated through WB quantification (A). GLO-1 activity (B) and GSH levels in pEAT were evaluated through commercial kits (C). Representative WB images are shown in the right panel. W – Wistar rats 14 weeks old and saline administration during 2 weeks; GK – Goto-Kakizaki rats 14 weeks old and saline administration during 2 weeks; WLira – Wistar rats 14 weeks old with liraglutide administration during 2 weeks twice/day; GKLira – GK rats 14 weeks old with liraglutide administration during 2 weeks twice/day. WB – western blotting; pEAT – periepididymal adipose tissue; GSH – reduced gluthathione GLO-1 – glyoxalase-1; CEL – N-epsilon (carboxyethyl)lysine. Bars represent means ± SEM, n = 6/group. * vs Ct; # vs GK; $ vs WLira. 1 symbol $p<0.05$; 2 symbols $p<0.01$.

Liraglutide improves pEAT angiogenesis in a glyoxalase-1-dependent manner

MG-induced glycation has been shown as a mechanism involved in the disturbance of the microvessel network in pEAT, leading to vascular dysfunction and loss of capillarization and blood flow (last section – 4.1). Using the AT angiogenesis assay, incubation of AT explants with methylglyoxal or the selective GLO-1 inhibitor BBGC, resulted in decreased pEAT capillarization area (MG and BBGC $p<0.001$ vs Ct), sprout length (MG and BBGC $p<0.001$ vs Ct) and vessel density (MG and BBGC $p<0.05$ vs Ct) (Figure 4.27A-C). Although no alterations have been observed in pEAT capillarization area and sprout length, vessel density was increased (Lira 50 nM $p<0.001$ vs Ct) in liraglutide-treated pEAT explants (Figure 4.27C). Additionally, liraglutide was able to prevent MG-induced inhibition of pEAT angiogenesis, by significantly improving the area of capillarization ($p<0.05$ vs MG 250 μM), vessel density ($p<0.01$ vs MG 250 μM) and partially the sprout length (Figure 4.27A-C). Interestingly, such effects of liraglutide were fully prevented in BBGC-incubated explants, suggesting that a fully functional GLO system is required for the angiogenesis-stimulating actions of liraglutide (Figure 4.27A-D).

D – Adipose tissue angiogenesis assay

Without Liraglutide, 5 days

Ct, 5 days   BBGC 10 μM 5 days   MG 250 μM 5 days

Liraglutide, 5 days

Lira 50 nM   Lira 50 nM + BBGC 10 μM   Lira 50 nM + MG 250 μM
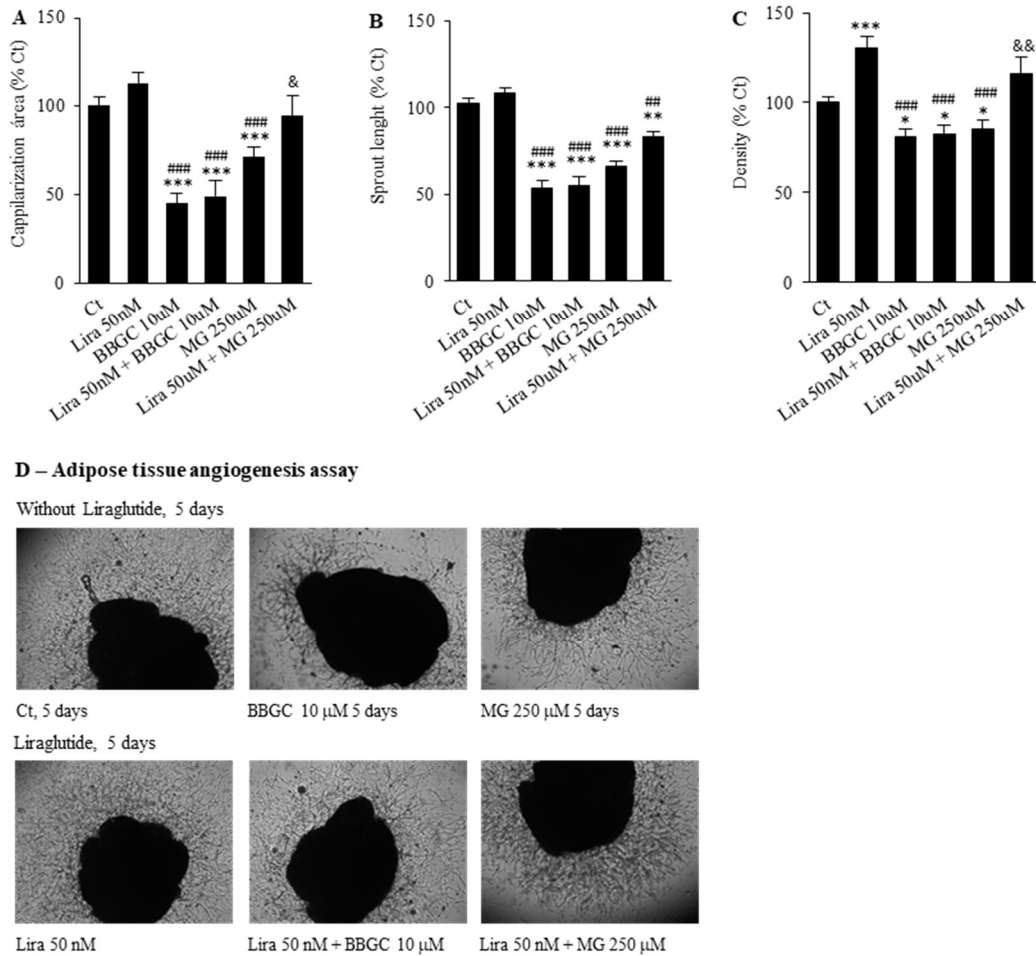
Figure 4.27 - Liraglutide improves pEAT angiogenesis through glyoxalase-1-dependent mechanisms

Using AT angiogenesis assay, capillarization area (A), sprout length (B) and vessel density (C) were evaluated. Representative bright field images of all conditions after five days are shown (50X) (D).

Ct – EGM-2MV plus vehicle (DMSO); Lira – EGM-2MV plus Lira (50 nM); BBGC – EGM-2MV plus BBGC (10 μM); Lira + BBGC – EGM-2MV plus Lira (50 nM) plus BBGC (10 μM); MG – EGM-2MV plus MG (250 μM); Lira + MG – EGM-2MV plus Lira (50 nM) plus MG (250 μM). EGM-2MV – supplemented endothelial growth medium; MG – methylglyoxal; DMSO – dimethyl sulfoxide; BBGC – bromobenzylglutathione cyclopentyl diester; Lira – liraglutide. Bars represent means ± SEM, n = 6x3/condition. * vs Ct; # vs Lira 50 nM; & vs MG 250 μM. 1 symbol $p<0.05$; 2 symbols $p<0.01$; 3 symbols $p<0.001$.

2.2 Highlights

✓ Early decrease of adipose tissue glyoxalase-1 activity is observed during progressive decline of β-cell and adipose tissue function in insulin resistant obese patients;

✓ Adipose tissue glyoxalase-1 activity is negatively correlated with impaired glycemic control in obese patients;

✓ Metabolic surgery increases GLP-1 receptor in adipose tissue and restores glyoxalase-1 levels and activity in diet-induced obese type 2 diabetic GK rats;

✓ Liraglutide restores adipose tissue GLO-1 levels and activity, as well as improves adipose tissue function and local and systemic insulin resistance in non-obese diabetic GK animals;

✓ Liraglutide prevents decreased angiogenesis induced by methylglyoxal;

✓ Liraglutide increases adipose tissue angiogenesis through glyoxalase-1-dependent mechanisms.

2.3 Discussion

In this work we have shown progressive loss of visceral adipose tissue GLO-1 activity and impaired markers of AT function in insulin resistant obese patients. Our data suggest, for the first time, the therapeutic potential of GLP-1-based strategies in restoring AT angiogenesis and function, by reducing glycation effects through GLO-1 dependent mechanisms. In fact, sleeve gastrectomy was able to enhance GLP-1R and restore GLO-1 levels in pEAT of diet-induced obese type 2 diabetic rats. Besides, human GLP-1 analogue, liraglutide, prevented MG-induced decrease of angiogenesis in matrigel plug angiogenesis assay. *In vivo*, liraglutide administration restored GLO-1 levels and activity leading to upregulation of AT angiogenic markers and angiogenesis improvement of AT explants in a GLO-1-dependent manner.

Glyoxalase system is critically involved in methylglyoxal detoxification. However, this system is impaired in type 2 diabetes, leading to the development of several diabetic complications (Brownlee, 2001; Matafome et al., 2015; Rabbani et al., 2014). Recently, a GLO-1 inducer formulation based on the NRF-2 activating effects of trans-resveratrol (tRES)-hesperetin (HESP) combination was developed as a possible new strategy for the improvement of metabolic and vascular health in obese patients, preventing the development of metabolic abnormalities and cardiovascular diseases (Rabbani and Thornalley, 2018; Rabbani et al., 2016; Xue et al., 2016). The impairment of this enzymatic system seems to far precede the development of diabetic complications, being present since the metabolic dysregulation occurring in obese patients. However, the real impact of GLO system in AT health in obesity is controversial and mostly unknown.

Masterjohn and colleagues have shown that liver GSH depletion in Sprague Dawley rats resulted in increased MG accumulation by impairing GSH-dependent glyoxalase-mediated

detoxification (Masterjohn et al., 2013a, 2013b). On the other hand, in red blood cells from leptin-deficient ob/ob mice and leptin receptor mutated db/db mice, GLO-1 was increased during the onset of type 2 diabetes, what may be a compensatory mechanism of these genetic models (Atkins and Thornally, 1989; Rabbani and Thornalley, 2011). In contrast, Bierhaus and colleagues suggested that increased RAGE activation by hyperglycemia-driven glycation and pro-inflammatory signaling may decrease GLO-1 expression, being diabetic RAGE knock-out mice more resistant to retinopathy (McVicar et al., 2015). In epicardial AT from patients with coronary artery disease, RAGE expression above the median induced lower GLO-1 expression, being also associated with decreased GLUT-4 and adiponectin expression, suggesting that impaired MG detoxification and increased dicarbonyl stress contribute to AT dysfunction (Vianello et al., 2015). Our data showed decreased pEAT GLO-1 levels and activity in diet-induced obese and non-obese diabetic GK rats. Furthermore, insulin sensitive obese patients have increased VAT GLO-1 activity following decreased insulin resistance. In contrast, poorer glycemic control evaluated by HbA1c, was correlated with lower adipose tissue GLO-1 activity in obese patients. Interestingly, these mechanisms may be crucial in human AT dysfunction, given the progressive decline in GLO-1 activity in pre-diabetic and type 2 diabetic obese patients. Considered together, these observations indicate tissue-specific and disease-specific alterations of glyoxalase system, although future studies are required to identify and describe all the mechanisms involved.

In order to understand the real impact of GLO-1 impairment in the mechanisms of AT dysfunction, which may be involved in the deterioration of metabolic homeostasis in obese patients, we determined the activity of the enzyme in visceral AT samples with different stages of insulin sensitivity and metabolic status. To the best of our knowledge, this is the first study addressing the activity of this enzyme in the AT of obese patients and correlating it with metabolic health. Here, we show that the activity of the enzyme in visceral AT is

associated with insulin sensitivity/resistance, being positively correlated with insulinemia in pre-diabetic obese patients. Thus, decreased GLO-1 activity in pre-diabetic obese patients when beta cell function starts its deterioration may reinforce the idea that GLO-1 activity in AT precedes the development of AT dysfunction markers, including hypoadiponectinemia and vascular disorders. Scherer and collaborators, performed the cohort Dallas Heart Study composed by 1557 participants without type 2 diabetes, showing higher triglycerides and lower HDL cholesterol and adiponectinemia (Neeland et al., 2018). In our data, unhealthy AT function was observed in type 2 diabetic obese patients, including increased triglyceridemia and decreased HDL cholesterol and adiponectinemia.

GLO-1 knockdown was shown to impair the angiogenic function in mouse aortic endothelial cells and to induce the formation of aberrant capillaries in zebrafish (Jörgens et al., 2015; Nigro et al., 2019). Moreover, we have shown that GLO-1 inhibition leads to a decrease of the angiogenic ability in AT explants. On the other hand, overexpression of GLO-1 improves tube formation of human endothelial cells, prevents MG-induced suppression of VEGFR2 expression and increases the angiogenic function of AT-derived stem cells through stimulation of VEGF expression (Ahmed et al., 2008; Liu et al., 2012; Peng et al., 2016). However, despite the development of an GLO inducer formulation by Xue and colleagues (2016) and a clinical trial with pyridoxamine by Schalkwijk and collaborators (2016), there is not a well-known strategy in order to achieve sustained GLO system activation in metabolic and vascular diseases (Rabbani and Thornalley, 2018; Schalkwijk, 2015; Xue et al., 2016).

The effects of metabolic surgery are known to be beyond the impact on food consumption and weight loss, being specifically relevant the remodeling of gut-derived hormones profile (Li et al., 2018; Trung et al., 2013). Our group has shown increased postprandial GLP-1 secretion in GK rats submitted to sleeve gastrectomy (Eickhoff et al., 2015) and, in the

present work, we observed that this surgical procedure increases GLP-1R levels in pEAT and restores GLO-1 levels and activity in this tissue. We have recently demonstrated that this surgical approach is able to stimulate pEAT angiogenesis, leading to increased levels of angiogenic, vasoactive and vascular differentiation markers (Eickhoff, in revision). Changes in the modulation of the glyoxalase system have never been addressed after bariatric/metabolic surgery and to the best of our knowledge, this is the first study reporting upregulation of GLO-1 following sleeve gastrectomy. Using HUVECs, GLP-1 directly promoted angiogenesis (Aronis et al., 2013) and liraglutide ameliorated palmitate-induced endothelial dysfunction (Li et al., 2016). Liraglutide also improved cardiac microvascular endothelial cells under hypoxia/reoxygenation through GLP-1R/PI3K (Zhang et al., 2016) and angiogenesis after islet transplantation, namely increasing CD31 and VEGF expression and secretion (Langlois et al., 2016). Furthermore, GLP-1 and liraglutide have been implicated in AT adipogenesis through GLP-1R signaling (Langlois et al., 2016). Regarding GLP-1 role in glycation, it has been shown to protect several biological models from the consequences of glycation and specifically methylglyoxal-induced effects (Chang et al., 2016; Kimura et al., 2009). In particular, native GLP-1 was effective in the protection from MG-induced apoptosis of beta cells (Chang et al., 2016) and neuronal (pheochromocytoma) cells (Kimura et al., 2009). GLP-1-mediated cytoprotective effects after exposure to MG were shown to occur through upregulation of survival pathways (PI3K/AKT/ mammalian target of rapamycin and AMPK pathways), as well as improvement of mitochondrial function and antioxidant defenses (Chang et al., 2016; Kimura et al., 2009; Sharma et al., 2014). Regarding antioxidant defenses, liraglutide may improve cell GSH levels, increasing GLO-1 activity indirectly, but future studies are still required. Furthermore, inhibition of DPP-IV by Linagliptin, the main enzyme involved in GLP-1 degradation, resulted in

decreased MG levels in the retina of diabetic rats (Dietrich et al., 2016) and prevented MG-induced peritoneal fibrosis (Nagai et al., 2016).

Different studies from Sharma et al (2014) and Wongchai et al (2016) demonstrated neuroprotective effects of liraglutide in neuroblastoma cells and C. Elegans after MG exposure (Sharma et al., 2014; Wongchai et al., 2016). Moreover, liraglutide was also shown to prevent MG-induced insulin resistance in L6 myotubes, including higher stimulation of GLUT-4 translocation and glucose uptake (Andreozzi et al., 2016). Here, along with improved insulin signaling, we demonstrated for the first-time protective effects of liraglutide in AT vascular dysfunction, including upregulation of key mediators of the angiogenic process and vascular function. In addition, we have also demonstrated that liraglutide is able to prevent the downregulation of the glyoxalase system, particularly in the AT of diabetic rats. Accordingly, in the AT angiogenic assay, we have shown that liraglutide is able to prevent the inhibitory effects of MG in the angiogenic process, restoring the capillarization area and vessel density. However, this is only observed when the glyoxalase system is functional, because selective GLO-1 inhibition abolishes the liraglutide-induced protective effects.

Given the role of glyoxalase system in preventing MG-induced angiogenic abnormalities in AT, the downregulation of AT GLO-1 activity since early stages of metabolic dysregulation in obese patients suggests that its modulation may be a promising strategy in improving AT vascular and metabolic function. Our results demonstrate for the first time the progressive loss of GLO-1 activity following the progressive metabolic dysregulation and insulin resistance in obesity. Moreover, this is the first report showing proangiogenic activity of liraglutide in the AT. In fact, the activation of AGE detoxification systems and particularly the glyoxalase system, has been suggested as an effective strategy to prevent dicarbonyl stress and diabetic vascular complications. Here, we show the efficacy of gut-derived

hormone therapies, sleeve gastrectomy and liraglutide treatment, in restoring GLO-1 levels and activity in AT from diabetic animal models (Figure 4.28).

Altogether, such results reveal new opportunities in the treatment of AT dysfunction in obesity and reinforce the role of metabolic surgery and GLP-1 analogues. Additionally, the regulation of GLO-1 by liraglutide also suggests that this mechanism may be useful in the prevention of diabetic complications in patients with established type 2 diabetes. Although future studies are necessary in this field, our results reinforced the importance of early prevention of adipose tissue vascular dysfunction and insulin resistance. Given the fact that GLP-1-based therapeutic approaches are already available and widely used, they may be introduced earlier to prevent adipose tissue dysfunction, metabolically unhealthy obesity and type 2 diabetes development.
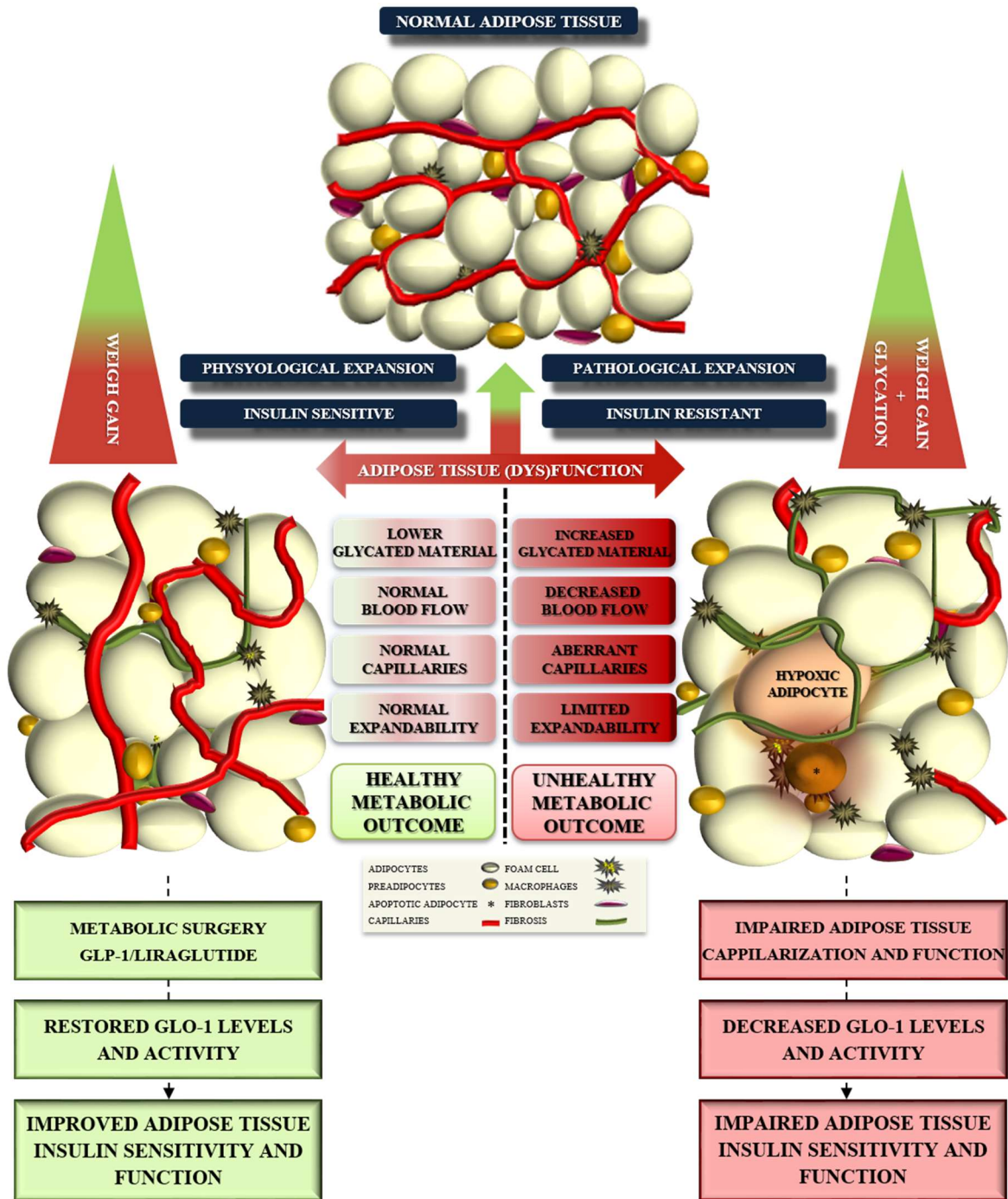
Figure 4.28 – Impaired adipose tissue expandability and function caused by MG-induced glycation, may be targeted by GLP-1-based therapies, namely metabolic surgery and liraglutide treatment. Both strategies restored adipose tissue GLO-1 levels/activity and angiogenesis, contributing to improved adipose tissue insulin sensitivity and function.

**Chapter 5 - GLOBAL CONSIDERATIONS
AND CONCLUSION**

1. Global considerations

Obesity prevalence is dramatically increasing worldwide and, in 2016, at least 1.9 billion adults (older than 17 years old), were overweight and 650 million of them were obese. Regarding children, more than 340 million children and adolescents (aged 5-19) were overweight or obese in 2016 (WHO, 2016). Obesity is a known risk factor for type 2 diabetes and therefore, type 2 diabetes prevalence is also rapidly increasing worldwide. In 2013, at least 382 million people were diabetic and a terrible rise to 592 million is expected in 2035 (Guariguata et al., 2014). Given the fact that lifestyle and dietary interventions have limited results, new therapeutic approaches are required as well as personalized and sophisticated therapeutic strategies to prevent early AT dysfunction, derived insulin resistance and progression to metabolic dysregulation and type 2 diabetes (Figure 5.1). In fact, targeting AT vasculature and function may prevent or delay metabolically unhealthy obesity and type 2 diabetes.

In the past, we have shown that MG-induced glycation resulted in structural and functional AT alterations as well as impaired adaptation to blood flow decrease and hypoxia, even in lean models (Matafome et al., 2012; Rodrigues et al., 2013b). Delayed intervention with pyridoxamine partially reverted MG-induced microvascular lesions (Rodrigues et al., 2013c). Based on these previous findings, we pursued the impact of "AGEing fat", including the mechanisms of glycation-induced microvascular dysfunction in adipose tissue expandability as well as potential therapeutic approaches. Consequently, in this work, our main goal was to understand the role of glycation-induced microvascular dysfunction in AT homeostasis, namely during tissue expansion, exploring the involved mechanisms and GLP-1-based therapeutics.

We have demonstrated adverse effects of MG-induced glycation during AT expansion, which originated impaired AT angiogenesis, blood flow, expandability and functionality (Figure 5.1). Furthermore, Rutkowski and Manneras-Holm and respective collaborators, described the crucial role of AT microvasculature and angiogenic capacity during AT expansion, preventing insulin resistance and tissue dysfunction (Mannerås-Holm and Krook, 2012; Rutkowski et al., 2009). On the other hand, Corvera and collaborators demonstrated that human highly active adipocytes (brite/beige/brown phenotype) may develop from capillary networks, and improve metabolic homeostasis in mice (Min et al., 2016; Tran et al., 2012). Altogether, such evidences reinforce the role of healthy microvasculature in AT function and related metabolic outcome. In agreement, compromised AT microvasculature and related mechanisms are nowadays recognized as key triggers to AT dysfunction, being deeply involved in the early unhealthy metabolic outcome (Farb et al., 2012c; Goossens, 2008; Kusminski et al., 2016; Mannerås-Holm and Krook, 2012; Rutkowski et al., 2009).

Our data from obese patients confirmed the existence of glycation-dependent mechanisms impairing human visceral AT function and systemic metabolic outcome. Body fat amount, commonly described through BMI and leptin levels, is insufficient to characterize metabolically healthy or unhealthy obesity. In fact, this role is nowadays attributed to AT function. Interestingly, we have shown that even morbidly obese subjects (median of 41.8 Kg/m^2) may have healthy AT, with preserved insulin sensitivity and metabolic homeostasis. Although controversial, several authors have identified this subset of obese patients with normal metabolic profile, but future studies are required to identify and describe all the mechanisms involved and potential therapeutic targets (Boonchaya-anant and Apovian, 2014; Gonçalves et al., 2016; Hinnouho et al., 2014; Naukkarinen et al., 2014). Conversely, insulin resistant and obese patients have shown a progressive decrease of pancreatic β cell compensation, which may be responsible for decreased insulin-dependent stimulation of

GLO-1 levels or activity in visceral AT. In fact, we demonstrated a decrease of GLO-1 activity in pre-diabetic and diabetic obese patients, what may reinforce the role of this key limiting enzyme in AT function, contributing to impaired insulin sensitivity and glucose dysmetabolism. Recently, Thornalley and collaborators have developed a clinical intervention study with a GLO-1 inducer (trans-resveratrol-hesperetin); they observed an improvement of insulin resistance and vascular inflammation as well as improved glycemic control and arterial function in overweight and obese subjects (Masania et al., 2016a; Rabbani and Thornalley, 2018). Thus, this data further reinforces the impact that MG and GLO-1 may have in AT structural and functional alterations, and therefore, in the development and progression of metabolic dysregulation in obesity. This study also suggests that GLO-1 inducers may have a key role in alleviating dicarbonyl stress in AT dysfunction and related metabolic burden. Dicarbonyl stress has pleiotropic effects on biological systems and is considered an early trigger to aging mechanisms, causing "AGEing"-induced cell and tissue dysfunction. Consequently, GLO-1 inducers may have a remarkably impact in aging-derived mechanisms and pathways in health and disease, which may contribute to improved healthy aging processes and prolonged lifespan.

Knowing the deleterious effects of "AGEing fat" and the involvement of glyoxalase system, we pursued strategies that could improve glycation and directly or indirectly GLO-1 levels and activity, expecting an improvement of AT angiogenesis and functionality. In the past, our group demonstrated ameliorated glycemic control in diabetic GK rats submitted to sleeve gastrectomy, related, at least in part, to gut-derived hormone profile restoration (Eickhoff et al., 2015). More recently, we showed in diet-induced obese type 2 diabetic GK rats submitted to the same surgical procedure, an increment in AT angiogenesis and function (Eickhoff, in revision). In our present study using this model, we have shown increased GLP-1R levels in pEAT, suggesting higher GLP-1 signaling in this tissue. Accordingly, Maessen and

collaborators demonstrated that energy restriction using Roux-en-Y gastric bypass reduce postprandial α-dicarbonyl stress in obese women with type 2 diabetes (Maessen et al., 2016a). Interestingly, metabolic surgery-induced effects, which have been firstly designed to promote weight loss (known as bariatric surgery) improves glucose tolerance few days after surgical procedures. Indeed, metabolic surgery effects were even more effective than any known intensive pharmaceutical or lifestyle intervention, even without major weight loss, causing durable remission (approximately 75%) in many patients with established type 2 diabetes (Cefalu et al., 2016; Cho et al., 2014). Furthermore, metabolic surgery was a surgical strategy mostly used in morbidly obese type 2 diabetic patients. However, clinical criteria have been recently adapted, and nowadays metabolic surgery is also recommended to class 1 ($30<BMI<34.9$ kg/m^2) obese patients with poor glycemic control (Rubino et al., 2016).

Based on our previous understanding about the metabolic effects of dicarbonyl stress, we aimed to develop new strategies to achieve sustained GLO-1 activation and prevention of MG-induced "AGEing fat". We explored the involvement of glyoxalase system in AT function after metabolic surgery, and particularly GLP-1-dependent mechanisms. Interestingly, both GLP-1-based strategies, vertical sleeve gastrectomy and liraglutide, restored GLO-1 levels and activity in pEAT, and improved its function and insulin sensitivity. Besides, the matrigel plug assay also showed that liraglutide prevents MG-induced inhibition of angiogenesis, and AT angiogenesis assay highlight its GLO-1-dependent effects. This effect was confirmed by the preventive action of GLO-1 inhibitor (BBGC) on liraglutide angiogenic effects. Thus, GLP-1-based strategies are effective in decreasing the impact of glycation in AT, contributing to healthy AT and metabolic outcome (Figure 5.1).

In line with previous findings, personalized pharmacological approaches may become as efficient as metabolic surgery by targeting gut-derived hormones mechanisms, restoring body weight, detoxifying mechanisms, insulin sensitivity and glucose tolerance. Despite the fact that GLP-1 analogues are effective, the administration requires periodic subcutaneous injections and may induce some side effects, decreasing therapeutic compliance. Several GLP-1 analogues and new formulations/associations are under development, to allow oral administration, reduced number of injections (long-acting agonists) and side-effects, contributing to improved therapeutic efficacy and compliance. Considering our data, future studies could address the role of gut-derived hormones and adipokines as regulators of detoxification systems, namely targeting the glyoxalase system, in order to identify new therapies against dicarbonyl stress and to avoid vascular disease and metabolic dysregulation associated with obesity and type 2 diabetes. Besides, these effects might be really valuable in decreasing the impact of glycation and oxidative stress in biological systems, being potentially effective in healthy aging mechanisms and preventing aging-related diseases like type 2 diabetes.

Altogether, our data suggests that early prevention of insulin resistance and unhealthy adipose tissue expandability and functionality by targeting "AGEing fat" may be a promising strategy to decrease the progressive metabolic dysregulation in obese and type 2 diabetic patients (Figure 5.1). However, future studies are required to explore the role of early/late interventions, new agonists, formulations and pharmacological associations, aiming to achieve sustained pleiotropic effects, as well as prevention and durable or even total remission of type 2 diabetes and related comorbidities.
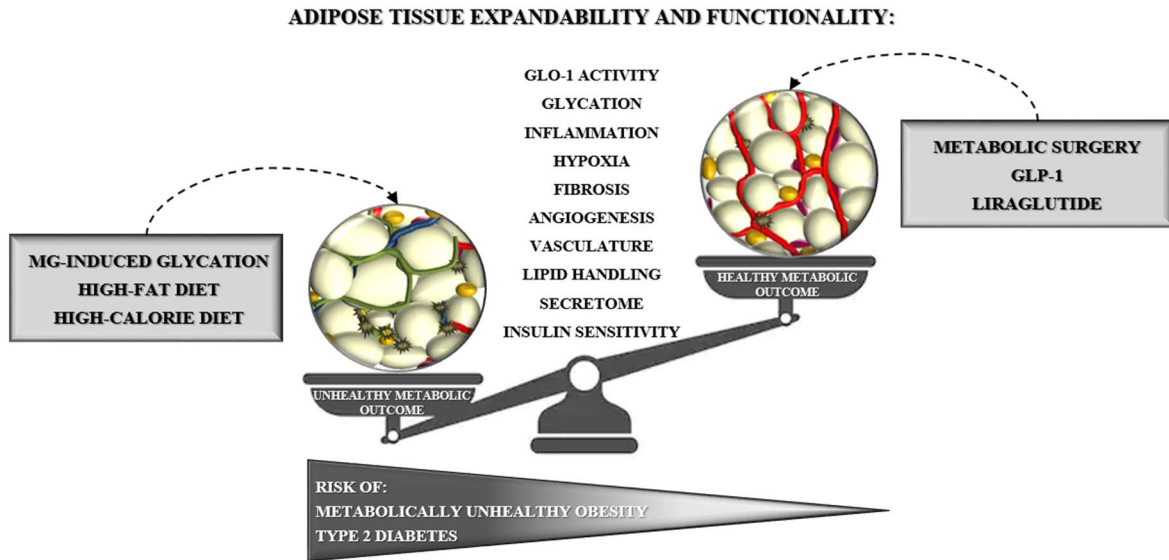
Figure 5.1 Methylglyoxal-induced glycation causes impaired adipose tissue expandability and function in obesity. However, unhealthy adipose tissue may be targeted by GLP-1-based therapies, which may improve tissue angiogenesis/vasculature through glyoxalase-1-dependent mechanisms, contributing to higher insulin sensitivity and a healthy metabolic outcome and, ultimately, to a lower risk of metabolically unhealthy obesity and type 2 diabetes.

2. Conclusions

Overall, our results demonstrate that glycation impairs adipose tissue microvasculature and expandability, contributing to increased insulin resistance and tissue dysfunction. Based on these findings, we propose the existence of adipovascular coupling mechanisms, being the crosstalk between adipocytes and vasculature crucial to healthy adipose tissue, preventing insulin resistance and the onset of metabolically unhealthy obesity and type 2 diabetes.

Our data showed that insulin resistant obese patients have a progressive decline of adipose tissue and β-cell function in pre-diabetic and diabetic obese patients. Adipose tissue glyoxalase-1 activity was negatively associated with glycemic control in obese patients, suggesting that this key enzyme involved in MG detoxification may be an important therapeutic target in obesity and type 2 diabetes in the near future.

GLP-1-based strategies, vertical sleeve gastrectomy and liraglutide treatment, increase adipose tissue angiogenesis and vascular remodeling, restoring glyoxalase-1 levels and activity and improving adipose tissue dysfunction and insulin resistance. The enzyme glyoxalase-1 is required to liraglutide-mediated improvement of adipose tissue angiogenesis, being potentially important in the prevention of glycation-induced vascular disease in obesity and type 2 diabetes.

BIBLIOGRAPHY

Adolphe, J.L., Drew, M.D., Huang, Q., Silver, T.I., and Weber, L.P. (2012). Postprandial impairment of flow-mediated dilation and elevated methylglyoxal after simple but not complex carbohydrate consumption in dogs. Nutrition Research. 32, 278–284.

Adya, R., Tan, B.K., Chen, J., and Randeva, H.S. (2012). Protective actions of globular and full-length adiponectin on human endothelial cells: Novel insights into adiponectin-induced angiogenesis. Journal of Vascular Research. 49, 534–543.

Agabiti-Rosei, C., Paini, A., De Ciuceis, C., Withers, S., Greenstein, A., Heagerty, A.M., and Rizzoni, D. (2018). Modulation of Vascular Reactivity by Perivascular Adipose Tissue (PVAT). Current Hypertension Reports. 20, 1–11.

Ahmed, M.U., Brinkmann Frye, E., Degenhardt, T.P., Thorpe, S.R., and Baynes, J.W. (1997). N-epsilon-(carboxyethyl)lysine, a product of the chemical modification of proteins by methylglyoxal, increases with age in human lens proteins. The Biochemical Journal. 324, 565–570.

Ahmed, U., Dobler, D., Larkin, S.J., Rabbani, N., and Thornalley, P.J. (2008). Reversal of hyperglycemia-induced angiogenesis deficit of human endothelial cells by overexpression of glyoxalase 1 in vitro. Annals of the New York Academy of Sciences. 1126, 262–264.

Ahmed, N., Mirshekar-Syahkal, B., Kennish, L., Karachalias, N., Babaei-Jadidi, R., and Thornalley, P.J. (2005). Assay of advanced glycation endproducts in selected beverages and food by liquid chromatography with tandem mass spectrometric detection. Molecular Nutrition & Food Research. 49, 691–699.

Akhand, A.A., Hossain, K., Mitsui, H., Kato, M., Miyata, T., Inagi, R., Du, J., Takeda, K., Kawamoto, Y., Suzuki, H., et al. (2001). Glyoxal and methylglyoxal trigger distinct signals for map family kinases and caspase activation in human endothelial cells. Free Radical Biology & Medicine. 31, 20–30.

Alfa, R.W., Park, S., Skelly, K.R., Poffenberger, G., Jain, N., Gu, X., Kockel, L., Wang, J., Liu, Y., Powers, A.C., et al. (2015). Suppression of Insulin Production and Secretion by a Decretin Hormone. Cell Metabolism. 21, 323–334.

Almeida, F., Santos-Silva, D., Rodrigues, T., Matafome, P., Crisóstomo, J., Sena, C., Gonçalves, L., and Seiça, R. (2013). Pyridoxamine reverts methylglyoxal-induced impairment of survival pathways during heart ischemia. Cardiovascular Therapeutics. 31, e79-85.

Amicarelli, F., Colafarina, S., Cattani, F., Cimini, A., Di Ilio, C., Ceru, M.P., and Miranda, M. (2003). Scavenging system efficiency is crucial for cell resistance to ROS-mediated methylglyoxal injury. Free Radical Biology & Medicine. 35, 856–871.

Andreozzi, F., Beguinot, F., Davalli, A.M., Miele, C., Sesti, G., Procopio, T., Mannino, G.C., Folli, F., Raciti, G.A., and Nigro, C. (2016). The GLP-1 receptor agonists exenatide and liraglutide activate Glucose transport by an AMPK-dependent mechanism. Journal of Translational Medicine. 14, 1–13.

Aouadi, M. (2014). HIF-2 Blows Out the Flames of Adipose Tissue Macrophages to Keep Obesity in a Safe Zone. Diabetes. 63, 3169–3171.

Aplin, A.C., and Nicosia, R.F. (2015). The Rat Aortic Ring Model of Angiogenesis. Methods in Molecular Biology. 1214, 255–264.

Aplin, A.C., Fogel, E., Zorzi, P., and Nicosia, R.F. (2008). The Aortic Ring Model of Angiogenesis. Methods in Enzymology. 443, 119–136.

Arner, P. (2005). Human fat cell lipolysis: Biochemistry, regulation and clinical role. Best Practice and Research: Clinical Endocrinology and Metabolism. 19, 471–482.

Arner, E., Westermark, P.O., Spalding, K.L., Britton, T., Ryde, M., Frise, J., Bernard, S., and Arner, P. (2010). Adipocyte Turnover: Relevance to Human Adipose Tissue Morphology. Diabetes. 59, 105–109.

Aronis, K.N., Chamberland, J.P., and Mantzoros, C.S. (2012). Glp-1 Promotes Angiogenesis in a Dose-Dependent Manner, Through the Pi3K/Akt, Pkc and Nitric Oxide Pathways. Journal of the American College of Cardiology. 59, 1279–1286.

Aronis, K.N., Chamberland, J.P., and Mantzoros, C.S. (2013). GLP-1 promotes angiogenesis in human endothelial cells in a dose-dependent manner, through the Akt, Src and PKC pathways. Metabolism: Clinical and Experimental. 62, 1279–1286.

Asterholm, I.W., Rutkowski, J.M., Fujikawa, T., Cho, Y.R., Fukuda, M., Tao, C., Wang, Z. V., Gupta, R.K., Elmquist, J.K., and Scherer, P.E. (2014). Elevated resistin levels induce central leptin resistance and increased atherosclerotic progression in mice. Diabetologia. 57, 1209–1218.

Atkins, T.W., and Thornally, P.J. (1989). Erythrocyte glyoxalase activity in genetically obese (ob/ob) and streptozotocin diabetic mice. Diabetes Research. 11, 125–129.

Baker, M., Robinson, S.D., Lechertier, T., Barber, P.R., Tavora, B., D'Amico, G., Jones, D.T., Vojnovic, B., and Hodivala-Dilke, K. (2012). Use of the mouse aortic ring assay to study angiogenesis. Nature Protocols. 7, 89–104.

Barreto, M., Gaio, V., Kislaya, I., Antunes, L., Rodrigues, A.P., Silva, A.C., Vargas, P., Prokopenko, T., Santos, A.J., Namorado, S., et al. (2016). 1st National Health Examination Survey (INSEF 2015): Health Status. INSA.

Batterham, R.L., and Cummings, D.E. (2016). Mechanisms of diabetes improvement following bariatric/metabolic surgery. Diabetes Care. 39, 893–901.

Baynes, J.W. (2002). The Maillard hypothesis on aging: time to focus on DNA. Annals of the New York Academy of Sciences. 959, 360–367.

Beisswenger, P.J., Howell, S.K., Touchette, A.D., Lal, S., and Szwergold, B.S. (1999). Metformin reduces systemic methylglyoxal levels in type 2 diabetes. Diabetes. 48, 198–202.

Benito, M. (2011). Tissue specificity on insulin action and resistance: past to recent mechanisms. Acta Physiologica. 201, 297–312.

Bento, C.F., and Pereira, P. (2011). Regulation of hypoxia-inducible factor 1 and the loss of the cellular response to hypoxia in diabetes. Diabetologia. 54, 1946–1956.

Bento, C., Marques, F., Fernandes, R., and Pereira, P. (2010a). Methylglyoxal Alters the Function and Stability of Critical Components of the Protein Quality Control. PLoS ONE. 5, 1–10.

Bento, C.F., Fernandes, R., Matafome, P., Sena, C., Seiça, R., and Pereira, P. (2010b). Methylglyoxal-induced imbalance in the ratio of vascular endothelial growth factor to angiopoietin 2 secreted by retinal pigment epithelial cells leads to endothelial dysfunction. Experimental Physiology. 95, 955–970.

Bento, C.F., Fernandes, R., Ramalho, J., Marques, C., Shang, F., Taylor, A., and Pereira, P. (2010c). The chaperone-dependent ubiquitin ligase CHIP targets HIF-1α for degradation in the presence of methylglyoxal.

PloS One. 5, 1–13.

Berlanga, J., Cibrian, D., Guillén, I., Freyre, F., Alba, J.S., Lopez-Saura, P., Merino, N., Aldama, A., Quintela, A.M., Triana, M.E., et al. (2005). Methylglyoxal administration induces diabetes-like microvascular changes and perturbs the healing process of cutaneous wounds. Clinical Science. 109, 83–95.

Berner, A.K., Brouwers, O., Pringle, R., Klaassen, I., Colhoun, L., McVicar, C., Brockbank, S., Curry, J.W., Miyata, T., Brownlee, M., et al. (2012). Protection against methylglyoxal-derived AGEs by regulation of glyoxalase 1 prevents retinal neuroglial and vasodegenerative pathology. Diabetologia. 55, 845–854.

Blonde, L., and Russell-Jones, D. (2009). The safety and efficacy of liraglutide with or without oral antidiabetic drug therapy in type 2 diabetes: An overview of the LEAD 1-5 studies. Diabetes, Obesity and Metabolism. 11, 26–34.

Blüher, M., and Mantzoros, C.S. (2015). From leptin to other adipokines in health and disease: Facts and expectations at the beginning of the 21st century. Metabolism: Clinical and Experimental. 64, 131–145.

De Bock, K., Georgiadou, M., and Carmeliet, P. (2013). Role of endothelial cell metabolism in vessel sprouting. Cell Metabolism. 18, 634–647.

Boden, G., She, P., Mozzoli, M., Cheung, P., Gumireddy, K., Reddy, P., Xiang, X., Luo, Z., and Ruderman, N. (2005). Free fatty acids produce insulin resistance and activate the proinflammatory nuclear factor-kB pathway in rat liver. Diabetes. 54, 3458–3465.

de Bona Castelan, J., Bettiol, J., d'Acampora, A.J., Castelan, J.V.E., de Souza, J.C., Bressiani, V., and Giroldi, S.B. (2007). Sleeve gastrectomy model in Wistar rats. Obesity Surgery. 17, 957–961.

Boonchaya-anant, P., and Apovian, C.M. (2014). Metabolically Healthy Obesity—Does it Exist? Current Atherosclerosis Reports. 16, 1–9.

Boydens, C., Maenhaut, N., Pauwels, B., Decaluwé, K., and Van de Voorde, J. (2012). Adipose tissue as regulator of vascular tone. Current Hypertension Reports. 14, 270–278.

Brownlee, M. (2001). Biochemistry and molecular cell biology of diabetic complications. Nature. 414, 813–820.

Brownlee, M. (2005). The pathobiology of diabetic complications: a unifying mechanism. Diabetes. 54, 1615–1625.

Buchwald, H. (2002). Overview of bariatric surgery. Journal of the American College of Surgeons. 194, 367–375.

Buechler, C., Krautbauer, S., and Eisinger, K. (2015). Adipose tissue fibrosis. World Journal Diabetes. 6, 548–553.

Cai, W., He, J.C., Zhu, L., Chen, X., Striker, G.E., and Vlassara, H. (2008). AGE-receptor-1 counteracts cellular oxidant stress induced by AGEs via negative regulation of p66shc-dependent FKHRL1 phosphorylation. American Journal of Physiology Cell Physiology. 294, C145-52.

Cai, W., Torreggiani, M., Zhu, L., Chen, X., He, J.C., Striker, G.E., and Vlassara, H. (2010). AGER1 regulates endothelial cell NADPH oxidase-dependent oxidant stress via PKC-delta: implications for vascular disease. American Journal of Physiology Cell Physiology. 298, C624-34.

Cantero, A.-V., Portero-Otín, M., Ayala, V., Auge, N., Sanson, M., Elbaz, M., Thiers, J.-C., Pamplona, R., Salvayre, R., and Nègre-Salvayre, A. (2007). Methylglyoxal induces advanced glycation end product (AGEs) formation and dysfunction of PDGF receptor-beta: implications for diabetic atherosclerosis. FASEB Journal.

21, 3096–3106.

Cao, Y. (2007). Angiogenesis modulates adipogenesis and obesity. Journal of Clinical Investigation. 117, 2362–2368.

Cao, Y. (2013). Angiogenesis and vascular functions in modulation of obesity, adipose metabolism, and insulin sensitivity. Cell Metabolism. 18, 478–489.

Carmeliet, P., and Jain, R.K. (2011). Molecular Mechanisms and and clinical applications of angiogenesis. Nature. 473, 298–307.

Cefalu, W.T., Rubino, F., and Cummings, D.E. (2016). Metabolic surgery for type 2 diabetes: Changing the landscape of diabetes care. Diabetes Care. 39, 857–860.

Ceriello, A., Ihnat, M.A., and Thorpe, J.E. (2009). Clinical review 2: The "metabolic memory": is more than just tight glucose control necessary to prevent diabetic complications? The Journal of Clinical Endocrinology and Metabolism. 94, 410–415.

Challa, T.D., Beaton, N., Arnold, M., Rudofsky, G., Langhans, W., and Wolfrum, C. (2012). Regulation of Adipocyte Formation by GLP-1/GLP-1R Signaling. Journal of Biological Chemistry. 287, 6421–6430.

Chan, W.-H., Wu, H.-J., and Shiao, N.-H. (2007). Apoptotic signaling in methylglyoxal-treated human osteoblasts involves oxidative stress, c-Jun N-terminal kinase, caspase-3, and p21-activated kinase 2. Journal of Cellular Biochemistry. 100, 1056–1069.

Chang, T., Wang, R., and Wu, L. (2005). Methylglyoxal-induced nitric oxide and peroxynitrite production in vascular smooth muscle cells. Free Radical Biology & Medicine. 38, 286–293.

Chang, T.J., Tseng, H.C., Liu, M.W., Chang, Y.C., Hsieh, M.L., and Chuang, L.M. (2016). Glucagon-like peptide-1 prevents methylglyoxal-induced apoptosis of beta cells through improving mitochondrial function and suppressing prolonged AMPK activation. Scientific Reports. 6, 1–11.

Chetyrkin, S. V, Zhang, W., Hudson, B.G., Serianni, A.S., and Voziyan, P. a (2008). Pyridoxamine protects proteins from functional damage by 3-deoxyglucosone: mechanism of action of pyridoxamine. Biochemistry. 47, 997–1006.

Cho, Y.M., Fujita, Y., and Kieffer, T.J. (2014). Glucagon-Like Peptide-1 : Glucose Homeostasis and Beyond. Annual Review of Physiology. 76, 535–559.

Choe, S.S., Shin, K.C., Ka, S., Lee, Y.K., Chun, J.S., and Kim, J.B. (2014). Macrophage HIF-2α ameliorates adipose tissue inflammation and insulin resistance in obesity. Diabetes. 63, 3359–3371.

Christiaens, V., and Lijnen, H.R. (2010). Angiogenesis and development of adipose tissue. Molecular and Cellular Endocrinology. 318, 2–9.

Consoli, A., Guagnano, M.T., Davì, G., Maccarone, M.T., Leo, M., Santilli, F., Federico, V., Tartaro, A., Bonadonna, R.C., Angelucci, E., et al. (2017). Effects of Liraglutide on Weight Loss, Fat Distribution, and β-Cell Function in Obese Subjects With Prediabetes or Early Type 2 Diabetes. Diabetes Care. 40, 1556–1564.

Corvera, S., and Gealekman, O. (2014a). Adipose tissue angiogenesis: Impact on obesity and type-2 diabetes. Biochimica et Biophysica Acta. 1842, 463–472.

Corvera, S., and Gealekman, O. (2014b). Adipose tissue angiogenesis: Impact on obesity and type-2 diabetes. Biochimica et Biophysica Acta. 1842, 463–472.

Crisóstomo, J., Matafome, P., Santos-Silva, D., Rodrigues, L., Sena, C.M., Pereira, P., and Seiça, R. (2013). Methylglyoxal chronic administration promotes diabetes-like cardiac ischaemia disease in Wistar normal rats.

Nutrition, Metabolism, and Cardiovascular Diseases. 23, 1223–1230.

Czech, M.P. (2017). Insulin action and resistance in obesity and type 2 diabetes. Nature Medicine. 23, 804–814.

Czech, M.P., Tencerova, M., Pedersen, D.J., and Aouadi, M. (2013). Insulin signalling mechanisms for triacylglycerol storage. Diabetologia. 56, 949–964.

Dakin, H., and Dudley, H. (1913). An enzyme concerned with the formation of hydroxy acids from ketonic aldehydes. Journal of Biological Chemistry. 14, 423–431.

Desai, K.M., Chang, T., Wang, H., Banigesh, A., Dhar, A., Liu, J., Untereiner, A., and Wu, L. (2010). Oxidative stress and aging: is methylglyoxal the hidden enemy? Canadian Journal of Physiology and Pharmacology. 88, 273–284.

Dhar, A., Desai, K., Kazachmov, M., Yu, P., and Wu, L. (2008). Methylglyoxal production in vascular smooth muscle cells from different metabolic precursors. Metabolism: Clinical and Experimental. 57, 1211–1220.

Dhar, A., Dhar, I., Jiang, B., Desai, K.M., and Wu, L. (2011). Chronic methylglyoxal infusion by minipump causes pancreatic beta-cell dysfunction and induces type 2 diabetes in Sprague-Dawley rats. Diabetes. 60, 899–908.

Dietrich, N., Kolibabka, M., Busch, S., Bugert, P., Kaiser, U., Lin, J., Fleming, T., Morcos, M., Klein, T., Schlotterer, A., et al. (2016). The dpp4 inhibitor linagliptin protects from experimental diabetic retinopathy. PLoS ONE. 11, e0167853.

Dimitriadis, G., Lambadiari, V., Mitrou, P., Maratou, E., Boutati, E., Panagiotakos, D., Economopoulos, T., and Raptis, S. (2007). Impaired Postprandial Blood Flow in Adipose Tissue May Be an Early Marker of Insulin Resistance in Type 2 Diabetes. Diabetes Care. 30, 3128–3130.

Dragos, S.M., Bergeron, K.F., Desmarais, F., Suitor, K., Wright, D.C., Mounier, C., and Mutch, D.M. (2017). Reduced SCD1 activity alters markers of fatty acid reesterification, glyceroneogenesis, and lipolysis in murine white adipose tissue and 3T3-L1 adipocytes. American Journal of Physiology Cell Physiology. 313, C295–C304.

Drucker, D.J. (2006). The biology of incretin hormones. Cell Metabolism. 3, 153–165.

Drucker, D.J. (2018). Mechanisms of Action and Therapeutic Application of Glucagon-like Peptide-1. Cell Metabolism. 27, 740–756.

Drucker, D.J., and Nauck, M.A. (2006). The incretin system: glucagon-like peptide-1 receptor agonists and dipeptidyl peptidase-4 inhibitors in type 2 diabetes. Lancet. 368, 1696–1705.

Du, J., Cai, S., Suzuki, H., Akhand, A. a, Ma, X., Takagi, Y., Miyata, T., Nakashima, I., and Nagase, F. (2003). Involvement of MEKK1/ERK/P21Waf1/Cip1 signal transduction pathway in inhibition of IGF-I-mediated cell growth response by methylglyoxal. Journal of Cellular Biochemistry. 88, 1235–1246.

Eickhoff, H., Louro, T.M., Matafome, P.N., Vasconcelos, F., Seiça, R.M., and Castro, F.S. (2015). Amelioration of Glycemic Control by Sleeve Gastrectomy and Gastric Bypass in a Lean Animal Model of Type 2 Diabetes: Restoration of Gut Hormone Profile. Obesity Surgery. 25, 7–18.

Elias, I., Franckhauser, S., Ferré, T., Vilà, L., Tafuro, S., Muñoz, S., Roca, C., Ramos, D., Pujol, A., Riu, E., et al. (2012). Adipose tissue overexpression of vascular endothelial growth factor protects against diet-induced obesity and insulin resistance. Diabetes. 61, 1801–1813.

Engelen, L., Stehouwer, C.D.A., and Schalkwijk, C.G. (2013). Current therapeutic interventions in the

glycation pathway: Evidence from clinical studies. Diabetes, Obesity and Metabolism. 15, 677–689.

Falone, S., D'Alessandro, A., Mirabilio, A., Petruccelli, G., Cacchio, M., Di Ilio, C., Di Loreto, S., and Amicarelli, F. (2012). Long term running biphasically improves methylglyoxal-related metabolism, redox homeostasis and neurotrophic support within adult mouse brain cortex. PloS One. 7, 1–11.

Fan, X., Xiaoqin, L., Potts, B., Strauch, C.M., Nemet, I., and Monnier, V.M. (2011). Topical application of L-arginine blocks advanced glycation by ascorbic acid in the lens of hSVCT2 transgenic mice. Molecular Vision. 17, 2221–2227.

Farb, M.G., Ganley-Leal, L., Mott, M., Liang, Y., Ercan, B., Widlansky, M.E., Bigornia, S.J., Fiscale, A.J., Apovian, C.M., Carmine, B., et al. (2012a). Arteriolar function in visceral adipose tissue is impaired in human obesity. Arteriosclerosis, Thrombosis, and Vascular Biology. 32, 467–473.

Farb, M.G.M., Ganley-Leal, L., Mott, M., Liang, Y., Ercan, B., Widlansky, M.E., Bigornia, S.J., Fiscale, A.J., Apovian, C.M., Carmine, B., et al. (2012b). Arteriolar function in visceral adipose tissue is impaired in human obesity. Arteriosclerosis, Thrombosis, and Vascular Biology. 32, 467–473.

Farb, M.G.M., Ganley-Leal, L., Mott, M., Liang, Y., Ercan, B., Widlansky, M.E., Bigornia, S.J., Fiscale, A.J., Apovian, C.M., Carmine, B., et al. (2012c). Arteriolar function in visceral adipose tissue is impaired in human obesity. Arteriosclerosis, Thrombosis, and Vascular Biology. 32, 467–473.

Fiory, F., Lombardi, A., Miele, C., Giudicelli, J., Beguinot, F., and Van Obberghen, E. (2011). Methylglyoxal impairs insulin signalling and insulin action on glucose-induced insulin secretion in the pancreatic beta cell line INS-1E. Diabetologia. 54, 2941–2952.

Frayn, K.N., and Karpe, F. (2013). Regulation of human subcutaneous adipose tissue blood flow. International Journal of Obesity. 38, 1019–1026.

Gaens, K.H.J., Niessen, P.M.G., Rensen, S.S., Buurman, W. a, Greve, J.W.M., Driessen, A., Wolfs, M.G.M., Hofker, M.H., Bloemen, J.G., Dejong, C.H., et al. (2012). Endogenous formation of Nε-(carboxymethyl)lysine is increased in fatty livers and induces inflammatory markers in an in vitro model of hepatic steatosis. Journal of Hepatology. 56, 647–655.

Gaens, K.H.J., Goossens, G.H., Niessen, P.M., Van Greevenbroek, M.M., Van Der Kallen, C.J.H., Niessen, H.W., Rensen, S.S., Buurman, W. a, Greve, J.W.M., Blaak, E.E., et al. (2014). Nε-(carboxymethyl)lysine-receptor for advanced glycation end product axis is a key modulator of obesity-induced dysregulation of adipokine expression and insulin resistance. Arteriosclerosis, Thrombosis, and Vascular Biology. 34, 1199–1208.

Galic, S., Oakhill, J.S., and Steinberg, G.R. (2010). Adipose tissue as an endocrine organ. Molecular and Cellular Endocrinology. 316, 129–139.

Galitzky, J., Lafontan, M., Nordenström, J., and Arner, P. (1993). Role of vascular alpha-2 adrenoceptors in regulating lipid mobilization from human adipose tissue. Journal of Clinical Investigation. 91, 1997–2003.

García-Martín, R., Alexaki, V.I., Qin, N., Rubín de Celis, M.F., Economopoulou, M., Ziogas, A., Gercken, B., Kotlabova, K., Phieler, J., Ehrhart-Bornstein, M., et al. (2016). Adipocyte-Specific Hypoxia-Inducible Factor 2α Deficiency Exacerbates Obesity-Induced Brown Adipose Tissue Dysfunction and Metabolic Dysregulation. Molecular and Cellular Biology. 36, 376–393.

Gealekman, O., Guseva, N., Hartigan, C., Apotheker, S., Gorgoglione, M., Gurav, K., Tran, K.-V. Van, Straubhaar, J., Nicoloro, S., Czech, M.P., et al. (2011). Depot-specific differences and insufficient

subcutaneous adipose tissue angiogenesis in human obesity. Circulation. 123, 186–194.

Gealekman, O., Burkart, A., Chouinard, M., Nicoloro, S.M., Straubhaar, J., and Corvera, S. (2008). Enhanced angiogenesis in obesity and in response to PPARgamma activators through adipocyte VEGF and ANGPTL4 production. American Journal of Physiology. Endocrinology and Metabolism. 295, E1056-64.

Gealekman, O., Brodsky, S. V., Zhang, F., Chander, P.N., Friedli, C., Nasjletti, A., and Goligorsky, M.S. (2004). Endothelial dysfunction as a modifier of angiogenic response in Zucker diabetic fat rat: Amelioration with Ebselen. Kidney International. 66, 2337–2347.

Gealekman, O., Guseva, N., Gurav, K., Gusev, A., Hartigan, C., Thompson, M., Malkani, S., and Corvera, S. (2012). Effect of rosiglitazone on capillary density and angiogenesis in adipose tissue of normoglycaemic humans in a randomised controlled trial. Diabetologia. 55, 2794–2799.

Gensberger, S., Glomb, M. a, and Pischetsrieder, M. (2013). Analysis of sugar degradation products with α-dicarbonyl structure in carbonated soft drinks by UHPLC-DAD-MS/MS. Journal of Agricultural and Food Chemistry. 61, 10238–10245.

Georgescu, A., Popov, D., Constantin, A., Nemecz, M., Alexandru, N., Cochior, D., and Tudor, A. (2011). Dysfunction of human subcutaneous fat arterioles in obesity alone or obesity associated with Type 2 diabetes. Clinical Science. 120, 463–472.

Ghaben, A.L., and Scherer, P.E. (2019). Adipogenesis and metabolic health. Nature Reviews Molecular Cell Biology. in press.

Giordano, A., Frontini, A., and Cinti, S. (2016). Convertible visceral fat as a therapeutic target to curb obesity. Nature Reviews - Drug Discovery. 15, 405–424.

Glassford, A.J., Yue, P., Sheikh, A.Y., Chun, H.J., Zarafshar, S., Chan, D. a, Reaven, G.M., Quertermous, T., and Tsao, P.S. (2007). HIF-1 regulates hypoxia- and insulin-induced expression of apelin in adipocytes. American Journal of Physiology Endocrinology and Metabolism. 293, E1590–E1596.

Golay, A., and Ybarra, J. (2005). Link between obesity and type 2 diabetes. Best Practice & Research Clinical Endocrinology & Metabolism. 19, 649–663.

Goldin, A., Beckman, J., Schmidt, A.M., and Creager, M. (2006). Advanced glycation end products: sparking the development of diabetic vascular injury. Circulation. 114, 597–605.

Golej, J., Hoeger, H., Radner, W., Unfried, G., and Lubec, G. (1998). Oral administration of methylglyoxal leads to kidney collagen accumulation in the mouse. Life Sciences. 63, 801–807.

Gómez-Ambrosi, J., Catalán, V., Rodríguez, A., Ramírez, B., Silva, C., Gil, M.J., Salvador, J., and Frühbeck, G. (2010). Involvement of serum vascular endothelial growth factor family members in the development of obesity in mice and humans. The Journal of Nutritional Biochemistry. 21, 774–780.

Gonçalves, C.G., Glade, M.J., and Meguid, M.M. (2016). Metabolically healthy obese individuals: Key protective factors. Nutrition. 32, 14–20.

Gondo, Y., Hirose, N., Inagaki, H., Homma, S., Kojima, T., Shimizu, K., Takayama, M., Masui, Y., Arai, Y., Kitagawa, K., et al. (2006). High adiponectin concentration and its role for longevity in female centenarians. Geriatrics and Gerontology International. 6, 32–39.

Goossens, G.H. (2008). The role of adipose tissue dysfunction in the pathogenesis of obesity-related insulin resistance. Physiology & Behavior. 94, 206–218.

Goossens, G.H., Bizzarri, A., Venteclef, N., Essers, Y., Cleutjens, J.P., Konings, E., Jocken, J.W.E.,

Cajlakovic, M., Ribitsch, V., Clément, K., et al. (2011). Increased adipose tissue oxygen tension in obese compared with lean men is accompanied by insulin resistance, impaired adipose tissue capillarization, and inflammation. Circulation. 124, 67–76.

Goossens, G.H., and Blaak, E.E. (2015). Adipose Tissue Dysfunction and Impaired Metabolic Health in Human Obesity: A Matter of Oxygen? Frontiers in Endocrinology. 6, 1–5.

Grimm, S., Horlacher, M., Catalgol, B., Hoehn, A., Reinheckel, T., and Grune, T. (2012). Cathepsins D and L reduce the toxicity of advanced glycation end products. Free Radical Biology & Medicine. 52, 1011–1023.

Group, U.P.D.S. (UKPDS) (1998). Intensive blood-glucose control with sulphonylureas or insulin compared with conventional treatment and risk of complications in patients with type 2 diabetes (UKPDS 33). Lancet. 352, 837–853.

Guariguata, L., Whiting, D.R., Hambleton, I., Beagley, J., Linnenkamp, U., and Shaw, J.E. (2014). Global estimates of diabetes prevalence for 2013 and projections for 2035. Diabetes Research and Clinical Practice. 103, 137–149.

Guilherme, A., Virbasius, J. V, Puri, V., and Czech, M.P. (2008). Adipocyte dysfunctions linking obesity to insulin resistance and type 2 diabetes. Nature Reviews - Molecular Cell Biology. 9, 367–377.

Halberg, N., Khan, T., Trujillo, M.E., Wernstedt-Asterholm, I., Attie, A.D., Sherwani, S., Wang, Z. V, Landskroner-Eiger, S., Dineen, S., Magalang, U.J., et al. (2009). Hypoxia-inducible factor 1alpha induces fibrosis and insulin resistance in white adipose tissue. Molecular and Cellular Biology. 29, 4467–4483.

Hattori, Y., Kakishita, H., Akimoto, K., Matsumura, M., and Kasai, K. (2001). Glycated serum albumin-induced vascular smooth muscle cell proliferation through activation of the mitogen-activated protein kinase/extracellular signal-regulated kinase pathway by protein kinase C. Biochemical and Biophysical Research Communications. 281, 891–896.

Hausman, G.J., and Richardson, R.L. (2004). Adipose tissue angiogenesis. Journal of Animal Science. 82, 925–934.

He, Q., Gao, Z., Yin, J., Zhang, J., Yun, Z., and Ye, J. (2011). Regulation of HIF-1alpha activity in adipose tissue by obesity-associated factors: adipogenesis, insulin, and hypoxia. American Journal of Physiology Endocrinology and Metabolism. 300, E877-85.

Hemmeryckx, B., Loeckx, D., Dresselaers, T., Himmelreich, U., Hoylaerts, M.F., and Lijnen, H.R. (2010). Age-associated adaptations in murine adipose tissues. Endocrine Journal. 57, 925–930.

Hinnouho, G.-M., Czernichow, S., Dugravot, A., Nabi, H., Brunner, E.J., Kivimaki, M., and Singh-Manoux, A. (2014). Metabolically healthy obesity and the risk of cardiovascular disease and type 2 diabetes: the Whitehall II cohort study. European Heart Journal. 36, 551–559.

Hj, K., Da, C., Schalkwijk, C.G., Gaens, K.H.J., Stehouwer, C.D.A., and Schalkwijk, C.G. (2013). Advanced glycation endproducts and its receptor for advanced glycation endproducts in obesity. Current Opinion in Lipidology. 24, 4–11.

Hocking, S., Wu, L., and Guilhaus, M. (2010). Intrinsic Depot-Specific Differences in the Secretome of Adipose Tissue, Preadipocytes, and Adipose Tissue–Derived Microvascular Endothelial Cells. Diabetes. 59, 3008–3016.

Hofmann, S.M.S., Dong, H.-J.H., Li, Z., Cai, W., Altomonte, J., Thung, S.N., Zeng, F., Fisher, E.A., and Vlassara, H. (2002). Improved insulin sensitivity is associated with restricted intake of dietary glycoxidation

products in the db/db mouse. Diabetes. 51, 2082–2089.

Hosogai, N., Fukuhara, A., Oshima, K., Miyata, Y., Tanaka, S., Segawa, K., Furukawa, S., Tochino, Y., Komuro, R., Matsuda, M., et al. (2007). Adipose tissue hypoxia in obesity and its impact on adipocytokine dysregulation. Diabetes. 56, 901–911.

Houben, a J., Eringa, E.C., Jonk, a M., Serne, E.H., Smulders, Y.M., and Stehouwer, C.D. (2012). Perivascular Fat and the Microcirculation: Relevance to Insulin Resistance, Diabetes, and Cardiovascular Disease. Current Cardiovascular Risk Reports. 6, 80–90.

Iacobini, C., Pugliese, G., Fantauzzi, C.B., Federici, M., and Menini, S. (2018). Metabolically healthy versus metabolically unhealthy obesity. Metabolism. 1–10.

Iantorno, M., Campia, U., Di Daniele, N., Nistico, S.P., Forleo, G.B., Cardillo, C., and Tesauro, M. (2014). Obesity, inflammation and endothelial dysfunction. Journal of Biological Regulators and Homeostatic Agents. 28, 169–176.

Jenkins, N.L., Johnson, J.O., Mageau, R.P., Bowen, J.B., and Pofahl, W.E. (2005). Who's who in bariatric surgery: The pioneers in the development of surgery for weight control. Current Surgery. 62, 38–44.

Jia, X., and Wu, L. (2007). Accumulation of endogenous methylglyoxal impaired insulin signaling in adipose tissue of fructose-fed rats. Molecular and Cellular Biochemistry. 306, 133–139.

Jia, X., Olson, D.J.H., Ross, A.R.S., and Wu, L. (2006). Structural and functional changes in human insulin induced by methylglyoxal. FASEB Journal. 20, 1555–1557.

Jones, B. (2016). Liraglutide and cardiovascular outcomes in type 2 diabetes. Annals of Clinical Biochemistry. 53, 712–712.

Jörgens, K., Stoll, S.J., Pohl, J., Fleming, T.H., Sticht, C., Nawroth, P.P., Hammes, H.-P., and Kroll, J. (2015). High Tissue Glucose Alters Intersomitic Blood Vessels in Zebrafish via Methylglyoxal Targeting the VEGF Receptor Signaling Cascade. Diabetes. 64, 213–225.

Juge-Aubry, C.E., Henrichot, E., and Meier, C. a (2005). Adipose tissue: a regulator of inflammation. Best Practice & Research Clinical Endocrinology & Metabolism. 19, 547–566.

Kadowaki, T., Yamauchi, T., Okada-Iwabu, M., and Iwabu, M. (2014). Adiponectin and its receptors: Implications for obesity-associated diseases and longevity. The Lancet Diabetes and Endocrinology. 2, 8–9.

Kalapos, M.P. (2013). Where does plasma methylglyoxal originate from? Diabetes Research and Clinical Practice. 99, 260–271.

Kalapos, M.P., Littauer, A., and de Groot, H. (1993). Has reactive oxygen a role in methylglyoxal toxicity? A study on cultured rat hepatocytes. Archives of Toxicology. 67, 369–372.

Kalupahana, N.S., Massiera, F., Quignard-Boulange, A., Ailhaud, G., Voy, B.H., Wasserman, D.H., and Moustaid-Moussa, N. (2012). Overproduction of angiotensinogen from adipose tissue induces adipose inflammation, glucose intolerance, and insulin resistance. Obesity. 20, 48–56.

Kamvissi, V., Salerno, A., Bornstein, S.R., Mingrone, G., and Rubino, F. (2015). Incretins or anti-incretins? A new model for the entero-pancreatic axis. Hormone and Metabolic Research. 47, 84–87.

Kaneto, H., Katakami, N., Matsuhisa, M., and Matsuoka, T. (2010). Role of reactive oxygen species in the progression of type 2 diabetes and atherosclerosis. Mediators of Inflammation. 2010, 1–11.

Karpe, F., Fielding, B.A., Ilic, V., Macdonald, I.A., Summers, L.K.M., and Frayn, K.N. (2002). Impaired Postprandial Adipose Tissue Blood Flow Response Is Related to Aspects of Insulin Sensitivity. Diabetes. 51,

2467–2473.

Ke, J., Wei, R., Yu, F., Zhang, J., and Hong, T. (2016). Liraglutide restores angiogenesis in palmitate-impaired human endothelial cells through PI3K/Akt-Foxo1-GTPCH1 pathway. Peptides. 86, 95–101.

Kersten, S., and Stienstra, R. (2017). The role and regulation of the peroxisome proliferator activated receptor alpha in human liver. Biochimie. 136, 75–84.

Kiess, W., Petzold, S., Töpfer, M., Garten, A., Blüher, S., Kapellen, T., Körner, A., and Kratzsch, J. (2008). Adipocytes and adipose tissue. Best Practice & Research Clinical Endocrinology & Metabolism. 22, 135–153.

Kim, K.M., Kim, Y.S., Jung, D.H., Lee, J., and Kim, J.S. (2012a). Increased glyoxalase I levels inhibit accumulation of oxidative stress and an advanced glycation end product in mouse mesangial cells cultured in high glucose. Experimental Cell Research. 318, 152–159.

Kim, J., Kim, O.S., Kim, C.-S., Sohn, E., Jo, K., and Kim, J.S. (2012b). Accumulation of argpyrimidine, a methylglyoxal-derived advanced glycation end product, increases apoptosis of lens epithelial cells both in vitro and in vivo. Experimental & Molecular Medicine. 44, 167–175.

Kimura, R., Okouchi, M., Fujioka, H., Ichiyanagi, A., Ryuge, F., Mizuno, T., Imaeda, K., Okayama, N., Kamiya, Y., Asai, K., et al. (2009). Glucagon-like peptide-1 (GLP-1) protects against methylglyoxal-induced PC12 cell apoptosis through the PI3K/Akt/mTOR/GCLc/redox signaling pathway. Neuroscience. 162, 1212–1219.

Kinsky, O.R., Hargraves, T.L., Anumol, T., Jacobsen, N.E., Dai, J., Snyder, S.A., Monks, T.J., and Lau, S.S. (2016). Metformin scavenges methylglyoxal to form a novel imidazolinone metabolite in humans. Chemical Research in Toxicology. 14, 227–234.

Konige, M., Wang, H., and Sztalryd, C. (2013). Role of adipose specific lipid droplet proteins in maintaining whole body energy homeostasis. Biochimica et Biophysica Acta. 1842, 1–9.

Koska, J., Saremi, A., Howell, S., Bahn, G., De Courten, B., Ginsberg, H., Beisswenger, P.J., and Reaven, P.D. (2018). Advanced glycation end products, oxidation products, and incident cardiovascular events in patients with type 2 diabetes. Diabetes Care. 41, 570–576.

Kusminski, C.M., Bickel, P.E., and Scherer, P.E. (2016). Targeting adipose tissue in the treatment of obesity-associated diabetes. Nature Reviews - Drug Discovery. 15, 639–660.

Ladenheim, E.E. (2015). Liraglutide and obesity: A review of the data so far. Drug Design, Development and Therapy. 9, 1867–1875.

Lambadiari, V., Triantafyllou, K., Dimitriadis, G.D., Lambadiari, V., Triantafyllou, K., and George, D. (2015). Insulin action in muscle and adipose tissue in type 2 diabetes : The significance of blood flow. World Journal Diabetes. 6, 626–633.

Lamers, D., Famulla, S., Wronkowitz, N., Hartwig, S., Lehr, S., Ouwens, D.M., Eckardt, K., Kaufman, J.M., Ryden, M., Müller, S., et al. (2011). Dipeptidyl peptidase 4 is a novel adipokine potentially linking obesity to the metabolic syndrome. Diabetes. 60, 1917–1925.

Langlois, A., Mura, C., Bietiger, W., Seyfritz, E., Dollinger, C., Peronet, C., Maillard, E., Pinget, M., Jeandidier, N., and Sigrist, S. (2016). In Vitro and In Vivo Investigation of the Angiogenic Effects of Liraglutide during Islet Transplantation. PloS One. 11, 1–14.

Lee, Y.S., Kim, J.W., Osborne, O., Oh, D.Y., Sasik, R., Schenk, S., Chen, A., Chung, H., Murphy, A., Watkins, S.M., et al. (2014). Increased adipocyte O_2 consumption triggers HIF-1α, causing inflammation and insulin

resistance in obesity. Cell. 157, 1339–1352.

Lee, Y.-H., Mottillo, E.P., and Granneman, J.G. (2013). Adipose tissue plasticity from WAT to BAT and in between. Biochimica et Biophysica Acta. 1842, 358–369.

Li, N., Zhao, Y., Yue, Y., Chen, L., Yao, Z., and Niu, W. (2016). Biochemical and Biophysical Research Communications Liraglutide ameliorates palmitate-induced endothelial dysfunction through activating AMPK and reversing leptin resistance. Biochemical and Biophysical Research Communications. 478, 46–52.

Li, L., Wang, X., Bai, L., Yu, H., Huang, Z., Huang, A., Luo, Y., and Wang, J. (2018). The effects of sleeve gastrectomy on glucose metabolism and glucagon-like peptide 1 in Goto-Kakizaki rats. Journal of Diabetes Research. 2018, 1–11.

Lijnen, H.R. (2008). Angiogenesis and obesity. Cardiovascular Research. 78, 286–293.

Liu, C.-S., Hsu, H.-S., Li, C.-I., Jan, C.-I., Li, T.-C., Lin, W.-Y., Lin, T., Chen, Y.-C., Lee, C.-C., and Lin, C.-C. (2010). Central obesity and atherogenic dyslipidemia in metabolic syndrome are associated with increased risk for colorectal adenoma in a Chinese population. BMC Gastroenterology. 10, 1–7.

Liu, H., and Gu, L. (2012). Phlorotannins from brown algae (Fucus vesiculosus) inhibited the formation of advanced glycation endproducts by scavenging reactive carbonyls. Journal of Agricultural and Food Chemistry. 60, 1326–1334.

Liu, H., Yu, S., Zhang, H., and Xu, J. (2012). Angiogenesis Impairment in Diabetes: Role of Methylglyoxal-Induced Receptor for Advanced Glycation Endproducts, Autophagy and Vascular Endothelial Growth Factor Receptor 2. PLoS ONE. 7, e46720.

Liu, J., Wang, R., Desai, K., and Wu, L. (2011a). Upregulation of aldolase B and overproduction of methylglyoxal in vascular tissues from rats with metabolic syndrome. Cardiovascular Research. 92, 494–503.

Liu, H., Liu, H., Wang, W., Khoo, C., Taylor, J., and Gu, L. (2011b). Cranberry phytochemicals inhibit glycation of human hemoglobin and serum albumin by scavenging reactive carbonyls. Food & Function. 2, 475–482.

Lorincz, A.M., and Sukumar, S. (2006). Molecular links between obesity and breast cancer. Endocrine-Related Cancer. 13, 279–292.

Lu, C., He, J.C., Cai, W., Liu, H., Zhu, L., and Vlassara, H. (2004). Advanced glycation endproduct (AGE) receptor 1 is a negative regulator of the inflammatory response to AGE in mesangial cells. Proceedings of the National Academy of Sciences of the United States of America. 101, 11767–11772.

Lu, M.-P., Wang, R., Song, X., Chibbar, R., Wang, X., Wu, L., and Meng, Q.H. (2008). Dietary soy isoflavones increase insulin secretion and prevent the development of diabetic cataracts in streptozotocin-induced diabetic rats. Nutrition Research. 28, 464–471.

Madiraju, A.K., Qiu, Y., Perry, R.J., Rahimi, Y., Zhang, X.M., Zhang, D., Camporez, J.P.G., Cline, G.W., Butrico, G.M., Kemp, B.E., et al. (2018). Metformin inhibits gluconeogenesis via a redox-dependent mechanism in vivo. Nature Medicine. 24, 1384–1394.

Maessen, D.E.M., Stehouwer, C.D. a., and Schalkwijk, C.G. (2015). The role of methylglyoxal and the glyoxalase system in diabetes and other age-related diseases. Clinical Science. 128, 839–861.

Maessen, D.E., Hanssen, N.M., Lips, M.A., Scheijen, J.L., Willems van Dijk, K., Pijl, H., Stehouwer, C.D., and Schalkwijk, C.G. (2016a). Energy restriction and Roux-en-Y gastric bypass reduce postprandial α-dicarbonyl stress in obese women with type 2 diabetes. Diabetologia. 59, 2013–2017.

Maessen, D.E., Brouwers, O., Gaens, K.H., Wouters, K., Cleutjens, J.P., Janssen, B.J., Miyata, T., Stehouwer, C.D., and Schalkwijk, C.G. (2016b). Delayed intervention with pyridoxamine improves metabolic function and prevents adipose tissue inflammation and insulin resistance in high-fat diet-induced obese mice. Diabetes. 65, 956–966.

Maher, P., Dargusch, R., Ehren, J.L., Okada, S., Sharma, K., and Schubert, D. (2011). Fisetin lowers methylglyoxal dependent protein glycation and limits the complications of diabetes. PloS One. 6, 1–11.

Maillard, L.C. (1912). Action des acides amines sur les sucres: formation des melanoidines par voie methodique. R Acad Sci Ser. 2, 66–68.

Mannerås-Holm, L., and Krook, A. (2012). Targeting adipose tissue angiogenesis to enhance insulin sensitivity. Diabetologia. 55, 2562–2564.

Marso, S.P., Daniels, G.H., Brown-Frandsen, K., Kristensen, P., Mann, J.F.E., Nauck, M.A., Nissen, S.E., Pocock, S., Poulter, N.R., Ravn, L.S., et al. (2016). Liraglutide and Cardiovascular Outcomes in Type 2 Diabetes. New England Journal of Medicine. 375, 311–322.

Masania, J., Malczewska-Malec, M., Razny, U., Goralska, J., Zdzienicka, A., Kiec-Wilk, B., Gruca, A., Stancel-Mozwillo, J., Dembinska-Kiec, A., Rabbani, N., et al. (2016a). Dicarbonyl stress in clinical obesity. Glycoconjugate Journal. 9, 581–589.

Masania, J., Malczewska-Malec, M., Razny, U., Goralska, J., Zdzienicka, A., Kiec-Wilk, B., Gruca, A., Stancel-Mozwillo, J., Dembinska-Kiec, A., Rabbani, N., et al. (2016b). Dicarbonyl stress in clinical obesity. Glycoconjugate Journal. 33, 581–589.

Mason, E.E., and Ito, C. (1969). Gastric bypass. Annals of Surgery. 170, 329–339.

Masterjohn, C., Park, Y., Lee, J., Noh, S.K., Koo, S.I., and Bruno, R.S. (2013a). Dietary Fructose Feeding Increases Adipose Methylglyoxal Accumulation in Rats in Association with Low Expression and Activity of Glyoxalase-2. Nutrients. 5, 3311–3328.

Masterjohn, C., Mah, E., Park, Y., Pei, R., Lee, J., Manautou, J.E., and Bruno, R.S. (2013b). Acute glutathione depletion induces hepatic methylglyoxal accumulation by impairing its detoxification to D-lactate. Experimental Biology and Medicine. 238, 360–369.

Matafome, P., Sena, C., and Seiça, R. (2013). Methylglyoxal, obesity, and diabetes. Endocrine. 43, 472–484.

Matafome, P., Rodrigues, T., and Seiça, R. (2015). Glycation and hypoxia: two key factors for adipose tissue dysfunction. Current Medicinal Chemistry. 22, 2417–2437.

Matafome, P., Eickhoff, H., Letra, L., and Seiça, R. (2017a). Neuroendocrinology of adipose tissue and gut–brain axis. Advances in Neurobiology. 19, 49–70.

Matafome, P., Rodrigues, T., Sena, C., and Seiça, R. (2017b). Methylglyoxal in Metabolic Disorders: Facts, Myths, and Promises. Medicinal Research Reviews. 37, 368–403.

Matafome, P., Santos-Silva, D., Crisóstomo, J., Rodrigues, T., Rodrigues, L., Sena, C., Pereira, P., and Seiça, R. (2012a). Methylglyoxal causes structural and functional alterations in adipose tissue independently of obesity. Archives of Physiology and Biochemistry. 118, 58–68.

Matafome, P., Santos-Silva, D., Crisóstomo, J., Rodrigues, T., Rodrigues, L., Sena, C.M., Pereira, P., and Seiça, R. (2012b). Methylglyoxal causes structural and functional alterations in adipose tissue independently of obesity. Archives of Physiology and Biochemistry. 118, 58–68.

Maury, E., and Brichard, S.M. (2010). Adipokine dysregulation, adipose tissue inflammation and metabolic

syndrome. Molecular and Cellular Endocrinology. 314, 1–16.

McVicar, C.M., Ward, M., Colhoun, L.M., Guduric-Fuchs, J., Bierhaus, A., Fleming, T., Schlotterer, A., Kolibabka, M., Hammes, H.-P., Chen, M., et al. (2015). Role of the receptor for advanced glycation endproducts (RAGE) in retinal vasodegenerative pathology during diabetes in mice. Diabetologia. 58, 1129–1137.

Meier, U., and Gressner, A.M. (2004). Endocrine Regulation of Energy Metabolism: Review of Pathobiochemical and Clinical Chemical Aspects of Leptin, Ghrelin, Adiponectin, and Resistin. Clinical Chemistry. 50, 1511–1525.

Min, S.Y., Kady, J., Nam, M., Rojas-Rodriguez, R., Berkenwald, A., Kim, J.H., Noh, H.L., Kim, J.K., Cooper, M.P., Fitzgibbons, T., et al. (2016). Human "brite/beige" adipocytes develop from capillary networks, and their implantation improves metabolic homeostasis in mice. Nature Medicine. 22, 312–318.

Moreno-Indias, I., and Tinahones, F.J. (2015). Impaired Adipose Tissue Expandability and Lipogenic Capacities as Ones of the Main Causes of Metabolic Disorders. Journal of Diabetes Research. 2015, 970375.

Muthenna, P., Akileshwari, C., and Reddy, G.B. (2012). Ellagic acid, a new antiglycating agent: its inhibition of Nlunate epsilon-(carboxymethyl) lysine. Biochemical Journal. 442, 221–230.

Nagai, T., Doi, S., Nakashima, A., Irifuku, T., Sasaki, K., Ueno, T., and Masaki, T. (2016). Linagliptin ameliorates methylglyoxal-induced peritoneal fibrosis in mice. PLoS ONE. 11, e0160993.

Nagaraj, R.H., Panda, A.K., Shanthakumar, S., Santhoshkumar, P., Pasupuleti, N., Wang, B., and Biswas, A. (2012). Hydroimidazolone modification of the conserved Arg12 in small heat shock proteins: studies on the structure and chaperone function using mutant mimics. PloS One. 7, 1–10.

Nakajou, K., Horiuchi, S., Sakai, M., Haraguchi, N., Tanaka, M., Takeya, M., and Otagiri, M. (2005). Renal clearance of glycolaldehyde- and methylglyoxal-modified proteins in mice is mediated by mesangial cells through a class A scavenger receptor (SR-A). Diabetologia. 48, 317–327.

Naukkarinen, J., Heinonen, S., Hakkarainen, A., Lundbom, J., Vuolteenaho, K., Saarinen, L., Hautaniemi, S., Rodriguez, A., Frühbeck, G., Pajunen, P., et al. (2014). Characterising metabolically healthy obesity in weight-discordant monozygotic twins. Diabetologia. 57, 167–176.

Neeland, I.J., Singh, S., McGuire, D.K., Vega, G.L., Roddy, T., Reilly, D.F., Castro-Perez, J., Kozlitina, J., and Scherer, P.E. (2018). Relation of plasma ceramides to visceral adiposity, insulin resistance and the development of type 2 diabetes mellitus: the Dallas Heart Study. Diabetologia. 61, 2570–2579.

Neels, J.G., Thinnes, T., and Loskutoff, D.J. (2004). Angiogenesis in an in vivo model of adipose tissue development. The FASEB Journal. 18, 983–1002.

Negre-Salvayre, A., Salvayre, Robert, Augé, N., Pamplona, R., Portero-Otín, M., and Salvayre, R. (2009). Hyperglycemia and glycation in diabetic complications. Antioxidants & Redox Signaling. 11, 3071–3109.

Negro, R. (2008). Endothelial effects of antihypertensive treatment: focus on irbesartan. Vascular Health and Risk Management. 4, 89–101.

Nemet, I., Varga-Defterdarovic, L., Turk, Z., Varga-Defterdarović, L., and Turk, Z. (2006). Methylglyoxal in food and living organisms. Molecular Nutrition & Food Research. 50, 1105–1117.

Neuberg, C. (1913). Uber die zerstorung von milch saurealdehyd und methylglyoxal durch tierische organe. Biochem. 49, 502–506.

Ng, M., Fleming, T., Robinson, M., Thomson, B., Graetz, N., Margono, C., Mullany, E.C., Biryukov, S.,

Abbafati, C., Abera, S.F., et al. (2014). Global, regional, and national prevalence of overweight and obesity in children and adults during 1980–2013: a systematic analysis for the Global Burden of Disease Study 2013. The Lancet. 384, 766–781.

Nguyen, N.T., and Varela, J.E. (2017). Bariatric surgery for obesity and metabolic disorders: State of the art. Nature Reviews Gastroenterology and Hepatology. 14, 160–169.

Nicosia, R.F., Tchao, R., and Leighton, J. (1982). Histotypic angiogenesis in vitro: Light microscopic, ultrastructural, and radioautographic studies. In Vitro. 18, 538–549.

Nielsen, T.S., Jessen, N., Jørgensen, J.O.L., Møller, N., and Lund, S. (2014). Dissecting adipose tissue lipolysis: Molecular regulation and implications for metabolic disease. Journal of Molecular Endocrinology. 52, 199–222.

Nielsen, N.B., Højbjerre, L., Sonne, M.P., Alibegovic, A.C., Vaag, A., Dela, F., and Stallknecht, B. (2009). Interstitial concentrations of adipokines in subcutaneous abdominal and femoral adipose tissue. Regulatory Peptides. 155, 39–45.

Nigro, C., Leone, A., Longo, M., Prevenzano, I., Fleming, T.H., Nicolò, A., Parrillo, L., Spinelli, R., Formisano, P., Nawroth, P.P., et al. (2019). Methylglyoxal accumulation de-regulates HoxA5 expression, thereby impairing angiogenesis in glyoxalase 1 knock-down mouse aortic endothelial cells. Biochimica et Biophysica Acta. 1865, 73–85.

Odegaard, J., Ricardo-Gonzalez, R., Goforth, M., Morel, C., Subramanian, V., Mukundan, L., Eagle, A., Vats, D., Brombacher, F., Ferrante, A., et al. (2007). Macrophage-specific PPARγ controls alternative activation and improves insulin resistance. Nature. 447, 1116–1120.

Okuno, Y., Fukuhara, A., Hashimoto, E., Kobayashi, H., Kobayashi, S., Otsuki, M., and Shimomura, I. (2018). Oxidative stress inhibits healthy adipose expansion through suppression of SREBF1-Mediated lipogenic pathway. Diabetes. 67, 1113–1127.

Olefsky, J.M., and Glass, C.K. (2010). Macrophages, inflammation, and insulin resistance. Annual Review of Physiology. 72, 219–246.

Otabe, S., Yuan, X., Fukutani, T., Wada, N., Hashinaga, T., Nakayama, H., Hirota, N., Kojima, M., and Yamada, K. (2007). Overexpression of human adiponectin in transgenic mice results in suppression of fat accumulation and prevention of premature death by high-calorie diet. American Journal of Physiology-Endocrinology and Metabolism. 293, E210–E218.

Padival, A.K., Crabb, J.W., and Nagaraj, R.H. (2003). Methylglyoxal modifies heat shock protein 27 in glomerular mesangial cells. FEBS Letters. 551, 113–118.

Paget, C., Lecomte, M., Ruggiero, D., Wiernsperger, N., and Lagarde, M. (1998). Modification of enzymatic antioxidants in retinal microvascular cells by glucose or advanced glycation end products. Free Radical Biology & Medicine. 25, 121–129.

Pais, R., Silaghi, H., Silaghi, A.C., Rusu, M.L., Dumitrascu, D.L., H, S., AC, S., ML, R., and DL, D. (2009). Metabolic syndrome and risk of subsequent colorectal cancer. World Journal of Gastroenterology. 15, 5141–5148.

Patel, A., MacMahon, S., Chalmers, J., Neal, B., Billot, L., Woodward, M., Marre, M., Cooper, M., Glasziou, P., Grobbee, D., et al. (2008). Intensive Blood Glucose Control and Vascular Outcomes in Patients with Type 2 Diabetes. New England Journal of Medicine. 358, 2560–2572.

Payne, J.H., and DeWind, L.T. (1969). Surgical treatment of obesity. American Journal of Surgery. 118, 141–147.

Pellegrinelli, V., Carobbio, S., and Vidal-Puig, A. (2016). Adipose tissue plasticity: how fat depots respond differently to pathophysiological cues. Diabetologia. 59, 1075–1088.

Peng, Z., Shi, H., Yang, X., Ye, K., Lu, X., Liu, X., Jiang, M., Qin, J., and Wang, X. (2016). Glyoxalase-1 Overexpression Reverses Defective Proangiogenic Function of Diabetic Adipose-Derived Stem Cells in Streptozotocin-Induced Diabetic Mice Model of Critical Limb Ischemia. Stem Cells Translational Medicine. 6, 261–271.

Peschechera, A., and Eckel, J. (2013). "Browning" of adipose tissue - regulation and therapeutic perspectives. Archives of Physiology and Biochemistry. 3455, 1–10.

Pi-Sunyer, X., Astrup, A., Fujioka, K., Greenway, F., Halpern, A., Krempf, M., Lau, D.C.W., le Roux, C.W., Violante Ortiz, R., Jensen, C.B., et al. (2015). A Randomized, Controlled Trial of 3.0 mg of Liraglutide in Weight Management. New England Journal of Medicine. 373, 11–22.

Pino, E., Wang, H., McDonald, M.E., Qiang, L., and Farmer, S.R. (2012). Roles for peroxisome proliferator-activated receptor γ (PPARγ) and PPARγ coactivators 1α and 1β in regulating response of white and brown adipocytes to hypoxia. The Journal of Biological Chemistry. 287, 18351–18358.

Pories, W.J. (1992). Why Does the Gastric Bypass Control Type 2 Diabetes Mellitus? Obesity Surgery. 2, 303–313.

Qatanani, M., and Lazar, M. a (2007). Mechanisms of obesity-associated insulin resistance: many choices on the menu. Genes & Development. 21, 1443–1455.

Qi, Q., Lu, L., Li, H., Yuan, Z., Chen, G., Lin, M., Ruan, Z., Ye, X., Xiao, Z., and Zhao, Q. (2017). Spatiotemporal delivery of nanoformulated liraglutide for cardiac regeneration after myocardial infarction. International Journal of Nanomedicine. 12, 4835–4848.

Rabbani, N., and Thornalley, P.J. (2008). The dicarbonyl proteome: proteins susceptible to dicarbonyl glycation at functional sites in health, aging, and disease. Annals of the New York Academy of Sciences. 1126, 124–127.

Rabbani, N., and Thornalley, P.J. (2011). Glyoxalase in diabetes, obesity and related disorders. Seminars in Cell & Developmental Biology. 22, 309–317.

Rabbani, N., and Thornalley, P.J. (2012). Methylglyoxal, glyoxalase 1 and the dicarbonyl proteome. Amino Acids. 42, 1133–1142.

Rabbani, N., and Thornalley, P.J. (2014a). The critical role of methylglyoxal and glyoxalase 1 in diabetic nephropathy. Diabetes. 63, 50–52.

Rabbani, N., and Thornalley, P.J. (2014b). Dicarbonyl proteome and genome damage in metabolic and vascular disease. Biochemical Society Transactions. 42, 425–432.

Rabbani, N., and Thornalley, P.J. (2015). Dicarbonyl stress in cell and tissue dysfunction contributing to ageing and disease. Biochemical and Biophysical Research Communications. 458, 221–226.

Rabbani, N., and Thornalley, P.J. (2018). Glyoxalase 1 Modulation in Obesity and Diabetes. Antioxidants & Redox Signaling. 30, ars.2017.7424.

Rabbani, N., Xue, M., and Thornalley, P.J. (2014). Activity, regulation, copy number and function in the glyoxalase system. Biochemical Society Transactions. 42, 419–424.

Rabbani, N., Xue, M., and Thornalley, P.J. (2016). Dicarbonyls and glyoxalase in disease mechanisms and clinical therapeutics. Glycoconjugate Journal. 33, 513–525.

Rafii, S., and Carmeliet, P. (2016). VEGF-B Improves Metabolic Health through Vascular Pruning of Fat. Cell Metabolism. 23, 571–573.

Rajala, M.W., and Scherer, P.E. (2003). Minireview: The Adipocyte--At the Crossroads of Energy Homeostasis, Inflammation, and Atherosclerosis. Endocrinology. 144, 3765–3773.

Ramasamy, R., Yan, S.F., and Schmidt, A.M. (2012). Advanced glycation endproducts: from precursors to RAGE: round and round we go. Amino Acids. 42, 1151–1161.

Reilly, S.M., and Saltiel, A.R. (2017). Adapting to obesity with adipose tissue inflammation. Nature Reviews Endocrinology. 13, 633–643.

Remor, A.P., de Matos, F.J., Ghisoni, K., da Silva, T.L., Eidt, G., Búrigo, M., de Bem, A.F., Silveira, P.C.L., de León, A., Sanchez, M.C., et al. (2011). Differential effects of insulin on peripheral diabetes-related changes in mitochondrial bioenergetics: involvement of advanced glycosylated end products. Biochimica et Biophysica Acta. 1812, 1460–1471.

Reshef, L., Olswang, Y., Cassuto, H., Blum, B., Croniger, C.M., Kalhan, S.C., Tilghman, S.M., and Hanson, R.W. (2003). Glyceroneogenesis and the triglyceride/fatty acid cycle. Journal of Biological Chemistry. 278, 30413–30416.

Riboulet-Chavey, A., Pierron, A., Durand, I., Murdaca, J., Giudicelli, J., and Van Obberghen, E. (2006). Methylglyoxal Impairs the Insulin Signaling Pathways Independently of the Formation of Intracellular Reactive Oxygen Species. Diabetes. 55, 1289–1299.

Riera-Guardia, N., and Rothenbacher, D. (2008). The effect of thiazolidinediones on adiponectin serum level: a meta-analysis. Diabetes, Obesity and Metabolism. 10, 367–375.

Robciuc, M.R., Kivelä, R., Williams, I.M., De Boer, J.F., Van Dijk, T.H., Elamaa, H., Tigistu-Sahle, F., Molotkov, D., Leppänen, V.M., Käkelä, R., et al. (2016). VEGFB/VEGFR1-Induced Expansion of Adipose Vasculature Counteracts Obesity and Related Metabolic Complications. Cell Metabolism. 23, 712–724.

Roberts, M.J., Wondrak, G.T., Laurean, D.C., Jacobson, M.K., and Jacobson, E.L. (2003). DNA damage by carbonyl stress in human skin cells. Mutation Research. 522, 45–56.

Rodrigue, T., Matafome, P., Daniela, S.-S., Cristina, S., and Raquel, S. (2013). Reduction of methylglyoxal-induced glycation by pyridoxamine improves adipose tissue microvascular lesions. Journal of Diabetes Research. 2013, 690650.

Rodrigues, T. (2013). O papel do metilglioxal nas adaptações metabólicas do tecido adiposo quando sujeito a uma redução parcial da irrigação. Universidade de Coimbra.

Rodrigues, T., Matafome, P., and Seiça, R. (2013a). A vascular piece in the puzzle of adipose tissue dysfunction: mechanisms and consequences. Archives of Physiology and Biochemistry. 120, 1–11.

Rodrigues, T., Matafome, P., and Seiça, R. (2013b). Methylglyoxal further impairs adipose tissue metabolism after partial decrease of blood supply. Archives of Physiology and Biochemistry. 119, 209–218.

Rodrigues, T., Matafome, P., Santos-Silva, D., Sena, C., Seiça, R., Rodrigues, T., and Matafome, P. (2013c). Reduction of methylglyoxal-induced glycation by pyridoxamine improves adipose tissue microvascular lesions. Journal of Diabetes Research. 2013, 1–9.

Rojas-Rodriguez, R., Gealekman, O., Kruse, M.E., Rosenthal, B., Rao, K., Min, S., Bellve, K.D., Lifshitz,

L.M., and Corvera, S. (2014). Adipose Tissue Angiogenesis Assay. Methods Enzymol. 537, 75–91.

Rubino, F. (2013). From bariatric to metabolic surgery: Definition of a new discipline and implications for clinical practice. Current Atherosclerosis Reports. 15, 369.

Rubino, F., Nathan, D.M., Eckel, R.H., Schauer, P.R., Alberti, K.G.M.M., Zimmet, P.Z., Del Prato, S., Ji, L., Sadikot, S.M., Herman, W.H., et al. (2016). Metabolic surgery in the treatment algorithm for type 2 diabetes: A joint statement by international diabetes organizations. Diabetes Care. 39, 861–877.

Rutkowski, J.M., Davis, K.E., and Scherer, P.E. (2009). Mechanisms of obesity and related pathologies: the macro- and microcirculation of adipose tissue. The FEBS Journal. 276, 5738–5746.

Rutkowski, J.M., Stern, J.H., and Scherer, P.E. (2015). The cell biology of fat expansion. Journal of Cell Biology. 208, 501–512.

Santilli, F., Blardi, P., Scapellato, C., Bocchia, M., Guazzi, G., Terzuoli, L., Tabucchi, A., Silvietti, A., Lucani, B., Renato, W., et al. (2015). Decreased plasma endogenous soluble RAGE , and enhanced adipokine secretion , oxidative stress and platelet / coagulative activation identify non-alcoholic fatty liver disease among patients with familial combined hyperlipidemia and / or metabolic syndrom. Vascular Pharmacology. 72, 16–24.

Santos-Oliveira, P., Correia, A., Rodrigues, T., Ribeiro-Rodrigues, T.M., Matafome, P., Rodríguez-Manzaneque, J.C., Seiça, R., Girão, H., and Travasso, R.D.M. (2015). The Force at the Tip--Modelling Tension and Proliferation in Sprouting Angiogenesis. PLoS Computational Biology. 11, e1004436.

Schalkwijk, C.G. (2015). Vascular AGE-ing by methylglyoxal: the past, the present and the future. Diabetologia. 58, 1715–1719.

Scherer, P.E. (2006). Adipose tissue: From lipid storage compartment to endocrine organ. Diabetes. 55, 1537–1545.

Scherer, P.E. (2016). The Multifaceted Roles of Adipose Tissue—Therapeutic Targets for Diabetes and Beyond. Diabetes. 65, 1452–1461.

Scherer, P.E. (2018). The many secret lives of adipocytes: implications for diabetes. Diabetologia. 62, 223–232.

Semenza, G.L. (2004). Hydroxylation of HIF-1: oxygen sensing at the molecular level. Physiology. 19, 176–182.

Sena, C., Matafome, P., Crisóstomo, J., Rodrigues, L., Fernandes, R., Pereira, P., and Seiça, R.M. (2012). Methylglyoxal promotes oxidative stress and endothelial dysfunction. Pharmacological Research. 65, 497–506.

Shao, Y., Yuan, G., Zhang, J., and Guo, X. (2015). Liraglutide reduces lipogenetic signals in visceral adipose of db/db mice with AMPK activation and akt suppression. Drug Design, Development and Therapy. 9, 1177–1184.

Sharma, M.K., Jalewa, J., and Hölscher, C. (2014). Neuroprotective and anti-apoptotic effects of liraglutide on SH-SY5Y cells exposed to methylglyoxal stress. Journal of Neurochemistry. 128, 459–471.

Shibata, R., Skurk, C., Ouchi, N., Galasso, G., Kondo, K., Ohashi, T., Shimano, M., Kihara, S., Murohara, T., and Walsh, K. (2008). Adiponectin promotes endothelial progenitor cell number and function. FEBS Letters. 582, 1607–1612.

Shimizu, I., and Walsh, K. (2015). The Whitening of Brown Fat and Its Implications for Weight Management in Obesity. Current Obesity Reports. 4, 224–229.

Shinohara, M., Thornalley, P.J., Giardino, I., Beisswenger, P., Thorpe, S.R., Onorato, J., and Brownlee, M. (1998). Overexpression of glyoxalase-I in bovine endothelial cells inhibits intracellular advanced glycation endproduct formation and prevents hyperglycemia-induced increases in macromolecular endocytosis. Journal of Clinical Investigation. 101, 1142–1147.

Sidossis, L., and Kajimura, S. (2015). Brown and beige fat in humans: Thermogenic adipocytes that control energy and glucose homeostasis. Journal of Clinical Investigation. 125, 478–486.

da Silva, K.S., Pinto, P.R., Fabre, N.T., Gomes, D.J., Thieme, K., Okuda, L.S., Iborra, R.T., Freitas, V.G., Shimizu, M.H.M., Teodoro, W.R., et al. (2017). N-acetylcysteine Counteracts Adipose Tissue Macrophage Infiltration and Insulin Resistance Elicited by Advanced Glycated Albumin in Healthy Rats. Frontiers in Physiology. 8, 723.

Smith, U. (2015). Abdominal obesity : a marker of ectopic fat accumulation. The Journal of Clinical Investigation. 125, 1790–1792.

Sotornik, R., Brassard, P., Martin, E., Yale, P., Carpentier, A.C., and Ardilouze, J.-L. (2012). Update on adipose tissue blood flow regulation. American Journal of Endocrinology and Metabolism. 302, E1157–E1170.

Spalding, K.L., Arner, E., Westermark, P.O., Bernard, S., Buchholz, B.A., Bergmann, O., Blomqvist, L., Hoffstedt, J., Näslund, E., Britton, T., et al. (2008). Dynamics of fat cell turnover in humans. Nature. 453, 783–787.

Spanneberg, R., Salzwedel, G., and Glomb, M. (2012). Formation of early and advanced Maillard reaction products correlates to the ripening of cheese. Journal of Agricultural and Food Chemistry. 60, 600–607.

Steckelings, U.M., Rompe, F., Kaschina, E., and Unger, T. (2009). The evolving story of the RAAS in hypertension, diabetes and CV disease: moving from macrovascular to microvascular targets. Fundamental & Clinical Pharmacology. 23, 693–703.

Stevens, G.A., Singh, G.M., Lu, Y., Danaei, G., Lin, J.K., Finucane, M.M., Bahalim, A.N., McIntire, R.K., Gutierrez, H.R., Cowan, M., et al. (2012). National, regional, and global trends in adult overweight and obesity prevalences. Population Health Metrics. 10, 22.

Sun, K., Wernstedt Asterholm, I., Kusminski, C.M., Bueno, A.C., Wang, Z. V, Pollard, J.W., Brekken, R.A., Scherer, P.E., Wernstedt, I., Kusminski, C.M., et al. (2012). Dichotomous effects of VEGF-A on adipose tissue dysfunction. Proceedings of the National Academy of Sciences of the United States of America. 109, 5874–5879.

Sun, K., Kusminski, C.M., Luby-Phelps, K., Spurgin, S.B., An, Y.A., Wang, Q.A., Holland, W.L., and Scherer, P.E. (2014). Brown adipose tissue derived VEGF-A modulates cold tolerance and energy expenditure. Molecular Metabolism. 3, 474–483.

Tam, J., Duda, D.G., Perentes, J.Y., Quadri, R.S., Fukumura, D., and Jain, R.K. (2009). Blockade of VEGFR2 and not VEGFR1 can limit diet-induced fat tissue expansion: role of local versus bone marrow-derived endothelial cells. PloS One. 4, e4974.

Tames, F.J., Mackness, M.I., Arrol, S., Laing, I., and Durrington, P.N. (1992). Non-enzymatic glycation of apolipoprotein B in the sera of diabetic and non-diabetic subjects. Atherosclerosis. 93, 237–44.

Tan, D., Wang, Y., Lo, C.-Y., Sang, S., and Ho, C.-T. (2008). Methylglyoxal: its presence in beverages and potential scavengers. Annals of the New York Academy of Sciences. 1126, 72–75.

Taneda, S., Honda, K., Tomidokoro, K., Uto, K., Nitta, K., and Oda, H. (2010). Eicosapentaenoic acid restores

diabetic tubular injury through regulating oxidative stress and mitochondrial apoptosis. American Journal of Physiology. Renal Physiology. 299, F1451-61.

Thieme, K., Da Silva, K.S., Fabre, N.T., Catanozi, S., Monteiro, M.B., Santos-Bezerra, D.P., Costa-Pessoa, J.M., Oliveira-Souza, M., Machado, U.F., Passarelli, M., et al. (2016). N-Acetyl Cysteine Attenuated the Deleterious Effects of Advanced Glycation End-Products on the Kidney of Non-Diabetic Rats. Cellular Physiology and Biochemistry. 40, 608–620.

Tikellis, C., Pickering, R.J., Tsorotes, D., Huet, O., Cooper, M.E., Jandeleit-Dahm, K., and Thomas, M.C. (2014). Dicarbonyl Stress in the Absence of Hyperglycemia Increases Endothelial Inflammation and Atherogenesis Similar to That Observed in Diabetes. Diabetes. 63, 3915–3925.

Tilg, H., and Moschen, A.R. (2006). Adipocytokines: mediators linking adipose tissue, inflammation and immunity. Nature Reviews - Immunology. 6, 772–783.

Tran, K., Gealekman, O., Frontini, A., Zingaretti, M., Morroni, M., Giordano, A., Smorlesi, A., Perugini, J., Matteis, R., Sbarbati, A., et al. (2012). The vascular endothelium of the adipose tissue gives rise to both white and brown fat cells. Cell Metabolism. 15, 222–229.

Trayhurn, P. (2013). Hypoxia and adipose tissue function and dysfunction in obesity. Physiological Reviews. 93, 1–21.

Trayhurn, P., Wang, B., and Wood, I.S. (2008a). Hypoxia in adipose tissue: a basis for the dysregulation of tissue function in obesity? The British Journal of Nutrition. 100, 227–235.

Trayhurn, P., Wang, B., and Wood, I.S. (2008b). Hypoxia and the endocrine and signalling role of white adipose tissue. Archives of Physiology and Biochemistry. 114, 267–276.

Treins, C., Giorgetti-Peraldi, S., Murdaca, J., Semenza, G.L., and Van Obberghen, E. (2002). Insulin stimulates hypoxia-inducible factor 1 through a phosphatidylinositol 3-kinase/target of rapamycin-dependent signaling pathway. The Journal of Biological Chemistry. 277, 27975–27981.

Trujillo, M.E., and Scherer, P.E. (2006). Adipose Tissue-Derived Factors: Impact on Health and Disease. Endocrine Reviews. 27, 762–778.

Trung, V.N., Yamamoto, H., Yamaguchi, T., Murata, S., Akabori, H., Ugi, S., Maegawa, H., and Tani, T. (2013). Effect of sleeve gastrectomy on body weight, food intake, glucose tolerance, and metabolic hormone level in two different rat models: Goto-Kakizaki and diet-induced obese rat. Journal of Surgical Research. 185, 159–165.

Ueno, H., Koyama, H., Shoji, T., Monden, M., Fukumoto, S., Tanaka, S., Otsuka, Y., Mima, Y., Morioka, T., Mori, K., et al. (2010). Receptor for advanced glycation end-products (RAGE) regulation of adiposity and adiponectin is associated with atherogenesis in apoE-deficient mouse. Atherosclerosis. 211, 431–436.

Uribarri, J., Cai, W., Woodward, M., Tripp, E., Goldberg, L., Pyzik, R., Yee, K., Tansman, L., Chen, X., Mani, V., et al. (2015a). Elevated serum advanced glycation endproducts in obese indicate risk for the metabolic syndrome: a link between healthy and unhealthy obesity? The Journal of Clinical Endocrinology and Metabolism. 100, 1957–1966.

Uribarri, J., del Castillo, M.D., de la Maza, M.P., Filip, R., Gugliucci, A., Luevano-Contreras, C., Macías-Cervantes, M.H., Markowicz Bastos, D.H., Medrano, A., Menini, T., et al. (2015b). Dietary Advanced Glycation End Products and Their Role in Health and Disease. Advances in Nutrition: An International Review Journal. 6, 461–473.

Uribarri, J., and He, J.C. (2015). The low AGE diet: a neglected aspect of clinical nephrology practice? Nephron. 130, 48–53.

Vázquez-Vela, M.E.F., Torres, N., and Tovar, A.R. (2008). White adipose tissue as endocrine organ and its role in obesity. Archives of Medical Research. 39, 715–728.

Vianello, E., Lamont, J., Tacchini, L., Corsi Romanelli, M.M., Briganti, S., Schmitz, G., and Dozio, E. (2015). Expression of the Receptor for Advanced Glycation End Products in Epicardial Fat: Link with Tissue Thickness and Local Insulin Resistance in Coronary Artery Disease. Journal of Diabetes Research. 2016, 1–8.

Villela, N., Kramer-Aguiar, L., Bottino, D., Wiernsperger, N., and Bouskela, E. (2009). Metabolic disturbances linked to obesity: the role of impaired tissue perfusion. Arquivos Brasileiros de Endocrinologia E Metabolismo. 53, 238–245.

Virtanen, K.A., Lönnroth, P., Parkkola, R., Peltoniemi, P., Asola, M., Viljanen, T., Tolvanen, T., Knuuti, J., Rönnemaa, T., Huupponen, R., et al. (2002). Glucose uptake and perfusion in subcutaneous and visceral adipose tissue during insulin stimulation in nonobese and obese humans. Journal of Clinical Endocrinology and Metabolism. 87, 3902–3910.

Vlassara, H., and Striker, G.E. (2013). AGE restriction in diabetes mellitus : a paradigm shift. Nature Reviews Endocrinology. 7, 526–539.

Vona-Davis, L., and Rose, D.P. (2009). Angiogenesis, adipokines and breast cancer. Cytokine & Growth Factor Reviews. 20, 193–201.

Vulesevic, B., McNeill, B., Geoffrion, M., Kuraitis, D., McBane, J.E., Lochhead, M., Vanderhyden, B.C., Korbutt, G.S., Milne, R.W., and Suuronen, E.J. (2014). Glyoxalase-1 overexpression in bone marrow cells reverses defective neovascularization in STZ-induced diabetic mice. Cardiovascular Research. 101, 306–316.

Wang, J., and Chang, T. (2010). Methylglyoxal content in drinking coffee as a cytotoxic factor. Journal of Food Science. 75, H167-71.

Wang, Z. V., and Scherer, P.E. (2016). Adiponectin, the past two decades. Journal of Molecular Cell Biology. 8, 93–100.

Wang, B., Wood, I.S., and Trayhurn, P. (2007). Dysregulation of the expression and secretion of inflammation-related adipokines by hypoxia in human adipocytes. Pflügers Archiv : European Journal of Physiology. 455, 479–492.

Wang, Z., Hsu, C., Huang, C., and Yin, M. (2010). Anti-glycative effects of oleanolic acid and ursolic acid in kidney of diabetic mice. European Journal of Pharmacology. 628, 255–260.

Wang, Z., Li, H., Zhang, D., Liu, X., Zhao, F., Pang, X., and Wang, Q. (2015a). Effect of advanced glycosylation end products on apoptosis in human adipose tissue-derived stem cells in vitro. Cell and Bioscience. 5, 3.

Wang, L., Zhang, X., Pang, N., Xiao, L., Li, Y., Chen, N., Ren, M., Deng, X., and Wu, J. (2015b). Glycation of vitronectin inhibits VEGF-induced angiogenesis by uncoupling VEGF receptor-2 – α v β 3 integrin cross-talk. Cell Death and Disease. 6, 1–8.

Watson, A.M.D., Soro-Paavonen, A., Sheehy, K., Li, J., Calkin, A.C., Koitka, A., Rajan, S.N., Brasacchio, D., Allen, T.J., Cooper, M.E., et al. (2011). Delayed intervention with AGE inhibitors attenuates the progression of diabetes-accelerated atherosclerosis in diabetic apolipoprotein E knockout mice. Diabetologia. 54, 681–689.

Weir, M.R. (2007a). Targeting mechanisms of hypertensive vascular disease with dual calcium channel and

renin-angiotensin system blockade. Journal of Human Hypertension. 21, 770–779.

Weir, M.R. (2007b). Effects of renin-angiotensin system inhibition end-organ protection: Can we do better? Clinical Therapeutics. 29, 1803–1824.

Wellen, K.E., and Hotamisligil, G.S. (2005). Inflammation, stress, and diabetes. Journal of Clinical Investigation. 115, 1111–1119.

WHO (2016). Obesity and Overweight. World Health Organization.

Wild, S., Roglic, G., Green, A., Sicree, R., and King, H. (2004). Global prevalence of diabetes: estimates for the year 2000 and projections for 2030. Diabetes Care. 27, 1047–1053.

WJ, P., Jr, M.K., EG, F., GL, D., MK, S., HA, B., HJ, M., P, K., MS, S., and E, M. (2006a). Is Type II Diabetes Mellitus (NIDDM) a Surgical Disease? Annals of Surgery. 215, 633–643.

WJ, P., MS, S., KG, M., SB, L., PG, M., BM, B., HA, B., RA, D., G, I., and JM, D. (2006b). Who Would Have Thought It? An Operation Proves to Be the Most Effective Therapy for Adult-Onset Diabetes Mellitus. Annals of Surgery. 222, 339–352.

Wongchai, K., Schlotterer, A., Lin, J., Humpert, P.M., Klein, T., Hammes, H.P., and Morcos, M. (2016). Protective Effects of Liraglutide and Linagliptin in Celegans as a New Model for Glucose-Induced Neurodegeneration. Hormone and Metabolic Research. 48, 70–75.

Wood, I.S., Heredia, F.P., Wang, B., and Trayhurn, P. (2009). Cellular hypoxia and adipose tissue dysfunction in obesity. The Proceedings of the Nutrition Society. 68, 370–377.

World Health Organization (2000). Obesity: preventing and managing the global epidemic. Report of a WHO consultation. World Health Organization Technical Report Series. 894, 1–253.

World Health Organization (2011). Use of glycated haemoglobin (HbA1c) in the diagnosis of diabetes mellitus: abbreviated report of a WHO consultation. 25.

Xiao-Yun, X., Zhao-Hui, M., Ke, C., Hong-Hui, H., and Yan-Hong, X. (2011). Glucagon-like peptide-1 improves proliferation and differentiation of endothelial progenitor cells via upregulating VEGF generation. Medical Science Monitor. 17, BR35-41.

Xue, J., Rai, V., Singer, D., Chabierski, S., Xie, J., Reverdatto, S., Burz, D.S., Schmidt, A.M., Hoffmann, R., and Shekhtman, A. (2011a). Advanced glycation end product recognition by the receptor for AGEs. Structure. 19, 722–732.

Xue, M., Weickert, M.O., Qureshi, S., Kandala, N.-B.B., Anwar, A., Waldron, M., Shafie, A., Messenger, D., Fowler, M., Jenkins, G., et al. (2016). Improved Glycemic Control and Vascular Function in Overweight and Obese Subjects by Glyoxalase 1 Inducer Formulation. Diabetes. 65, 2282–2294.

Xue, M., Rabbani, N., and Thornalley, P.J. (2011b). Glyoxalase in ageing. Seminars in Cell & Developmental Biology. 22, 293–301.

Yamakawa, M., Liu, L.X., Date, T., Belanger, A.J., Vincent, K. a, Akita, G.Y., Kuriyama, T., Cheng, S.H., Gregory, R.J., and Jiang, C. (2003). Hypoxia-inducible factor-1 mediates activation of cultured vascular endothelial cells by inducing multiple angiogenic factors. Circulation Research. 93, 664–673.

Yamawaki, H., Saito, K., Okada, M., and Hara, Y. (2008). Methylglyoxal mediates vascular inflammation via JNK and p38 in human endothelial cells. American Journal of Physiology. Cell Physiology. 295, C1510-7.

Yan, S.F., Ramasamy, R., Naka, Y., and Schmidt, A.M. (2003). Glycation, inflammation, and RAGE: a scaffold for the macrovascular complications of diabetes and beyond. Circulation Research. 93, 1159–1169.

Yao, D., and Brownlee, M. (2010). Hyperglycemia-induced reactive oxygen species increase expression of the receptor for advanced glycation end products (RAGE) and RAGE ligands. Diabetes. 59, 249–255.

Ye, J. (2008). Emerging role of adipose tissue hypoxia in obesity and insulin resistance. International Journal of Obesity. 33, 54–66.

Ye, J., Gao, Z., Yin, J., and He, Q. (2007). Hypoxia is a potential risk factor for chronic inflammation and adiponectin reduction in adipose tissue of ob/ob and dietary obese mice. American Journal of Physiology Endocrinology and Metabolism. 293, E1118-28.

Zhang, Y., Zhou, H., Wu, W., Shi, C., Hu, S., Yin, T., Ma, Q., Han, T., Zhang, Y., Tian, F., et al. (2016). Free Radical Biology and Medicine Liraglutide protects cardiac microvascular endothelial cells against hypoxia / reoxygenation injury through the suppression of the SR-Ca 2 þ – XO – ROS axis via activation of the GLP-1R / PI3K / Akt / survivin pathways. 95, 278–292.

Zheng, Y., Ley, S.H., and Hu, F.B. (2017). Global aetiology and epidemiology of type 2 diabetes mellitus and its complications. Nature Reviews Endocrinology. 14, 88–98.